SESS REPORT 2022

The State of Environmental Science in Svalbard – an annual report

SIOS
SVALBARD INTEGRATED ARCTIC EARTH OBSERVING SYSTEM

SESS REPORT 2022

The State of Environmental Science
in Svalbard – an annual report

Marjolein Gevers, Divya David T, Roseline C
Thakur, Christiane Hübner, Jacek Jania (Editors)

SESS report 2022
The State of Environmental Science in Svalbard
– an annual report

ISSN 2535-809X (printed)
ISSN 2535-6321 (pdf)
ISBN 978-82-93871-07-1 (printed, stapled)
ISBN 978-82-93871-06-4 (pdf)

Publisher: Svalbard Integrated Arctic Earth Observing System (SIOS)
Editors: Marjolein Gevers, Divya David T, Roseline C Thakur, Christiane Hübner, Jacek Jania
Editor popular science summaries: Janet Holmén
Layout: Melkeveien designkontor, Oslo

CITATION:
Entire report: Gevers M, David DT, Thakur RC, Hübner C, Jania J (eds) 2023: SESS report 2022, Svalbard Integrated Arctic Earth Observing System, Longyearbyen
Chapters in report: All authors (2023) Title of chapter. In: Gevers et al (eds) SESS report 2022, Svalbard Integrated Arctic Earth Observing System, Longyearbyen, pp xx-xx. DOI-link of chapter

The report is published as electronic document, available from the SIOS web site
https://sios-svalbard.org/SESSreport

Contents

Foreword

You are reading the 5th State of Environmental Science in Svalbard (SESS) report. This report includes six chapters on topics ranging from snow to the Sun's activity. The report is again an enjoyable collection of articles describing science and scientific tools in Svalbard and how to develop them. This is the first time I was not in the editorial board and only excitedly followed the creation of the 5th SESS report from the sidelines.

Last year I wrote in the foreword about living under the shadow of the COVID-19 pandemic, and just when we were almost back to normal the world took a tragic negative turn with the unjustified Russian invasion of Ukraine. This has also had a significant impact on polar science and scientific collaboration, with nearly half of the Arctic suddenly being inaccessible in many ways. The consequences are also seen here in Svalbard: collaboration at all levels between Russian settlements and research institutions has almost completely ceased. My honest hope is that cooperation will resume one day; how far in the future that day lies, we do not know. What we know is that science diplomacy will certainly play an important role. Arctic nations have always managed to collaborate despite the geopolitical turbulences, and it might well turn out that it is through the Arctic we start to build the bridges again.

Svalbard Integrated Arctic Earth Observing System (SIOS) entered a new funding phase this year. It was a natural time to renew our strategy, which we have started to implement. It includes among other things new methods to develop the observing system: the optimisation call programme. The first call is designed to make extensive use of the SESS reports' recommendations.

A synthesis of recommendations from the first four SESS reports was published this fall and it is being used to develop the observing system together with SIOS core data and the infrastructure optimisation report. As I write this, I have the new draft of the infrastructure optimisation report on my desk. The task force has taken big leaps forward spurred by its leader, who is new in the SIOS environment. It is refreshing to be observed from outside the SIOS bubble, in which our working groups and we staffers at the SIOS Knowledge Centre occasionally find ourselves. With the same idea in mind, it has been agreed that an external evaluation of SIOS will be conducted next year, and I am looking forward to receiving input on how SIOS could be even better.

I really appreciate the reviewers of the chapters in this SESS report; peer review is the cornerstone of the scientific process. I would like to express my gratitude to the editorial board for their engagement in the preparation of this report. It is hard work, but you have managed to find time to share your expertise. I would like to acknowledge my colleagues here at the SIOS Knowledge Centre; it is a privilege to work with such an enthusiastic and supportive team.

Longyearbyen, December 2022

Prof. Heikki Lihavainen
Director, SIOS

Authors from following institutions contributed to this report:

4s	forScience Foundation, Toruń, Poland
AMU	Adam Mickiewicz University in Poznań, Poznań, Poland
AWI	Alfred Wegener Institute, Helmholtz Centre for Polar and Marine Research, Bremerhaven, Germany
BAS	British Antarctic Survey, Cambridge, UK
BCSS	Birkeland Centre for Space Studies, University of Bergen, Bergen, Norway
CWU	Central Washington University, Ellensburg, USA
CZU	Czech University of Life Sciences Prague, Prague, Czech Republic
EPFL	École Polytechnique Fédérale de Lausanne, Switzerland
FMI	Finnish Meteorological Institute, Helsinki, Finland
Gdansk Tech	Gdansk University of Technology, Gdansk, Poland
Hereon	Institute of Coastal Environmental Chemistry, Helmholtz-Zentrum Hereon, Geesthacht, Germany
HVL	Western Norway University of Applied Sciences, Bergen, Norway
IG PAS	Institute of Geophysics, Polish Academy of Sciences, Warsaw, Poland
IOPAN	Institute of Oceanology of the Polish Academy of Sciences, Sopot, Poland
IPS-CNR	Institute of Polar Sciences, National Research Council of Italy, Venice, Italy
KWU	The Kazimierz Wielki University in Bydgoszcz, Bydgoszcz, Poland
LBHI	Agricultural University of Iceland, Hvanneyri, Iceland
MU	Masaryk University, Brno, Czech Republic
NCSR 'Demokritos'	Environmental Radioactivity Laboratory, NCSR 'Demokritos', Athens, Greece
NCU	Nicolaus Copernicus University, Toruń, Poland
NILU	NILU – Norwegian Institute for Air Research, Kjeller, Norway
NMBU	Norwegian University of Life Sciences, Ås, Norway

NORCE	Norwegian Research Centre AS, Tromsø, Norway
NPI	Norwegian Polar Institute, Tromsø, Norway
NTNU	Norwegian University of Science and Technology, Trondheim, Norway
NU	Northumbria University at Newcastle, Newcastle-upon-Tyne, UK
PMOD/WRC	Physikalisch-Meteorologisches Observatorium Davos, World Radiation Center, Davos, Switzerland
SEHS	SEHS, Bern, Switzerland
TU Braunschweig	Technische Universität Braunschweig, Braunschweig, Germany
TU/e	Eindhoven University of Technology, the Netherlands
UiB	University of Bergen, Bergen, Norway
UiO	University of Oslo, Oslo, Norway
UL	École Centrale de Lyon University of Lyon, Lyon, France
UMCS	Maria Curie-Skłodowska University, Lublin, Poland
UmU	Umeå University, Umeå, Sweden
Uni Bonn	University of Bonn, Bonn, Germany
UNIPG	University of Perugia, Perugia, Italy
UNIS	University Centre in Svalbard, Longyearbyen, Norway
UNIVE	University of Venice, Venice, Italy
UoS	University of Silesia in Katowice, Katowice, Poland
UU	Uppsala University, Uppsala, Sweden
UVA	University of Valladolid, Facultad de Ciencias, Valladolid, Spain
UWR	University of Wroclaw, Wroclaw, Poland
WWU	Western Washington University, Bellingham, USA

Executive Summary

Marjolein Gevers[1], Divya David T[2], Roseline C Thakur[3], Christiane Hübner[4], Jacek Jania[5]

1 Institute of Earth Surface Dynamics, University of Lausanne, Lausanne, Switzerland
2 National Centre for Polar and Ocean Research, Goa, India
3 Institute for Atmospheric and Earth Systems Research, University of Helsinki, Helsinki, Finland
4 SIOS Knowledge Centre, Longyearbyen, Norway
5 Institute of Earth Science, University of Silesia, Katowice, Poland

The State of Environmental Science in Svalbard (SESS) reports document the current condition of the Arctic environment in and around Svalbard. The chapters highlight research conducted within the Svalbard Integrated Arctic Earth Observing System (SIOS). This contributes to a better understanding of the present status of the Arctic environment as a whole.

The chapters in this report emphasise atmospheric studies on temperature trends, show the importance of studying of dust in Svalbard, summarise two decades of columnar aerosol observations in and around Svalbard, plus 25 years of snow thickness studies. One chapter highlights the guidelines for operating Uncrewed Aerial Vehicles (UAVs) in Svalbard and is therefore relevant to researchers working within a variety of disciplines; it is an extension of the UAV Svalbard chapters in the 2020 and 2021 SESS reports.

Air temperatures are rising under a changing climate; changes for the Arctic exceed those for the globe. The Arctic warming trend is expected to strengthen in the coming decades and extend beyond the Arctic region (Rantanen et al. 2022[1]; Chylek et al. 2022[2]). The climate of the Arctic archipelago of Svalbard is very sensitive to these climatic changes. Between 1899 and 2018, Svalbard warmed 3.5 times more than the global mean air temperature (Nordli et al. 2020[3]).

Temperature measurements from several observatories in and above Svalbard are used by the authors of the first chapter, *Seasonal asymmetries and long-term trends in atmospheric and ionospheric temperatures in polar regions and their dependence on solar activity* (SATS), to study air temperature variations and their relation to solar activity. Their measurements show a trend towards higher values, less difference between summer and winter over the last decades, and an increasing seasonal asymmetry between air temperatures and season. No clear correlation was found between solar activity and air temperatures near the ground or in the lower atmosphere. However, the mesosphere and the ionosphere show a clear correlation between solar activity and air temperature.

Aerosols are an important constituent of the atmosphere, both influencing the climate system and contributing to increased pollution of the Arctic. The chapter *Long-term observations of aerosol optical depth and their relation to in-situ aerosol properties in the Svalbard region* (LOAD-RIS) shows that Arctic haze, aerosols from anthropogenic pollution at lower latitudes, has decreased significantly over the last two decades, while aerosols from biomass burning events in spring and summer have increased in number and severity.

1 Rantanen M, Karpechko AY, Lipponen A, Nordling K, Hyvärinen O, Ruosteenoja K, Vihma T, Laaksonen A (2022) The Arctic has warmed nearly four times faster than the globe since 1979. Nature Commun Earth Environ 3:168. https://doi.org/10.1038/s43247-022-00498-3

2 Chylek P, Folland C, Klett JD, Wang M, Hengartner N, Lesins G, Dubey MK (2022) Annual mean Arctic amplification 1970–2020: observed and simulated by CMIP6 climate models. Geophys Res Letters 49(13):e2022GL099371. https://doi.org/10.1029/2022GL099371

3 Nordli Ø, Wyszyński P, Gjelten H, Isaksen K, Łupikasza E, Niedźwiedź T, Przybylak R (2020) Revisiting the extended Svalbard Airport monthly temperature series, and the compiled corresponding daily series 1898–2018. Polar Res 39. https://doi.org/10.33265/polar.v39.3614

One of the aerosols conditioning the atmosphere and cryosphere in Svalbard is dust, which is produced in the lithosphere, travels in the atmosphere, can be deposited on the cryosphere and biosphere and can alter the hydrosphere. *Dust in Svalbard: local sources versus long-range transported dust* (SVALDUST) aims to summarise existing knowledge on local and long-range dust sources in Svalbard.

Harmonising environmental research and monitoring of priority pollutants and impurities in the Svalbard atmosphere (HERMOSA) shows that collecting information on many characteristics of the air may help solve some long-standing scientific problems in Svalbard, such as the origins of what floats in the air and the future of Arctic pollution in the changing world. It also links to SVALDUST by providing a rich list of analytical techniques used to characterise and quantify pollutants.

Surveys of the snow cover have been conducted in Svalbard for more than 25 years. The chapter *Ground penetrating radar measurement of snow in Svalbard - past, present, future* (SnowGPR), compiles information about the conducted GPR snow cover measurements and standards for measurements and data sharing. These measurements provide an insight on the spatial distribution of snow accumulation and its interannual variability.

As a part of a series of SESS chapters that give a comprehensive overview of research involving drones, *Practical guidelines for scientific application of uncrewed aerial vehicles in Svalbard* (UAV Svalbard 3), highlights practical issues related to planning and conducting fieldwork with Uncrewed Aerial Vehicles (UAV) in Svalbard, as well as storing and sharing drone-based datasets. The proposed practical recommendations are intended to guide scientists to become more successful in drone missions in Svalbard. This benefits the whole SIOS community as various research disciplines can make good use of these recommendations.

The authors have identified gaps and highlighted some unanswered questions in the above-mentioned critical areas of research. Concise and relevant recommendations summarise each chapter.

Furthermore, the concluding remarks by the editorial board sets the content of this years' report in the context of previous reports and reflects upon the bigger interdisciplinary picture of environmental research in Svalbard.

At the end of the report, the authors have provided answers to Frequently Asked Questions (FAQ) from the general public, as a contribution to the growing SIOS reference book for environmental science facts.

The editors would like to thank the authors for their valuable contributions to the SESS Report 2022.

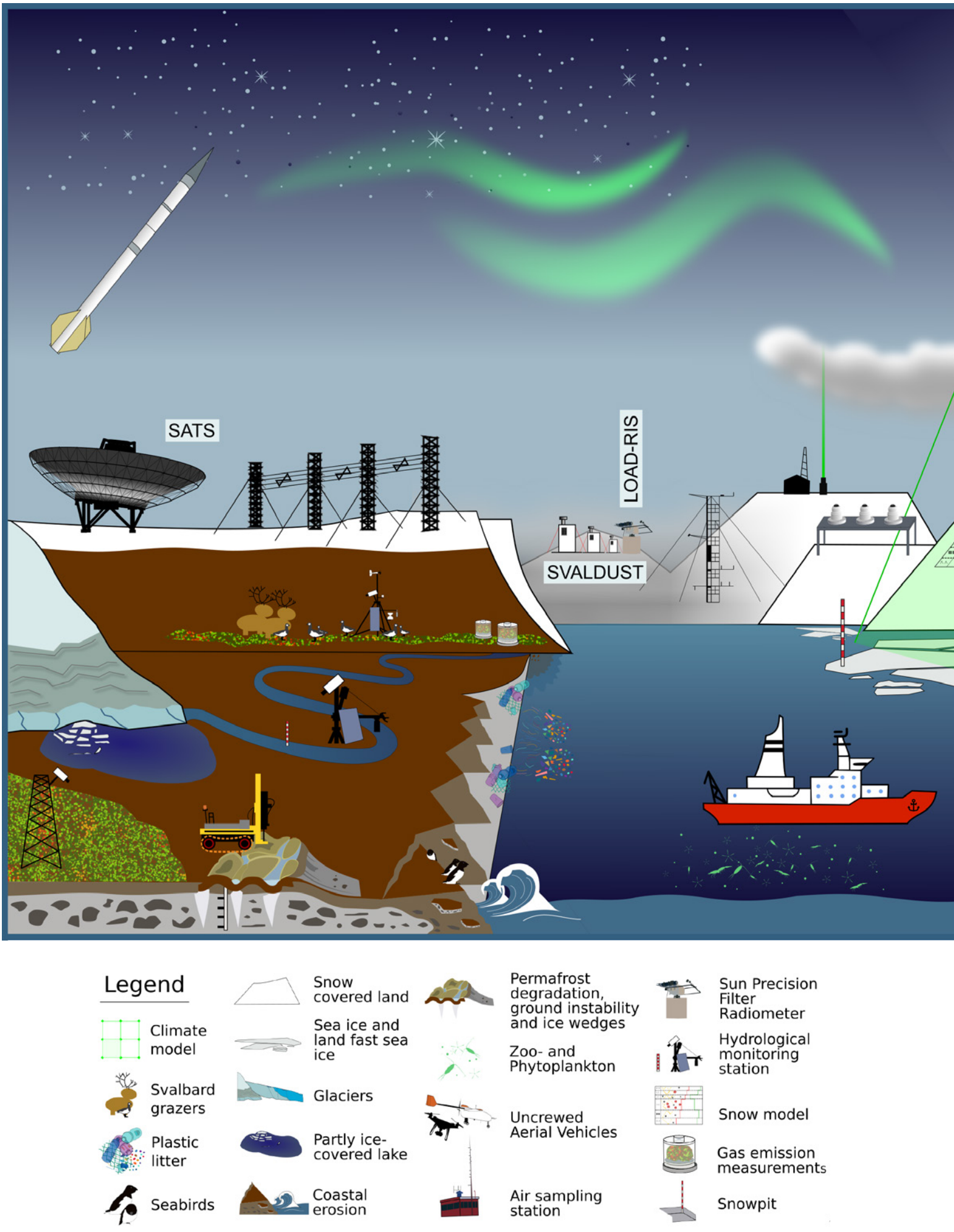
SATS
LOAD-RIS
SVALDUST
Legend
Climate model
Svalbard grazers
Plastic litter
Seabirds
Snow covered land
Sea ice and land fast sea ice
Glaciers
Partly ice-covered lake
Coastal erosion
Permafrost degradation, ground instability and ice wedges
Zoo- and Phytoplankton
Uncrewed Aerial Vehicles
Air sampling station
Sun Precision Filter Radiometer
Hydrological monitoring station
Snow model
Gas emission measurements
Snowpit

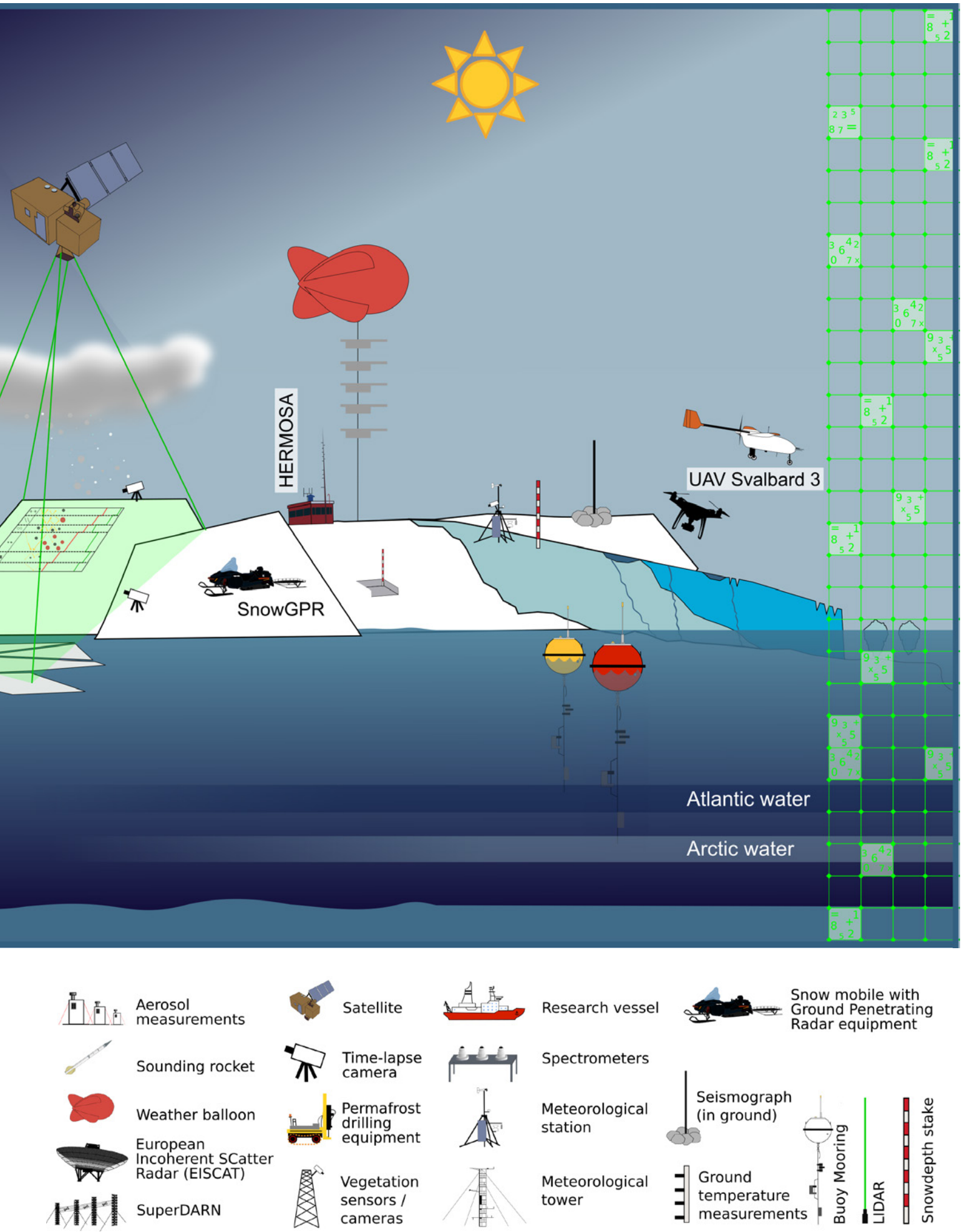

Earth system science in Svalbard as described in the SESS report series. Acronyms of the chapters in the current report are shown. (Figure: Floor van den Heuvel).

CHAPTER 1

The EISCAT radar at Breinosa, Svalbard. This radar provides profiles of ion and electron temperatures in the altitude 100-1000 km. (Photo: Christer van den Meeren, Creative Commons)

Seasonal asymmetries and long-term trends in atmospheric and ionospheric temperatures in polar regions and their dependence on solar activity (SATS)

Click here for full chapter

HIGHLIGHTS

1. On ground and in the lower atmosphere we observe a trend towards higher yearly average temperatures, and less difference between winter and summer temperatures.
2. We observe an increasing asymmetry between temperatures and season over the last decades; the day with maximum temperatures tends to occur later in the year.
3. While there is a significant phase shift between season and temperatures on ground and in the troposphere, there is little or no phase shift above the tropopause.
4. We do not find any strong relation between the temperatures on ground or in the sea and solar activity.
5. In the higher parts of the thermosphere, in particular the ionosphere, but to some extent also the mesosphere, there is a pronounced correlation between solar input energy and temperatures.

AUTHORS

S Haaland (BCSS, SEHS, UNIS)
A Radlwimmer (UNIS, Uni Bonn)
B van Schaik (TU/e, EPFL)
A Schillings (UmU)
L Bjoland (UNIS, UiB)

We have used temperature measurements from a number of observatories in and above Svalbard to study temperature variations, and their relation to solar activity. Sea temperatures from the mouth of Isfjorden, several ground stations as well as weather balloon measurements were used to study long-term trends of temperatures on ground and in the atmosphere. Radar and optical measurements were used to infer temperatures in the mesosphere and ionosphere.

RECOMMENDATIONS

- Enhance cooperation between science disciplines: space science, meteorology, oceanography and glaciology.
- Promote cross-disciplinary studies and modern data assimilation techniques like machine learning to identify couplings between processes.
- Make sure long-term measurements from space, from the atmosphere, from ground and in the sea/ice are easily available.
- Continue to promote open access to observations, and make sure measurements are well calibrated and contain sufficient metadata.

The measurements show a trend towards higher temperatures and less difference between summer and winter over the last decades. An increasing seasonal asymmetry between temperatures and season over the last decades is also observed; the day with maximum temperatures tends to occur later in the year.

Ground based temperature measurement station near Longyearbyen airport (Photo: Antonia Radlwimmer)

Ground and atmospheric temperatures were also compared to solar input energies, but no clear correlation between solar activity and temperatures on ground or in the lower atmosphere was found. We attribute the observed trends in the ground and atmospheric conditions to a combination of climate warming and local conditions such as sea currents and changes in the extension of the ice shelf.

At higher altitudes, in the mesosphere and in the ionosphere, we observe a clear correlation between solar activity and temperatures, suggesting that a significant transfer of energy from the Sun and its solar wind to the upper part of the thermosphere takes place. This coupling can be explained by electromagnetic processes and enhanced Joule heating due to collisions between neutrals and ions.

1m 'Silver' Ebert-Fastie Spectrometer mounted at the Kjell Henriksen Aurora Observatory (KHO). This instrument uses measurements of airglow to provide mesospheric temperatures from ca 90 km altitude during the dark season. (Photo: Antonia Radlwimmer)

CHAPTER 2

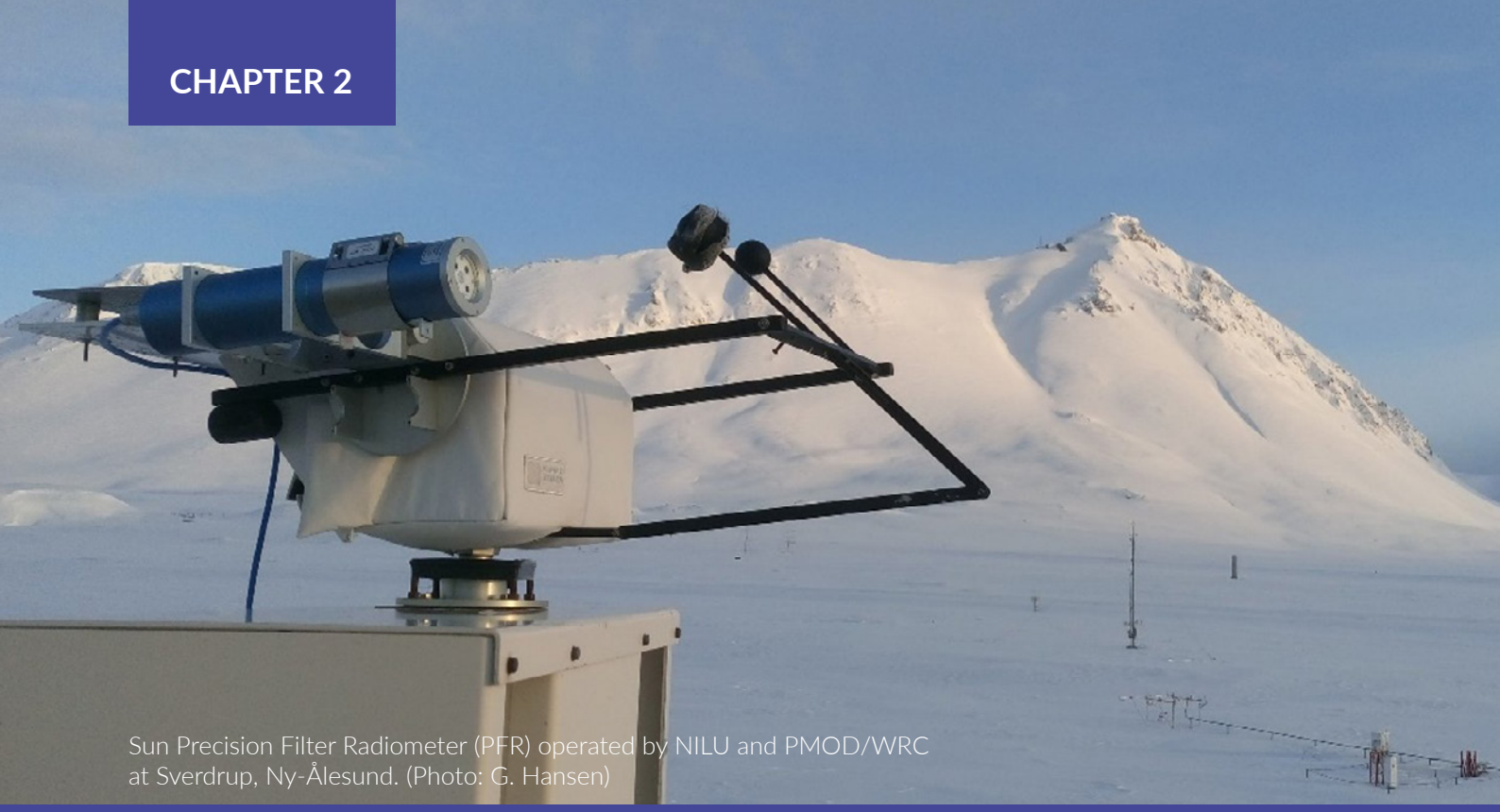

Sun Precision Filter Radiometer (PFR) operated by NILU and PMOD/WRC at Sverdrup, Ny-Ålesund. (Photo: G. Hansen)

Long-term observations of aerosol optical depth and their relation to in-situ aerosol properties in the Svalbard region (LOAD-RIS)

Click here for full chapter

HIGHLIGHTS

Aerosols are an important element of the climate system and can lead to both heating and cooling in the polar regions. In Svalbard, Arctic haze, aerosols from anthropogenic pollution at lower latitudes, has decreased significantly in the last 2 decades, while aerosols from biomass burning events in spring and summer increase in number and severity.

AUTHORS

Georg Hansen (NILU)
Natalia Kouremeti (PMOD/WRC)
Stefania Gilardoni (IPS-CNR)
Kerstin Stebel (NILU)
Nikolaos Evangeliou (NILU)
Christoph Ritter (AWI)
Tymon Zielinski (IOPAN)
Sara Herrero (UVA)
Stelios Kazadzis (PMOD/WRC)
David Mateos (UVA)
Mauro Mazzola (IPS-CNR)
Paulina Pakszys (IOPAN)
Konstantinos Eleftheriadis (NCSR 'Demokritos')

Aerosols are an important constituent of the atmosphere both influencing the climate system and contributing to increasing pollution of the Arctic. At the same time, their adequate monitoring is a big challenge, as instruments on the ground only can sample aerosols in the lowermost atmosphere. For this reason, these measurements are complemented with observations of aerosol optical depth (AOD) which quantify the total amount of aerosols throughout the atmosphere from the attenuation of direct sunlight (and moonlight). This procedure requires extremely careful instrument calibration and removal of cloud contaminated data. In Svalbard, such measurements have been performed by several research groups with different instruments, mostly in Ny-Ålesund and in Hornsund, but also on research vessels offshore. In the framework of the SSF Strategic Grant project ReHearsol, all AOD data from the Svalbard region since 2002 have been collected and made available to the SIOS research

community. They indicate that number and intensity of Arctic haze episodes occurring in late winter and spring have decreased consistently and significantly in the two decades, while pollution events in summer/early autumn, caused by boreal biomass burning, are on the rise, though not as consistently. Comparison between in-situ measurements at Gruvebadet Atmosphere Laboratory in Ny-Ålesund and AOD measurements indicate that most (more than 65%) of the episodes with high aerosol load are not captured by surface measurements. This finding does not change when one includes in-situ measurements at Zeppelin Observatory (475 m a.s.l.). Studying extensive high-AOD episodes such as those in summer 2019 requires a multi-tool approach including in-situ and remote-sensing measurements combined with model tools.

RECOMMENDATIONS

- Sun AOD measurements should continue at both Hornsund and Ny-Ålesund as at present, while a third station in eastern Svalbard connected to a meteorological station should be considered.
- An observation capacity for in-situ aerosol measurements on board a mobile platform (uncrewed autonomous vehicle, aircraft) to be used during periods of elevated AOD measurements should be developed.
- More emphasis should be put on collecting data during the polar night, possibly through the establishment of a star photometer and further development of lunar AOD observations.

View from Zeppelin Observatory to Ny-Ålesund and Kongsfjorden during the high-pollution episode in April/May 2006. (Photo: Webcam Zeppelin Observatory)

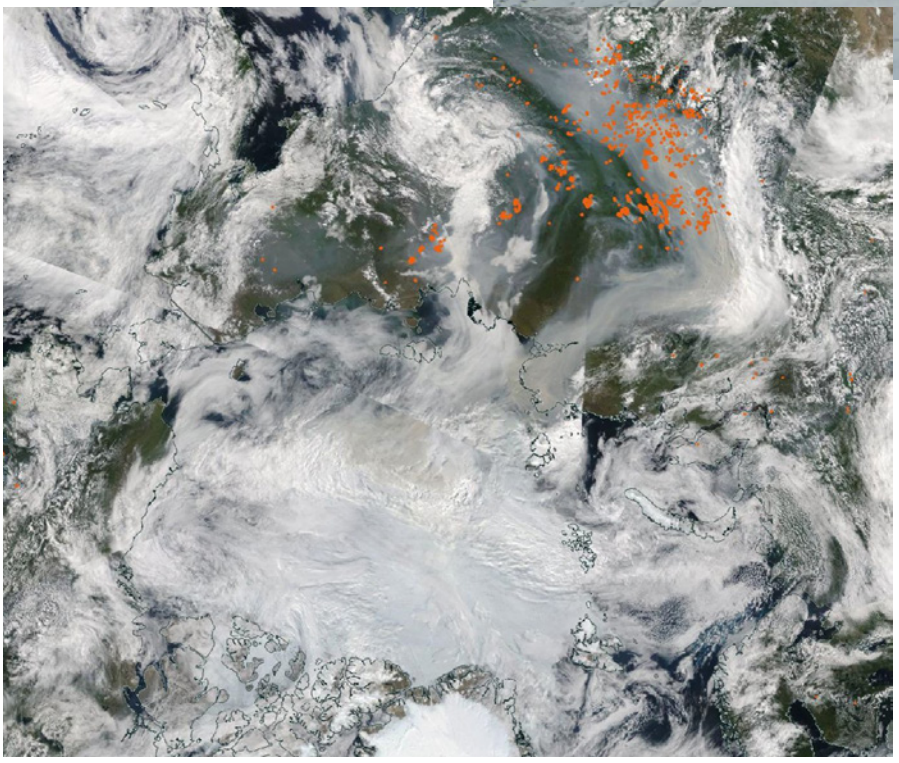

Satellite image of the Arctic (Aqua/MODIS, corrected true reflectance) on 10 August 2019. Greenland is at the lower edge in the centre, Svalbard to the right of Greenland, and Siberia in the upper half of the image. Red dots: forest fires in central and eastern Siberia, releasing large plumes of smoke spreading towards the North Pole. The image is produced by NASA's EOSDIS Worldview tool.

CHAPTER 3

Mine 7 near Longyearbyen (Breinosa mountain). Note the dark coal dust deposits on surface snow. (Photo: Alia Khan)

Dust in Svalbard: local sources versus long-range transported dust (SVALDUST)

Click here for full chapter

HIGHLIGHTS

- Dust has an impact on both the atmosphere and the cryosphere in Svalbard.
- In the Svalbard archipelago, dust can have both local and long-range sources.
- Dust can lower snow albedo and trigger a melting feedback.

AUTHORS

Biagio Di Mauro (ISP-CNR)
David Cappelletti (ISP-CNR, UNIPG)
Beatrice Moroni (UNIPG)
Mauro Mazzola (ISP-CNR)
Stefania Gilardoni (ISP-CNR)
Bartłomiej Luks (IG PAS)
Adam Nawrot (IG PAS)
Marek Lewandowski (IG PAS)
Pavla Dagsson Waldhauserova (LBHI, CZU)
Outi Meinander (FMI)
Monika Wittmann (Independent)
Susan Kaspari (CWU)
Alia Khan (WWU)

Dust consists of fine and coarse particles that travel in the atmosphere and are deposited on the Earth's surface. Dust particles deposited on snow and ice can cause snow darkening and contribute to melting. In this chapter, we summarise existing knowledge on local and long-range dust sources in Svalbard, and describe current methodologies for studying dust from both an observational and modelling perspective. Dust science in Svalbard is still in its infancy; future research will help to disentangle the complex role of dust in the Svalbard environment.

Coal and other local dust from melted snow samples collected in Adventdalen. (Photo: Alia Khan)

Sampling sites locations described in the SVALDUST chapter. 1 – Woodfjorden; 2 – Gruvebadet; 3-7 – Ny-Ålesund; 8 – Pyramiden; 9 – Breinosa; 10-11 – Recherchebreen; 12-13 – Storbreen; 14-15 – Hornbreen; 16-21 – Werenskioldbreen; 22 – Hansbreen; 23 – Ariekammen. Coordinate Reference System: WGS84 / UTM 33N. Map made based on the NPI S100 Topographic Raster Data for Svalbard. © Norwegian Polar Institute. (Maps by: Adam Nawrot)

RECOMMENDATIONS

We propose following recommendations for future dust research in Svalbard:

- Identify and characterise dust sources in Svalbard.
- Systemise the observation and remote detection of dust emission/uplift and dust storm events on Svalbard by means of adequate monitoring systems.
- Investigate the influence of local sources in the lower troposphere and long-range transport at higher altitudes by continuous measurements and devoted campaigns.
- Establish an inventory of the long-range dust sources by source profiling in order to cooperate with the modellers for the quantification of the dust load from different sources.
- Attribute the role of dust, black carbon and living organisms (e.g. algae) to snow albedo reductions and melt.

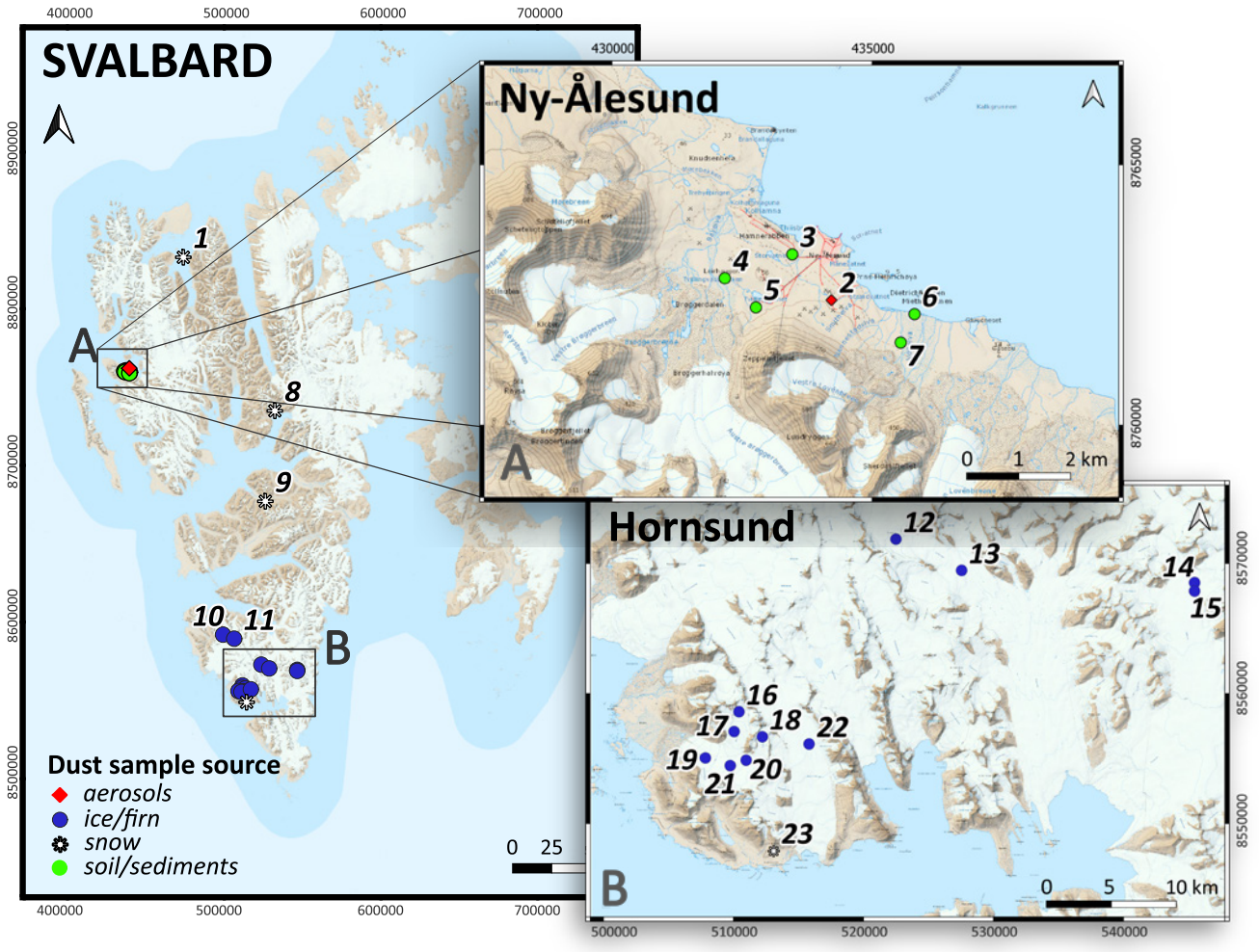

CHAPTER 4

For air sampling for microorganisms, a number of instruments are available. Key requirements for research are: a) a filter size which captures bacteria, b) relatively high flow through the instrument to study DNA, c) the ability of the instrument to cope with the Arctic environment, d) a convenient power source (e.g. a battery) and e) best if there are other users in the scientific world. The sampler in this photo, the SAS (Surface Air System) Air Sampler, meets all these requirements. Here it is seen mounted aboard a ship. (Photo: David Pearce)

Harmonising environmental research and monitoring of priority pollutants and impurities in the Svalbard atmosphere (HERMOSA)

Click here for full chapter

HIGHLIGHTS

- Air impurities, from sulphur to pollen, were measured in Svalbard already before 1980s.
- Air quality monitoring is spatially uneven – the Ny-Ålesund hub needs to be supported by other regular sites.
- Methods of impurity measurement show similarities which can be exploited for better problem solving.

AUTHORS

Krystyna Koziol (KWU, Gdansk Tech)
Roland Kallenborn (UNIS, NMBU)
Zhiyong Xie (Hereon)
Catherine Larose (UL, 4S)
Andrea Spolaor (ISP-CNR)
Elena Barbaro (UNIVE)
Jan Kavan (UWR, MU, 4S)
Daniel Kępski (IG PAS)
Anna Nikulina
Krzysztof Zawierucha (AMU)
David Pearce (NU, BAS)
Luke Cockerton (NU)
Adam Nawrot (IG PAS, 4S)
Filip Pawlak (Gdansk Tech)
Paulina Pakszys (IOPAN)
David Cappelletti (UNIPG)

Many characteristics of atmospheric air are measured in Svalbard, including levels of chemical pollution, dark dust connected to soot, and living organisms, but most of these studies happen in Ny-Ålesund. Air monitoring was initiated as early as the 1970s, and multiple atmospheric components have been added to the monitoring over time (especially since 2010; in the early 2000s a few parameters measured at Hornsund joined the regular programme). New types of contaminants are being discovered and

measured in Svalbard. Methods for detecting simpler substances and particles have been established for a long time, while certain complex chemicals and small living organisms are more difficult to capture and study. Laboratory and field equipment upgrades help improve understanding of the Svalbard environment. In this chapter, we find that collecting information on many characteristics of the air at the same time helps solve long-standing scientific questions in Svalbard, such as the origins of pollution in the Arctic air and the future of the Arctic atmosphere in a changing world. This is especially important since the Arctic is changing fast, both due to global warming and to the shift in local people's activity from mining to services, e.g. tourism.

RECOMMENDATIONS

- Researchers should agree on important parameters of the atmospheric composition to be measured in at least three places across Svalbard (we propose Ny-Ålesund, Longyearbyen and Hornsund as site, and black carbon (soot), the greenhouse gas methane, inorganic ions, pollen and novel organic chemicals as parameters).
- Change over time (between seasons and years) of a few such parameters should be measured simultaneously to better study the influence of human activity and climate change. This would be easier to study in the future if organic chemical analyses were saved for future searches for novel chemicals (that is, if an electronic sample bank was founded).
- Ny-Ålesund is the best place to study how such parameters change between sea level and mountaintops, but the effects of altitude should be tested in other places too, with shorter experiments. Methods at various locations need to be harmonised and laboratories compared for robust results.

The environmental chamber of the Polish Polar Station in Hornsund also has a few instruments sampling the air on its roof. Regular measurements of aerosol in Hornsund started in 2002. (Photo: Krystyna Koziol)

A collection of instruments monitoring air composition (and pollution) atop Gruvebadet Atmosphere Laboratory roof in Ny-Ålesund. Ny-Ålesund is the main place in Svalbard for air monitoring, with two main sites – Gruvebadet near sea level and Zeppelin Observatory near the mountain top. (Photo: Marco Casula)

CHAPTER 5

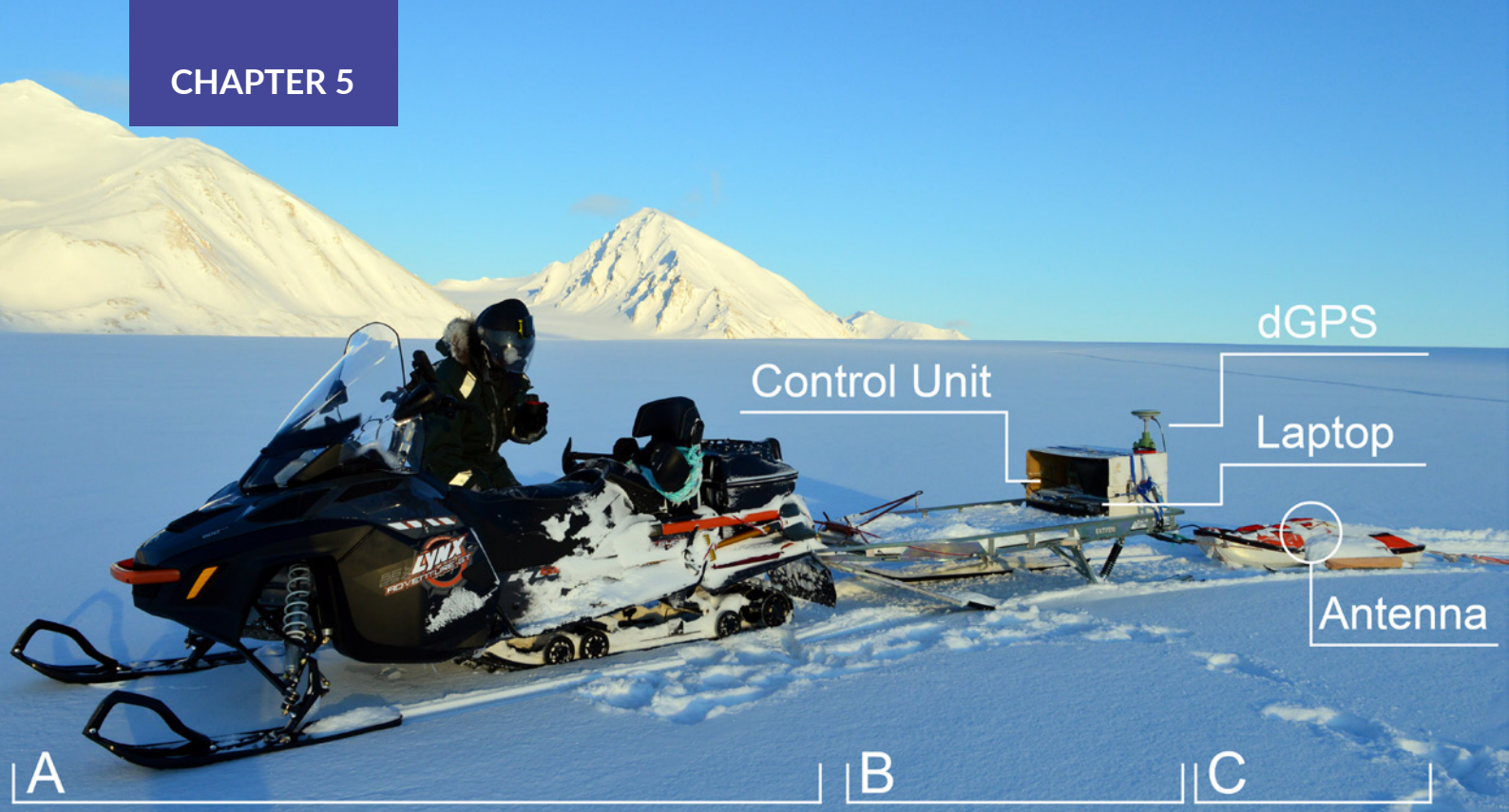

Example of the GPR system configuration: A – snowmobile with navigator, B – sledge with GPR operator, C – pulkas with antenna(s) in a waterproof cover (Photo: Mariusz Grabiec)

Ground penetrating radar measurement of snow in Svalbard – past, present, future (SnowGPR)

Click here for full chapter

HIGHLIGHTS

- Snow thickness surveys by ground penetrating radar (GPR) have been conducted in Svalbard for over 25 years, thus permitting assessment of long-term changes.
- More than 5000 km of GPR profiles have been collected in Svalbard.
- Standards for the metadata of the GPR snow measurements have been proposed.

AUTHORS

D Ignatiuk (UoS)
T Dunse (HVL)
J-C Gallet (NPI)
L Girod (UiO)
M Grabiec (UoS)
D Kępski (IG PAS)
J Kohler (NPI)
M Laska (UoS)
B Luks (IG PAS)
W van Pelt (UU)
R Pettersson (UU)
V Pohjola (UU)
TV Schuler (UiO)

Snowpack covers 60-100% of all land in Svalbard, depending on the season, and it is very sensitive to changes in climate. Knowledge about the snowpack is important not just in itself, but also to understand how snow cover affects other components of Svalbard's natural environment – land, sea, permafrost, glaciers, and the ecosystems that they support. Monitoring the evolution of Svalbard's snow cover will be crucial as the world's climate continues to warm.

Ground-penetrating radars (GPRs) towed by snowmobile across glaciers and snowfields provide vital information about snowpack thickness and structure. Ideally, such surveys should be repeated annually for continuous monitoring of climate-induced change. Three decades ago, a GPR programme catalogued regional variations in snow accumulation. This should be repeated and expanded to cover all of Svalbard. The GPR method

should also be further developed e.g. by mounting GPRs on drones, giving access to parts of glaciers that are too dangerous for researchers to visit. Lastly, women are encouraged to join the field of GPR-based research on snow.

Most of the GPR data collected so far are not currently available in any data repository. The comprehensive compilation of available studies presented in this report, and the recommendations for metadata and data quality, are important first steps to making GPR data more accessible.

RECOMMENDATIONS

- Repeated measurements in successive years should be made along the same tracks whenever safety conditions allow.
- GPR results should be validated with data from snow pits (snow depth, stratigraphy, snow water equivalent (SWE)) or shallow coring (snow depth, SWE).
- The shared GPR data should be accompanied by a full metadata description as proposed in this report.
- UAVs should be adapted to perform autonomous GPR measurements of snow cover.
- The programme conducted in the late 1990s to chart regional variations of snow accumulation in W–E and N–S transects should be repeated for all of Svalbard.

GPR measurements during a blizzard, Hansbreen (Photo:Dariusz Ignatiuk)

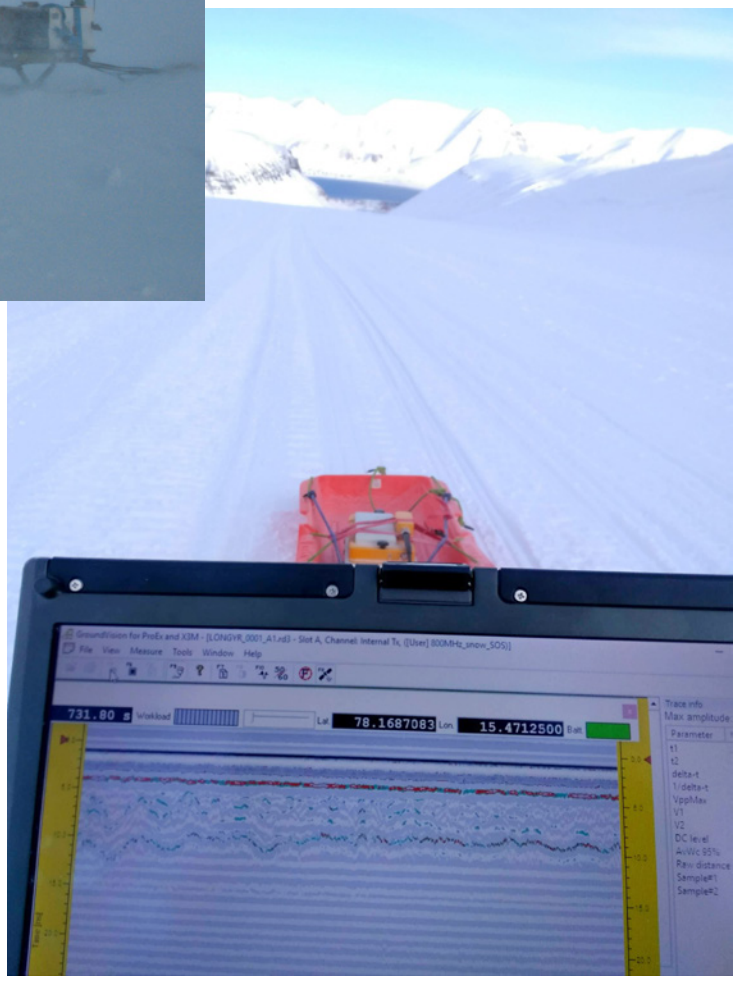

GPR measurements on Longyearbreen for the SIOS Access Project in 2018. The screen shows a raw, unprocessed radarogram recorded in real time. Reflections of horizons in the snow cover at the snow/firn/ice border can be seen. (Photo: Bartłomiej Luks)

CHAPTER 6

Off-the-shelf commercial drone in Adventdalen (Photo: Richard Hann)

Practical guidelines for scientific application of uncrewed aerial vehicles in Svalbard (UAV Svalbard 3)

Click here for full chapter

HIGHLIGHTS

1. Recommendations for data storage and data accessibility for drone-based data.
2. Framework for planning drone-based fieldwork in Svalbard.
3. Practical guidelines and recommendations for conducting fieldwork in Svalbard.
4. Recommendations on how to strengthen and expand scientific drone applications in Svalbard.

AUTHORS

R Hann (NTNU)
P Betlem (UNIS, UiO)
K Deja (IOPAN)
M Ewertowski (AMU)
B Harm-Altstädter (TU Braunschweig)
M Jonassen (UNIS)
A Lampert (TU Braunschweig)
M Laska (UoS)
I Sobota (NCU)
R Storvold (NORCE)
A Tomczyk (AMU)
P Zaorski (UMCS)

Uncrewed aerial vehicles (UAVs), or drones, have become an established tool for a wide range of scientific applications. Today, UAVs are used for example for mapping geomorphic features, glaciers, and heritage sites, counting reindeer, atmospheric measurements, sea ice monitoring and in many other ways.

However, the technology is still relatively new and there is a substantial untapped potential for using UAVs for scientific goals. This report's main focus is to highlight practical issues related to planning and conducting fieldwork in Svalbard, as well as storing and sharing drone-based datasets. One of the key challenges in the field is related to a lack of standardised data storage and metadata requirements. This means that many datasets are not adequately described and/or archived so they are publicly available This means that drone-based data can often not be reused, for example for long-term monitoring studies. The practical

recommendations about planning and conducting fieldwork with UAVs in Svalbard is intended to help and guide scientists to become more successful in conducting drone missions. Svalbard has several special challenges related to its remoteness, high latitude, and fauna.

Recommendations are given on how SIOS can strengthen and expand scientific drone applications in Svalbard. The recommendations are intended to make it easier to conduct more complex missions in Svalbard and to train and fund new users. Furthermore, it is recommended to create a forum for scientists to discuss drone-related issues, e.g. to develop community standards for data.

RECOMMENDATIONS

1. Efforts to lower barriers for advanced and complex operations with drones in Svalbard.
2. Develop community standards for data storage and data accessibility for drone-based data.
3. Develop and provide an interdisciplinary forum for scientific drone users in Svalbard.
4. Provide training and funding for basic and advanced scientific drone missions in Svalbard.

Off-the-shelf commercial drone in Adventdalen (Photo: Richard Hann)

Fixed-wing UAV operations in Ny-Ålesund (Photo: Alexander Peuker)

Seasonal asymmetries and long-term trends in atmospheric and ionospheric temperatures in polar regions and their dependence on solar activity (SATS)

Stein Haaland[1,2,3], Antonia Radlwimmer[3,4], Brandon van Schaik[5,6], Audrey Schillings[7], Lindis Bjoland[3,8]

1 Birkeland Centre for Space Science, Bergen, Norway
2 SEHS, Bern, Switzerland
3 The University Centre in Svalbard, Longyearbyen, Svalbard
4 University of Bonn, Bonn, Germany
5 Eindhoven University of Technology, Eindhoven, the Netherlands
6 École Polytechnique Fédérale de Lausanne, Lausanne, Switzerland
7 Department of Physics, Umeå University, Umeå, Sweden
8 Space Plasma Physics Group, University of Bergen, Bergen, Norway

Corresponding author: Stein Haaland, Stein.Haaland@uib.no
ORCID number: 0000-0002-1241-7570

Keywords: Temperatures, seasonal asymmetry, atmosphere, mesosphere, ionosphere, solar activity

DOI: https://doi.org/10.5281/zenodo.7371477

1. Introduction

Solar radiation is fundamental for all life on Earth. Radiation in the infrared and visible part of the solar spectrum is more or less constant over time. In the ultraviolet (UV) range, and in particular in the extreme ultraviolet (EUV) range, however, there are significant variations, which largely follow the solar cycle with its 11-year period. This UV radiation ionises parts of the upper atmosphere, and an electrically conductive layer – the ionosphere – is formed at a height of 100-300 km. Since UV radiation only constitutes a small fraction of the total radiation, the total variation in solar irradiance, and thus the variation in radiation energy from the Sun is only about 0.1% over the solar cycle (Coddington et al. 2019).

Around vernal and autumnal equinoxes, the incoming solar radiation is nearly identical for both hemispheres. The local temperature at a given altitude, however, is strongly influenced by local conditions. Landmasses (including glaciers) and water (sea) have large heat capacities, and energy transport in the form of wind and ocean currents cause large local variations on different timescales. Still, it is usually much warmer, in the sea, on land, and in the atmosphere during autumnal equinox than vernal equinox: there is a seasonal asymmetry in temperatures on ground.

Such seasonal asymmetries are strongest at high latitudes. In Svalbard, average temperatures around vernal equinox (March) can be as much as 15 degrees lower than at autumnal (September) equinox, and the yearly maximum temperature typically occurs almost 50 days after solstice as illustrated in Figure 1. At higher altitudes in the atmosphere, where the heat capacity of land or sea is less important, the seasonal asymmetry is expected to be smaller.

Somewhat surprisingly, similar seasonal asymmetries in temperatures have also been detected in space. Specifically, plasma temperatures inferred from EISCAT Svalbard radar measurements and observations from satellite measurements in the high latitude ionosphere at 200-400 km altitudes have shown such asymmetries (Aruliah et al. 1996; Hatch et al. 2020). There are also indications that such asymmetries exist in the magnetosphere (Haaland et al. 2017).

In space, electromagnetic forces play a key role for the temperature and motion of gases. Much of the dynamics, including transport and heating, is driven by the interaction between the solar wind and the Earth's magnetic field. In particular, solar activity and the orientation of the interplanetary magnetic field play crucial roles. Measurements from satellites (Förster et al. 2008) indicate that the motion of plasma in space also influences the neutral atmosphere, and sets up circulation and redistribution of energy in the upper atmosphere. This effect is most pronounced at high latitudes where the magnetic field is directly coupled to the interplanetary space.

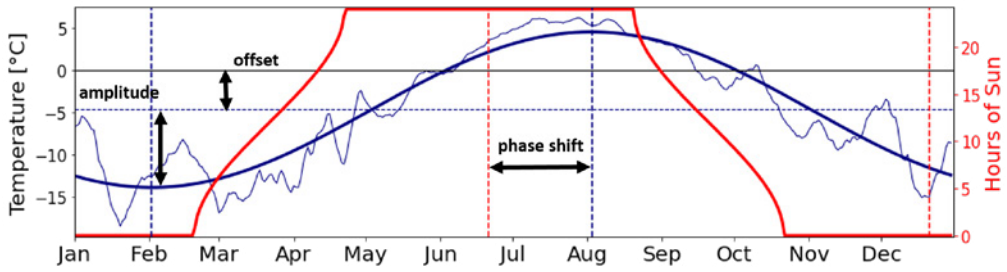

Figure 1: Illustration of temperature asymmetry at Ny-Ålesund airport. The ragged blue line shows the daily median temperature (smoothed with a 7-day rolling window) as a function of season based on daily averages between 2000 and 2002. The solid blue curve is a model fit to the measurements, using a simple sinusoidal variation as the model. The red curve shows the corresponding number of daylight hours. We quantify the seasonal asymmetry as the **phase shift** (in number of days) between solar illumination maximum (at solstice) and the maximum temperature of the fitted curve (early August). **Amplitude** is defined as the difference between lowest and highest temperatures of the model fit, and **offset** is the difference between the yearly average model temperature and 0°C.

Conversely, transport of neutral material due to thermal effects may also affect plasma motions in the ionosphere and even the magnetosphere. Since the atmosphere is the prime supplier of plasma to the magnetosphere (through a process called ionospheric outflow), the seasonal asymmetry can have a profound effect on supply of plasma to the magnetosphere, and thus space weather phenomena such as geomagnetic substorms and auroral activity. This cross-coupling between the atmosphere and space is still poorly understood, partly because it spans two science disciplines: space science and atmospheric science.

In this report, we have used measurements from a number of observations in and above Svalbard (see Figure 2) to study how the temperature asymmetry varies with altitude, and whether this asymmetry has changed over time. We also investigated whether a relation (possibly cause/effect) exists between solar activity and temperatures in the sea, on ground, and in the atmosphere.

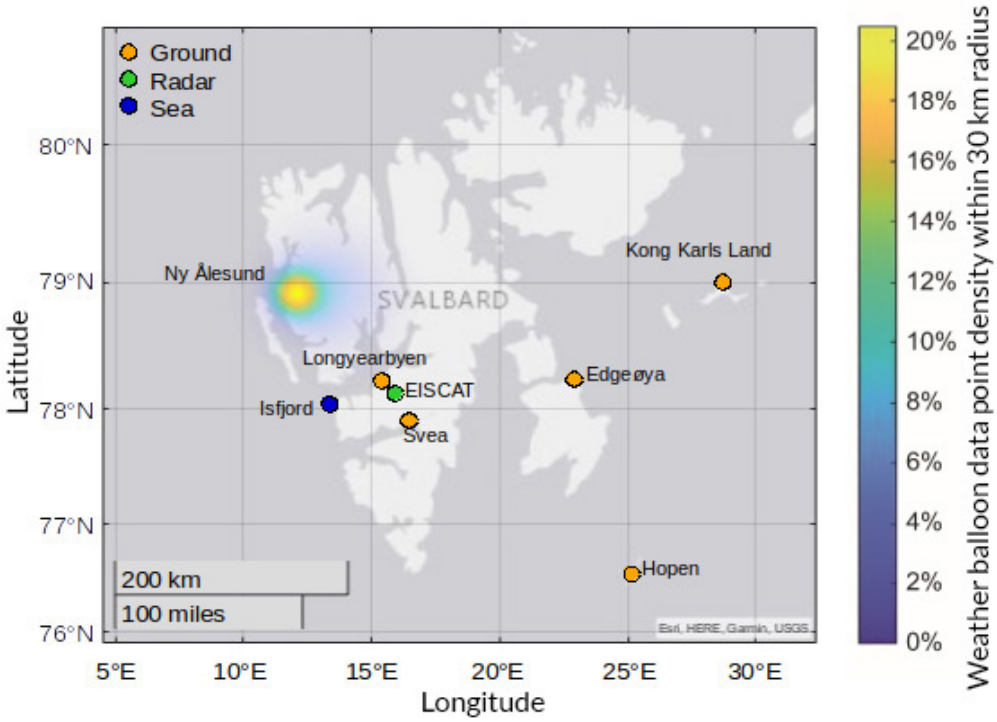

Figure 2: Map of ground stations with temperature measurements (yellow circles), the EISCAT Svalbard radar (green) and the mouth of Isfjorden where sea temperatures have been measured (blue). Balloon measurements are obtained from Ny-Ålesund, and the horizontal spread of the balloons as they rise is indicated as a colour-coded cloud.

2. Data and methodology

Tables 1 and 2 and the map in Figure 2 provide an overview of observatories, their location and availability of data used for this study. In the following subsections we briefly describe the data sources and methodology used.

A note about temperatures and units: traditionally, temperatures are given either as absolute temperatures in units of Kelvin – hereafter denoted [K], or in degrees Celsius [°C]. The freezing point of water (0°C) is equivalent to 273.15 K, with a temperature difference of 1°C equivalent to a difference of 1 K, meaning the unit size in each scale is the same.

2.1. Svalbard Sea temperatures

For the present study, we had access to a limited set of measurements of ocean temperatures obtained from buoys deployed at various depths from ships

near the mouth of Isfjorden (Skogseth et al. 2020). Measurements exist for the period September 2005 until August 2018, but with intermittent data gaps. Notably, there are no data between February 2008 and August 2010.

Table 1: List of observatories, their geographic location and elevation, time of operation and data availability.

Station	Lat [°]	Lon [°]	Alt [m]	Time period	Number of records	Tavg
Isfjord mouth	78.06	13.52	≥ -210	2005-09-16 - 2021-10-08	95969	3.0 °C
Hopen (HOP)	76.51	25.01	6	1970-01-01 - 2022-05-04	19098	-1.9 °C
Ny-Ålesund (NAL)	78.92	11.89	8	1974-08-01 - 2022-06-16	17146	-3.5 °C
Longyearbyen Airport (LYR)	78.24	15.49	9	1975-08-01 - 2022-06-16	17037	-3.1 °C
Svea (SVE)	77.89	17.72	9	1978-05-01 - 2022-05-04	15422	-3.8 °C
Edgeøya (EDG)	78.25	22.81	14	2006-01-11 - 2022-06-16	4797	-3.7 °C
Kong Karl VII øya (KXI)	78.92	28.72	5	2006-03-02 - 2022-06-13	3111	-3.1 °C
Mesosphere (nightglow)	78.15	16.04	ca 90km	1980-12-08 - 2022-02-27	2198	207.3 K **(1)**
Mesosphere (radar)	78.17	16.00	ca 90km	2001-10-16 - 2022-06-12	6679	181.1 K **(2)**
EISCAT Svalbard	78.09	16.03	**(3)**	1999-12-01 - 2021-03-23	4837	486.0 K

(1) During the dark season only, thus different averages from radar (2) measurements, from which measurements are available throughout the year. (3) EISCAT provides height profiles of plasma parameters. Depending on programme, the range can be from 100 to 1200 km. See Section 2.5 for more details.

2.2. Ground based temperatures

For near surface atmospheric temperatures, we find a wealth of observations in the region, dating back several decades. The stations chosen for this study are maintained by the Norwegian Meteorological Institute and listed in Table 1. Each station is presently equipped with a PT100 temperature sensor (standard for all MET Norway stations), succeeding manual readings taken for 2000 sec every 6 hours. As our research interest lies with seasonal patterns and long-time trends, daily means provide sufficient temporal resolution. Where possible, these means are given as the arithmetic mean of 24-hourly observations. However, before the early 21st century hourly observations are often unavailable. Here, the mean is taken from fewer, manual daily readings. The temperatures are measured at a default height of 2 m above ground.

All near surface atmospheric temperature data used in this study are taken from MET Norway's services. We downloaded the daily mean air temperatures directly from the Norwegian Centre for Climate Services[1].

2.3. Atmospheric weather balloon data

The temperature of the atmosphere can be directly measured with fast-response temperature sensors

1 https://seklima.met.no/

on weather balloons. The Norwegian Meteorological Institute and Alfred Wegner Institute have been collecting empirical temperature data from the lower atmosphere (0-40 km) at Ny-Ålesund on a daily basis since 1 January 1993. From this location, weather balloons are launched in fixed time frames, 09:00, 12:00 and 16:00 UTC, and the balloons rise with a rate of approximately 5 m/s.

We have calculated aggregate values at various pressure levels (isobars) as shown in Table 2. Since the pressure varies exponentially, and the height ranges are given in metres, the number of samples varies greatly between the isobars.

Since the weather balloon data are intermittent in time, microwave radiometer measurements from Ny-Ålesund, collected since January 2018 by the German Meteorological Institute, are used to identify daily fluctuations in temperatures. This analysis shows that the daily fluctuations are negligible with respect to temperature variations that are observed at altitude. Therefore, the time of day is disregarded and all data points can be averaged on a daily basis without correction.

Moreover, weather balloon data tends to vary in location during flight due to horizontal motion caused by winds. In Figure 2, the data point density of the weather balloon data is plotted as a heat map over Svalbard. Since the majority of data are taken within 15 km of the launch site, we disregard the effects of horizontal motion.

Table 2: Aggregate values from weather balloon observations from Ny-Ålesund (78.92 N, 11.89 E) at 11 different pressure heights between ground (pressure level 1000) to the upper stratosphere (pressure level below 100 hPa).

Pressure level [hPa]	Average height [m]	Number of records	Tavg [°C]
1000	75	54507	-2.4
900 - 1000	500	527903	-5.2
800 - 900	1,375	735815	-9.8
700 - 800	2,325	651119	-13.9
600 - 700	3,400	724818	-19.7
500 - 600	4,625	833663	-27.3
400 - 500	6,050	975353	-36.8
300 - 400	7,775	1205420	-48.1
200 - 300	9,873	1566151	-53.5
100 - 200	13,550	2531448	-51.8
0 - 100	22,900	7156433	-52.6

2.4. Mesospheric temperatures

We have used two different data sets for the temperatures near the mesopause. The first data set contains data from 1980 and estimates mesospheric temperatures from the spectral emissions of the excited hydroxyl (OH*), commonly called nightglow.

Hydroxyl emissions are taken at approximately 90 km altitude for an area of approximately 9 km to 12 km, using a Ebert-Fastie spectrometer currently located at the KHO, Longyearbyen (Sigernes et al. 2003). Until 2007, the spectrometer was located at the auroral station in Adventdalen. At high latitude, the nighttime OH* layer is directly proportional to the atomic oxygen concentration (Grygalashvyly 2015), thus we observe the OH* layer with the lowest altitudes and highest number densities during the winter.

The second data set consists of temperatures derived from daily echoes caused by ablation of meteors in the mesosphere (Hocking et al. 1997) using he Nippon/Norway Svalbard Meteor Radar, located in Adventdalen (Hall et al. 2002). This technique uses the ambipolar diffusion coefficient from the plasma trail formed by a meteor while

entering the atmosphere. Unlike the nightglow technique, radar measurements are available throughout the year. Measurements are available since 2001.

Both data sets, calculations and instrumentation are well described in Holmen (2016), and we refer to this thesis for details. Mesospheric temperature derivations are subject to larger uncertainties than ground-based or balloon-based temperatures. Still, these derived temperatures provide information in an altitude range too high for weather balloons and below the altitude of satellites.

2.5. Ionospheric temperatures

The European Incoherent SCatter Radar (EISCAT) in Svalbard (Folkestad et al. 1983; Maeda et al. 2002) provides height profiles of plasma temperatures (electron and ion temperatures) from approximately 100 km to ca 1000 km altitude depending on the experiment. Below ca 300 km, the ion temperature can be used as an approximation for the neutral temperature (Brekke 1993).

Note that EISCAT does not provide continuous data; measurements are typically taken during campaigns. The best data coverage was obtained during the international geophysical year (2007-2008). In this study, we use a specially prepared data set consisting of daily EISCAT temperatures from the fixed direction 42 m antenna for local noon.

2.6. Solar activity and solar wind input energy

To investigate correlations and possible cause/effects between temperatures and solar conditions, we looked at two different parameters: solar illumination and solar wind electromagnetic energy coupling.

As a proxy for solar UV illumination and solar activity, we use the F10.7 index. This is a measure of the radio emissions at 10.7 cm wavelength, and has been measured every day at local noon at the Dominion Radio Astrophysical Observatory (DRAO) in Penticton, Canada, since 1947. It correlates well with sunspot numbers, and is often referred to when discussing solar activity; a high F10.7 index means high solar activity.

Additionally, we estimated the solar energy input (similar to Poynting flux) to the Earth's magnetosphere derived from the solar wind parameters. This is the amount of electromagnetic energy transferred from the solar wind into the Earth's magnetosphere. Based on the original Vasyliunas formula (Vasyliunas et al. 1982), a later paper by Tenfjord and Østgaard (2013) proposed the following formula to quantify solar wind electromagnetic energy input for long time series:

$$P_{input}[W] = \frac{M_A \cdot V_{SW,x} \cdot B_T^2}{\mu_0} \cdot \sin\left(\frac{\theta}{2}\right)^4 \frac{167}{5 \cdot 10^{22} |B_z|^3 + 1} R_E^2 \quad (1)$$

where M_A is the solar wind Alfvèn Mach number, $\mu_0 = 4\pi \times 10^{-7}$ [kg m A^{-2} s^{-2}] the vacuum permeability, $V_{SW,x}$ [m s^{-1}] the solar wind velocity, $B_T = \sqrt{B_Y^2 + B_Z^2}$ [T] the transverse component of the interplanetary magnetic field (IMF), θ [rad] the clock angle and $\frac{167}{5 \cdot 10^{22} |B_z|^3 + 1} R_E^2$ is the effective area in which the solar wind interacts with the Earth's magnetosphere (R_E = Earth radius = 6371 km).

2.7. Estimation of seasonal asymmetry

In order to coherently quantify the seasonal temperature asymmetries at all altitudes, a relative measure of the seasonal temperature cycle is needed. Hence, where data availability allowed, a sinusoidal model was fitted to the observations as follows:

$$T = A \cdot sin\left(\frac{2\pi}{365.242} \cdot (t - 81) - B\right) + C \quad (2)$$

where $T = T(t)$ is the temperature [K] as a function of time, with fit parameters **A the amplitude** [K], **B the phase shift** [days] and **C the temperature offset** [K] (see Figure 1). These fit parameters are used in the following as proxy for the characteristics of the annual temperature cycle. Note that the fitted sinusoidal model has a period of 365.242 days and that the ascending node through equilibrium position is set to the 81st day of the year. The 81st day of the year, somewhat unintuitively, does

not correspond to spring equinox. Instead, it was chosen for its position halfway between winter and summer solstice, which, as summer on the northern hemisphere is nine days longer than winter, is two days after spring equinox. The fitted phase shift can thus be thought of as spring time phase shift.

In the following, the fit is used on a five-year moving window, shifting by one year for each time step of the analysis. Thus, the fit parameters associated to a specific year resemble the parameters of the fit of five years, with the year in question at the centre. Five years was chosen to smooth out the more extreme fluctuations in any one year's seasonal cycle.

2.8. Caveats, statistical spreads and uncertainties in measurements and methodology

As with any collection of experimental data, there are uncertainties related to both measurements, methodology and the underlying assumptions. In terms of measurement accuracy, in-situ measurements (e.g. sea, ground, balloon temperature and solar wind measurements) are more accurate than derived temperatures e.g. mesospheric temperatures derived from radar or optical methods.

In this study, we also discuss averages, for example daily averages, which are based on a number of individual samples throughout the day. Consequently, there is a statistical spread in the measurements. Note that these spreads mainly reflect the genuine variability of nature, and should not be confused with uncertainty or error in the data. Statistical spread in the measurements is usually much larger than any measurement errors.

A challenge when assessing statistical spread in measurements based on several different methods is the role of sampling frequency and number of samples used to establish statistical moments. In the figures below, we therefore do not show error bars, as these would be misleading and strongly dominated by sample frequency and number of samples.

3. Results

Figure 3 shows the timeline of some of the key measurements used for this study. Already from this plot, variations on a number of time scales can be discerned. In the sea, on ground, and in the atmosphere, seasonal variations are dominating. These can be explained by the sinusoidal variation in the Earth's rotation axis throughout the year. The 11-year solar cycle (which is primarily an effect of the periodic polarity change Sun's intrinsic magnetic field) is also clearly discernible as modulations of the F10.7 index as shown in panel a) and the electromagnetic input energy (solar wind Poynting flux calculated using Equation 1) in panel b). Note that the electromagnetic input energy from the Sun lags the F10.7 index; The strongest solar wind–magnetosphere coupling takes place in the waning phase of the solar cycle, not during its peak.

Ionospheric temperatures (e.g. EISCAT ion temperatures shown in panel c) seem to be modulated by solar cycle variation. The other parameters, plotted in panels d) to g) possess strong seasonal variations (as well as diurnal variations, but as we use daily averages and focus on long term trends, these are ignored), and will be discussed in some detail below.

3.1. Seasonal asymmetry and trends in ground and atmospheric temperatures

We now discuss in more detail the parameters A - amplitude, B - phase shift (seasonal asymmetry), and C - offset as introduced above. These are derived from the model fit (Equation 2) applied to the various temperature measurements.

Figure 4 shows the evolution of the three key parameters (phase shift, amplitude, offset) for ground stations (left columns) during the last four decades, and for balloon measurements (right columns) since 1993. The coloured curves give the

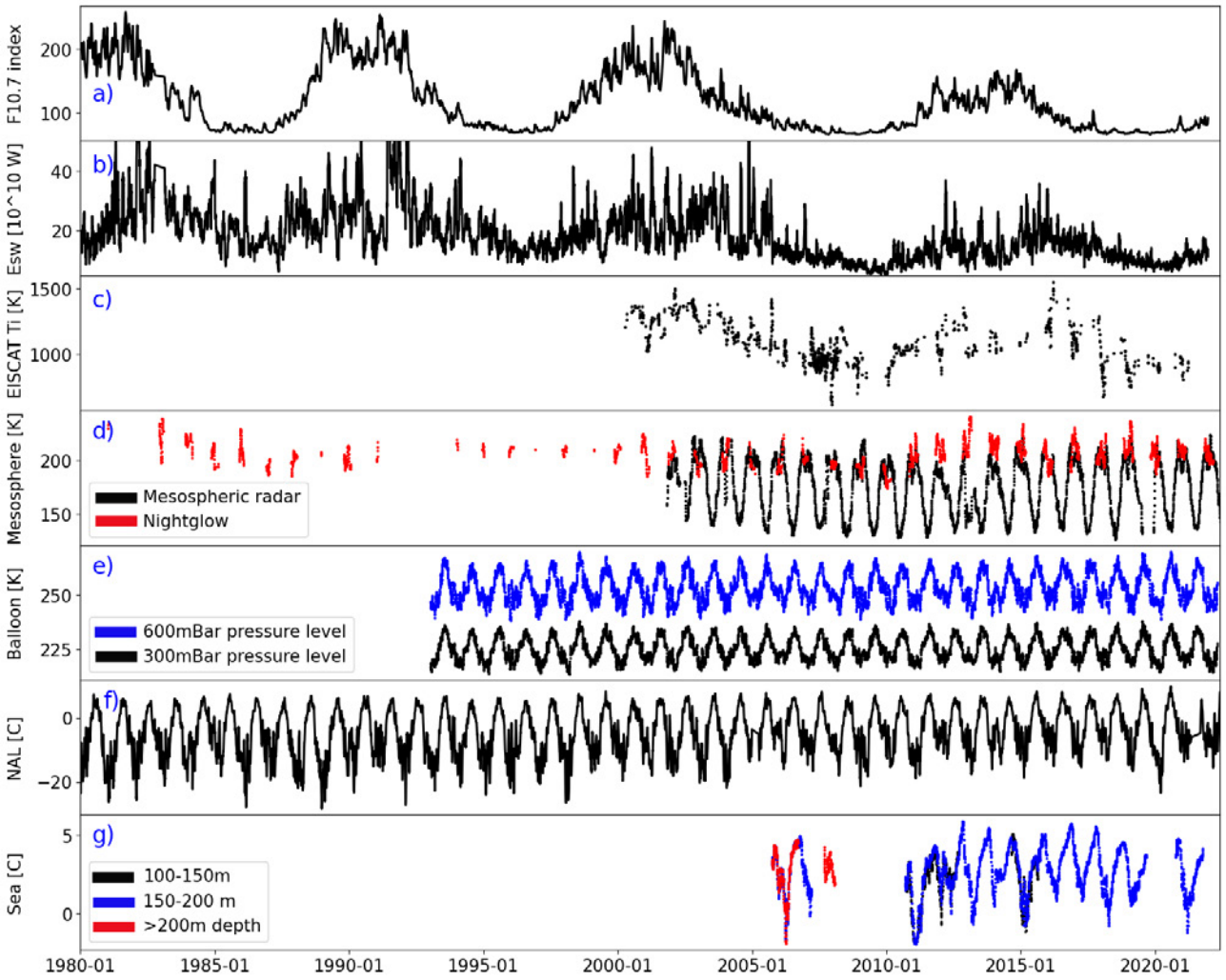

Figure 3: Timelines of some of the key measurements used for this study. Panel a) F10.7 index; b) Solar wind electromagnetic input energy (Poynting flux - see Equation 1); c) EISCAT ion temperatures; d) Mesospheric temperatures from radar (black solid lines) and nightglow observations (red dots, dark season only); e) Atmospheric temperatures at two altitudes (pressure levels) based on balloon measurements; f) Ground temperature [°C] from Ny-Ålesund airport (NAL); g) Sea temperatures [°C] from three different depth ranges in Isfjorden.

different ground stations, whereas the coloured dots represent different altitudes (or pressure levels) of the balloon measurements. We find several familiar traits: the signature of climate warming may be seen in the steady increase in temperature offset in the ground stations (panel e) over the last decades; the steady decrease of amplitude on ground (panel c) follows the warming of the winter months. For reference, we have also plotted the F10.7 index (panel g) for the same time period.

In terms of seasonal asymmetries, an increasing phase shift (panel a) can be observed from around 1990. Generally, all stations used exhibit a similar evolution of all three parameters. However, slight differences may be traced back to the local environments of the stations. Edgeøya (light blue curve) and Karl-XII-øya (dark blue curve), as islands on the east coast of Svalbard, are usually surrounded by sea ice for large portions of the year, leading to cooler mean temperatures. Svea (orange curve), which likewise is surrounded by ice in winter, is next coolest, while the stations on the ice-free west coast are warmest. In the phase shift the effect of ocean waters is also apparent. Stations located on smaller islands, e.g. Hopen (green curve), experience a greater phase shift. The pattern of the evolution of the phase shift parameter is difficult to interpret. There seems to be a diffuse oscillation signal. A possible cause is the yearly variation of sea ice extent. A quick crosscheck with the yearly minimum sea ice area (NASA[2]), however, did not seem promising.

2 https://climate.nasa.gov/vital-signs/arctic-sea-ice/

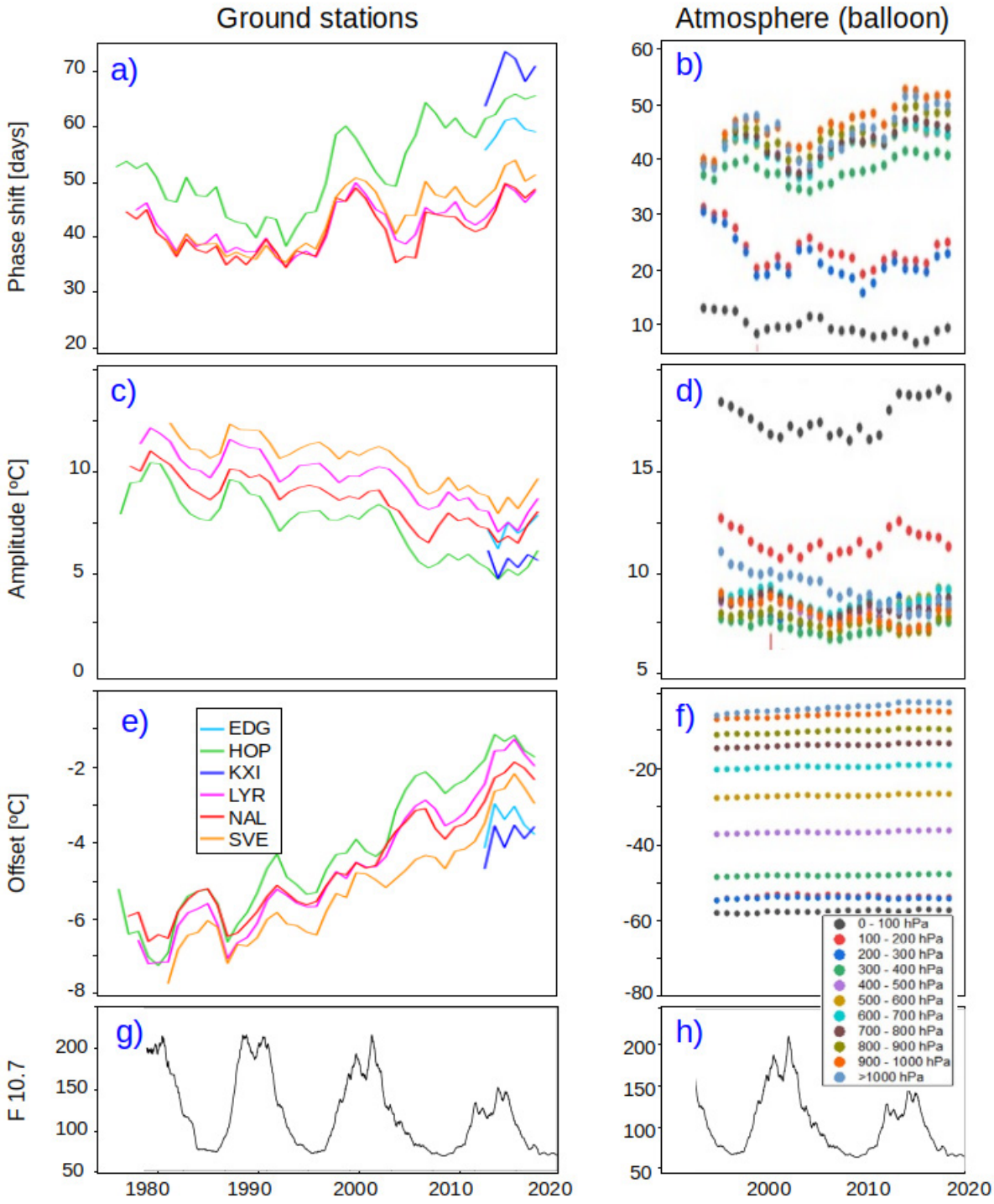

Figure 4: Evolution of key parameters on ground and in the atmosphere over the last decades. Panel a) Phase shift (seasonal shift) from ground stations; b) Phase shifts at various pressure altitudes derived from balloon measurements; c) Temperature amplitudes, ground stations; d) Temperature amplitudes from balloon measurements; e) Temperature offset, ground stations; f) Temperature offset, balloon measurements; g) F10.7 index for 1980-2020; h) F10.7 index for 1990-2020.

Atmospheric temperatures, derived from the balloon measurements (see Figure 4) generally show a similar evolution. Near ground (≥ 1000 hPa), the trends in phase shift (panel b) are similar to those derived from ground stations. Interestingly, the temporal variances in both the phase shift and the amplitude appear to be inverted for the high-altitude isobars (0-300 hPa) compared to lower altitudes. This phenomenon is likely caused by the absorption of UV radiation in this upper layer of air where more ozone is present (Randel and Wy 2010).

Moreover, much larger variances in the amplitude and phase shift can be observed in the ground station data compared to the lowest weather

balloon isobar. On average, these results should be equal; however, as there are more data points throughout the day for the ground stations, it is more likely that outliers will be observed, which explains why these parameters vary. It can furthermore be concluded that these short-term variances in amplitude and phase-shift cannot be observed in the weather balloon data due to insufficient number of data points to accurately map these outliers.

Figure 5 synthesises observations from the sea, ground, and atmosphere for more recent years. Each dot in this plot is the mean temperature over the years 2014-2021, i.e. when we have reasonable coverage from all observations. We once again note a significant phase shift (panel a) near the Earth's surface, suggesting that landmasses, glaciers and the ocean have a great impact on the local temperature. As we ascend further through the troposphere, this phase shift seems to reduce only slightly. However, as the tropopause is reached around the 200-300 hPa isobar (approximately 9 km altitude), there is a significant drop in the phase shift, and the phase shift eventually disappears completely vertical solid red line) at the highest balloon altitude, although a nearly half-year phase shift is observed in the mesosphere. Underwater (red dots and lines) the phase shift is amplified to greater temperature response lag, primarily due to the much larger heat capacity of water, though sea currents also probably play a role. The dotted line in the underwater phase shift indicates the lack of sufficient data points at pressures between12500 and 15000 hPa to enable an accurate fit.

In Panel b), which shows amplitude as function of pressure level, we observe a similar discrepancy between the troposphere and tropopause. The amplitude (i.e. average seasonal variation) does not vary significantly below the tropopause, whereas larger seasonal variations are seen above the tropopause, suggesting that the temperature is primarily modulated by solar irradiance. Below the sea surface, the temperature amplitude only varies a few degrees. Solar irradiation does not reach such depths underwater, and variations at these depths are primarily influenced by ocean currents. Panel c) shows the calculated offset. Being averages over several years, the offsets can be interpreted as the average temperature at that pressure level. A consistent decrease in the average temperature is observed as we move from underwater via ground and upwards through the troposphere. Above the tropopause (where pressure is below ca. 300 hPa), the temperature remains relatively constant.

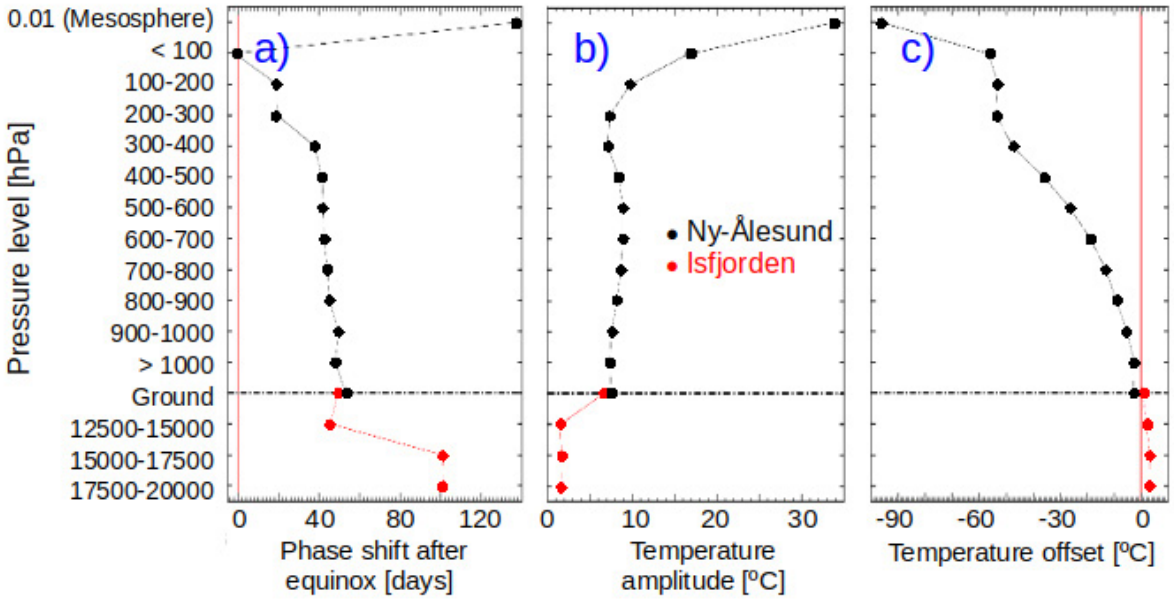

Figure 5: Fit parameters; a) Phase shift; b) Amplitude, and c) Temperature offset for various pressure levels in the atmosphere, ground (black lines and symbols) and under water (red), averaged between 2014-2021.

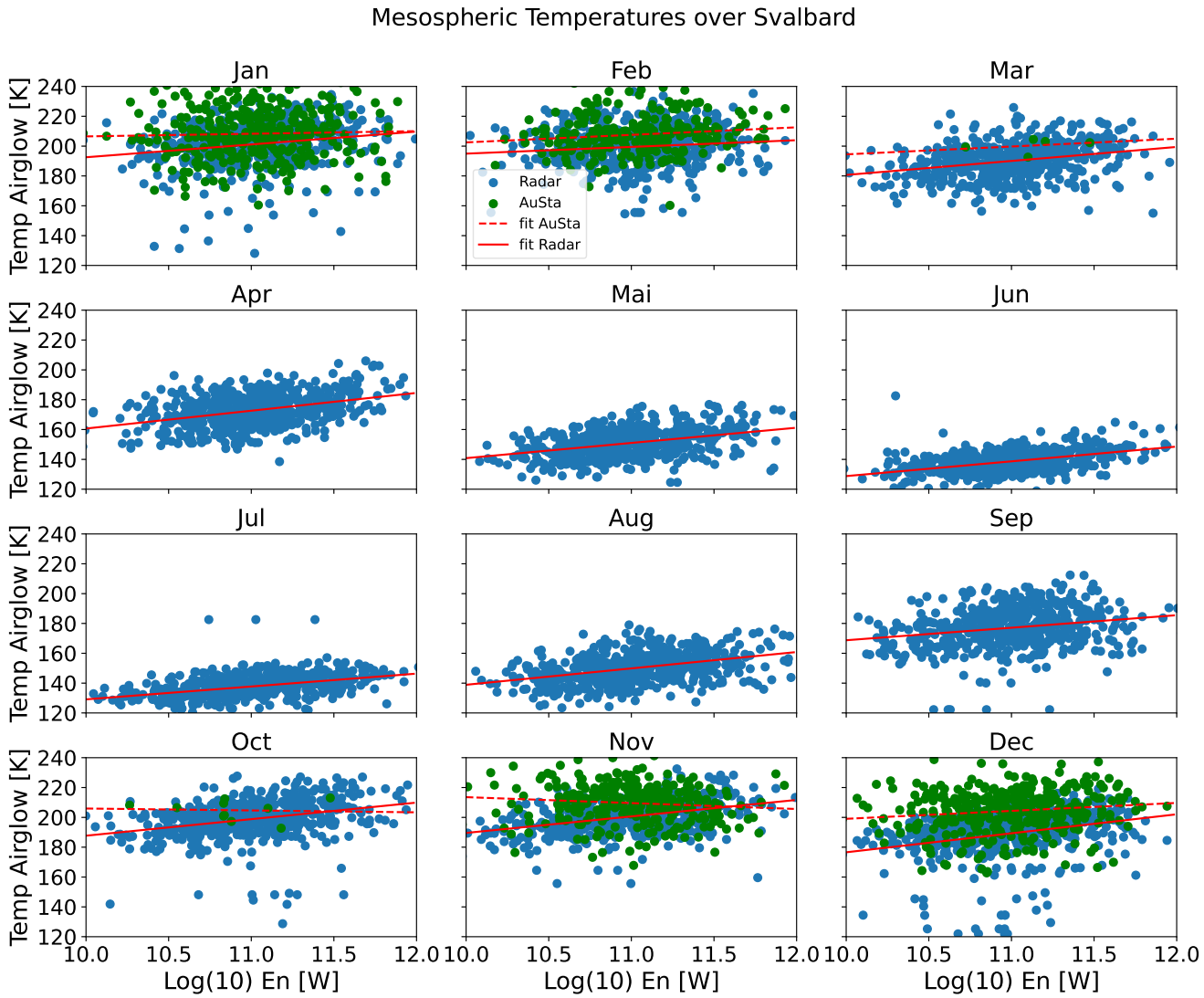

Figure 6: Monthly mesospheric temperatures between 1980 and 2021 as a function of the solar wind energy input in the Earth's magnetosphere. The temperatures are estimated at around 90 km derived from radar (blue dots) or spectrometer (green dots) measurements. Red lines represent a first-degree polynomial fitting for the spectrometer (dashed lines) and radar data (solid lines). Positive correlations, indicating a vertical coupling with some transfer of energy from the solar wind to the mesosphere, can be observed throughout the year.

3.2. Trends in the mesosphere and ionosphere and coupling to solar activity

Whereas the temperatures (and their trends) in the sea, on ground, and in the atmosphere do not show any clear correlation with solar activity or solar wind input, we do find a correlation between energy input and temperatures higher up. Figure 6 shows mesospheric temperatures as a function of the solar wind energy input (see Equation 1) for each month. Nightglow measurements (green dots) are only available during the dark season (late October to early March), whereas mesospheric temperatures derived from radar (blue dots) are available throughout the year. Despite some variability during the year, a general trend towards higher temperatures during periods with high solar wind energy input is seen for all months.

Figure 7 shows similar correlations, but this time between EISCAT measurements of ion temperatures around 300 km and the electromagnetic solar wind energy input. The correlation between the two parameters is even more pronounced. As noted above, around 300 km, neutral temperatures are on average very similar to ion temperatures.

Heating in the ionosphere can either be produced by Joule heating or through precipitation of soft electrons. The direct relation between the ion temperatures and Poynting flux has been shown by Banks and Kockarts (1973) at the altitude of the ionospheric E region (ca 90-150 km altitude) and lower F region (150-250 km). At higher altitudes, ion heating produced is sufficient to lead to direct ion outflow (Strangeway et al. 2000, 2005; Zheng et al. 2005).

3.3. Vertical coupling

In the mesosphere and above, a correlation between temperatures and electromagnetic energy from the Sun is observed, suggesting a vertical coupling and transfer of energy between regions. This coupling is most pronounced in ionospheric temperatures (Figure 7), where a clear correlation between solar activity and temperature can be observed. As shown in Figure 6, mesospheric temperatures are also correlated with the solar wind input energy, but the coupling is less pronounced than in the ionosphere.

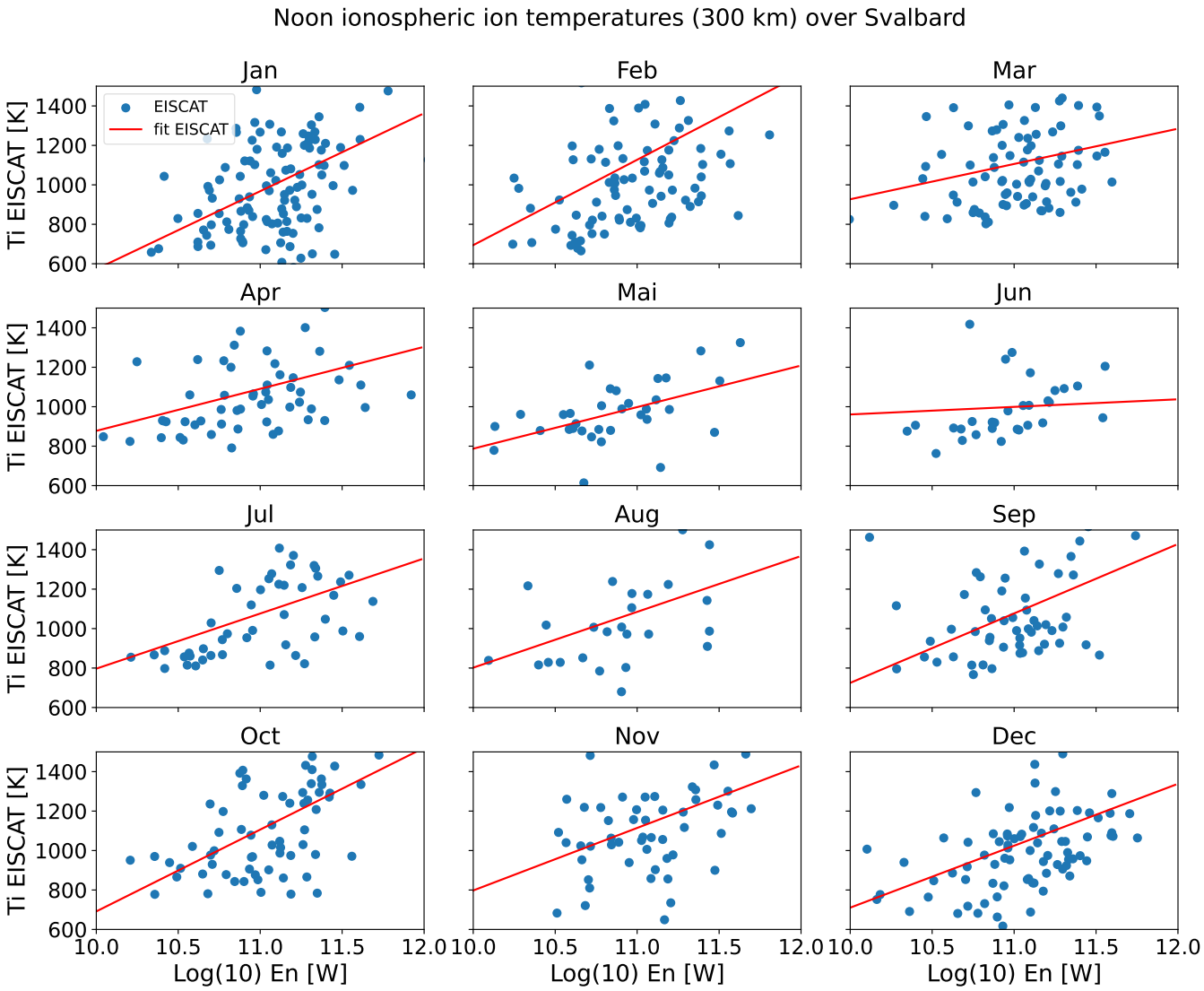

Figure 7: *Similar to figure 6, but now showing ionospheric ion temperatures at noon from EISCAT as a function of the solar wind energy input in the Earth's magnetosphere throughout the year. Solid red lines represent a first-degree polynomial fitting. Once again, there is a clear positive correlation between the solar wind input energy and ionospheric ion temperatures, indicating a transfer of energy from the solar wind to the ionosphere.*

Correlations between electromagnetic solar wind energy and the neutral atmosphere have been reported in earlier studies from high latitudes (Kosch and Nielsen 1995; Fujii et al. 1999). Such correlations have been attributed to Joule heating due to frictional forces between ions and neutrals (Cai et al. 2014), or heating due to small-scale field aligned currents (Lühr et al. 2004; Lühr and Marker 2013).

The former is related to enhanced ionospheric convection driven by solar wind–magnetosphere coupling through the so-called Dungey cycle (Dungey 1958). As a consequence, ions start moving faster than the neutrals. The resulting friction causes Joule heating. Signatures of field aligned currents in the thermosphere have been inferred from magnetic field measurements by the CHAMP satellites (Reigber et al. 2002), and one theory is that the Joule heating is caused by the combination of these fine structure currents and finite conductivity at 90-140 km altitude (Neubert and Christiansen 2003; Lühr et al. 2004).

Within the neutral atmosphere, at least below the tropopause, there is a strong vertical coupling where temperatures and their seasonal variation are correlated. Both diurnal and seasonal variations are observed, and these can be attributed to a combination of solar illumination and heat capacity in the sea, ground and ice/glaciers.

The existence of a direct coupling of solar wind input and the neutral atmosphere temperature cycles seems unlikely. If we calculate correlation coefficients between F10.7 and various ground stations, we note the values never exceed 0.25, and thus do not provide any convincing argument for direct relation between solar input and ground temperatures. Still, as shown in Figure 8, the evolution of the phase shift parameter from many ground stations bears an uncanny resemblance to that of the F10.7 parameter. The behaviour of the phase shift may be a coincidence, but this signal needs to be further explored in future studies.

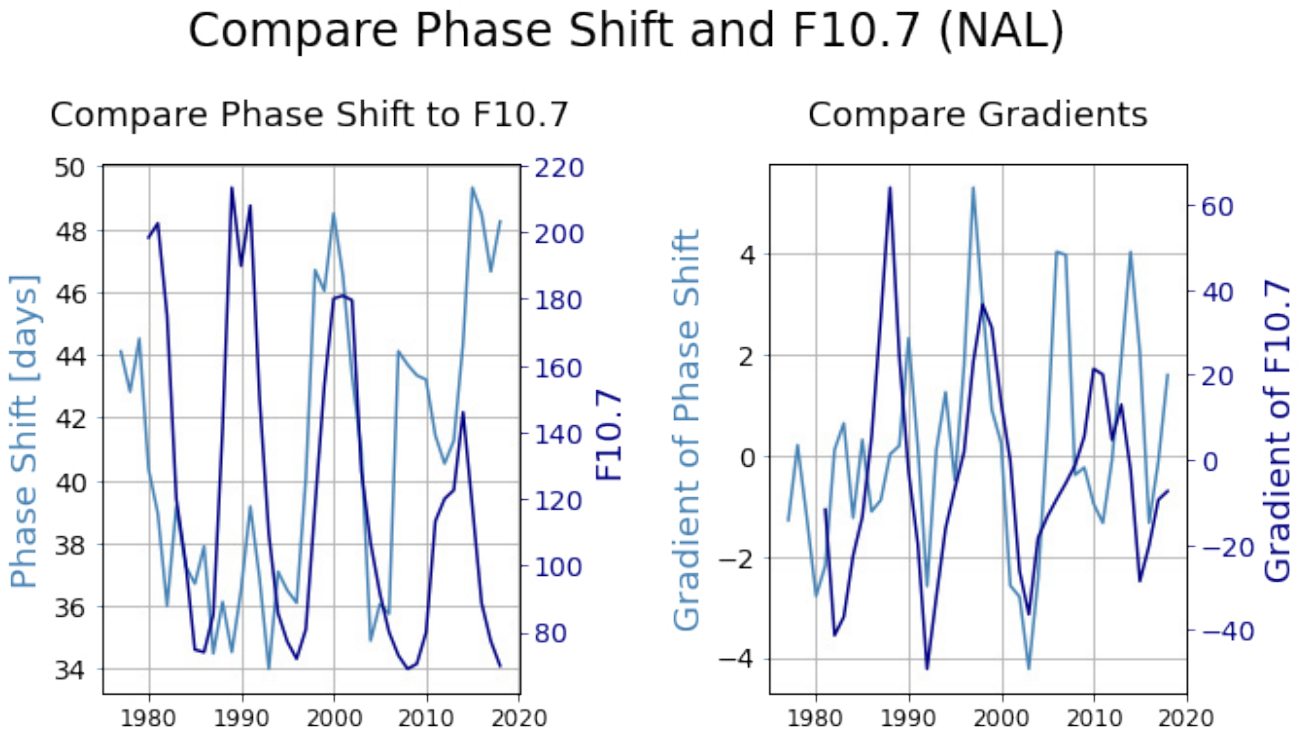

Figure 8: Left: Oscillation of phase shift in ground temperatures (with 5-year floating window), plotted with associated F10.7 values. Right: Gradients of self-same parameters. Data from Ny-Ålesund ground station.

4. Contributions to interdisciplinarity

We have studied long-term trends in temperatures in the sea, on ground, in the atmosphere in Svalbard, as well as the mesosphere and ionosphere above Svalbard. In particular, we have investigated how the seasonal asymmetry depends on altitude, and whether any of the trends observed can be explained by solar activity or enhanced energy transfer from the Sun and solar wind into the thermosphere.

The study spans several science disciplines: space physics, atmospheric physics, meteorology and oceanography. This interdisciplinarity implies some challenges. While the fundamental concepts such as temperature, density and convection are similar, forces responsible are very different in the different regions. Electromagnetic forces dominate in space, but are largely irrelevant on ground and in the atmosphere below the ionosphere. There are also practical challenges with data handling. In space, temperatures are frequently given in units of electronvolt [eV] or in K (Kelvin) whereas °C is more common in meteorology and oceanography. Still, the study has provided some interesting results, and new knowledge. Below we summarise the main results, list a couple of open questions and provide some recommendations for future utilisation of observations.

4.1. Main findings

The results of this study can be summarised as follows:

- On ground and in the lower atmosphere we observe a trend towards higher yearly average temperatures, and less difference between winter and summer temperatures. Over the ca 40 year time period considered, the difference in temperature between summer and winter has decreased about 2-3°C at the ground stations included in this study.
- We observe an increasing seasonal asymmetry between temperatures and season over the last decades; the day of the year with maximum temperatures tends to occur later in the year.
- While there is a significant phase shift between season and temperatures on ground and in the troposphere, there is little or no phase shift above the tropopause.
- We do not find any strong relation between the temperatures on ground or in the sea and solar activity.
- Likewise, there is little or no direct correlation between atmospheric temperatures and solar activity.
- In the higher parts of the thermosphere, in particular the ionosphere, but to some extent also the mesosphere, there is a pronounced correlation between solar input energy and temperatures.
- The most recently completed solar cycle, the 24th since systematic measurements started in 1755, shows a lower activity (lower EUV irradiance and electromagnetic energy transfer) than the earlier cycles for which we have reasonable data coverage. Despite this lower solar activity, the trend shows increased ground temperatures.

4.2. Open questions

While the study reveals some interesting trends and correlation between measurements from space, the atmosphere, the ground and the ocean, it also raises a couple of questions:

- What is the underlying reason for the observed trends? Is it primarily a result of global warming due to increased release of CO2 to the atmosphere, or are the observed trends primarily caused by local conditions and indirect effects, such as change of the ice-cap extent or ocean currents?
- Will the observed trends (as seen in e.g. Figure 4) continue in the coming years? An obvious follow-up question is: 'What consequences will these changes have in the future?'
- We do not observe any significant correlation between solar activity and ground temperatures. Does solar activity play any role for local temperatures in Arctic at all?

4.3. Recommendations for the future

With its extensive infrastructure, Svalbard is an ideal place to conduct studies focusing on the relation between solar activity on one side and processes and properties of the Earth's thermosphere on the other side. Still, this is a complex system involving several science disciplines. To enhance utilisation of data, we propose the following:

- Enhance cooperation between science disciplines: space science, meteorology, oceanography and glaciology. There are several conceivable ways to achieve this, for example by promoting cross-disciplinary study programs at universities, and by enhancing funding for cross-discipline and system science studies. Promoting common formats (such as netdcf, csv, cdf) within the disciplines could also facilitate interdisciplinary studies.
- Make sure measurements of critical parameters from space, from the atmosphere, from ground and in the sea/ice are available over extended epochs (ideally several solar cycles). Observations should ideally be continuous and without any major data gaps. In our study, we faced the measurements gap between highest altitude of atmospheric balloon (about 30 km) and the first altitude of EISCAT (about 80 km running on special Programme). The mesospheric measurements are very sporadic and not enough balloon data are available to make a feasible comparison with ground stations' data (see Section 3.1).
- Promote cross-disciplinary studies and modern data assimilation techniques like machine learning to identify couplings between processes.
- Continue to promote open access to observations, and make sure observations are well calibrated and contain sufficient metadata such as exact time and location of the observations, proper units, information about data gap handling and links to instrumentation papers with further details about the measurements and techniques.

5. Data availability

Data used for this study are available from public archives. Provider and Uniform Resource Locator (URL) is given in Appendix 1. See also Table 1 and 2 for details about location, parameters and time periods for the individual observations.

6. Acknowledgements

This work was supported by the Research Council of Norway, project number 322387, Svalbard Integrated Arctic Earth Observing System – Knowledge Centre, operational phase 2022. The authors also thanks staff and colleagues at the University Centre in Svalbard (UNIS), the Kjell Henriksen Observatory (KHO) and EISCAT for fruitful discussions and support in preparing this report. EISCAT is an international association supported by research organisations in China (CRIRP), Finland (SA), Japan (NIPR and ISEE), Norway (NFR), Sweden (VR), and the United Kingdom (UKRI).

7. References

Aruliah AL, Farmer AD, Fuller-Rowell TJ, Wild MN, Hapgood M, Rees D (1996) An equinoctial asymmetry in the high-latitude thermosphere and ionosphere. J Geophys Res: Space Physics 101:15713–15722. https://doi.org/10.1029/95JA01102

Banks PM, Kockarts G (1973) Aeronomy, Part B. Elsevier, New York.

Brekke A (1993) Physics of the Upper Atmosphere. Springer, Berlin, Heidelberg. https://doi.org/10.1007/978-3-642-27401-5

Cai L, Aikio AT, Nygrén T (2014) Solar wind effect on Joule heating in the high-latitude ionosphere. J Geophys Res: Space Physics 119 (10):440–10,455. https://doi.org/10.1002/2014JA020269

Coddington O, Lean J, Pilewskie P, Snow M, Richard E, Kopp G, Lindholm C, DeLand M, Marchenko S, Haberreiter M, Baranyi T (2019) Solar Irradiance Variability: Comparisons of Models and Measurements. Earth Space Sci 6:2525–2555. https://doi.org/10.1029/2019EA000693

Dungey JW (1958) Cosmic electrodynamics. Q J R Meteorolog Soc 85:450–450. https://doi.org/10.1002/qj.49708536628

Folkestad K, Hagfors T, Westerlund S (1983) EISCAT: An updated description of technical characteristics and operational capabilities. Radio Sci 18:867–879. https://doi.org/10.1029/RS018i006p00867

Förster M, Haaland SE, Rentz S, Liu H (2008) IMF Dependence of High-Latitude Thermospheric Wind Pattern Derived from CHAMP Cross-Track Accelerometer Data and the Corresponding Magnetospheric Convection from Cluster EDI Measurements. 37th COSPAR Scientific Assembly (Montreal, Canada)

Fujii R, Nozawa S, Buchert SC, Brekke A (1999) Statistical characteristics of electromagnetic energy transfer between the magnetosphere, the ionosphere, and the thermosphere. J Geophys Res: Space Physics 104:2357–2366. https://doi.org/10.1029/98JA02750

Grygalashvyly M (2015) Several notes on the OH* layer. Ann Geophys 33:923–930. https://doi.org/10.5194/angeo-33-923-2015

Haaland S, Lybekk B, Maes L, Laundal K, Pedersen A, Tenfjord P, Ohma A, Østgaard N, Reistad J, Snekvik K (2017) North-south asymmetries in cold plasma density in the magnetotail lobes: Cluster observations. J Geophys Res: Space Physics 122:136–149. https://doi.org/10.1002/2016JA023404

Hall CM, Aso T, Tsutsumi M (2002) An examination of high latitude upper mesosphere dynamic stability using the Nippon/Norway Svalbard Meteor Radar. Geophys Res Lett 29:1280. https://doi.org/10.1029/2001GL014229

Hatch SM, Haaland S, Laundal KM, Moretto T, Yau AW, Bjoland L, Reistad JP, Ohma A, Oksavik K (2020) Seasonal and Hemispheric Asymmetries of F Region Polar Cap Plasma Density: Swarm and CHAMP Observations. J Geophys Res 125:e28084. https://doi.org/10.1029/2020JA028084

Hocking WK, Thayaparan T, Jones J (1997) Meteor decay times and their use in determining a diagnostic mesospheric Temperature-pressure parameter: Methodology and one year of data. Geophys Res Lett 24:2977–2980. https://doi.org/https://doi.org/10.1029/97GL03048

Holmen SE (2016) Trends and variability of polar mesopause region temperatures attributed to atmospheric dynamics and solar activity. Dissertation, UiT - The Arctic University of Norway. https://munin.uit.no/handle/10037/10740

Kosch MJ, Nielsen E (1995) Coherent radar estimates of average high-latitude ionospheric Joule heating. J Geophys Res: Space Physics 100:12201–12216. https://doi.org/10.1029/95JA00821

Lühr H, Marker S (2013) High-Latitude Thermospheric Density and Wind Dependence on Solar and Magnetic Activity. In Lübken FJ (ed) Climate and Weather of the Sun-Earth System (CAWSES). Springer Atmospheric Sciences. Springer, Dordrecht, pp 189–205. https://doi.org/10.1007/978-94-007-4348-9_11

Lühr H, Rother M, Köhler W, Ritter P, Grunwaldt L (2004) Thermospheric up-welling in the cusp region: Evidence from CHAMP observations. Geophys Res Lett 31(6):L06805. https://doi.org/10.1029/2003GL019314

Maeda S, Nozawa S, Sugino M, Fujiwara H, Suzuki M (2002) Ion and neutral temperature distributions in the E-region observed by the EISCAT Tromsø and Svalbard radars. Ann Geophys 20:1415–1427. https://doi.org/10.5194/angeo-20-1415-2002

NASA's Jet Propulsion Laboratory, E S Arctic Sea Ice Minimum Extent. https://climate.nasa.gov/vital-signs/arctic-sea-ice/. Accessed 22 July 2022.

Neubert T, Christiansen F (2003) Small-scale, field-aligned currents at the top-side ionosphere. Geophys Res Lett 30:2010. https://doi.org/10.1029/2003GL017808

Randel WJ, Wu F (2010) The Polar Summer Tropopause Inversion Layer. J Atmos Sci 67:2572–2581. https://doi.org/10.1175/2010JAS3430.1

Reigber C, Lühr H, Schwintzer P (2002) CHAMP mission status. Adv Space Res 30:129–134. https://doi.org/10.1016/S0273-1177(02)00276-4

Sigernes F, Shumilov N, Deehr CS, Nielsen KP, Svenøe T, Havnes O (2003) Hydroxyl rotational temperature record from the auroral station in Adventdalen, Svalbard (78°N, 15°E). J Geophys Res: Space Physics 108(A9):1342. https://doi.org/10.1029/2001JA009023

Skogseth R, Olivier LL, Nilsen F, Falck E, Fraser N, Tverberg V, Ledang AB, Vader A, Jonassen MO, Søreide J, Cottier F, Berge J, Ivanov BV, Falk-Petersen S (2020) Variability and decadal trends in the Isfjorden (Svalbard) ocean climate and circulation - An indicator for climate change in the European Arctic. Prog Oceanogr 187:102394. https://doi.org/10.1016/j.pocean.2020.102394

Strangeway RJ, Russell CT, Carlson CW, McFadden JP, Ergun RE, Temerin M, Klumpar DM, Peterson WK, Moore TE (2000) Cusp field-aligned currents and ion outflows. J Geophys Res: Space Physics 105:21129-21141. https://doi.org/10.1029/2000JA900032

Strangeway R, Ergun R, Su Y-J, Carlson C, Elphic R (2005) Factors controlling ionospheric outflows as observed at intermediate altitudes. J Geophys Res: Space Physics 110: A03221. https://doi.org/10.1029/2004JA010829

Tenfjord P, Østgaard N (2013) Energy transfer and flow in the solar wind-magnetosphere-ionosphere system: A new coupling function. J Geophys Res: Space Physics, 118:5659–5672. https://doi.org/10.1002/jgra.50545

Vasyliunas VM, Kan JR, Siscoe GL, Akasofu S-I (1982) Scaling relations governing magnetospheric energy transfer. Planet Space Sci 30:359-365. https://doi.org/10.1016/0032-0633(82)90041-1

Zheng Y, Moore TE, Mozer FS, Russell CT, Strangeway RJ (2005) Polar study of ionospheric ion outflow versus energy input. J Geophys Res: Space Physics 110:A07210. https://doi.org/10.1029/2004JA010995

Appendix 1: Datasets used and their providers

Dataset	Provider and access (URL)	Data responsible / contact person for this SIOS project
Solar wind and solar indices	Coordinated Data Analysis Web, NASA, USA https://cdaweb.gsfc.nasa.gov/index.html Data description of the OMNI data set used for this study can be found on: https://cdaweb.gsfc.nasa.gov/misc/NotesO.html#OMNI_HRO_1MIN	Audrey Schillings, *Umeå University, Sweden* Audrey.Schillings@space.umu.se
EISCAT radar data	**EISCAT Scientific Association** http://pc115.seg20.nipr.ac.jp/www/eiscatdata/esr/ascii/42m_ascii/5min/	Lindis Bjoland, *UNIS, Svalbard* lindisb@unis.no
Atmospheric temperatures (balloon measurements)	Norwegian Meteorological Institute https://thredds.met.no/thredds/catalog/remotesensingradiosonde/catalog.html Alfred Wegener Institute, Germany: http://doi.pangaea.de/10.1594/PANGAEA.845373	Brandon van Schaik, b.j.a.v.schaik@student.tue.nl *École Polytechnique Fédérale de Lausanne, Switzerland*
Ground temperatures	Norwegian Centre for Climate Research https://www.seklima.met.no	Antonia Radlwimmer, UNIS, Svalbard Quivi@web.de
Ocean temperatures	Norwegian Polar Institute https://data.npolar.no/dataset/?filter-links.rel=data&q=Mooring	Lindis Bjoland, *Space Physics Group, University of Bergen* Lindis.Bjoland@uib.no

Long-term observations of aerosol optical depth and their relation to in-situ aerosol properties in the Svalbard region (LOAD-RIS)

Georg Hansen[1], Natalia Kouremeti[2], Stefania Gilardoni[3], Kerstin Stebel[1], Nikolaos Evangeliou[1], Christoph Ritter[4], Tymon Zielinski[5], Sara Herrero[6], Stelios Kazadzis[2], David Mateos[6], Mauro Mazzola[3], Paulina Pakszys[5], Konstantinos Eleftheriadis[7]

1 NILU – Norwegian Institute for Air Research, Kjeller, Norway
2 Physikalisch-Meteorologisches Observatorium Davos, World Radiation Center, Davos, Switzerland
3 Institute of Polar Sciences, National Research Council of Italy, Bologna, Italy
4 Alfred Wegener Institute, Helmholtz Centre for Polar and Marine Research, Bremerhaven, Germany
5 Institute of Oceanology of the Polish Academy of Sciences, Sopot, Poland
6 University of Valladolid, Facultad de Ciencias, Valladolid, Spain
7 Environmental Radioactivity Laboratory, NCSR 'Demokritos', Athens, Greece

Corresponding author: Georg Hansen, ghh@nilu.no, georghh@msn.com

Keywords: Aerosols, Arctic haze, biomass burning, black carbon, optical thickness

DOI: https://doi.org/10.5281/zenodo.7376140

1. Introduction

Measurements of aerosol optical depth (AOD) at different wavelengths and the resulting Ångström exponent (AE) by means of sun photometers provide information about the total extinction and, except multimodal aerosols, the size of aerosols in the atmospheric column. This is of great importance for investigations of long-range pollution transport, mostly occurring in the free troposphere. A comprehensive overview of AOD and supplementary in-situ measurements of aerosols both in the Arctic and in Antarctica was given by Tomasi et al. (2015), while an in-depth study of AOD and black carbon (BC) at the three Arctic core sites (Ny-Ålesund, Point Barrow and Alert) in the period 2001–2011 was published by Stone et al. (2014). Recently, Xian et al. (2022 a, b) presented an analysis of (pan-) Arctic spring and summertime AOD trends and extreme events in 2003–2019.

AOD measurements in Svalbard started in 2002 and have continued until today. In other words, a considerable part of the measurements – including the more recent development of increasing summer aerosol load in the Arctic due to biomass burning – is not covered by the above-mentioned publications.

Despite extensive collaboration between groups who have developed the instruments and post-processing algorithms in use, there are different routines both regarding data quality control and cloud flagging, and regarding data aggregation routines (e.g. Kazadzis et al. 2018, Giles et al. 2019). Usually, these challenges are addressed in dedicated inter-comparison campaigns at suitable sites with stable observation conditions, e.g. Izaña Observatory, Tenerife, Spain, for two of the instrument types involved in this project (Cuevas et al. 2019). However, at high-latitude locations, inter-comparison results may differ from those at lower latitudes (Mazzola et al. 2012). Comparing three types of instruments and their respective evaluation routines at one high-latitude location thus offers a valuable contribution to data harmonisation efforts. The value of such an exercise can be further enhanced by also including in-situ measurements of aerosol extinction, absorption and scattering as well as black carbon observations.

In this report, we give an overview over columnar aerosol observations from two sites in Svalbard (Ny-Ålesund, Hornsund) in the time period 2002–2021, links to selected in-situ observations at Gruvebadet Atmosphere Laboratory ('Gruvebadet') and Zeppelin Observatory ('Zeppelin') in Ny-Ålesund, and satellite observations combined with FLEXPART model simulations complementing the two observation methods. The two sites are both located on the western coast of the main island of Spitsbergen, few kilometres into a fjord, but about 200 km apart in N-S direction and, according to a previous study, similar, but not 'identical', in terms of AOD characteristics (Pacszys and Zielinski 2017). However, while at the northern site of Ny-Ålesund sea-ice has been practically absent year-round for more than a decade, sea-ice conditions are still quite variable at Hornsund, due to the strong coastal current there.

2. Data analysis and overview

In the framework of the ReHearsol and the LOAD-RIS projects, AOD and AE datasets were collected from several on- and offshore instruments, AOD usually on 4 wavelengths and AE derived from these. The data sources are listed in Table 1.

Besides AOD and AE measurements, (in-situ) aerosol extinction, absorption and scattering coefficients collected at Gruvebadet (78.918°N, 11.895°E, 30 m a.s.l.) since 2011 and BC extinction coefficients mostly collected at Zeppelin since the 1990s have been included in the data analysis. These are available through the NILU EBAS[1] and the IADC[2] databases.

1 https://ebas.nilu.no/
2 https://iadc.cnr.it/cnr/

Table 1: Sources/instruments of AOD and AE measurements collected in the framework of the ReHearsol/LOAD-RIS projects.

Location	Photometer	Type	Measurement period	Comments
Sverdrup, Ny-Ålesund*	PFR	sun	April 2002–September 2021	1-min. resolution, quality-assured, temperature-stabilised sensor; https://doi.org/10.5281/zenodo.7191072
AWIPEV, Ny-Ålesund**	SP1A	sun	March 2003–October 2020	1-min. resolution, 5 wavelengths out of up to 13 selected
Polish Polar Station, Hornsund***	CIMEL	sun	April 2005–October 2021	2021: level 1.5 quality
AWIPEV, Ny-Ålesund	CIMEL	sun	2017–2021	2021: level 1.5 quality
Zeppelin Observatory, Ny-Ålesund****	SP1A	sun	2015, 2016, 2017, 2019, 2020	10 wavelengths, 4 wavelength AE
AWIPEV, Ny-Ålesund	CIMEL	lunar	2017–2019	
Sverdrup, Ny-Ålesund	PFR	lunar	2018–2020	
on board *R/V Oceania*	Microtops	sun	2007, 2009–2020	geographical area: 72–85°N, 0–50°E
on board *R/V Polarstern*	Microtops	sun	2009, 2012, 2015, 2017, 2020	geographical area: 72–85°N, 0–50°E

*78.923°N, 11.929°E, 5 m a.s.l.
**78.923°N, 11.923°E, 5 m a.s.l.
***77.002°N, 15.540°E, 5 m a.s.l.
****78.907°N, 11.889°E, 475 m a.s.l.

2.1. Inter-comparison of long-term AOD observations in Svalbard

The comparison of the AOD/AE datasets was performed with the primary goal to identify the level of agreement in the collocated instruments and establish an uncertainty level above which AOD spatial differences in the Svalbard area can be considered significant using different instruments, calibration and processing protocols. According to WMO two instruments are equivalent when more than 95% of the compared data show AOD differences within 0.005 ± 0.010/airmass (WMO 2016). This strict limit is difficult to reach at polar monitoring stations due to challenging observation conditions (low temperatures and resulting sensor stability issues, icing) and limited staff.

2.1.1. Comparison of Ny-Ålesund data sets

In Ny-Ålesund, two sun photometers have been run quasi-continuously for 20 years (and more): the SP1A by Alfred Wegener Institute at AWIPEV (since the late 1990s) and the sun PFR at Sverdrup close to AWIPEV (since 2002). In recent years AWI decided to replace the SP1A with a CIMEL instrument; this has been in operation since 2017 and will take over as the only instrument at AWIPEV after a transition period with SP1A and CIMEL running in parallel. In the framework of the ReHearsol project the whole time series of PFR, SP1A and CIMEL measurements has been inter-compared; this has not been done at such a scale at a polar station so far. The overall comparison results are summarised in Table 2, while details about this exercise are given in Appendix 1. For Ny-Ålesund we consider 66% of the AOD differences between different instruments being within the WMO limits as a statistically significant and satisfactory agreement given the conditions of the station.

In Figure 1 the level of agreement of the compared instruments is presented as median AOD differences at four wavelengths over each year along with the 5th and 95th percentiles (error bars). The filled symbols indicate that more than 66% (small) and 95% (large) of the compared values are within the WMO limit. It is evident that the level of agreement between SP1A and PFR has significantly improved since 2009. For the CIMEL-AWIPEV the highest level of agreement is observed in 2017

Table 2: Summary of long-term AOD differences between PFR, SP1A and CIMEL sun photometer at Ny-Ålesund. For wavelength pairs marked with * PFR values were interpolated to match CIMEL wavelengths, using the PFR AE.

	Wavelength/nm	AOD difference			% within WMO limits	Correlation Coefficient
		Median	5th percentile	95th percentile		
PFR-SP1A	368/368	0.002	-0.034	0.023	51.4	0.93
	412/412	0.007	-0.029	0.031	40.0	0.91
	500/500	0.006	-0.017	0.026	48.3	0.90
	862/862	0.001	-0.017	0.017	68.7	0.69
PFR-CIMEL	367/380*	0.013	0.004	0.027	26.5	0.99
	412/440*	0.013	0.005	0.028	19.2	0.98
	500/500	0.007	0.002	0.017	63.9	0.98
	862/870	0.002	-0.002	0.010	92.5	0.94

and 2018 (AERONET level-2 product) especially for the common wavelengths 500 nm and 870 nm, almost reaching or exceeding the WMO traceability criterium (91% to 99%). The level of agreement of the instruments poses difficulties in merging the datasets, but it is possible to fill gaps due to technical failures and secure continuous AOD measurements at Ny-Ålesund, at least in the near-infrared wavelength (870 nm). The overall comparison results are summarised in Table 2.

2.1.2. Comparison of SP1A observations at AWIPEV and Zeppelin Observatory

Since 2015, sun photometer measurements by means of an SP1A instrument have also been carried out at Zeppelin. Here we present a comparison for the year 2017, in which 25 480 isochronal (time difference < 10 minutes) one-minute measurements are available during the whole sunlit season.

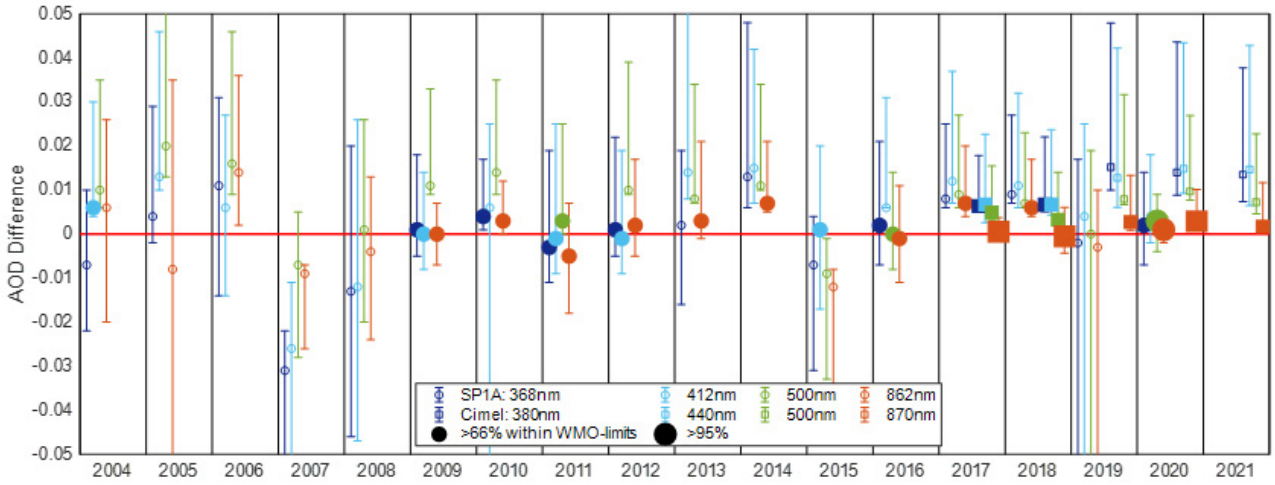

Figure 1: Yearly median AOD difference at four wavelengths for the SP1A (open circles) and CIMEL (open squares). The error bars represent the 5th and 95th percentile of the differences observed with in the year. The small and big filled circles and squares indicate datasets with agreement within the WMO uncertainty limit to better than 66% and 95%, respectively. Red line: zero difference level.

The AOD at 500 nm measured at AWIPEV ('Ny-Ålesund', in blue) and the difference between these and the corresponding measurements from Zeppelin (in red) are shown in Figure 2. Obviously, the AOD absolute differences between both sites are small. At 500 nm the median AOD at Zeppelin is 0.0033 (7.55%) lower than at AWIPEV. Only in 12.1% of all cases is the AOD difference larger than 0.01. The correlation between the two AOD at 500 nm data series over time is r = 0.9596, and at 368 nm it is even larger (0.9709). Moreover, we found that the small difference in AOD does not depend on the AOD itself. This means that observations at Zeppelin do not simply miss a constant fraction of aerosol. Instead, based on this work, one can expect that the aerosol in-situ samplers at Zeppelin and at Gruvebadet, averaged over a season, should measure almost the same aerosol in accumulation and coarse mode.

On the other hand, the Ångström exponent values (not shown here) reveal slight differences: Whenever the Ångström exponent (at Zeppelin) is larger than 1.5 it is even higher at, indicating that Zeppelin is missing some of the newly formed particles in the Aitken mode from the ocean in summer.

2.1.3. Comparison of Hornsund CIMEL data with Ny-Ålesund CIMEL data

A comprehensive analysis of aerosol measurements in the Svalbard region in the years 2000–2015 was made in the PhD thesis of Dr. Paulina Pakszys (2018); the comparison between Hornsund and Ny-Ålesund in the same period is discussed in Pakszys and Zielinski (2017). Both studies concluded with a generally high correlation between AOD observations at the two sites, but with a bias towards slightly higher mean values and larger variability at Hornsund. These analyses were based on different instruments at the two sites. From 2017, data from the same instrument type with identical calibration and analysis procedures (AERONET) became available, allowing a direct and simultaneous comparison of AOD at the two AERONET sites.

A total of 180 data pairs were obtained in the period 2017–2019. To increase this number we decided to use level 1.5 data (upgraded to level 2 data shortly before the end of the project period); this yielded 849 data pairs instead. Results from this enhanced data set are shown for two wavelengths in Figure 3; level 2.0 data results agree with this. The statistics of the comparison show Mean Bias Error (MBE) values below 0.009 for all channels and Root Mean Square Error (RMSE) values ranging from 0.02 at 1020 nm to 0.29 at 340 nm. Overall, about half of the differences are within the WMO U95 limits (analysis not shown here) despite the distance between two sites. However, the other half of the data proves that different aerosol conditions are measured frequently at the two sites. Generally, AOD values are slightly larger at Hornsund than at Ny-Ålesund, especially at shorter wavelengths.

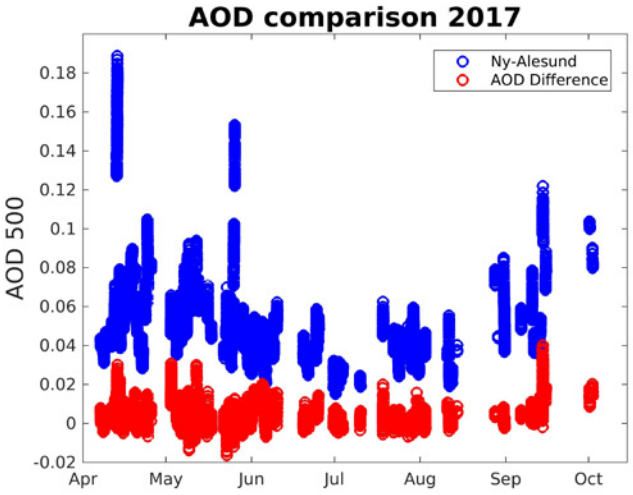

Figure 2: SP1A AOD observations at 500 nm in 2017 at AWIPEV, Ny-Ålesund (blue) and difference AOD (AWIPEV) – AOD (Zeppelin) (red).

2.2. High-AOD episodes

Initially, a threshold value of 0.15 for AOD at 500 nm was chosen to identify high-AOD events. All hourly means >0.1 and >0.15 (for moderate and high AOD events) from all instruments were identified and stored in annual files. Moreover, annual files listing all single measurements of AOD (500 nm) >0.1 and >0.15, respectively, from all instruments were created. Figure 4 shows the percentage of AOD hourly means >0.15 for four instruments included in the analysis (Ny-Ålesund: PFR, SP1A, CIMEL; Hornsund: CIMEL), the left panel from the period March–May and the right panel from the period June–August. The most prominent feature

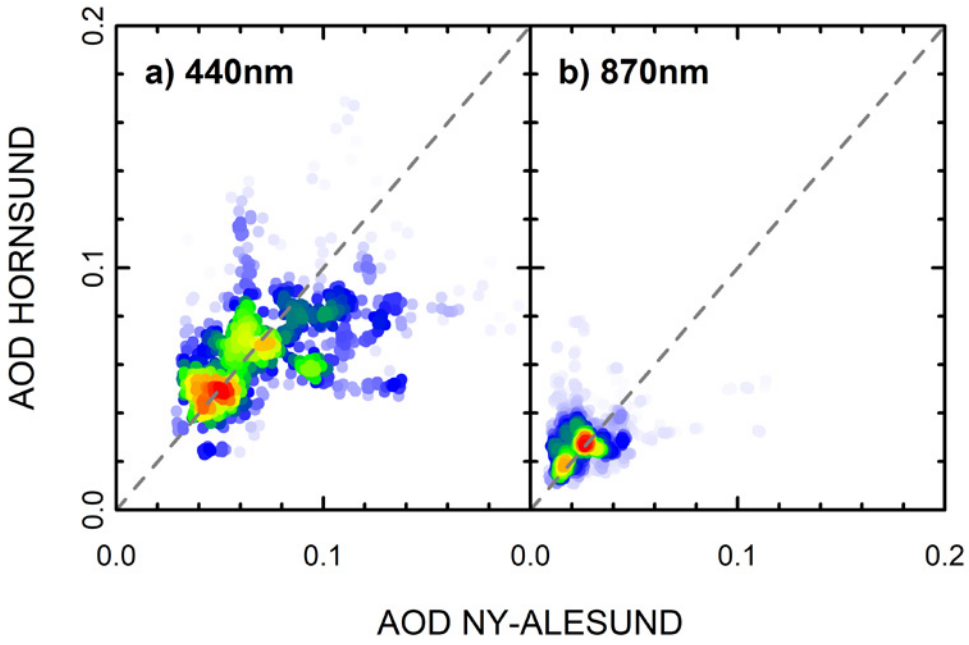

Figure 3: AOD scatterplot between CIMEL measurements in Hornsund and Ny-Ålesund at two wavelengths (440 nm, 870 nm). Colour scale indicates the density concentration from high (red) to low (blue).

is the decrease in number of high-AOD episodes in the March–May period since the early 2000s. In the June–August period there is no clear trend, but a tendency towards more frequent high-AOD episodes since 2014, with 2019 as a case of exceptionally persistent high-AOD conditions both in Ny-Ålesund and in Hornsund. We propose this is related to more frequent summer biomass burning episodes which more easily reach Hornsund (200 km closer to the Eurasian mainland).

Observations of aerosol originating from biomass burning events have been published for selected cases. The most prominent is the spring 2006 event which caused unprecedented levels of pollution in Svalbard (e.g. Stohl et al. 2007). More typical summer episodes originating from boreal forest fires in North America and Siberia in 2015 and 2017, respectively, were analysed and published by Markowicz et al. (2016) and Zielinski et al. (2020).

2.2.1. Comparison of columnar and in-situ aerosol properties at Ny-Ålesund – Arctic haze vs. summer biomass burning events

To better characterise the observed columnar aerosol, the AOD data were compared with aerosol properties derived from in-situ measurements, including aerosol absorption, scattering and extinction coefficients from Gruvebadet, and aerosol absorption coefficients from Zeppelin. Gruvebadet is located at about 1 km from the Ny-Ålesund settlement at 30 m a.s.l., while Zeppelin is sited at the top of the Zeppelin Mountain at 474 m a.s.l., about 2 km from the coast and 1 km from Gruvebadet. Aerosol absorption coefficient time series at Zeppelin and Gruvebadet are described, e.g. in Eleftheriadis et al. (2009) and Stathopoulos et al. (2021), while the chapter 'ABC Svalbard' in SESS report 2019 (Gilardoni et al. 2020) compares the time series at the two sites.

To compare aerosol properties depending on the aerosol load, three aerosol situations have been distinguished using columnar information: low, moderate, and extreme AOD. Following an automatic methodology proposed by Mateos et al. (2020) and based on an AERONET AOD measurement strategy with a quality-control algorithm (Giles et al. 2019), AOD for fine and coarse modes at 500 nm (AOD_F and AOD_C respectively), are analysed for hourly data from Ny-Ålesund. If AOD_F is higher than the 85th percentile of all the time series or AOD_C is higher than the 93rd percentile (we select a higher percentile because of the lower probability that this mode will appear at the current location) an aerosol event is identified. When considering only those events with a total AOD (500 nm) <0.15, a mean value of AOD (500 nm) of 0.1 for them is obtained, which has been selected as threshold for moderate

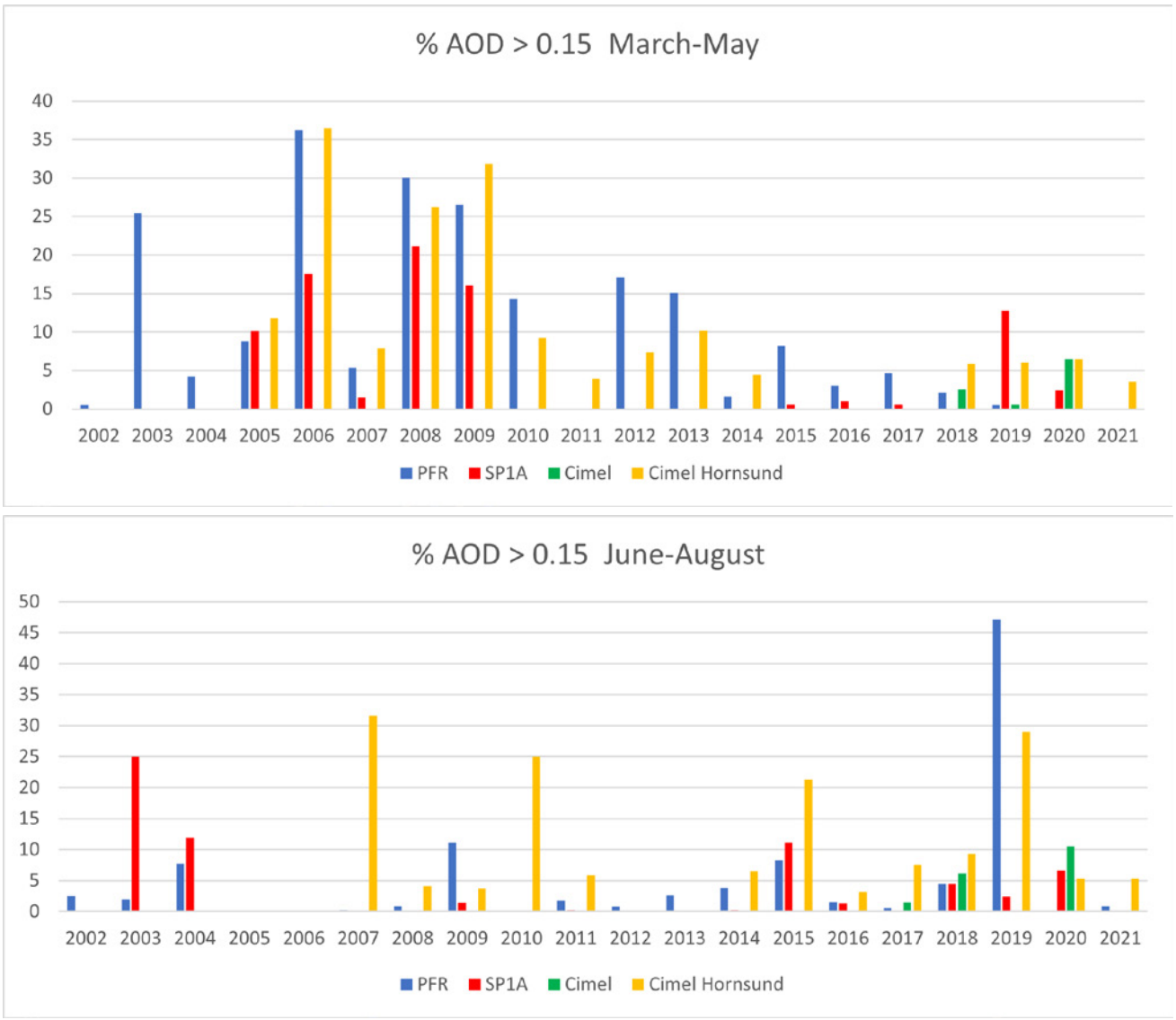

Figure 4: Frequency of high-AOD (>0.15 at 500 nm) episodes in the periods March–May (left panel) and June–August (right panel) for 4 sun photometers (3 in Ny-Ålesund, 1 in Hornsund). The CIMEL in Ny-Ålesund started operations in June 2017.

conditions. Therefore, a columnar low aerosol load is considered if the total AOD (500 nm) is below 0.1. If only those events with total AOD (500 nm) >0.15 are considered, a mean value of 0.24 is obtained, which has been selected as threshold for extreme conditions. Columnar moderate aerosol events correspond to total AOD between 0.1 and 0.24. And finally, columnar extreme aerosol events are those showing an AOD (500 nm) larger than 0.24.

Figure 5 compares the aerosol scattering, absorption, and extinction coefficients at 530 nm measured at the ground sites during periods characterised by low, moderate, and high AOD. The period from 9 July to 28 August 2019 was excluded from the analysis and is addressed separately. In general, higher coefficients are observed for moderate and high AOD episodes, with statistically significant differences compared to low-AOD periods (significance level 0.05). Differences are more pronounced for scattering and extinction coefficients, and during extreme AOD events.

We identified the time periods characterised by high aerosol extinction coefficient at ground level as those days characterised by coefficient values larger than the de-seasonalised average plus three times the standard deviation of the average. The comparison between the occurrences of moderate and high AOD and high extinction coefficient values indicate that a small fraction of aerosol transport episodes to Svalbard are detected at the

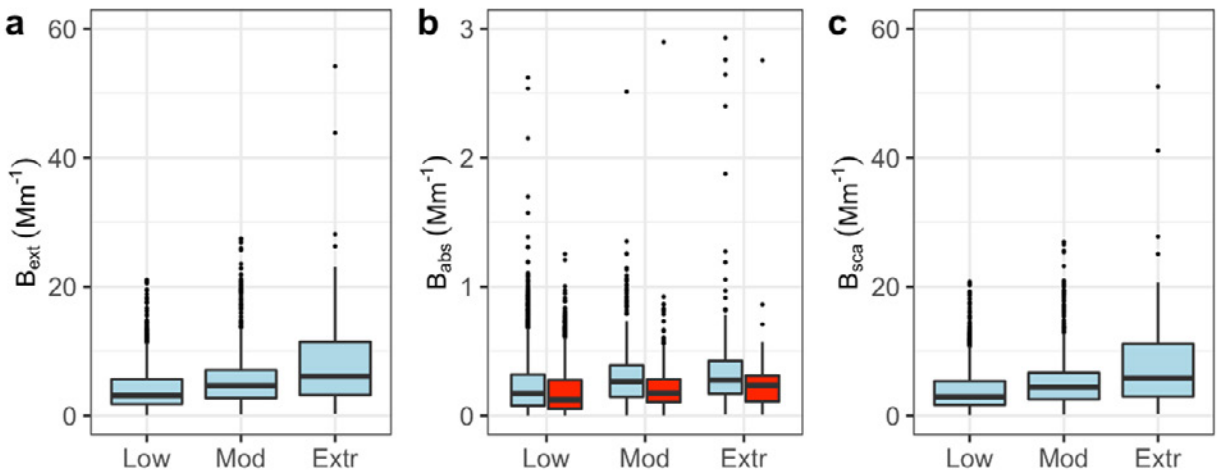

Figure 5: Box-whisker plot of extinction (panel a) absorption (panel b) and scattering (panel c) coefficients at Gruvebadet (in light blue) and Zeppelin (in red) during low, moderate and high AOD episodes. The box identifies the 25th and 75th percentile, the line inside the box corresponds to the median, the vertical lines extend to the minimum and maximum without outliers, while the dots indicate outliers. Gruvebadet and Zeppelin time series overlap partially and a direct comparison of the two sites is not discussed in this context.

ground. Depending on the AOD record, 67–89% of the moderate and high AOD events were not associated with a significant increase of the in-situ aerosol extinction coefficient (Hansen et al. 2022).

PFR AOD measurements in Ny-Ålesund, CIMEL measurements in Hornsund and Microtops measurements on board the research vessel *Oceania* in the Fram Strait revealed significantly elevated AOD values almost continuously from early July to early September 2019 (see Figure 6). For comparison, the 20-year monthly mean AOD values (PFR) are also included in the figure, proving that summer 2019 was exceptional, with July and August monthly means 2 to 3 times higher than long-term means. The general agreement between the three observation sites indicates that this must have been due to large-scale presence of aerosols. High aerosol loading was simultaneously observed by integrated column and in-situ measurements on 7–9 July, 17 July, and 5 August, but many high-AOD observations later in August are not seen in the in-situ data. The only way to clarify this discrepancy is through information about the altitude of the aerosol layer, which can be obtained from ground-based lidar (dependent on clear-sky conditions) and from space-based lidar observations.

2.2.2. Satellite observations of high-AOD episodes over Svalbard: a case study from July/August 2019

Satellite data can be of great value both to complement total column data in periods of cloudy ground conditions (caveat: AOD data usually are only derived for cloud-, ice- and snow-free pixels) and to identify the altitude distribution of aerosols and thus cast light on when AOD and in-situ measurements can be combined. Vertical profile information on aerosol extinction and polarisation can be obtained from the Cloud-Aerosol Lidar with Orthogonal Polarisation (CALIOP) on board the Cloud-Aerosol Lidar and Infrared Pathfinder Satellite Observations (CALIPSO) platform (Winker et al. 2009). Furthermore, the V4 level 2 cloud–aerosol discrimination (CAD) algorithm distinguishes between tropospheric and stratospheric aerosol subtypes (Kim et al. 2018). The data were downloaded from the ICARE Data and Services Center[3].

In Figure 7, we show two examples of level 2 data (version 4.20) curtains of the aerosol extinction at 532 nm to evaluate the vertical representation of the aerosols during the 2019 high-AOD episodes. White areas present regions with no signal (clouds inhibiting the observations below), clouds

3 https://www.icare.univ-lille.fr, last access: 08 August 2022

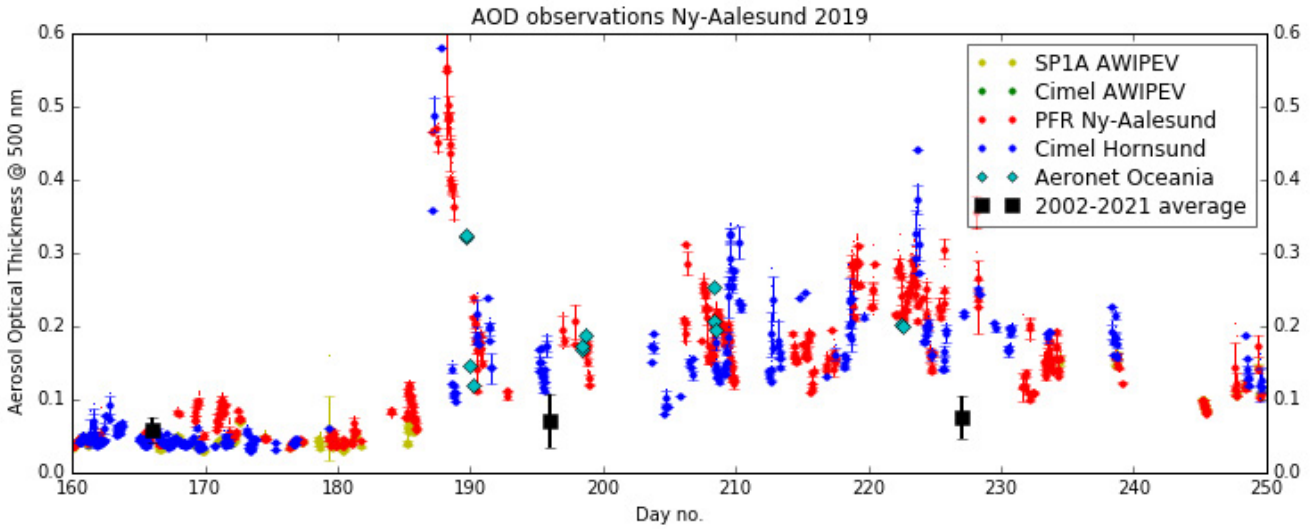

Figure 6: AOD measurements (hourly means with standard deviation of single measurements) performed in and around Svalbard in summer 2019 (9 June–6 September), with data from Ny-Ålesund, Hornsund and *R/V Oceania* (in the Fram Strait). Long-term monthly means of PFR measurements in Ny-Ålesund are shown as black squares with error bars. No CIMEL measurements were made in Ny-Ålesund in this time interval of 2019.

in the respective area or no aerosols. The most prominent case is from 6–7 July, with by far most PFR measurements on 7 July starting at 05:00 with values of around 0.5 (at 500 nm) and continuing until around 18:00 with AOD dropping to 0.36. On that occasion there are few data from Hornsund. On 7 July 03:15 UTC there was a CALIPSO overpass over Svalbard, close to Ny-Ålesund. Low-level clouds were obstructing the scenes between Ny-Ålesund and Hornsund, around 13°E and the view below 3 km altitude at Ny-Ålesund. The tropospheric aerosol layer reaching up to about 4 km altitude above Svalbard was classified as elevated smoke. A second, extended, period of high AOD values at Ny-Ålesund occurred from 6 (from 17:00) to 11 August (until 16:00), with AOD hourly means ranging from 0.2 to 0.31. There are few data from Hornsund at the beginning and end of the period which fit into the Ny-Ålesund measurements. Here, we show an example of a CALIOP curtain above Svalbard from the morning of 6 August, 09:05 UTC. Also on this occasion cloud cover around 5 km altitude obstructs some of the lower tropospheric aerosol observations over mid-/west Svalbard. The thick aerosol layer at 4–5 km altitude west of Svalbard is classified as elevated smoke, the three layers between Ny-Ålesund and Hornsund at about 6–7 km altitude are labelled as dust, polluted dust, and elevated smoke.

As an additional complication, a stratospheric sulphate aerosol layer occurred in summer 2019. This aerosol which could be observed from mid-July onward, was caused by the Raikoke volcano on the Kuril Islands in the western Pacific Ocean, which had a series of eruptions on 21–22 June 2019. The layer contributed an estimated AOD of up to 0.03 at 500 nm from mid-July to the end of August, i.e. exactly in the period with elevated AOD values in Svalbard, but it cannot alone explain the elevated AOD summer values seen in Figure 6. The event is discussed in detail in a recent publication by Kloss et al. (2021). Not considered here is the potential self-lifting of the large forest fires in Siberia, which could have caused an ascent of the smoke layer into the lower stratosphere, potentially leading to a misclassification of the CALIOP aerosol typing (see Ansmann et al. 2021).

2.2.3. Aerosol back-trajectory studies: A case study of the summer 2019 event

To investigate the possible origin of the aerosols on the two occasions presented in the previous section, the Lagrangian particle dispersion model FLEXPART (FLEXible PARTicle dispersion model) version 10.4 was used (Pisso et al. 2019). The model was driven by 3-hourly operational meteorological fields from the European Centre for Medium-Range Weather Forecasts (ECMWF) with 137 vertical

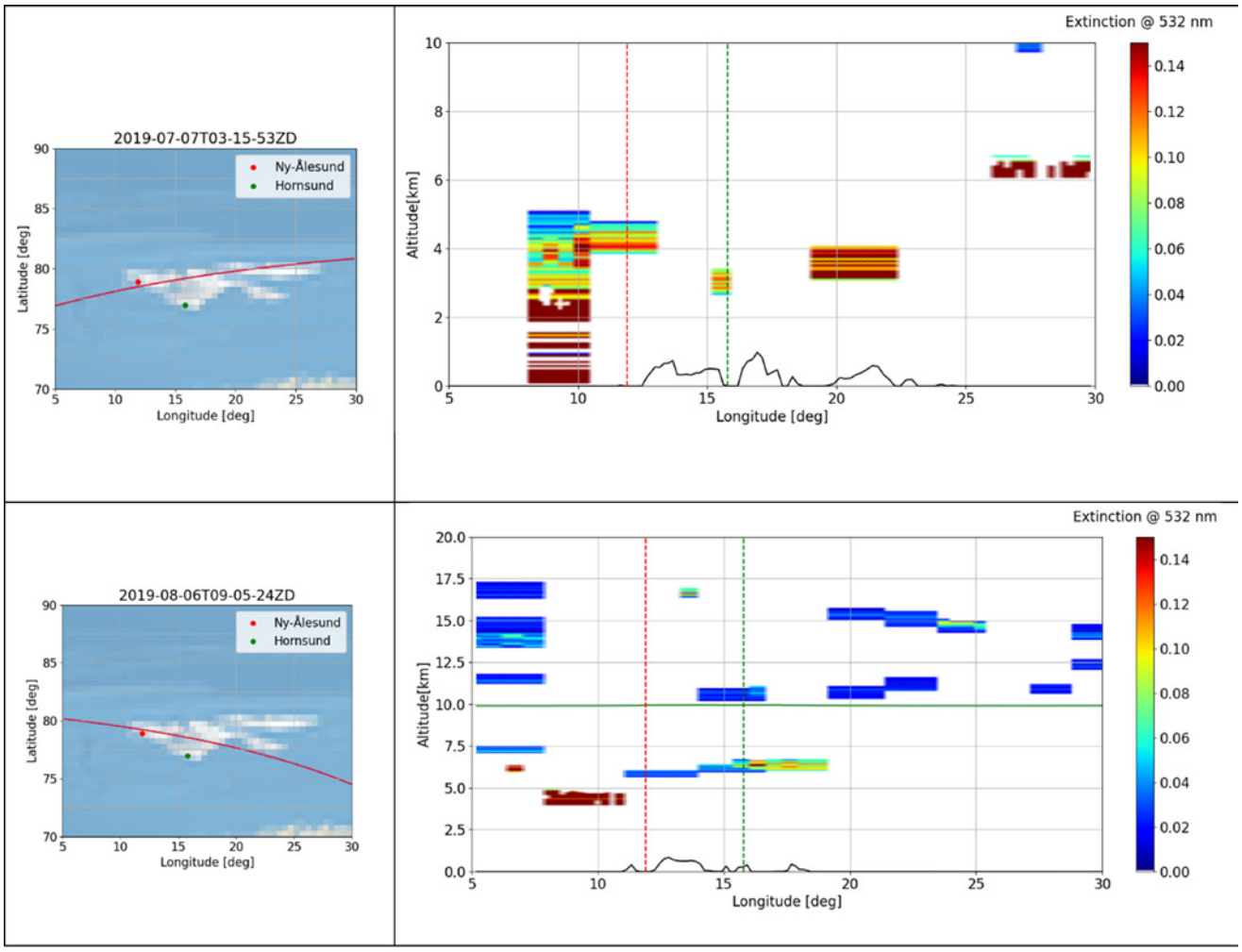

Figure 7: Aerosol extinction at 532 nm [units: km^{-1}] during two CALIOP overpasses (left panels: satellite geo-location): 7 July 2019, 03:15 (upper panel) and 6 August 2019, 09:05 (lower panel). Vertical dashed lines: ground station longitudes (red: Ny-Ålesund, green: Hornsund). Left panels: satellite geolocation maps.

levels and a horizontal resolution of 1°×1°. In FLEXPART, computational particles are released at the altitudes where they were detected by CALIOP and are tracked backward in time in FLEXPART's 'retroplume' mode. Simulations extended over 10 days backward in time, sufficient to include aerosol emissions from biomass burning arriving at the measurement site, given a typical aerosol lifetime of 1 week (Bond et al. 2013). The tracking includes gravitational settling for spherical particles of the size observed. FLEXPART differs from trajectory models due to its ability to simulate dry and wet deposition of gases or aerosols, turbulence, unresolved mesoscale motions, while it includes a deep convection scheme (see Pisso et al. 2019). For our simulations, we assumed that aerosols have a density of 1500 kg/m^3 (similar to black carbon) and follow a logarithmic size distribution with an aerodynamic mean diameter of 0.25 µm and a logarithmic standard deviation of 0.3 (Long et al. 2013).

Figure 8, left panel, shows the result for 7 July, 03:00 UTC, for an assumed aerosol height above Ny-Ålesund of 4–4.5 km. As the plume altitude was not known, the integrated footprint from 1 to 10 km was used. The figure shows a well-defined source region in Central Siberia which coincides very well with the location of extensive forest fires at the end of June and early July. The aerosols moved essentially straight northeastward towards Svalbard. This pattern was geographically very stable throughout 7 July. On 6 August, shown for one time slot in Figure 8, right panel, the situation was very different. On this day, the back-trajectories, now with a release height of 6 to 6.5 km, point towards northern Canada and Alaska, with an extension towards Siberia. In this

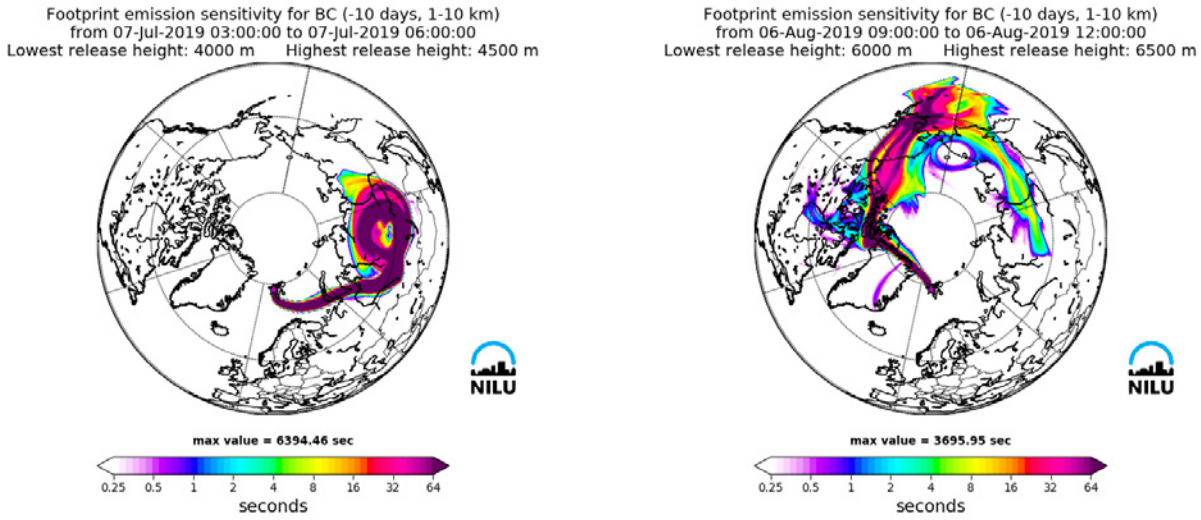

Figure 8: FLEXPART 10-day back-trajectory calculation of aerosols observed on 7 July (left panel) and 6 August (right panel), 2019.

case, the 10-day limitation probably was too short to mark Siberia as the origin of the aerosol; in Alaska, there were few fires in the 10 days prior to 6 August. There are also differences between Ny-Ålesund and Hornsund on this day, with clearly lower AOD values in the morning of 6 August over Hornsund increasing throughout the day. Back-trajectories from Hornsund show source regions over Greenland and the northwestern Atlantic for the morning of 6 August, then shifting to the same pattern as in Ny-Ålesund over the day, at the same time as AOD values reach the same level as in Ny-Ålesund.

These few samples of ground-based, satellite and model data show the potential of combining such data, but also the complexity to be considered. For example, we have not discussed here the possible contribution of the volcano aerosols mentioned above or the impact of deep injection processes of fire aerosols possibly reaching the lower stratosphere. The situation of summer 2019 definitely deserves a much more careful analysis than is possible within the scope of this SESS chapter. Thus, developing adequate tools for such occasions, which probably will occur more frequently in the future, will serve studies using a wide range of observations.

3. Contributions to interdisciplinarity

Aerosols and their effect on the atmosphere are an important aspect of the climate system, influencing both solar irradiation and formation of cloud nuclei with further implications on cloudiness. In the most recent published assessment (AR6) of the IPCC (IPCC 2021) the contribution from aerosols to changes in effective radiative forcing since 1750 remains the one with the largest uncertainty, especially the contribution of aerosol–cloud interactions. In the polar areas this uncertainty is even greater. During winter conditions, aerosol can warm the surface, favouring cloud formation and trapping long-wave radiation. In spring, deposition of light-absorbing aerosol reduces snow and ice albedo, accelerating their melting (e.g. Skiles et al. 2018). Finally, in spring and summer, aerosol contributes to scattering and absorption of incoming short-wave radiation, in addition to altering cloud properties. An improved monitoring of aerosol load will contribute to reducing these uncertainties. A second important field of interdisciplinary research is that of aerosols as a carrier of pollution from lower to high latitudes, i.e. from regions with high pollution load to those with little local and regional pollution (although also this pattern is changing with the increasing number of biomass burning events in the boreal zone).

4. Unanswered questions

Although the different photometers presented in this study do agree quite well in general, noticeable differences have been observed. The dominance of small-scale, micrometeorological phenomena in fjords affects sites like Ny-Ålesund and Hornsund in a complex manner, e.g. through aerosol advection at different altitudes. Potential resulting differences between the various AOD data sets are not yet fully understood, and efforts should continue to clarify these.

The closure between aerosol properties derived by in-situ and remote sensing instruments is still a challenging topic. Thanks to their very high time resolution and their availability at different places in and around Ny-Ålesund, photometer data are helpful to interpret, e.g. filter-based aerosol measurements in terms of uniform conditions or consistency.

The fraction of aerosol, which is principally missed by in-situ measurements due to advection altitudes in the free troposphere or even stratosphere is hard to assess. If the optical properties of aerosol at the ground and the height and stability of the boundary layer were known, the photometers could easily estimate the aerosol fraction aloft.

So far, there are far fewer AOD observations during polar night. This report is based on sun-photometer data. Hence a significant part of the annual cycle (about 5 months of the year) is still severely under-represented.

5. Recommendations for the future

- Sun AOD measurements should continue at both Hornsund and Ny-Ålesund as at present, while a third station in eastern Svalbard connected to a meteorological station should be established;
- An observation capacity on board a mobile platform (UAV, aircraft) with the possibility to perform limited campaigns during periods of elevated AOD measurements should be developed and stationed at Ny-Ålesund or Longyearbyen;
- More emphasis should be put on collecting data during the polar night, possibly through the establishment of a star photometer and further development of lunar AOD observations.
- Efforts to integrate in-situ, columnar, lidar (which have been performed at AWIPEV for many years), and satellite remote-sensing observations and combining them with various modelling tools such as FLEXPART should be intensified and streamlined for near-real-time applications in high-AOD episodes.

6. Data availability

Dataset	Parameter	Period	Location	Metadata access (URL)	Dataset contact
Aggregated AOD/ AE data from the Svalbard region	Aeorosol Optical Depth (4/5 wavelengths), Ångström Exponent	2002-2021	Sverdrup, AWIPEV (both Ny-Ålesund), Polish Polar Station (Hornsund)	https://doi.org/10.21343/1GAJ-4645	Kerstin Stebel (NILU) kst@nilu.no
Gruvebadet Atmosphere Laboratory data	Aerosol absorption coefficient and aerosol scattering coefficient	2010-2020	Gruvebadet	https://metadata.iadc.cnr.it/geonetwork/srv/eng/catalog.search#/metadata/ee3fb49e-c3e2-4572-95b8-1e7ff6361ac5 https://metadata.iadc.cnr.it/geonetwork/srv/eng/catalog.search#/metadata/534d6e9e-8bb5-40d1-8ddd-1092e0373584	Stefania Gilardoni (IPS-CNR) stefania.gilardoni@cnr.it
Zeppelin Observatory data	Aerosol absorption coefficient	2005-2021	Zeppelin Mt	https://ebas-data.nilu.no/Pages/DataSetList.aspx?key=8AFF59A5D-0A845C7833AE6F65D-990D5C	Kostas Eleftheriadis (NCSR Demokritos) eleftheriadis@ipta.demokritos.gr

7. Acknowledgements

This work was supported by the Research Council of Norway, project number 322387, Svalbard Integrated Arctic Earth Observing System – Knowledge Centre, operational phase 2022. We are grateful for the technical support from the Norwegian Polar Institute for the PFR measurements in Ny-Ålesund and in-situ measurements at Zeppelin Observatory. We also gratefully acknowledge the use of imagery provided by services from NASA's Global Imagery Browse Services (GIBS), part of NASA's Earth Observing System Data and Information System (EOSDIS).

8. References

Ansmann A, Ohneiser K, Chudnovsky A, Baars H, Engelmann R (2021) CALIPSO Aerosol-Typing Scheme Misclassified Stratospheric Fire Smoke: Case Study From the 2019 Siberian Wildfire Season. Front Environ Sci 9:769852. https://doi.org/10.3389/fenvs.2021.769852

Bond TC, Doherty SJ, Fahey DW, Forster PM, Berntsen T, DeAngelo BJ et al (2013) Bounding the role of black carbon in the climate system: A scientific assessment. J Geophys Res Atmos 118(11):5380-5552. https://doi.org/10.1002/jgrd.50171

Cuevas E, Romero-Campos PM, Kouremeti N Kazadzis S, Räisänen P, Garcia RD, Barretto A, Guirado-Fuentes C, Ramos R, Toledano C, Almansa F, Grübner J (2019) Aerosol optical depth comparison between GAW-PFR and AERONET-Cimel radiometers from long-term (2005-2015) 1 min synchronous measurements. Atmos Meas Tech 12:4309-4337. https://doi.org/10.5194/amt-12-4309-2019

Eleftheriadis K, Vratolis S, Nyeki S (2009) Aerosol black carbon in the European Arctic: Measurements at Zeppelin station, Ny-Ålesund, Svalbard from 1998–2007. Geophys Res Lett 36(2). https://doi.org/10.1029/2008GL035741

Gilardoni S, Lupi A, Mazzola M, Cappelletti DM, Moroni B, Ferrero L, Markuszewski P, Rozwadowska A, Krecji R, Zieger P, Tunved P, Karlsson L, Vratolis S, Eleftheriadis K, Viola AP (2020) Atmospheric black carbon in Svalbard. In: Van den Heuvel et al. (eds): SESS report 2019, Svalbard Integrated Arctic Earth Observing System, Longyearbyen, pp 196–211. https://doi.org/10.5281/zenodo.4707201

Giles DM, Sinyuk A, Sorokin MG, Schafer JS, Smirnov A, Slutsker I, Eck TF, Holben BN, Lewis JR, Campbell JR, Welton EJ, Korkin SV, Lyapustin AI (2019) Advancements in the Aerosol Robotic Network (AERONET) Version 3 database

– automated near-real-time quality control algorithm with improved cloud screening for Sun photometer aerosol optical depth (AOD) measurements. Atmos Meas Tech 12:169-209. https://doi.org/10.5194/amt-12-169-2019

Hansen GH, Zielinski T, Pakszys P, Rittre C, Gilardoni S, Eleftheriadis K, Kouremeti N, Mateos D, Herrero S, Kazadzis S, Mazzola M, Stebel K (2022) Re-evaluation and Homogenization of Aerosol Optical Depth Observations in Svalbard (ReHearsol). RCN Project No: 311250/E40 - ReHearsol Final Report (NILU report 03/2022). Kjeller: NILU

Holben BN, Eck TF, Slutsker I, Tanré D, Buis JP, Setzer A, Vermote E, Reagan JA, Kaufman YJ, Nakajima T, Lavenu F, Jankowski I, Smirnov A (1998) AERONET – A Federated Instrument Network and Data Archive for Aerosol Characterization. Rem Sens Envir 66(1):1-16. https://doi.org/10.1016/S0034-4257(98)00031-5

IPCC (2021) Climate Change 2021: The Physical Science Basis. Contribution of Working Group I to the Sixth Assessment Report of the Intergovernmental Panel on Climate Change. Masson-Delmotte V, Zhai P, Pirani A et al (eds) Cambridge: Cambridge University Press. In Press

Kazadzis S, Kouremeti N, Nyeki S, Gröbner J, Wehrli C (2018) The World Optical Depth Research and Calibration Center (WORCC) quality assurance and quality control of GAW-PFR AOD measurements. Geosci Instrum Method Data Syst 7(1):39-53. https://doi.org/10.5194/gi-7-39-2018

Kim M-H, Omar AH, Tackett JL et al (2018) The CALIPSO version 4 automated aerosol classification and lidar ratio selection algorithm Atmos Meas Tech 11:6107-6135. https://doi.org/10.5194/amt-11-6107-2018

Kloss C, Berthet G, Sellitto P et al (2021) Stratospheric aerosol layer perturbation caused by the 2019 Raikoke and Ulawun eruptions and their radiative forcing. Atmos Chem Phys 21:535-560. https://doi.org/10.5194/acp-21-535-2021

Long CM, Nascarella MA, Valberg PA (2013) Carbon black vs. black carbon and other airborne materials containing elemental carbon: Physical and chemical distinctions. Environ Pollut 181:271-286. https://doi.org/10.1016/j.envpol.2013.06.009

Markowicz KM, Pakszys P, Ritter C et al (2016) Impact of North American intense fires on aerosol optical properties measured over the European Arctic in July 2015. J Geophys Res Atmos 121(24):14487-14512. https://doi.org/10.1002/2016JD025310

Mateos D, Cachorro VE, Velasco-Merino C et al (2020) Comparison of three different methodologies for the identification of high atmospheric turbidity episodes. Atmos Res 237(26):104835. https://doi.org/10.1016/j.atmosres.2019.104835

Mazzola M, Stone RS, Herber A et al (2012) Evaluation of sun photometer capabilities for retrievals of aerosol optical depth at high latitudes: The POLAR-AOD intercomparison campaigns. Atmos Env 52:4-17. https://doi.org/10.1016/j.atmosenv.2011.07.042

Pacszys P, Zielinski T (2017) Aerosol optical properties over Svalbard: a comparison between Ny-Ålesund and Hornsund. Oceanologia 59(4):431-444. https://doi.org/10.1016/j.oceano.2017.05.002 Pisso I, Sollum E, Grythe H (2019) The Lagrangian particle dispersion model FLEXPART version 10.4, Geosci Model Dev 12:4955-4997. https://doi.org/10.5194/gmd-12-4955-2019

Skiles SM, Flanner M, Cook JM, Dumont M, Painter TH (2018) Radiative forcing by light-absorbing particles in snow. Nature Climate Change 8:964-971. https://doi.org/10.1038/s41558-018-0296-5

Stathopoulos VK, Evangeliou N, Stohl A, Vratolis S, Matsoukas C, Eleftheriadis K (2021) Large circulation patterns strongly modulate long-term variability of Arctic black carbon levels and areas of origin. Geophys Res Lett 48(19) https://doi.org/10.1029/2021GL092876

Stohl A, Berg T, Burkhart JF et al (2007) Arctic smoke – record high air pollution levels in the European Arctic due to agricultural fires in Eastern Europe in spring 2006. Atmos Chem Phys 7:511-534. https://doi.org/10.5194/acp-7-511-2007

Stone RS, Sharma S, Herber A, Eleftheriadis K, Nelson DW (2014) A characterization of Arctic aerosols on the basis of aerosol optical depth and black carbon measurements. Elementa: Science of the Anthropocene 2:000027 https://doi.org/10.12952/journal.elementa.000027

Tomasi, C, Kokhanovsky AA, Lupi A, Ritter C et al (2015) Aerosol remote sensing in polar regions. Earth Sci Rev 140:108-157. https://doi.org/10.1016/j.earscirev.2014.11.001

Winker DM, Vaughan MA, Omar A et al (2009) Overview of the CALIPSO mission and CALIOP data processing algorithms. J Atmos Ocean Tech 26(11):2310-2323. https://doi.org/10.1175/2009JTECHA1281.1

WMO (2016) Aerosol Measurement Procedures, Guidelines and Recommendations, 2nd Edition. WMO No 1177. https://library.wmo.int/doc_num.php?explnum_id=3073

Xian P, Zhang J, O'Neill NT et al (2022a) Arctic spring and summertime aerosol optical depth baseline from long-term observations and model reanalyses – Part 1: Climatology and trend. Atmos Chem Phys 22:9915-9947. https://doi.org/10.5194/acp-22-9915-2022

Xian P, Zhang J, O'Neill NT et al (2022b) Arctic spring and summertime aerosol optical depth baseline from long-term observations and model reanalyses – Part 2: Statistics of extreme AOD events, and implications for the impact of regional biomass burning processes. Atmos Chem Phys 22:9949-9967. https://doi.org/10.5194/acp-22-9949-2022

Zielinski T, Bolzacchini E, Cataldi M et al (2020) Study of Chemical and Optical Properties of Biomass Burning Aerosols during Long-Range Transport Events toward the Arctic in Summer 2017. Atmosphere 11(1):84. https://doi.org/10.3390/atmos11010084

Appendix 1: Ny-Ålesund AOD inter-comparison – details

The PFR is a temperature-stabilised filter radiometer equipped with four interference filters. The calibration of the PFR is performed on a yearly basis at PMOD/WRC against the WMO AOD reference instruments (Kazadzis et al. 2018). The SP1A has been calibrated on an annual or biannual basis using the Langley method during 3-month campaigns at Izaña, Tenerife. Finally, the CIMEL instrument as a part of AERONET is following the standard calibration procedure of the network (Holben et al. 1998).

The basic characteristics of the compared filter radiometers are shown in Table A1.

The comparison has been done against the PFR instruments. Specifically, the PFR AOD measurements at the nominal wavelengths 368, 412, 500 and 862 nm have been compared to the SP1A AOD at the same nominal wavelengths with the actual differences of the centroid wavelengths of the interference filters to be within ±3 nm. For the CIMEL instrument the AOD values at 500 nm, and 870 nm have been directly compared to 500 nm and 862 nm (negligible AOD differences in that spectral region) respectively, while 380 nm and 440 nm (CIMEL) were compared interpolating the PFR-AOD to those wavelengths using the PFR Ångström exponent. The single AOD measurements have been synchronised to ±30 sec time windows.

The differences as a function of time are shown in Figure A1 for PFR and SP1A and in Figure A2 for PFR and CIMEL, while in the right panel the distribution of these differences is given. The normalised distributions are scaled to the percentage of measurements of the peak of the histogram. The overall comparison results are summarised in Table 2 (main document) and the statistics per year in Tables A2 and A3.

The dataset of the PFR instruments is described in 'WORCC-PMOD/WRC quality-assured aerosol optical depth and Ångström exponent for Ny-Ålesund GAW station (2002–present).[1]

Table A1: Basic characteristics of filter radiometers.

	Centroid wavelengths (nm)	Bandwidth (nm)	Field of View (FWHM, deg)	Dataset period	Temperature stabilisation
PFR	368, 412, 500, 862	4-5	2.5	2002-2021	Yes
SP1A	368,412,500,610,675,778,861,945,1020	4-10	2.5	2004-2020	No
CIMEL	340,380,440,500,675,870,945,1020	3-10	1.2	2017-2021	No

1 https://doi.org/10.5281/zenodo.7191072

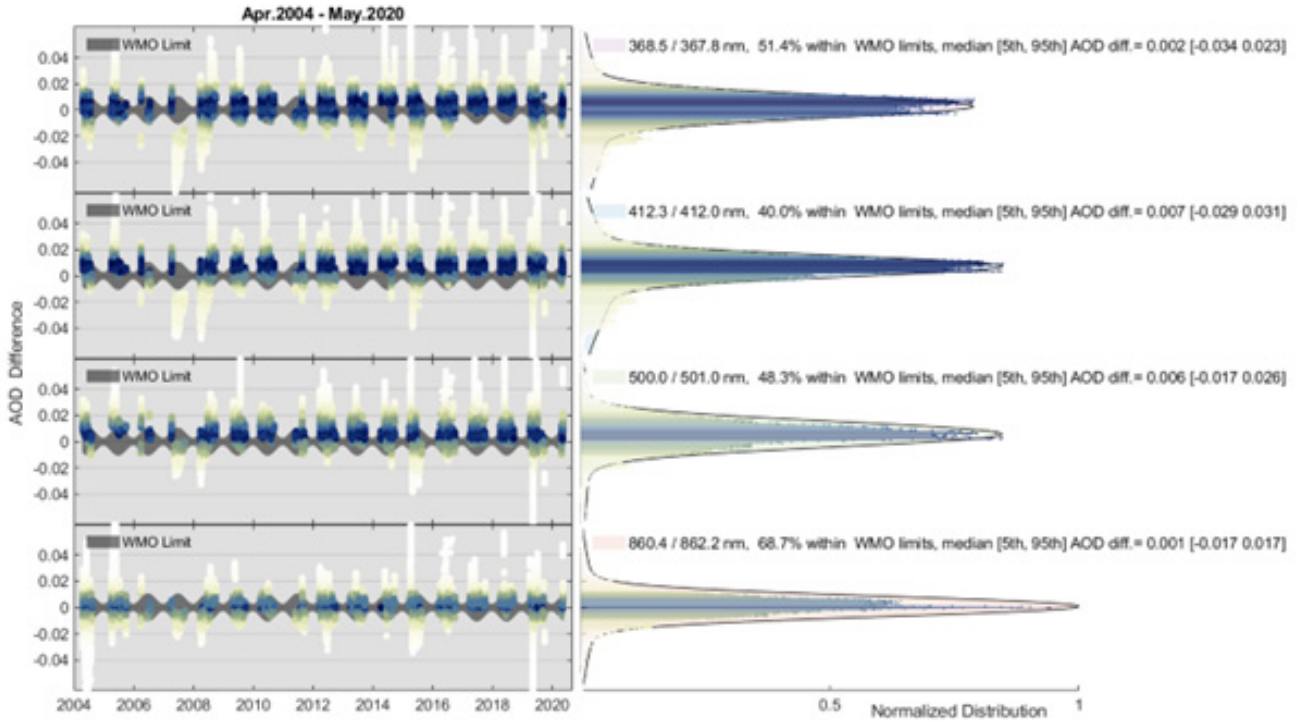

Figure A1: Left panels: AOD difference PFR-SP1A at nominal wavelength 368 nm, 412 nm, 500 nm and 862 nm for the period Apr 2004 to May 2020. The dark shaded area represents the WMO limit for AOD agreement between two instruments. The AOD difference (dots) is coloured based on the probability density function shown in the coloured bars on the right panel. Right panels: Normalised probability density functions of the AOD differences for each wavelength (bars) and approximated by triple gaussian distribution functions (coloured shaded areas).

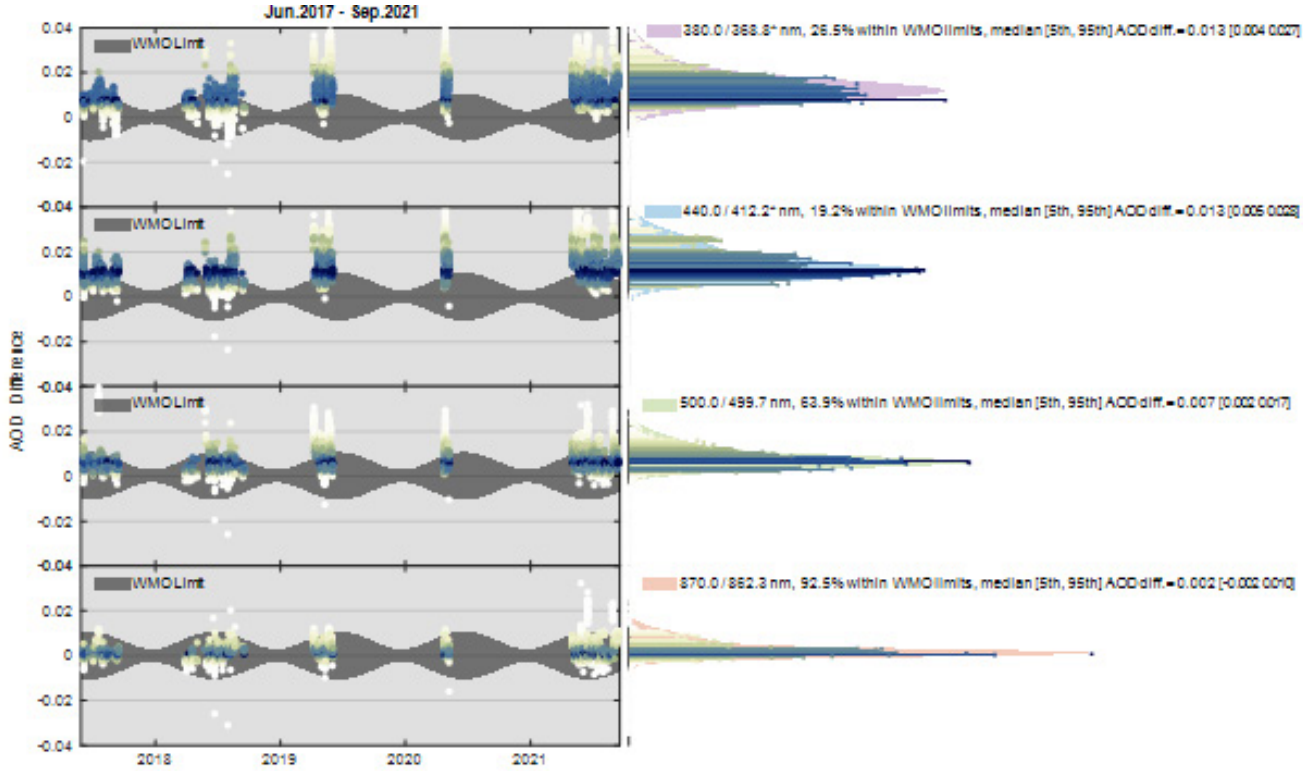

Figure A2: Left panels: AOD difference PFR-CIMEL at nominal wavelength 380 nm, 440 nm, 500 nm and 870 nm for the period Jun 2017 to Sep 2021. The dark shaded area represents the WMO limit for AOD agreement between two instruments. The AOD difference (dots) is coloured based on the probability density function shown in the coloured bars on the right panel. Right panels: Normalised probability density functions of the AOD differences for each wavelength (bars) and approximated by triple gaussian distribution functions (coloured shaded areas).

Table A2: Comparison result of AOD at four common wavelengths between PFR and SP1A. The statistics are presented per year and for the whole dataset.

	Median AOD difference (PFR-SP1A)				Standard deviation				Within WMO limit (%)				Correlation Coefficient				Number of compared points (x1000)
year	368 nm	412 nm	500 nm	862 nm	368 nm	412 nm	500 nm	862 nm	368 nm	412 nm	500 nm	862 nm	368 nm	412 nm	500 nm	862 nm	
2004	-0.007	0.006	0.010	0.006	0.009	0.008	0.009	0.015	54	**67**	44	47	0.982	0.985	0.966	0.487	10
2005	0.005	0.015	0.023	0.017	0.015	0.016	0.012	0.019	54	32	5	21	0.976	0.965	0.967	0.523	4
2006	0.011	0.006	0.016	0.014	0.015	0.013	0.012	0.012	29	32	39	31	0.947	0.952	0.941	0.890	2
2007	-0.031	-0.026	-0.007	-0.009	0.016	0.014	0.009	0.005	1	0	52	40	0.905	0.912	0.935	0.873	17
2008	-0.013	-0.012	0.001	-0.004	0.019	0.021	0.012	0.011	11	10	61	56	0.958	0.941	0.968	0.857	14
2009	0.001	0.000	0.011	0.000	0.008	0.007	0.010	0.005	**85**	**85**	36	**92**	0.984	0.982	0.951	0.909	14
2010	0.004	0.007	0.014	0.003	0.005	0.009	0.005	0.004	**75**	61	14	**93**	0.982	0.932	0.953	0.919	16
2011	-0.003	-0.001	0.003	-0.005	0.009	0.011	0.007	0.007	**85**	**84**	**89**	**74**	0.933	0.878	0.896	0.483	5
2012	0.001	-0.001	0.010	0.002	0.010	0.009	0.009	0.007	**75**	**74**	33	**77**	0.967	0.965	0.944	0.852	24
2013	0.002	0.014	0.008	0.003	0.010	0.010	0.007	0.006	51	13	46	**83**	0.960	0.955	0.953	0.837	23
2014	0.014	0.015	0.011	0.007	0.010	0.008	0.007	0.006	5	2	33	**70**	0.974	0.983	0.974	0.911	15
2015	-0.006	0.001	-0.008	-0.010	0.029	0.028	0.026	0.024	45	60	34	25	0.793	0.756	0.698	0.309	24
2016	0.002	0.006	0.000	-0.001	0.009	0.009	0.007	0.007	**77**	59	**89**	**88**	0.977	0.972	0.971	0.852	32
2017	0.008	0.012	0.009	0.007	0.006	0.009	0.007	0.004	51	15	45	**71**	0.985	0.960	0.953	0.911	20
2018	0.009	0.011	0.007	0.006	0.007	0.007	0.008	0.005	39	15	60	**78**	0.987	0.985	0.965	0.926	18
2019	-0.002	0.004	0.001	-0.002	0.043	0.041	0.038	0.024	46	31	50	55	0.696	0.704	0.598	0.234	19
2020	0.002	0.004	0.003	0.001	0.008	0.007	0.006	0.005	**66**	56	**96**	**98**	0.925	0.905	0.894	0.689	7
All Years	**0.002**	**0.007**	**0.006**	**0.001**	**0.020**	**0.020**	**0.017**	**0.013**	**51**	**40**	**48**	**69**	**0.907**	**0.891**	**0.863**	**0.656**	**265**

Table A3: Comparison result of AOD at four wavelengths between PFR and CIMEL. The PFR-AOD at 380 nm and 440 nm has been retrieved from interpolation of 368 nm and 412 nm AOD using the PFR-AE. The statistics are presented per year and for the whole dataset. Wavelengths marked with * were interpolated using the Ångström exponent to match the CIMEL wavelength.

	Median AOD difference (PFR-SP1A)				Standard deviation				within WMO limit (%)				Correlation Coefficient				Number of compared points
CIMEL	380 nm	440 nm	500 nm	870 nm	380 nm	440 nm	500 nm	870 nm	380 nm	440 nm	500 nm	870 nm	380 nm	440 nm	500 nm	870 nm	
PFR	368 nm*	412 nm*	500 nm	862 nm	368 nm*	412 nm*	500 nm	862 nm	368 nm*	412 nm*	500 nm	862 nm	368nm*	412 nm*	500 nm	862 nm	
2017	**0.006**	**0.007**	**0.005**	**0.001**	**0.003**	**0.003**	**0.002**	**0.001**	**82.4**	**66.4**	**90.8**	**99.5**	**0.97**	**0.98**	**0.96**	**0.97**	666
2018	**0.007**	**0.007**	**0.003**	**-0.001**	**0.004**	**0.004**	**0.003**	**0.003**	**71.1**	**71.2**	**93.2**	**97.7**	**0.99**	**0.99**	**0.98**	**0.96**	789
2019	0.015	0.013	0.008	0.003	0.007	0.006	0.006	0.003	13.7	14.6	52.5	91.4	0.95	0.96	0.92	0.87	747
2020	0.014	0.015	0.010	0.003	0.006	0.006	0.004	0.002	22.9	16.2	39.3	98.0	0.89	0.87	0.91	0.93	1423
2021	0.014	0.015	0.007	0.002	0.005	0.005	0.003	0.003	16.8	7.2	64.3	89.4	0.99	0.98	0.98	0.94	5404
All Years	**0.013**	**0.013**	**0.007**	**0.002**	**0.006**	**0.006**	**0.004**	**0.003**	**26.5**	**19.2**	**63.9**	**92.5**	**0.99**	**0.98**	**0.98**	**0.94**	**8722**

Dust in Svalbard: local sources versus long-range transported dust (SVALDUST)

Biagio Di Mauro[1], David Cappelletti[1,2], Beatrice Moroni[2], Mauro Mazzola[1], Stefania Gilardoni[1], Bartłomiej Luks[3], Adam Nawrot[3], Marek Lewandowski[3], Pavla Dagsson Waldhauserova[4,5], Outi Meinander[6], Monika Wittmann[7], Susan Kaspari[8], Alia Khan[9]

1 Institute of Polar Sciences, National Research Council of Italy, Venice, Italy
2 University of Perugia, Perugia, Italy
3 Institute of Geophysics, Polish Academy of Sciences, Warszawa, Poland
4 Agricultural University of Iceland, Hvanneyri, Iceland
5 Czech University of Life Sciences Prague, Prague, Czech Republic
6 Finnish Meteorological Institute, Aerosols and Climate, Helsinki, Finland
7 Independent researcher
8 Central Washington University, Ellensburg, USA
9 Western Washington University, Bellingham, USA

Corresponding author: Biagio Di Mauro, biagio.dimauro@cnr.it
ORCID number: 0000-0002-8161-3962

Keywords: Dust, aerosol, Svalbard, snow, radiative forcing

DOI: https://doi.org/10.5281/zenodo.7377518

1. Introduction

1.1. What is dust

Dust particles are commonly defined according to their size, including clay-sized (<4 µm), silt-sized (4–62.5 µm) or sand-sized (62.5 µm –2 mm) material (UNCCD 2022). Giant dust particles (>75 µm in diameter) of wind-blown mineral have been observed at large (>10 000 km) distances from their source, and individual giant Saharan dust particles of up to 450 µm in diameter have been sampled in air over the Atlantic Ocean at 2 400 and 3 500 km from the west African coast (van der Does et al. 2018). The dust cycle contains sediments that travel within the atmosphere mainly by suspension, and that can be deposited on land, in lakes, or in the ocean (Bullard et al. 2016). The main source of these microscopic particles is the ground and the lifting energy is provided by the wind; thus the usual terminology for these particles is 'mineral dust' or 'aeolian dust'.

The role of aeolian dust for the radiation balance of the Earth is size-dependent. Dust has a direct cooling effect when particles of size <2 µm are transported into the high atmosphere and block incoming sunlight (e.g. Claquin et al. 2003). Mineral dust deposited and trapped on the cryosphere (cryodust; see Lewandowski et al. 2020) can impact snow and ice properties, contributing to the mass balance of glaciers, lowering their albedo (Lambert et al. 2013; Goelles et al. 2017, as well as influencing rheological properties of ice (Green and Mahajan 2005). Dust records from the ice core may illustrate potential changes in dust emissions or transportation pathways over long time scales.

Dust loading in the atmosphere has increased by 25-100% since pre-industrial time (Kok et al. 2021). There is an estimated two billion tonnes of dust travelling in the atmosphere every year, and double this mass if sand and giant particles are included (van der Does et al. 2018; Dagsson-Waldhauserova et al. 2019). Changes in the emission of high latitude dust (HLD) have not yet been estimated, but first estimates are that HLD contributes about 5% to global dust emissions (Bullard et al. 2016;

Dust types used in this chapter

High Latitude Dust – dust originating from cold arid areas of ≥ 50°N and ≥ 40°S with size up to 100 µm. Northern dust sources are in Alaska, Canada, Denmark, Greenland, Iceland, Svalbard, Sweden, and Russia and southern dust sources are in Antarctica, Patagonia and New Zealand.

Volcanic dust – dust of volcanic origin which was re-suspended/emitted from old to ancient tephra deposits in volcanic deserts often located in proximity to glaciers. Volcanic dust is mainly driven by glaciofluvial processes and by wind-recycled tephra sediment transport. It is sometimes referred to as dust from the volcaniclastic deserts in high latitudes. Volcanic dust is dark in colour and has greater radiative forcing impacts than mineral dust, especially when deposited on the cryosphere where the impacts are similar to those of black carbon.

Glacigenic dust – dust suspended during glacial periods, but also refers to contemporary dust from cold regions. This term was used before HLD was defined.

Cryodust – natural abiotic particulate matter deposited and trapped in glaciers.

Coal dust – dark dust particles from coal mines at high latitudes, usually deposited on the cryosphere that is in close proximity or downwind of the mine.

Light Absorbing Impurities / Light Absorbing Particles – the term light-absorbing impurities (LAI) refers to impurities (including also other than particles, e.g. algae) in snow and ice, while the term light absorbing particles (LAP) refers to particles in the atmosphere or in snow and ice.

Meinander et al. 2022). Sand and dust storms, including HLD, were identified as a hazard that affects 11 of the 17 Sustainable Development Goals (UNCCD 2022).

1.2. General information on dust at high latitudes

High-latitude (HL) sites and regions can be sources and receptors of dust. In the latter case, dust can be both local and long-range transported to the receptor sites.

Like desert dust around the world, HLD also consists of various parent materials. Icelandic, Alaskan, some Canadian, and some Antarctic sources are of volcanic origin with high proportion of iron oxides and low proportion of quartz compared to low latitude deserts (Bachelder et al. 2020; Baldo et al. 2020; Crusius et al. 2021). Dust from the other source areas show variable amounts of a dual component from sedimentary covers and metamorphic complexes (Moroni et al. 2016, 2018).

It is estimated that HLD contributes 5% to the global dust budget and active HLD sources cover >1 500 000 km^2 (Bullard et al. 2016 Meinander et al. 2022). Arctic HLD sources are estimated to contribute 1-3% of the global dust with area of >1 000 000 km^2 (Groot Zwaafting et al. 2016; Meinander et al. 2022). It is estimated that during years when dust activity in enhanced, about 5.5% of the Arctic land areas are active dust sources (>1 mil. km^2, Meinander et al. 2022). The most active research has been done in Iceland, Canada, Alaska, and Greenland (Crusius et al. 2011; Arnalds et al. 2016; Bachelder et al. 2020). Model simulations by Groot Zwaaftink et al. (2016) showed that dust surface concentrations and deposition in the Arctic are dominated by the local high-latitude sources, due to limited convection and efficiency of removal processes.

1.3. Objectives of this report

The main objectives of this report are as follows:

- to identify and characterise local and long-range dust sources in Svalbard
- to summarise available information on dust sources in Svalbard and evaluate contributions to dust load from long-range transport
- to propose for the future a plan/strategy for the collection, treatment, evaluation, and harmonisation of new data on the subject

2. Overview of existing knowledge

2.1. Dust sources over Svalbard

Local and long-range sources of dust have been recognised in Svalbard, which are quite well distinguishable from each other due to the presence of specific mineral phases and / or mineralogical assemblies. Estimated dust loads in central and southern Svalbard from different sources range from 4 g up to 4-5 kg per m^2 per year (Rymer et al. 2022). In the Hornsund region the annual aeolian accumulation rate was estimated to between 29-117 g/m^2 (Pekala 1980) and 300-400 g/m^2 (Czeppe 1968) and to 2.66-24.56 g/m^2 per snow season (Kavan et al. 2020). At lower elevations up to 300 metres above sea level, local dust is more prevalent than dust from long-distance transport.

2.2. Local sources

Svalbard has been recognised as an important HLD source with several active hotspots in northwestern, central and southern Svalbard (Meinander et al. 2022). In Ny-Ålesund local dust dominates in the summer–fall period (Moroni et al. 2016, 2018), while Hornsund reports local dust as early as late spring and throughout the melting season (Zwolinski et al. 2013; Kavan et al. 2020; Lewandowski et al. 2020; Spolaor et al. 2021). Dust storms have been reported in Longyearbyen (Dörnbrack et al. 2010; Khan et al. 2017; Kandler et al. 2020), in Pyramiden and Ebba Valley (Strzelecki and Long 2020; Kavan et al. 2020), as well as at the forefield of the Werenskioldbreen glacier (Migała

and Sobik 1984). Although it has been shown that HLD sources can also be active during winter (Dagsson-Waldhauserova et al. 2019; Meinander et al. 2022), no evidence of dust emissions occurring in this season is reported for Svalbard.

Periglacial and proglacial areas are the main local dust sources in Svalbard (Zwoliński et al. 2013). These areas develop at the edge of glaciers or within glacial valleys, and they are increasing in size due to accelerated glacier ablation. These areas affect the narrow coastal or nearshore plains that border the entire archipelago. Glacial valleys, instead, develop radially from the inland to the coast. They are very extensive, quite stable in general and, thus, able to supply dust sediments more regularly than coastal plains during the year.

The mineralogical assemblage and the mineral chemistry of local dust (Moroni et al. 2016, 2018; Lewandowski et al. 2020) clearly reflect the geological features of the sites, marked by the presence of different sedimentary units overlying diverse metamorphic complexes, and small magmatic units (Dallmann 2015).

The presence and production of anthropogenically-derived dust on Svalbard is also evident from observational studies of dust collected in proximity to coal mines near Longyearbyen and Svea, which were active at the time of the studies (Aamaas et al. 2011; Khan et al. 2017). Up to 4863 ng/g of coal dust was found near Mine 7 in Longyearbyen and in Svea while the mines were active, and has been shown to reduce spectral albedo of surface snow by up to 84% directly next to the mine and up to 55% within 0.5 km downwind of the mine (Khan et al. 2017). These coal dust deposits are visible dark scars along the otherwise pristine landscape (Figure 1).

2.3. Long-range sources

Long-range transport to Spitsbergen involves dust from high- to low-latitude regions. According to global transport model simulations (Groot Zwaaftink et al. 2016; Figure 2), the largest contribution to Svalbard comes from Africa, Asia and, above all, Eurasia, while the contribution from Iceland, North America and, especially, from Greenland is much smaller. In addition, dust from remote sources shows a marked seasonal trend with highs in late winter/spring and lows in summer/autumn.

Results from field observations confirm some of the model results. In particular, Crocchianti et al. (2021)

Figure 1. Mine 7 near Longyearbyen (Breinosa mountain). Note the dark coal dust deposits on surface snow. Photo: Alia Khan

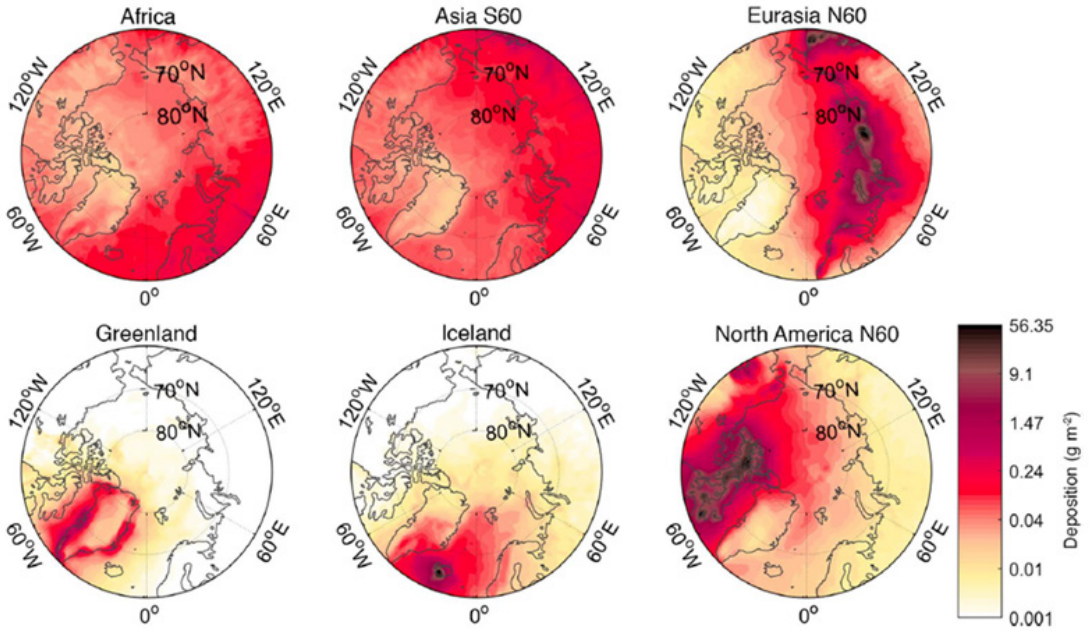

Figure 2. Simulated annual wet and dry deposition of dust (g/m^2) in the Arctic originating from different source regions averaged for the period 2010-2012. Reprinted from Groot Zwaafting et al. 2016, with permission of the authors.

have identified HL sources for the dust reaching Ny-Ålesund to be Eurasia, Greenland, Arctic-Alaska and Iceland. In addition, the mineralogy and the mineral chemistry of dust with respect to the parent soils made it possible to distinguish the local dust fraction from those of Iceland, Siberia and Alaska (Moroni et al. 2016, 2018, 2020). The presence of Saharan dust, including giant quartz particles, and Asian dust is documented over the Arctic (Groot Zwaafting et al. 2016; Varga et al. 2021), but not directly in Svalbard. In a study comparing dust deposition at Pyramiden and Hornsund, Kavan et al. (2020) showed that dust deposited at high altitudes is dominated by long-range transport.

2.4. Dust impact on the atmosphere

Dust is an important air pollutant with severe impacts on human health, visibility, and traffic safety (Querol et al. 2019; Monteiro et al. 2022). It can cause extreme particulate matter concentrations (PM10) up to 50 000 µg/m^3 (1000x higher the health limit) as measured for example in Iceland and elsewhere (Querol et al. 2019). PM10 concentrations >1 000 µg/m^3 have been reported during dust storms from several locations in high latitudes, including populated areas (Arnalds et al. 2016; Bachelder et al. 2020; Butwin et al. 2020). Aeolian transport of 11 tonnes of dust over a one-metre transect was measured during an extreme wind erosion event in Iceland in 2010 and evaluated as one of the most extreme wind erosion events measured on Earth (Arnalds et al. 2013). Experiments and observations have shown that HLD such as that from Iceland has impacts on atmospheric chemistry (Urupina et al. 2019; Romanias et al. 2020). HLD uptake of gases (both greenhouse gases with their precursors and gases controlling global warming) has been investigated in the laboratory and during in situ observations. Icelandic dust particles efficiently scavenge SO_2 and NO_2 to form sulphites/sulphates and nitrous acid. Dust is also an important agent in cloud formation as dust particles serve as ice nucleating particles (INPs) and cloud condensation nuclei, allowing ice and liquid droplet formation. HLD and particularly Icelandic and Svalbard dusts are efficient INPs and significant INP contributors in the Arctic, having impact on the mid- to high-latitude mixed phase clouds (Sanchez-Marroquin et al. 2020; Tobo et al. 2019; Meinander et al. 2022; Rinaldi et al. 2021). Th high ice nucleating ability of HLD is likely due to its origin in glacial valleys rich in primary minerals (olivenes, pyroxenes, feldspars, and amphiboles) and less rich in clays compared to low latitude dust. Increased INP concentrations can lead to a

reduction in supercooled water and a decrease in shortwave reflectivity of clouds to produce a positive climate feedback.

2.5. Dust impact on the cryosphere

The cryosphere is an important part of the climate system and small changes in surface properties can have large radiative impacts. Dust deposition has a great effect on the cryosphere because it lowers the surface albedo and therefore influences the surface energy balance and melt rates. A mainly local source of HLD is fine sediment from glacier forefields. Glaciers produce this glacial flour which gets airborne due to katabatic winds in areas with limited vegetation cover. Due to glacier retreat, more land surface is exposed to wind and therefore dust emissions are likely to increase (Bullard 2013). Light-absorbing HLD particles can induce snow optical characteristics that impact Arctic amplification and cryosphere melt via radiative feedback (Boy et al. 2019; Meinander et al. 2022).

Snow and ice darkening due to the deposition of light-absorbing particles is a global phenomenon with regional characteristics (Di Mauro et al. 2021). The impact of dust on the optical properties of snow and ice strongly depends on the nature and size of mineral particles (Skiles et al. 2018; Shi et al. 2022) and also snow and ice properties, such as grain size and snow age (Warren and Wiscombe 1980). Most of the radiative impact of dust on snow occurs at wavelengths below 600 nm, and it is possible to analyse this effect by measuring the spectral reflectance of snow and ice (Di Mauro et al. 2015, 2017; Khan et al. 2017). Black carbon has instead a rather flat absorption spectrum.

3. Methods

The methods reported here are part of long-term monitoring activities continuously performed in observatory labs (e.g. Gruvebadet, Zeppelin, Hornsund), and during short-term fieldwork campaigns (e.g. balloon experiments, snow/ice sampling on glaciers). Sampling, sample treatment and analysis appear to be quite varied and heterogeneous, and this has often made data integration and comparison quite complex.

3.1. Sample collection and treatment

Dust sampling is part of both long-term and short-term monitoring activities. Dust sampling has been performed in air, ice/firn and snow. Dust sources such as bare soils and sedimentary deposits have been also sampled in some cases. Sampling site locations are presented in Figure 3, while aerosol, snow and ice/firn sampling techniques commonly employed in Svalbard are reported in appendix 1.

3.2. Continuous measurements

Long-term HLD atmospheric observations (ground and balloon-borne) have been conducted in Iceland, Canada and Antarctica (Thorsteinsson et al. 2011; Dagsson-Waldhauserova et al. 2014a,b; Arnalds et al. 2016; Kavan et al. 2020; Bachelder et al. 2020; Butwin et al. 2020). The analysis of aerosol chemical composition is a useful approach to quantify aerosol dust. Sharma et al. (2019) studied dust variability at Alert through the analysis of aluminium and calcium aerosol concentration from 1980 until 2013. Higher dust contributions were observed in late summer – early fall and during spring. The most common instruments to measure dust in situ are particle counters, able to measure particle number concentration in specific size ranges. Examples of particle counters are Optical Particle Counter (OPC 3330, EDM365, 22 or 31 size bins PM0.25–32), Dusttrak DRX 8533EP (4 size bins PM1-10), Light Aerosol Optical Counter (LOAC, 19 size bins PM0.2–100), and Thermo EMS Andersen FH 62 I-R instrument and Grimm EDM 365. Dust concentration is generally derived as the concentration of particle number or mass in the coarse size range (above 1 or 2.5 micrometers). Song et al. (2021) investigated dust occurrence in Svalbard through cluster analysis of particle size distribution and aerosol bulk chemical composition

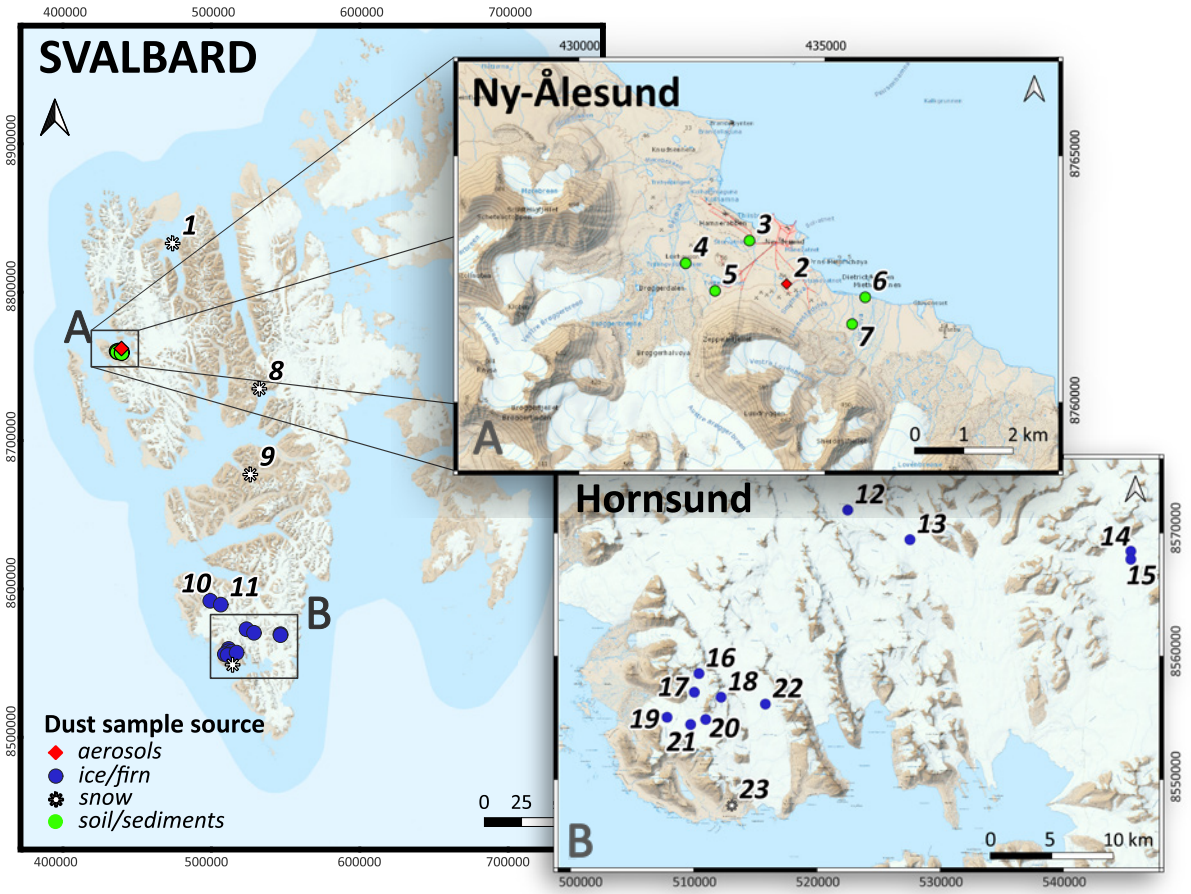

Figure 3. Sampling site locations: 1 – Woodfjorden; 2 – Gruvebadet; 3-7 – Ny-Ålesund; 8 – Pyramiden; 9 – Breinosa; 10-11 – Recherchebreen; 12-13 – Storbreen; 14-15 – Hornbreen; 16-21 – Werenskioldbreen; 22 – Hansbreen; 23 – Ariekammen. Coordinate Reference System: WGS84 / UTM 33N. Map made based on the NPI S100 Topographic Raster Data for Svalbard. © Norwegian Polar Institute.

at Gruvebadet. Dust-dominated aerosol was characterised by coarse particles (volume size distribution peaking at 3 µm and 12-14 µm) and an average calcium to sodium ion ratio of 1.8. Dust was observed mainly from June to October. Finally, the analysis of aerosol optical properties allows the identification of dust transport episodes, because dust particles are generally characterised by small scattering Angstrom exponents and might show large absorption Angstrom exponents (Russell et al. 2010; Costabile et al. 2013).

Long term measurements of aerosol chemical composition, particle size distribution, and aerosol optical properties have been routinely performed at the Zeppelin Observatory (78.9071 N - 11.8867 E, 474 m a.s.l.) and at the Gruvebadet Atmospheric Laboratory (78.918 N - 11.895 E, 61 m a.s.l.) since 2010. A complete list of analytical techniques used to characterise and quantify dust in the aerosol phase is reported in the chapter 'HERMOSA' of this report (Koziol et al. 2023).

The Polish Polar Station in Hornsund, together with NASA, has been conducting Aerosol Optical Depth (AOD) monitoring since 2004. A CE318 (Cimel's Sun Sky Multispectral Photometer) is used for this purpose. Automatic measurements are taken during the polar day, usually from April to September. Later, the device is sent to NASA for review and calibration. The data obtained goes to the AERONET (Aerosol Robotic Network) database maintained by NASA.

From October 2009 to 2017, measurements were made with a ground-based bistatic lidar system with multilevel elastic and Raman scattering. It allowed regular vertical soundings of the troposphere and lower stratosphere over the Polish Polar Station in Hornsund (77.00°N, 15.55°E, 10 m above sea level; Karasiński et al. 2014). The Nd:YAG laser generated three wavelengths simultaneously, i.e. 1064 nm;

532 nm and 355 nm. Automatic measurements of PM10 and PM2.5 particulate matter are planned to be launched in Hornsund in the near future.

3.3. Field campaigns

Field spectral reflectance measurements of dust deposited on snow, such as with field spectrometers, are necessary to quantify the impacts of dust on snow albedo, as well as to develop indices that can be used to map dust on snow from space (Khan et al. 2017; Di Mauro et al. 2015). More research is needed to continue to develop indices specific to the dust sources found in Svalbard beyond the local coal dust, which absorbs broadly in the visible wavelengths (Khan et al. 2017), as well as to monitor dust impacts on the local cryosphere.

Dust measurement campaigns in the Hornsund area have so far taken place irregularly. Measurements have been conducted in late June/early July (Kavan et al. 2020) or in spring (Lewandowski et al. 2020). In the first case, snow was taken in the vertical profile of the Ariekammen slope to determine the amount and mineral composition of dust. In the second case, the focus was on shallow firn-ice cores. In both cases, efforts were made to determine the impact of local and long-distance transport on dust delivery to the Svalbard archipelago. Different analytical methods were used. The results obtained confirmed the greater contribution of dust of local origin. Attention was drawn to the need for further research to confirm the results obtained.

Other studies conducted seasonally in the Hornsund area include AOD measurements using solar photometers. Since the focus of this chapter is on mineral dust, we refer the reader to Koziol et al. 2023.

3.4. Source identification: analytical methods

An inventory of solid phases in ice or snow can be indicative for localisation of source rocks, at least for their most general classification. The dating of radioactive minerals found in dust further constrains sourcing area to orogens formed at the given time. For instance, Lewandowski et al. (2020) used the Electron MicroProbe (EMP) for U-Th-Pb chemical dating of monazite grains, and magnetic methods for identification of magnetically active minerals, found in an ice core from southern Spitsbergen.

To distinguish between different HLD sources the geochemical features of HLD can be treated by means of potential source contribution function analysis (Crocchianti et al. 2021). Soil dust from potential source areas can also be used in resuspension chambers to segregate the aeolian part (less than 10 µm) onto filters for successive analysis (Bertinetti et al. 2022).

3.5. Source identification: Back-trajectories modelling and sand/dust forecast

Atmospheric dust in the Arctic originates from resuspension of soil dust from high latitude local sources, as well as from long-range transport events. The origin of aerosol particles in the Arctic has been investigated by tracing back air mass origin using Lagrangian back trajectory models, including HYSPLIT and LAGRANTO models (Stohl 2006).

Based on HYSPLIT back trajectories, Tobo et al. (2019) observed that air masses that spent a relatively long time over the Svalbard region in summer 2016 were enriched in larger mineral particles, indicating a significant contribution of local sources to the observed atmospheric dust. The contribution of local and long distance dust sources to the Svalbard aerosol loading was reported by Crocchianti et al. (2021) in spring and summer 2015, as well.

Young et al. (2016) studied dust particles over the European Arctic in spring 2013 during the ACCACIA campaign. Local snow excluded the impact of local dust sources and the HYSPLIT back trajectories indicated that air masses passed over North America and northern Europe at high altitudes before reaching Svalbard. Such observations suggested that dust originated from lower latitudes, potentially Asia, and was transported through the free troposphere with weak cloud scavenging.

4. Contributions to interdisciplinarity

The study of dust is intrinsically interdisciplinarity. In fact, dust is produced in the lithosphere, travels in the atmosphere and it can be deposited on the cryosphere and biosphere, and it can alter the hydrosphere. Our chapter helps in putting the role of dust in Svalbard in the right perspective. We hereafter discuss possible interactions among spheres that involve dust transport and impact.

By accelerating the melt of snow and ice, dust is potentially able to change the surface hydrology of glaciers and snowfields in Svalbard. These particular interactions have not been explored in detail, neither with observational data nor with modelling. Snow dynamical models such as Crocus are able to assimilate dust flux from the atmosphere and estimate the reduction of snow season length due to dust (Di Mauro et al. 2019). Furthermore, dust can be involved in complex interactions on the surface of melting glaciers. For example, it can enhance the development of organic material on ice and further induce surface melting of the glaciers (Di Mauro et al. 2021).

The contribution from bioaerosols (e.g. Conen et al. 2016; Baloh et al. 2021) on the ice nucleating ability of windblown dust and on cryoconite state and development has been recognised. Bioaerosol includes bacteria, fungi, pollen and terrestrial/marine organics amongst others (Kanji et al. 2017). The source(s) and nature of such particles are at present poorly studied and understood, and this is a point to call for interdisciplinarity in the characterisation of bioparticles and their interaction with both the atmosphere and the cryosphere. Combined bio-geochemical bio-physical characterisation of aerosol and dust in Svalbard may be the starting point for widespread activity (as for disciplines and research groups involved) regarding both the cryosphere and the atmosphere in their interaction with bioparticles and bioaerosols.

To investigate and understand the life cycle of dust, measurements can be coupled with modelling approaches on emission, long-range transport and deposition. Models can also have capacity to indicate where more direct observations are needed (Meinander et al. 2022). The World Meteorological Organisation Sand and Dust Storm Warning Advisory and Assessment System (WMO SDS-WAS) monitors and predicts dust storms from the world's major deserts[1,2]. High latitude sources have recently been included in the SDS-WAS dust forecasts for the first time. Svalbard dust sources have been identified also in the SDS Source Base-Map developed by the secretariat of the United Nations Convention to Combat Desertification, in collaboration with UN Environment Programme and the WMO[3]. Models could be developed to predict albedo changes due to dust deposition from northern circumpolar dust sources.

1 https://community.wmo.int/activity-areas/gaw/science-for-services/sds-was
2 https://dust.aemet.es/
3 https://maps.unccd.int/sds/

5. Unanswered questions

Hereafter we list a series of unanswered questions that arose during the writing of this SVALDUST Chapter.

1. What is the impact of dust on the cryosphere in Svalbard? And how does dust influence the melting of Svalbard's glaciers?

2. Is dust able to trigger a bio-albedo feedback, mediated by dark photosynthetic organisms?

3. What are the interactions between black carbon and dust both in the atmosphere and the cryosphere?

4. Are radionuclides present in the aeolian dust, and, if so, what is their concentration?

5. Can dust be a vector/medium transporting micro/nanobiotic organisms on a cross-regional scale?

6. Recommendations for the future

1. Identify and characterise new dust sources in Svalbard, e.g. those caused by permafrost thaw or related to human activities (e.g. road dust).

2. Intensify and/or regularise (=make systematic) the observation and remote detection of dust emission/uplift and dust storm events in Svalbard by means of adequate monitoring systems (such as those already in use in other HL dust sources/regions such as Iceland), installed at different sites, starting from the localities (such as Adventdalen valley near Longyearbyen) where these phenomena have already been observed.

3. Further investigation, by continuous/direct measurements and devoted campaigns, of the influence of local sources in the lower troposphere and long-range transport at higher altitudes.

4. Establish an inventory of the long-range dust sources by source profiling in order to cooperate with the modellers for quantification of the dust load from different sources.

5. Disentangle the relative contribution of black carbon and dust on snow and ice albedo reduction in Svalbard. Furthermore, a detailed study on the possible mechanism promoting bio-albedo feedbacks (i.e. biological reduction of snow/ice albedo) should be conducted in Svalbard, and then results should be compared with those presented for the so called 'dark zone' of the Greenland Ice Sheet.

7. Data availability

Data availability is presented in appendix 2.

8. Acknowledgements

This work was supported by the Research Council of Norway, project number 322387, Svalbard Integrated Arctic Earth Observing System – Knowledge Centre, operational phase 2022. Additional funding for Outi Meinander from the Academy of Finland (ACCC Flagship funding grant No. 337552) and Ministry for Foreign Affairs of Finland (IBA-project No. PC0TQ4BT-20) is gratefully acknowledged. Authors from the Institute of Geophysics Polish Academy of Sciences would like to acknowledge the support from the Polish Ministry of Education and Science Project No. DIR/WK/201805. The work was partly funded by the Czech Science Foundation (20-06168Y) and Orkurannsóknasjóður (National Power Agency of Iceland).

9. References

Aamaas B, Bøggild CE, Stordal F, Berntsen T, Holmèn K, Strùm J (2011) Elemental carbon deposition to Svalbard snow from Norwegian settlements and long-range transport. Tellus B: Chem Phys Meteorol 63(3):340-351. https://doi.org/10.1111/j.1600-0889.2011.00531.x

Arnalds O, Thorarinsdottir EF, Thorsson J, Waldhauserova PD, Agustsdottir AM (2013) An extreme wind erosion event of the fresh Eyjafjallajökull 2010 volcanic ash. Sci Rep 3(1):1-7. https://doi.org/10.1038/srep01257

Arnalds O, Dagsson-Waldhauserová P, Olafsson H (2016) The Icelandic volcanic aeolian environment: Processes and impacts – A review. Aeolian Res 20:176–195. https://doi.org/10.1016/j.aeolia.2016.01.004

Bachelder J, Cadieux M, Liu-Kang C, Lambert P, Filoche A, Galhardi JA, Hadioui M, Chaput A, Bastien-Thibault M-P, Wilkinson KJ, King J, Hayes PL (2020) Chemical and microphysical properties of wind-blown dust near an actively retreating glacier in Yukon, Canada. Aerosol Sci Tech 54:2–20. https://doi.org/10.1080/02786826.2019.1676394

Baldo C, Formenti P, Nowak S, Chevaillier S, Cazaunau M, Pangui E, Di Biagio C, Doussin J-F, Ignatyev K, Dagsson-Waldhauserova P, Arnalds O, MacKenzie AR, Shi Z (2020) Distinct chemical and mineralogical composition of Icelandic dust compared to northern African and Asian dust. Atmos Chem Phys 20:13521–13539. https://doi.org/10.5194/acp-20-13521-2020

Baloh P, Hanlon R, Anderson C, Dolan E, Pacholik G, Stinglmayr D, Burkart J, Felgitsch L, Schmale D G III, Grothe H (2021) Seasonal ice nucleation activity of water samples from alpine rivers and lakes in Obergurgl, Austria. Sci Total Environ 800:149442. https://doi.org/10.1016/j.scitotenv.2021.149442

Bertinetti S, Bolea-Fernandez E, Malandrino M, Moroni B, Cappelletti D, Grotti M, Vanhaecke F (2022) Strontium isotopic analysis of environmental microsamples by inductively coupled plasma–tandem mass spectrometry. J Anal Atomic Spectr 37(1):103-113. https://doi.org/10.1039/D1JA00329A

Bullard JE (2013) Contemporary glacigenic inputs to the dust cycle. Earth Surf Proc Land 38:71–89. https://doi.org/10.1002/esp.3315

Bullard JE, Baddock M, Bradwell T, Crusius J, Darlington E, Gaiero D, Gassó S, Gisladottir G, Hodgkins R, McCulloch R, McKenna-Neuman C, Mockford T, Stewart H, Thorsteinsson T (2016) High-latitude dust in the Earth system. Rev Geophys 54(2):447–485. https://doi.org/10.1002/2016RG000518

Butwin MK, Pfeffer MA, von Löwis S, Støren EW, Bali E, Thorsteinsson T (2020) Properties of dust source material and volcanic ash in Iceland. Sedimentology 67(6):3067-3087. https://doi.org/10.1111/sed.12734

Claquin T, Roelandt C, Kohfeld K, Harrison S, Tegen I, Prentice I, Balkanski Y, Bergametti G, Hansson M, Mahowald N, Rodhe H, Schulz M (2003) Radiative forcing of climate by ice-age atmospheric dust. Clim Dyn 20:193-202. https://doi.org/10.1007/s00382-002-0269-1

Conen F, Stopelli E, Zimmermann L (2016) Clues that decaying leaves enrich Arctic air with ice nucleating particles. Atmos Environ 129:91–94. https://doi.org/10.1016/j.atmosenv.2016.01.027

Costabile F, Barnaba F, Angelini F, Gobbi G (2013) Identification of key aerosol populations through their size and composition resolved spectral scattering and absorption. Atmos Chem Phys 13:2455–2470. https://doi.org/10.5194/acp-13-2455-2013

Crocchianti S, Moroni B, Waldhauserová PD, Becagli S, Severi M, Traversi R, Cappelletti D (2021) Potential Source Contribution Function Analysis of High Latitude Dust Sources over the Arctic: Preliminary Results and Prospects. Atmosphere 12:347. https://doi.org/10.3390/atmos12030347

Crusius J, Schroth AW, Gassó S, Moy CM, Levy RC, Gatica M (2011) Glacial flour dust storms in the Gulf of Alaska: Hydrologic and meteorological controls and their importance as a source of bioavailable iron. Geophys Res Lett 38:L06602. https://doi.org/10.1029/2010GL046573

Crusius J (2021) Dissolved Fe supply to the central Gulf of Alaska is inferred to be derived from Alaskan glacial dust that is not resolved by dust transport models. J Geophys Res: Biogeosci 126:6. https://doi.org/10.1029/2021JG006323

Czeppe Z (1968) The annual rhythm of morphogenetic processes in Spitsbergen. Geographia Polonica 14:57-65

Dagsson-Waldhauserova P, Arnalds O, Olafsson H (2014) Long-term variability of dust events in Iceland (1949–2011). Atmos Chem Phys 14(24):13411-13422.

Dagsson-Waldhauserova P, Renard J-B, Olafsson H, Vignelles D, Berthet G, Verdier N, Duverger V (2019) Vertical distribution of aerosols in dust storms during the Arctic winter. Sci Rep 9:16122. https://doi.org/10.1038/s41598-019-51764-y

Dallmann WK (2015) Geoscience Atlas of Svalbard. Report Series No. 148. Tromsø, Norwegian Polar Institute

Di Mauro B, Baccolo G, Garzonio R, Giardino C, Massabò D, Piazzalunga A, Rossini M, Colombo R (2017) Impact of impurities and cryoconite on the optical properties of the Morteratsch Glacier (Swiss Alps). The Cryosphere 11:2393–2409. https://doi.org/10.5194/tc-11-2393-2017

Di Mauro B, Fava F, Ferrero L, Garzonio R, Baccolo G, Delmonte B, Colombo R (2015) Mineral dust impact on snow radiative properties in the European Alps combining ground, UAV, and satellite observations. J Geophys Res Atmos 120:6080–6097. https://doi.org/10.1002/2015JD023287

Di Mauro B, Garzonio R, Rossini M, Filippa G, Pogliotti P, Galvagno M, et al (2019) Saharan dust events in the European Alps: role in snowmelt and geochemical characterization. The Cryosphere 13(4):1147-1165. https://doi.org/10.5194/tc-13-1147-2019

Di Mauro B, Garzonio R, Baccolo G, Gilardoni S, Rossini M, Colombo R (2021) Light-Absorbing Particles in Snow and Ice: A Brief Journey Across Latitudes. In: Kokhanovsky A (ed) Springer Series in Light Scattering. Springer, Cham. https://doi.org/10.1007/978-3-030-87683-8_1

Dörnbrack A, Stachlewska IS, Ritter C, Neuber R (2010) Aerosol distribution around Svalbard during intense easterly winds. Atmos Chem Phys 10(4):1473-1490. https://doi.org/10.5194/acp-10-1473-2010

Goelles T, Bøggild CE (2017) Albedo reduction of ice caused by dust and black carbon accumulation: a model applied to the K-transect, West Greenland. J Glaciol 63:1063–1076. https://doi.org/10.1017/jog.2017.74

Groot Zwaaftink CD, Grythe H, Skov H, Stohl A (2016) Substantial contribution of northern high-latitude sources to mineral dust in the Arctic. J Geophys Res Atmos 121(22):13,678–13,697. https://doi.org/10.1002/2016JD025482

Kandler K, Schneiders K, Heuser J, Waza A, Aryasree S, Althausen D, Hofer J, Abdullaev SF, Makhmudov AN (2020) Differences and Similarities of Central Asian, African, and Arctic Dust Composition from a Single Particle Perspective. Atmosphere 11:269. https://doi.org/10.3390/atmos11030269

Kanji ZA, Ladino LA, Wex H, Boose Y, Burkert-Kohn M, Cziczo DJ, Krämer, M (2017) Overview of ice nucleating particles. Meteorol Monographs 58:1-1. https://doi.org/10.1175/AMSMONOGRAPHS-D-16-0006.1

Karasiński G, Posyniak M, Bloch M, Sobolewski P, Małarzewski Ł, Soroka J (2014) Lidar Observations of Volcanic Dust over Polish Polar Station at Hornsund after Eruptions of Eyjafjallajökull and Grímsvötn. Acta Geophysica 62(2):316-339. https://doi.org/10.2478/s11600-013-0183-4

Kavan J, Láska K, Nawrot A, Wawrzyniak T (2020) High Latitude Dust Transport Altitude Pattern Revealed from Deposition on Snow, Svalbard. Atmosphere 11:1318. https://doi.org/10.3390/atmos11121318

Khan AL, Dierssen H, Schwartz J, Schmitt C, Hermanson M, Painter T, McKnight D (2017) Impacts of coal dust on the spectral reflectance of Arctic surface snow in Svalbard, Norway. J Geophys Res Atmos 122(3):1767-78. https://doi.org/10.1002/2016JD025757

Kok JF, Adebiyi AA, Albani S, Balkanski Y, Checa-Garcia R, Chin M, Colarco PR, Hamilton DS, Huang Y, Ito A, Klose M, Li L, Mahowald NM, Miller RL, Obiso V, Pérez García-Pando C, Rocha-Lima A, Wan JS (2021) Contribution of the world's main dust source regions to the global cycle of desert dust. Atmos Chem Phys 21:169–8193. https://doi.org/10.5194/acp-21-8169-2021

Koziol K, Kallenborn R, Xie Zhiyong, Larose C, Spolaor A, Barbaro E, *Kępski* D, Nikulina A, Zawierucha K, Pearce D, Cockerton L, Nawrot A, Pawlak F, Pakszys P, Cappelletti D (2023) Harmonising Environmental Research and Monitoring of Priority Pollutants and Impurities in the Svalbard Atmosphere. In: Gevers et al (eds) SESS report 2022, Svalbard Integrated Arctic Earth Observing System, Longyearbyen, pp 78-115. https://doi.org/

Lanci L, Delmonte B, Salvatore MC, Baroni C (2020) Insight Into Provenance and Variability of Atmospheric Dust in Antarctic Ice Cores During the Late Pleistocene From Magnetic Measurements. Front Earth Sci 8:258. https://doi.org/10.3389/feart.2020.00258

Lambert F, Kug J-S, Park RJ, Mahowald N, Winckler G, Abe-Ouchi A, O'ishi R, Takemura T, Lee J-H (2013) The role of mineral-dust aerosols in polar temperature amplification. Nat Clim Change 3:487–491. https://doi.org/10.1038/nclimate1785

Lewandowski M, Kusiak MA, Werner T, Nawrot A, Barzycka B, Laska M, Luks B (2020) Seeking the Sources of Dust: Geochemical and Magnetic Studies on 'Cryodust' in Glacial Cores from Southern Spitsbergen (Svalbard, Norway). Atmosphere 11(12):1325. https://doi.org/10.3390/atmos11121325

Meinander O, Dagsson-Waldhauserova P, Amosov P, Aseyeva E, Atkins C, Baklanov A et al (2022) Newly identified climatically and environmentally significant high latitude dust sources. Atmos Chem Phys 22:11889–1193. https://doi.org/10.5194/acp-2021-963

Migała K, Sobik M (1984) Deflation and nival-eolian phenomena observed under conditions of congelation in the forefield of the Werenskiold Glacier, SW Spitsbergen. Zeitschrift fur Gletscherkunde und Glazialgeologie, Innsbruck 20:197-206.

Monteiro A et al. (2022) Multi-sectoral impact assessment of an extreme African dust episode in the Eastern Mediterranean in March 2018. Sci Total Environ 843:156861. https://doi.org/10.1016/j.scitotenv.2022.156861

Moroni B, Cappelletti D, Ferrero L, Crocchianti S, Busetto M, Mazzola M, Becagli S, Traversi R, Udisti R (2016) Local vs. long-range sources of aerosol particles upon Ny-Ålesund (Svalbard Islands): mineral chemistry and geochemical records. Rend Lincei-Sci Fis 27:115–127. https://doi.org/10.1007/s12210-016-0533-7

Moroni B, Arnalds O, Dagsson-Waldhauserová P, Crocchianti S, Vivani R, Cappelletti D (2018) Mineralogical and Chemical Records of Icelandic Dust Sources Upon Ny-Ålesund (Svalbard Islands). Front Earth Sci 6:187. https://doi.org/10.3389/feart.2018.00187

Moroni B, Ritter C, Crocchianti S, Markowicz K, Mazzola M, Becagli S, Traversi R, Krejci R, Tunved P, Cappelletti D (2020) Individual particle characteristics, optical properties and evolution of an extreme long-range transported biomass burning event in the European Arctic (Ny-Ålesund, Svalbard Islands). J Geophys Res Atmos 125:e2019JD031535. https://doi.org/10.1029/2019JD031535

Pękala K (1980) Morphogenetic processes and cover deposits of nunataks in the Hornsund area (SW Spitsbergen). Polish Polar Research 1(2–3):9-44

Querol X, Tobías A, Pérez N, Karanasiou A, Amato F, Stafoggia M, et al (2019) Monitoring the impact of desert dust outbreaks for air quality for health studies. Environ Int 130:104867. https://doi.org/10.1016/j.envint.2019.05.061

Rinaldi M, Hiranuma N, Santachiara G, Mazzola M, Mansour K, Paglione M, Rodriguez CA, Traversi R, Becagli S, Cappelletti D, Belosi F (2021) Ice-nucleating particle concentration measurements from Ny-Ålesund during the Arctic spring–summer in 2018. Atmos Chem Phys 21:14725–14748. https://doi.org/10.5194/acp-21-14725-2021

Romanias, M. N., Ren, Y., Grosselin, B., Daële, V., Mellouki, A., Dagsson-Waldhauserova, P., & Thevenet, F. (2020). Reactive uptake of NO2 on volcanic particles: A possible source of HONO in the atmosphere. Journal of Environmental Sciences 95:155–164. https://doi.org/10.1016/j.jes.2020.03.042

Russell PB, Bergstrom RW, Shinozuka Y, Clarke AD, DeCarlo PF, Jimenez JL, Livingston JM, Redemann J, Dubovik O, Strawa A (2010) Absorption Angstrom Exponent in AERONET and related data as an indicator of aerosol composition. Atmos Chem Phys 10:1155–1169. https://doi.org/10.5194/acp-10-1155-2010

Rymer KG, Rachlewicz G, Buchwal A, Temme AJ, Reimann T, van der Meij WM (2022) Contemporary and past aeolian deposition rates in periglacial conditions (Ebba Valley, central Spitsbergen). Catena 211:105974. https://doi.org/10.1016/j.catena.2021.105974

Sanchez-Marroquin A, Arnalds O, Baustian-Dorsi KJ, Browse J, Dagsson-Waldhauserova P, Harrison AD, Murray BJ (2020) Iceland is an episodic source of atmospheric ice-nucleating particles relevant for mixed-phase clouds. Sci Adv 6:26. https://doi.org/10.1126/sciadv.aba8137

Sharma S, Barrie LA, Magnusson E, Brattström G, Leaitch WR, Steffen A, Landsberger S (2019) A Factor and Trends Analysis of Multidecadal Lower Tropospheric Observations of Arctic Aerosol Composition, Black Carbon, Ozone, and Mercury at Alert, Canada. J Geophys Res Atmos 124:14133–14161. https://doi.org/10.1029/2019JD030844

Shi T, He C, Zhang D, Zhang X, Niu X, Xing Y, Chen Y, Cui J, Pu W, Wang X (2022) Opposite effects of mineral dust nonsphericity and size on dust-induced snow albedo reduction. Geophys Res Lett 49:e2022GL099031. https://doi.org/10.1029/2022GL099031

Song C, Dall'Osto M, Lupi A, Mazzola M, Traversi R, Becagli S, Gilardoni S, Vratolis S, Yttri KE, Beddows DCS, Schmale J, Brean J, Kramawijaya AG, Harrison RM, Shi Z (2021) Differentiation of coarse-mode anthropogenic, marine and dust particles in the High Arctic islands of Svalbard. Atmos Chem Phys 2:11317–11335. https://doi.org/10.5194/acp-21-11317-2021

Spolaor A, Moroni B, Luks B, Nawrot A, Roman M, Larose C, et al (2021) Investigation on the sources and impact of trace elements in the annual snowpack and the firn in the Hansbreen (Southwest Spitsbergen). Front Earth Sci 8:536036. https://doi.org/10.3389/feart.2020.536036

Stohl A (2006) Characteristics of atmospheric transport into the Arctic troposphere. J Geophys Res 111:D11306. https://doi.org/10.1029/2005JD006888

Strzelecki MC, Long AJ (2020) Tales from an Arctic Beach, Little Shells and Return to the Past—Petuniabukta 2010 Fieldwork, Billefjorden, Svalbard. J Coast Res 101:339–345

Tobo Y, Adachi K, DeMott PJ, Hill TCJ, Hamilton DS, Mahowald NM, Nagatsuka N, Ohata S, Uetake J, Kondo Y, Koike M (2019) Glacially sourced dust as a potentially significant source of ice nucleating particles. Nat Geosci 12:253–258. https://doi.org/10.1038/s41561-019-0314-x

Thorsteinsson T, Gísladóttir G, Bullard J, McTainsh G (2011) Dust storm contributions to airborne particulate matter in Reykjavík, Iceland. Atmos Environ 45(32):5924-5933. https://doi.org/10.1016/j.atmosenv.2011.05.023

United Nations Convention to Combat Desertification (UNCCD) (2022) Sand and Dust Storms Compendium: Information and Guidance on Assessing and Addressing the Risks. Bonn, Germany, 345 pp.

Urupina D, Lasne J, Romanias MN, Thiery V, Dagsson-Waldhauserova P, Thevenet, F (2019) Uptake and surface chemistry of SO2 on natural volcanic dusts. Atmos Environ 217:116942. https://doi.org/10.1016/j.atmosenv.2019.116942

Van Der Does M, Knippertz P, Zschenderlein P, Harrison RG, Stuut JBW (2018) The mysterious long-range transport of giant mineral dust particles. Sci Adv 4(12). https://doi.org/10.1126/sciadv.aau2768

Varga G, Dagsson-Waldhauserová P, Gresina F, Helgadottir A (2021) Saharan dust and giant quartz particle transport towards Iceland. Sci Rep 11(1):1-12. https://doi.org/10.1038/s41598-021-91481-z

Warren SG, Wiscombe WJ (1980) A Model for the Spectral Albedo of Snow. II: Snow Containing Atmospheric Aerosols. J Atmos Sci 37(12):2734-2745. https://doi.org/10.1175/1520-0469(1980)037<2734:AMFTSA>2.0.CO;2

Young G, Jones HM, Darbyshire E, Baustian KJ, McQuaid JB, Bower KN, Connolly PJ, Gallagher MW, Choularton TW (2016) Size-segregated compositional analysis of aerosol particles collected in the European Arctic during the ACCACIA campaign. Atmos Chem Phys 16:4063–4079. https://doi.org/10.5194/acp-16-4063-2016

Zwoliński Zb, Kostrzewski A, Pulina M (2013) Dawne i współczesne geoekosystemy Spitsbergenu. Polskie badania geomorfologiczne / Ancient and modern geoecosystems of Spitsbergen. Polish geomorphological research/Bogucki Wydawnictwo Naukowe, Poznań 456 pp

Appendix 1: Aerosol, snow and ice/firn sampling techniques commonly employed in Svalbard

Aerosol	
Time resolution	From a few hours up to 7 days, depending on the analytical technique employed
Size fractionation	Bulk aerosol samples (PM10 and TSP -Total Suspended Particulate matter sampling head) or size segregated samples (impactors)
Sampling substrate	Different filter substrates according to specific analytical needs (i.e. quartz for organics, teflon for trace elements, polycarbonate for Scanning Electron Microscopy (SEM), cellulose for microbial population)
Snow and ice/firn	
Sampling depth	Surface snow layer up to 10 cm; snow in a vertical profile (snow pits, snow cores) to the ground or to the glacier ice; shallow ice/firn cores (1-2 m).
Sampling techniques	Bulk samples collected manually or with ice core drilling equipment. Samples should be collected according to the protocol given by Gallet et al. (2018)
Sample preparation	Mineral fractions in the ice and snow samples are extracted by filtering the meltwater. Filters with mineral residuum are dried and divided into parts, each part being subjected to different analytical methods.

Reference:

Gallet J-C, Björkman MP, Larose C, Luks B, Martma T, Zdanowicz C (2018) Protocols and recommendations for the measurement of snow physical properties, and sampling of snow for black carbon, water isotopes, major ions and microorganisms. Norwegian Polar Institute Brief Report 046, 27 pp. http://hdl.handle.net/11250/2486183

Appendix 2: Availability of data referenced in this chapter

Dataset	Parameter	Period	Location	Metadata access (URL)	Dataset provider
High Latitude Dust deposited on snow	Sediment concentration	June-July 2019	Ariekammen and Pyramiden	https://doi.org/10.5281/zenodo.6790469	Jan Kavan (Masaryk University), jan.kavan.cb@gmail.com
Aerosol chemical speciation	Concentration of Na+, Cl-, NH4+, nssK, nssSO4, C org, EC and BC	July 2015	Gruvebadet, Ny-Ålesund	https://doi.org/10.1594/PANGAEA.908250	Beatrice Moroni, University of Perugia, Italy (UNIPG), b.moroni@tiscali.it
Aerosol chemical speciation	concentration of metals	July 2015	Gruvebadet, Ny-Ålesund	https://doi.org/10.1594/PANGAEA.908251	Beatrice Moroni, University of Perugia, Italy (UNIPG), b.moroni@tiscali.it
Percent mass fraction of aerosol particles from SEM observations	mass fraction of aerosol particles	July 2015	Gruvebadet, Ny-Ålesund	https://doi.org/10.1594/PANGAEA.908276	Beatrice Moroni, University of Perugia, Italy (UNIPG), b.moroni@tiscali.it
Aerosol optical properties	aerosol optical properties	July 2015	Gruvebadet, Ny-Ålesund	https://doi.org/10.1594/PANGAEA.908239	David Cappelletti, niversity of Perugia, Italy (UNIPG), david.cappelletti@unipg.it
Aerosol size distribution	aerosol size distribution	July 2015	Gruvebadet, Ny-Ålesund	https://doi.org/10.1594/PANGAEA.90818	Beatrice Moroni, University of Perugia, Italy (UNIPG), b.moroni@tiscali.it
Aerosol size distribution	aerosol size distribution	July 2015	Zeppelin Observatory, Ny-Ålesund	https://doi.org/10.1594/PANGAEA.908186	Beatrice Moroni, University of Perugia, Italy (UNIPG), b.moroni@tiscali.it
Results of the geochemical and magnetic studies on cryodust from glacial cores of southern Spitsbergen (Svalbard, Norway)	Sample specification; Chemical dating; Magnetic slope correction; Magnetic susceptibillity	April 2018	Recherchebreen, Hornbreen (Flatbreen), Storbreen, Werenskiold-breen, Hansbreen	https://doi.org/10.5281/zenodo.6801558	Adam Nawrot, Institute of Geophysics, Polish Academy of Sciences (IG PAS), anawrot@igf.edu.pl

Harmonising environmental research and monitoring of priority pollutants and impurities in the Svalbard atmosphere (HERMOSA)

Krystyna Koziol[1,2], Roland Kallenborn[3,4], Zhiyong Xie[5], Catherine Larose[6,16], Andrea Spolaor[7], Elena Barbaro[8], Jan Kavan[9,10,16], Daniel Kępski[11], Anna Nikulina[12], Krzysztof Zawierucha[13], David Pearce[14,15], Luke Cockerton[14], Adam Nawrot[11,16], Filip Pawlak[2], Paulina Pakszys[17], David Cappelletti[18]

1 Institute of Geography, The Kazimierz Wielki University in Bydgoszcz, Bydgoszcz, Poland
2 Chemical Faculty, Gdansk University of Technology, Gdansk, Poland
3 Arctic Technology Department, University Centre in Svalbard, Longyearbyen, Svalbard, Norway
4 Faculty of Chemistry, Biotechnology and Food Sciences, Norwegian University of Life Sciences, Ås, Norway
5 Institute of Coastal Environmental Chemistry, Helmholtz-Zentrum Hereon, Geesthacht, Germany
6 École Centrale de Lyon University of Lyon, Écully, France
7 Institute of Polar Sciences, National Research Council of Italy, Venice, Italy
8 Department of Environmental Sciences, Informatics and Statistics, University of Venice, Venice, Italy
9 Alfred Jahn Cold Regions Research Centre, Institute of Geography and Regional Development, University of Wroclaw, Wroclaw, Poland
10 Polar-Geo Lab, Department of Geography, Faculty of Science, Masaryk University, Brno, Czechia
11 Institute of Geophysics, Polish Academy of Sciences, Warsaw, Poland
12 Saint Petersburg, Russia
13 Faculty of Biology, Adam Mickiewicz University in Poznań, Poznań, Poland
14 Northumbria University at Newcastle, Newcastle-upon-Tyne, UK
15 British Antarctic Survey, Cambridge, UK
16 forScience Foundation, Toruń, Poland
17 Institute of Oceanology, Polish Academy of Sciences, Sopot, Poland
18 Department of Chemistry, Biology and Biotechnology, University of Perugia, Perugia, Italy

Corresponding author: Krystyna Koziol, k.a.koziol@gmail.com / krykozio@ukw.edu.pl
ORCID number: 0000-0003-1678-3647

Keywords: Aerosol, atmospheric pollution, monitoring coordination, aerobiology, dust deposition, contaminants of emerging Arctic concern (CEACs)

DOI: https://doi.org/10.5281/zenodo.7406842

1. Introduction

Atmospheric pollution research and monitoring in Svalbard occupies a significant position in pan-Arctic research on priority pollutants (AMAP 2016, 2017), providing observations of their long-range atmospheric transport (Iversen and Joranger 1985; Hung et al 2010). Atmospheric research in Svalbard has been increasing in diversity and magnitude in recent years, with more comprehensive long-term observational efforts and numerous short-term intensive field experiments. Coordination of the research and scientific exchange in terms of common sampling and analytical protocols, joint data analysis, publications, and related planning of future research has growing potential. Coordination offers two advantages: it lowers the environmental footprint of researchers coming to Svalbard (by reducing the number of people necessary to collect samples for various impurities) and allows researchers to see a bigger, interconnected picture of environmental processes.

In this chapter, we collect information from various sources on the state of the research and monitoring of priority pollutants and other impurities in the atmosphere over Svalbard, bridging the chemical, biological and supportive physical monitoring efforts. By atmospheric impurity we mean any kind of substance that is dispersed in the atmosphere, whether in gaseous or particulate form. The definition encompasses molecules of various sizes and chemical composition, as well as biological cells and small organisms, referred to as aerial plankton. Among physical properties of the atmospheric aerosol, we mention mainly the aerosol optical depth (AOD) as a basic parameter monitored in Svalbard, however AOD is elaborated on elsewhere (e.g. Hansen et al 2023). Unfortunately, it is impossible to list every short-term dataset from campaigns conducted in Svalbard, hence we only strive for a representative overview with a focus on long-term monitoring programmes. The opportunities for harmonising several types of measurements are sought in this work, and the distribution of measurements across Svalbard is both an opportunity and a hindrance; hence, the first iteration of the problem is divided by geographical locations. Direct monitoring of atmospheric impurities is also closely connected to their deposition in precipitation. Therefore, we also mention efforts in precipitation sampling which may lead to synergy with aerosol or air sampling, though we must restrict considerations of the topic to such cases alone (excluding, for example, the literature on ice cores collected in Svalbard).

Abbreviations used in the text

AOD	aerosol optical depth
BC	black carbon
CCN	cloud condensation nuclei
CEACs	chemicals of emerging Arctic concern
CFCs	chlorofluorocarbons
eBC	equivalent black carbon
GC	gas chromatograph
NILU	Norwegian Institute for Air Research
NOAA/ CMDL	US National Oceanic and Atmospheric Administration/ Climate Monitoring and Diagnostics Laboratory
PAHs	polycyclic aromatic hydrocarbons
PCBs	polychlorinated biphenyls
PFAS	per- and polyfluoroalkyl substances
PM	particulate matter
POPs	persistent organic pollutants

Previous SESS Reports have included a few chapters showing a fraction of the vast topic of atmospheric impurities (Gallet et al 2019; Malard et al 2019; Petkov et al 2019; Viola et al 2019; Gilardoni et al 2020; Mazzola et al 2020; Sipilä et al 2020; Singh et al 2021; Traversi et al 2021; Petkov et al 2022). In the interest of efficient information processing, we will only refer to topics previously described in SESS reports to the extent which is necessary to understand the potential for harmonisation between the already described and other atmospheric components. The same approach is taken with the parallel chapters in this report on mineral dust (SVALDUST, Di Mauro et al 2023) and AOD measurements (LOAD-RIS, Hansen et al 2023). Due to the focus on measurement harmonisation and the best potential to do so for lower tropospheric, ground-based measurements, we will narrow our focus to these kinds of experiments and monitoring programmes.

2. Overview of existing knowledge

2.1. Existing monitoring and available datasets

2.1.1. Atmospheric impurity monitoring in Ny-Ålesund

Ny-Ålesund has an unparalleled position for atmospheric impurity monitoring in the Arctic and Svalbard, holding two main facilities with an elevation difference of 425 m (Gruvebadet Atmosphere Laboratory 'Gruvebadet' at 50 m and Zeppelin Observatory 'Zeppelin' at 475 m asl), and several facilities dispersed in its vicinity (Figure 1). It offers a unique opportunity for harmonised studies of atmospheric impurity differences with elevation (within and beyond the boundary layer) and between multiple impurities. For example, a recent study (Song et al 2022) explored the sources of atmospheric particles in Ny-Ålesund with machine learning, showing the importance of secondary aerosol in cloud condensation processes and predicting non-linear changes in aerosol composition with temperature changes (resulting from climate change).

The earliest regular monitoring work at Ny-Ålesund was conducted by the Norwegian Institute for Air Research (NILU), starting as early as 1989 (for SO_2 and SO_4^{2-} measurements), although short-term studies had been conducted there earlier, e.g. in 1980-83 on organochlorine persistent organic pollutants (POPs) by Oehme and Ottar (1984). NILU's main facility is located on top of Zeppelin (joined since by other institutions), a unique site where local contamination factors exert a much smaller influence than at any other land-based station in Svalbard due to its elevation. NILU is collecting data on a wide range of variables there, from inorganic ions and gaseous compounds (oxides of carbon, sulphur and nitrogen, also H_2 and NH_3), through various forms of mercury in atmospheric air, to metals and metalloids in precipitation. Carbon dioxide concentrations are monitored there by Stockholm University; in parallel, weekly flask samples have been analysed for trace gas concentrations by the US National Oceanic and Atmospheric Administration's Climate Monitoring and Diagnostics Laboratory (NOAA/CMDL). The monitoring programme at Zeppelin also spans organic compounds: greenhouse gases (CH_4, fluorinated gases), POPs and selected contaminants of emerging Arctic concern (CEACs) (AMAP 2011, 2016, 2017; Carlsson et al 2016; Platt et al 2022; Xie et al 2022b), saccharides, volatile organic compounds and more (ebas-data.nilu.no/; see also section 6. *Data availability*). Furthermore, selected POPs and CEACs have been detected in air samples from Ny-Ålesund (as well as Longyearbyen, Barentsburg and Hornsund) via diverse national research projects (Appendix 1 & 2). The concentrations of most POPs listed for control under the Stockholm Convention, e.g. polychlorinated biphenyls (PCBs) polybrominated diphenyl esters (PBDEs), and organochlorine pesticides, showed clearly seasonal variation and declining trends over the years from the 1990s to 2021 (AMAP 2016; Wong et al 2021). Given the advances in sampling and analytical techniques,

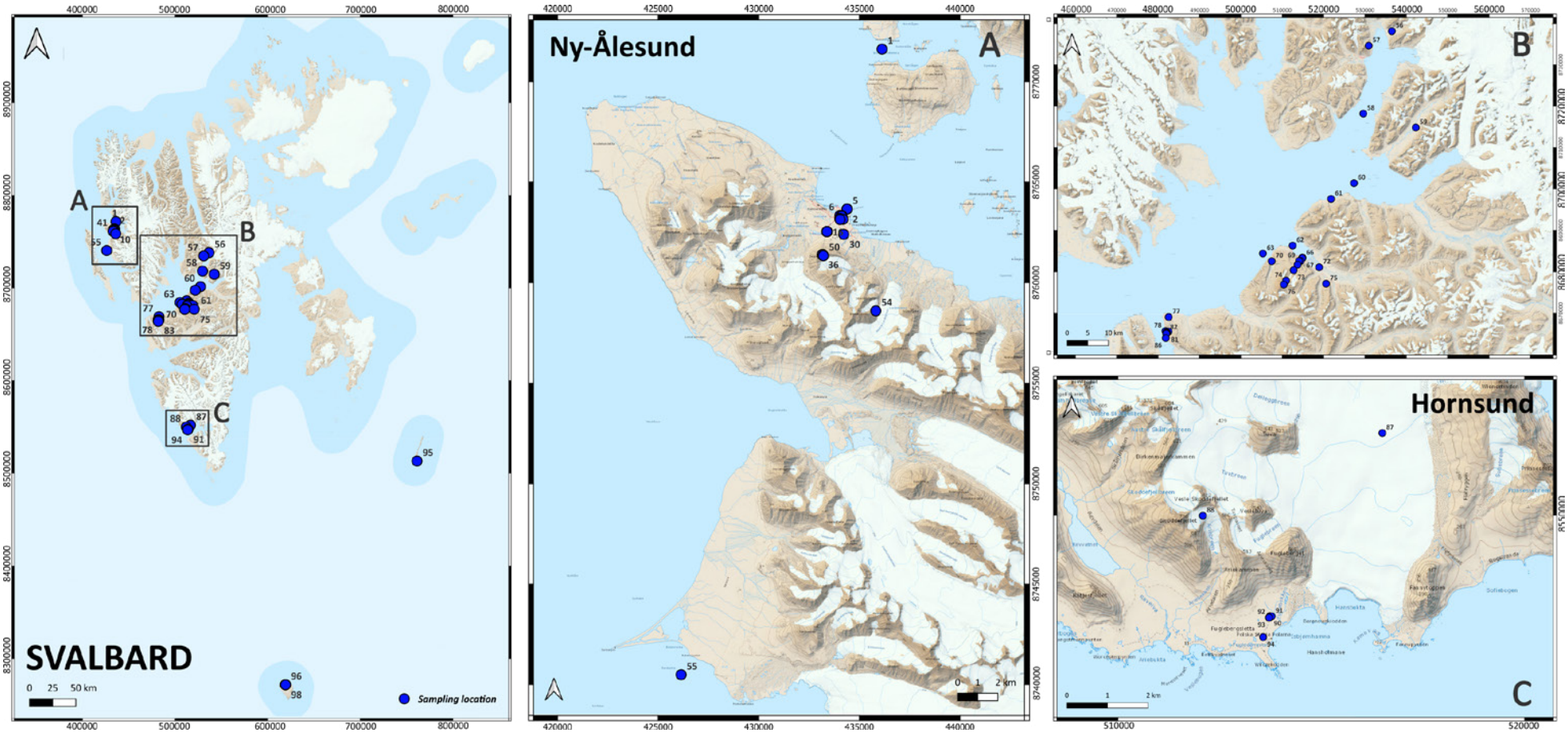

Figure 1: Distribution map, showing measurement sites relevant to the topic of atmospheric impurity monitoring and harmonisation across Svalbard. The numbered locations are described in Appendix 2. Map source: Norwegian Polar Institute, toposvalbard.npolar.no.

more and more novel CEACs have been identified and quantitatively detected in Arctic air (see Appendix 1; Xie et al 2015; Wong et al 2021). Unfortunately, the time trends of CEACs are not as clear as those for classic POPs, and the relatively high concentrations of CEACs in Arctic summer imply the impact of local sources or reemission from cryosphere (AMAP 2017; Xie et al 2022a). Studies of CEACs from Svalbard also testify to the transport, persistence, and impacts of these chemicals in the Arctic (Hao et al 2021; Li et al 2022).

A large part of the atmospheric impurity research at Ny-Ålesund is now carried out in Gruvebadet, about 1 km away from the main settlement. Gruvebadet is dedicated to the study of the atmospheric composition and the atmosphere–cryosphere interaction. It is equipped with several instruments for aerosol studies (see positions 12-29 in Appendix 2). The accessible roof holds an installation of both sampling heads and full samplers (Figure 2). Several continuous measurements are performed at Gruvebadet to fully characterise the aerosol composition within the planetary boundary layer during the entire year, alongside dedicated experimental campaigns. Specialty areas of Gruvebadet laboratory include size-segregated chemical and optical analyses of particulate matter (PM, in this case PM10, which has a maximum diameter of 10 µm), including trace elements, water-soluble organic carbon, and forms of black carbon (BC), microplastics, additives, plasticisers and other CEACs, as well as properties of ice nucleating particles, all performed with state-of-the-art analytical techniques. Multi-decadal results on equivalent black carbon (eBC; see section 2.2) in Svalbard are available from Zeppelin; since 2010, these data have been integrated into the measurements at the Gruvebadet laboratory (cf. Gilardoni et al 2020). Continuous monitoring of the optical (scattering and absorption) and physical (dimensional distribution) properties of the in-situ aerosol is conducted using semi-automatic instrumentation (nephelometer, scanning mobility particle sizer and aerodynamic particle sizer absorption photometer) in collaboration between Italian institutions running Gruvebadet and the Alfred Wegener Institute (Germany), the Institute for Atmospheric and Earth System Research (Finland), Stockholm University (Sweden), the National Centre of Science Research 'Demokritos' (Greece) and the Korean Polar Research Institute (Republic of South Korea). Recently (in 2021), a campaign was conducted to measure particle fluxes using the eddy covariance technique, encompassing measurement of momentum flows and ultrafine particles with a sonic anemometer and a condensation particle counter. Flow measurements of dimensionally segregated particles were conducted through the use of an optical particle counter. A passive sampler for dry deposition of aerosol, and a 'Cyclone' sampler collecting spores and pollen, complement the programme at this supersite.

The Gruvebadet facility is also used to study the atmosphere–cryosphere interaction (in tune with a SESS report recommendation by Gallet et al 2019), through a parallel programme of snow monitoring (for wet and dry deposition), showing the role of snowpack as a chemical sink for emissions from rock weathering, forest fires, marine and biogenic emissions, and anthropogenic contaminants, such as BC, secondary aerosols (e.g. SOx, NOx), complex organic pollutants (e.g. POPs) and heavy metals (e.g. As, Cd, Pb). Quantifying the concentrations of those impurities in the seasonal snowpack allows us to understand the accumulation and depletion mechanisms, and consequently to assess the total load of contaminants potentially released by spring melt into the local food chain. Furthermore, air–snow exchange may significantly interfere with atmospheric concentrations of per- and polyfluoroalkyl substances (PFAS) at Ny-Ålesund, showing strong snow to air evaporation for fluorotelomer alcohol and fluorotelomer acrylates (Xie et al 2015). For atmosphere–cryosphere interaction studies, a weekly sampling of the entire snowpack has been adopted – by snow pit approach, with a vertical resolution of 10 cm. Snow is then analysed to quantify the concentration of elements and compounds of interest (at the National Research Council of Italy, Institute of Polar Sciences), the BC loading (at the Norwegian Polar Institute) and to characterise the microbial community (at Université de Lyon, Centre national de la recherche scientifique). Snow density and stratigraphy data support interpretation of the

Figure 2: Overview of the instruments placed atop the roof of Gruvebadet Atmosphere Laboratory. (Photo: Marco Casula)

chemical data, and an automated nivometric station has been working near the Gruvebadet site since 2020.

It is worth mentioning that at Gruvebadet, several measurements have been integrated into one sampling protocol, described partially in the studies using the data collected there (Scalabrin et al 2012; Zangrando et al 2013; Turetta et al 2016, 2021; Feltracco et al 2019, 2020, 2021b, a). The currently developing project BETHA-NyÅ[1] aims to further harmonise aerosol measurements at Gruvebadet and Zeppelin, as proposed by Traversi et al (2021).

2.1.2. Other land-based atmospheric impurity research in Svalbard

Besides the atmospheric measurement hub at Ny-Ålesund, the main air impurity screening sites in Svalbard are located in Longyearbyen, Barentsburg, and Hornsund; however, studies on specific topics may be encountered in other locations, such as Petuniabukta. One of the earliest monitoring sites in the Norwegian Arctic (including Svalbard) was Bjørnøya – inorganic compounds in atmospheric air and aerosol have been measured there since 1977[2] (SO_2 in atmospheric air). Important discoveries at that time were made possible by this station functioning, e.g. Iversen (1989) showing the meteorological mechanism of long-range atmospheric transport causing winter/spring pollution maxima. The measurements in Bjørnøya were phased out in 1989.

In Longyearbyen, a strong focus of atmospheric impurity research was on local and regional pollution. A fully equipped sampling observatory has been established on the roof of UNIS, with several high volume air samplers (TISCH, Cleves, OH, USA, Type TE-1000BL; US Environmental Protection Agency TO-A4, TO-9A). Further campaignbased studies were conducted at the former Aurora

1 RiS ID 11924
2 http://ebas.nilu.no/

observatory in Adventdalen, and in collaboration with SvalSat on the adjacent mountain Platåfjellet. During the past years, in Longyearbyen, POPs and novel CEACs have been detected in gaseous and/or particle phase during research projects (including novel PFAS, polychlorinated biphenyls [PCBs] and polycyclic aromatic hydrocarbons [PAHs] and their major transformation products).

The research conducted in Longyearbyen has been instrumental in documenting the transition from a coal-mining-based community to a settlement relying mostly on services as an income source, with both sources contributing to local air pollution. Coal mining has been present in Longyearbyen (and Svalbard in general) since the early 1900s when John Munro Longyear established the first mining infrastuctures in Adventdalen (Westby and Amundsen 2003; Kvello 2004). Since then, five major locations across Svalbard have had large coal mining infrastructures established and in operation (Appendix 3). After the Norwegian government decided to abandon coal mining in Svalbard (in 2017), other activities such as services, municipal administration, research, education, construction and maintenance, as well as international tourism, have replaced coal mining as the main source of employment in Svalbard (Avango 2020).

Today, around 3000 inhabitants are living and working in Svalbard, mainly in Longyearbyen (2400) and Barentsburg (400). All settlements in Svalbard are isolated infrastructures: life-supporting services such as heating, electric power, water supply, and waste handling need to be provided on-site. In addition to high costs of infrastructure operation, settlements in Svalbard have a significantly higher ecological footprint per inhabitant compared to mid-latitude locations, where infrastructure is shared. An earlier report by the Norwegian Environmental Agency concluded that Svalbard's man-made CO_2 emissions (produced by ca 3000 people = 0.06% of the total population) accounted for ca 1% of the total Norwegian CO_2 emissions in 2009 (Vestreng et al 2009). Hence, it is important to control local emissions, not least to minimise the risk of exposure for local populations (e.g. to CEACs).

For two decades now, Svalbard settlements have been comprehensively investigated for local pollution. Transportation and emissions from gasoline-fuelled engines are an important local contamination source in Svalbard. Shipping, the operation of heavy vehicles that run of fossil fuels (e.g. lorries), and private transportation (cars, snowmobiles) contribute significantly to the local pollution profile. Reimann et al (2009) reported on the emission of volatile organic compounds in Longyearbyen, especially aromatics, from snowmobile exhaust. Elevated levels of aromatics were attributed to the extensive use of two-stroke engine snowmobiles between November and June. Aromatics were emitted at levels similar to those of a medium-sized European city, like Zürich (400 000 inhabitants). Also for PAHs, elevated air concentrations were confirmed to come from fossil-fuel-driven engines, both in and around Longyearbyen. A variety of local sources such as a local petrol station, the coal power plant and various municipal installations were confirmed. Unlike aromatics, PAHs are environmentally stable contaminants and hence were subsequently found in surface soil along major snowmobile tracks near Longyearbyen.

PAHs are relevant local pollutants, and coal-fired power plants both in Longyearbyen and Barentsburg are identified as their major local source. A recent comprehensive study investigated the emission profile and the rapid atmospheric transformation process for PAHs (Marquès et al 2017; Drotikova et al 2020, 2021). Air samples from three locations, at increasing distances from the source (0 to 8 km from the power plant), were investigated for PAHs and their major transformation products (oxy- and nitro-PAHs). Seasonal profiles have been described: during polar day, rapid photochemical transformation eliminates nitro-PAHs, while oxy-PAHs are less affected.

In the past years, a variety of new organic pollutants were identified as local contaminants in Svalbard (AMAP 2017; Kallenborn et al 2018). Among CEACs, PFAS were found to be directly emitted from Svalbard installations, mainly at the local airports (Longyearbyen, Ny-Ålesund, Svea – the fire fighting training locations) and local waste dumps

(Skaar et al 2019; Ali et al 2021). Elevated levels of PFAS in the local food webs were confirmed both in Ny-Ålesund and Longyearbyen. Recently, a study on surface snow revealed the presence of novel ultra-short PFAS in the vicinity of Longyearbyen (Foxfonna glacier). Here, the photochemical transformation of long-chain precursor PFAS led to elevated levels of trifluoroacetate and trifluoromethane sulphonic acid in surface snow. Trifluoroacetate was also identified in drinking water in Longyearbyen (Nödler, pers. comm.), proving the importance of PFAS emission screening.

In Barentsburg, aerosol measurements started in 2011 (Sakerin et al 2012; Golobokova et al 2013). Since 2016, systematic measurements of optical, microphysical and chemical aerosol properties have been conducted by researchers from the Russian Academy of Sciences and the Arctic and Antarctic Research Institute (Chernov et al 2016, Sakerin et al 2018; Sakerin et al 2019). AOD, and other physical properties including eBC concentration, have been measured by sun photometer (since 2015), aethalometer, integrating nephelometer and a photoelectric particle counter (Sakerin et al 2012, 2019; Chernov et al 2016). Aerosol was sampled for further measurements of chemical composition, for example the concentration of major inorganic ions and trace metals (Chernov et al 2016; Sakerin et al 2018; Golobokova et al 2020). The sampling was performed according to international guidelines (EMEP 2001; EANET 2003). Alternating daily and weekly modes, 14 to 18 m^3 of air was pumped through a four-stage filter holder at 2 m above the ground on the south side of Barentsburg Meteorological Observatory (V. Radionov, pers. comm.). Concentrations of 17 PAHs were also measured there in aerosol (Sep-Oct 2017; Golobokova et al 2020).

The chemical composition of the atmospheric boundary layer was observed daily from April to September in 2011-2015, and monthly from April 2016 to 2018. Since 2016, atmospheric gases (CO_2, CO, SO_2, H_2S, NO_x, O_3 and gaseous Hg) have been automatically monitored, maintained by the Arctic and Antarctic Research Institute, and the data were occasionally used for comparisons with other sites in Svalbard. Since 2019, aerosol is sampled weekly. The highest ion concentrations were measured in 2011-2012 during the renovation of Barentsburg. After the introduction of a filter system on Barentsburg power plant in 2012, the total ion concentrations were halved by 2016, but subsequently increased slightly (Sakerin et al 2018). Generally, ion concentrations increase in winter-spring and drop slightly in May-June, with sea spray as a main source of aerosol throughout the year and the local influence of coal mining and power plant exhaust being more prominent during the polar night (Golobokova et al 2020).

The ground-based monitoring programme Northwest branch of RPA 'Typhoon' (Saint Petersburg) includes the analysis of atmospheric aerosol for 16 PAHs, PCBs and trace metals, since 2002 (Demin et al 2011). Apart from direct measurements, method development and intercalibration exercises with NILU were conducted. Samples have been collected twice a year in spring (March) and late summer (August) with a multichannel low-volume sampler simultaneously on three AFA-HA-20 filters (acetate cellulose fibrous material with electrostatic effect, 20 cm^2) at three sites in Barentsburg and outside the settlement (Demin et al 2011; E. Yaeski, pers. comm.). The methods of sampling and analysis remained unaltered for the whole observation period.

The Governor of Svalbard, in collaboration with the Norwegian Environmental Protection Agency (Miljødirektoratet), commissioned a Svalbard-wide survey on potential local sources of PCBs in 2007 (Lundkvist et al 2008). In virtually all settlements in Svalbard, elevated PCB concentrations were found in the local environment; decommissioned and defective technical equipment (like transformers) was identified and removed for proper destruction. This first survey noted the paucity of information on PCB contamination from Russian settlements and hence a dedicated campaign for mapping PCB contamination in Barentsburg and Pyramiden was initiated (Evenset and Ottesen 2009). The latter authors concluded that although local emissions could be considered high, the majority of PCB pollution in Svalbard stems from decades of long-range atmospheric transport.

In southern Spitsbergen, long-term monitoring of several atmospheric pollution parameters is carried out at the Polish Polar Station in Hornsund. This station is the site that has been operating longest in the AERONET network in Svalbard, among other things providing continuous cloud-screened observations of spectral AOD since 2004. Aerosol studies have been complemented with ceilometer data since 2017. Extended measurements of aerosols in the atmosphere were conducted there in the years 2009-2015, when Raman lidar was operational (Pietruczuk and Karasiński 2010), detecting the impact of volcanic ash (Karasiński et al 2013) or wildfires (Markowicz et al 2016) on the atmosphere of Svalbard. In the spring of 2021, more detailed data on the concentration of the aerosol and its size distribution were collected using OPS 3330 and NanoScan SMPS 3910 TSI spectrometers.

The chemical composition of aerosol is also monitored at the Polish Polar Station in Hornsund, albeit less comprehensively. This is one of the northernmost continuous monitoring sites for radionuclides in the ground-level atmosphere since 2002 (Mysłek-Laurikainen et al 2006) and was recently expanded to include an EcoGamma environmental gamma radiation monitor. This monitoring additionally provides information on the concentration of dust deposited on Petrianov filters in an AZA-1000 high-volume air sampler, which are replaced at weekly intervals (Burakowska et al 2021). The measurements have confirmed an influx of radioactive isotopes into Svalbard after the Fukushima nuclear power plant disaster (Burakowska et al 2021), which was visible also in Ny-Ålesund (Paatero et al 2012). Besides this ongoing programme, recent measurements have been made in Hornsund within the scope of short-term projects (Sea-snow POPs[3] and HiLDA[4]) since 2019, to determine the concentration of organic compounds in the atmosphere at Hornsund and to characterise mineral and anthropogenic compounds in atmospheric particulate matter.

Since 2004, monitoring of the chemical composition of precipitation (rain and snow) has been carried out in Hornsund (Figure1, see also Appendix 2). Samples are collected: a) ~500 m north of the station (from a high-density polyethylene precipitation collector), after each rain or snowfall; b) on glaciers (Hansbreen until 2019; Ariebreen since then) after each snowfall near the ablation poles (into polyethylene bags); c) in an elevation transect from the seashore to the summit of Fugleberget, irregularly (into polyethylene bags). All physico-chemical analyses are carried out in the station's chemical laboratory. After pH, conductivity and HCO_3^- titration measurements, samples are filtered (on 0.45 µm cellulose membrane filters) and analysed for the major ion composition using ion chromatography (now a Methrom 930 Compact chromatograph). The data on precipitation composition collected at Hornsund, before and after 2004, allows characterisation of the origin of rain and snow (e.g. Pulina 1991; Głowacki and Leszkiewicz 1994; Głowacki and Pulina, 2000; Burzyk et al 2001; Krawczyk et al 2002; Krawczyk and Skręt 2005; Kozak et al 2015), spatial differences in precipitation chemistry (e.g. Krawczyk et al 2008), and the impact of wildfires and long-range transport (e.g. Bryś 2002; Głowacki and Krawczyk 2002; Ruman et al 2014; Kozak et al 2015; Nawrot et al 2016).

2.1.3. Specific study topics with atypical or sparse spatial representation

Aeolian dust studies in Svalbard, which recently started again after lying dormant since the 1980s (e.g. Pękala 1980; Åkerman 1983; Gębica and Szczęsny 1988), are limited to a few sites. Direct observational data exist only for Ny-Ålesund (Moroni et al 2015, 2016, 2018; Gallet et al 2018; Conca et al 2019; Jacobi et al 2019), Hornsund (Migała and Sobik 1984; Kavan et al 2020; Lewandowski et al 2020; Spolaor et al 2021), and Longyearbyen (e.g. Khan et al 2017; Kandler et al 2020). Apart from that, there are only two studies from Petuniabukta area in central Svalbard (Kavan et al 2020; Rymer et al 2022). The studies at Ny-Ålesund were conducted using ground level active filtering (Conca et al 2019), or vertical profiling (Moroni et al 2015, 2016); the

3 RiS ID 11108
4 RiS ID 11195

detailed mineralogical and chemical composition of the aerosol was reported by Moroni et al (2018). Aeolian processes are also monitored as the deposition of material on snow (Khan et al 2017; Gallet et al 2018; Jacobi et al 2019; Kavan et al 2020; Lewandowski et al 2020; Spolaor et al 2021). The only direct deposition of dust was observed by Rymer et al (2022) using passive samplers in central Spitsbergen. Quantifying mineral dust deposition remains a challenge due to its large spatial and temporal variability – the measured deposition rates vary, are site-specific, and depend on the method used.

Another type of measurement sparsely distributed across Svalbard is aerobiological sampling. Aerobiology research is a relatively nascent field in Svalbard; few studies have been published from the archipelago on aerial microbiology and aerial plankton, or on the transport of pollen and eukaryotic spores, both of local and distant origin (cf. Figure 1). Johansen and Hafsten (1988) detected pollen, bryophyte and fungal spores in Bürkard traps at Ny-Ålesund, most of them of local origin. However, Polunin (1955) found mostly exotic pollen species for Svalbard including *Pinus* pollen, highlighting the role of long-range transport. In a study on bacterial diversity in the air over Svalbard (Cuthbertson et al 2017), biodiversity was found to be similar to that in other environments, both polar and non-polar. The identification of viable bacteria suggests that living bacteria are ubiquitous in the air around Svalbard. In a six-month study on the composition of the bacterial community in the atmosphere at NyÅlesund, community structure exhibited seasonal dynamics that mimicked the different stages of bacterial colonisation of algal blooms in the surrounding fjords. This highlights the importance of open water as a source of airborne microorganisms (Feltracco et al 2021a). In a cultivation-dependent study (likely to underestimate the number of live airborne microorganisms), fifteen fungal taxa were isolated from the air of Longyearbyen (Pusz and Urbaniak 2021). Currently, no long-term monitoring programmes focus on aeromicrobiology in Svalbard, although the project ArcticBioAir[5] is generating pilot data to determine the potential of such monitoring. Finally, even though microinvertebrates predominate in the faunal diversity of polar regions and play a pivotal role in matter flow, the majority of studies investigate microinvertebrate transport only by migratory birds, humans or imported soils (Coulson et al 2013; Pilskog et al 2014). Few studies discuss passive transport of invertebrates by wind at all (Hodkinson et al 2001; Coulson et al 2002, 2003; Coulson 2015), and among them, only two test aerial transport empirically (Coulson et al 2002, 2003).

2.1.4. Atmospheric impurities research from the seas surrounding Svalbard

A complementary element of atmospheric impurity monitoring in Svalbard is that it is also done in the seas around the archipelago. While the sampling techniques and protocols match those used on land, the research done at sea is tied geographically to cruise routes and thus repeated measurements concern a wider area rather than an exact location. Challenging atmospheric conditions at sea introduce potential obstacles to measurement, e.g. dense fog, strong winds and breaking waves.

Since 2004, AOD instruments have been deployed periodically on various ships navigating around Svalbard: *RV Oceania* (2007, 2009-2020, e.g. Leck et al 2001; Tjernström et al 2014; Heintzenberg et al 2015), the Swedish icebreaker *Oden* (2008; ASCOS campaign – Chang et al 2011; Sierau et al 2014), *RV Polarstern* (2012, 2015, 2017, 2020), *RV Jan Mayen* (2009); *RV Akademik Mstislav Keldysh* (2016; Terpugova et al 2018) and *RV Alliance* (2021). *RV Oceania*, owned by the Institute of Oceanology, Polish Academy of Sciences, participates in the Maritime Aerosol Network, a component of the AERONET network, and has been providing AOD measurements from the Norwegian and Greenland Seas since 2007. Since 1987, the Institute of Oceanology has been conducting a regular, annual AREX Arctic Expedition (Węsławski and Sagan 2020), performing meteorological surveys, measuring aerosol fluxes, and the physical and optical properties of aerosols right from the

5 RiS ID 11752

start. The cruises are conducted year by year with almost the same research plan, with continuity and repeatability both in time and space, covering about 90 days in the Arctic each summer (Ferrero et al 2019; Pakszys et al 2020). The annual summer cruise of *RV Oceania* cruise is one of the longest monitoring programmes conducted in the Svalbard seas. Recently, in collaboration with the University of Mila Bicocca, PAHs, n-alkanes, organic matter and trace elements have occasionally been included in the monitoring.

The German research icebreaker *RV Polarstern* (of the Alfred Wegener Institute) has a longer Arctic history than *RV Oceania*, starting in 1991, continuing between 2001 and 2021 (2009, 2012, 2015, 2017, 2020, 2021), and crowned with the longest expedition across the ArcticOcean: the MOSAiC cruise, which lasted over a year. This was the first year-round expedition into the central Arctic to explore the Arctic climate system, drifting with the sea ice across the central Arctic from September 2019 to October 2020, launching radiosondes along the way. The Institute's polar research aircraft and UAVs played an important part in atmospheric investigations throughout MOSAiC (Mazzola et al 2020; Griesche et al 2020).

Air quality monitoring at sea is especially important in the context of sea–air exchange phenomena. Substantial evidence from observations and modelling shows the impact of climate change on the biogeochemical cycle of POPs and CEACs in the Arctic, pertinent to both the seas and the atmosphere (Ma et al 2016). For instance, many legacy POPs have revolatilised into air from water, snow or ice as a consequence of sea ice retreat and rising temperatures (Ma et al 2011). Besides, many CEACs were likely transported with ocean currents and waves from the low and medium latitudes to the High Arctic. The warm Atlantic seawater may bring CEACs such as ionic PFAS, organophosphate esters, and compounds from pharmaceuticals and personal care products into the waters surrounding Svalbard and influence their atmospheric levels through air–water gas exchange or sea spray (Li et al 2017; Sha et al 2022). Both ship-based and stationary observations in Svalbard have shown that gas exchange between air and water/snow alters the atmospheric concentrations of chemicals (Yu et al 2019; Araujo et al 2022; Dastoor et al 2022).

2.2. Sampling techniques and data collection protocols

The liquids and solids dispersed in the atmospheric air (e.g. aerosols, PM) encompass both iorganic and organic chemicals, frequently in mixed particles, particles with specific optical properties, such as BC, and more complex and larger airborne impurities, such as pollen, microplastics, and small living organisms. Some of these substances have closely related aerosol and gaseous forms, e.g. sulphate in aerosol which comes from the dissolution of gaseous SO_2. With such a variety of analytes, a suite of analytical approaches need to be employed for their qualitative and quantitative characterisation. However, since the mode of transport is similar for multiple species of similar molecular or particle size, similar sample collection approaches can be used, which allows for harmonisation of several measurement types in one monitoring protocol. In harmonisation attempts, key variables to consider are the types of sampling consumables required (e.g. filter material or pore size), exposure time (or sampled air volume), and the analytical steps leading to final results.

The first group of chemicals with harmonised sampling regimes in the Svalbard monitoring includes gaseous constituents measured online, such as the greenhouse gases (CH_4, CO_2, hydrofluorocarbons, SF_6), O_3, and several ozone-depleting chemicals (chlorofluorocarbons [CFCs], hydrochlorofluorocarbons [HCFCs], halones, and other halogenated organic gases). The online measurements offer quick access to analytical results and high sampling frequencies, e.g. NILU monitors 23 gases at Zeppelin at least once per 4 hours (every 5 minutes for O_3). Most of these measurements are provided by automated gas chromatography (GC) systems with different detectors: flame ionisation for methane, MgO-UV for carbon monoxide, and mass spectrometry for halogenated compounds (Myhre et al 2010). CH_4 concentrations may also be measured with cavity ring-down spectroscopy (ebas-data.nilu.no/). For

longer-term averages, weekly flask sampling has also been used for trace gas analysis by NOAA CMDL.

Inorganic ionic species in atmospheric aerosol play an important role as source indices (Giardi et al 2016; Udisti et al 2016; Amore et al 2022): for example, sodium and chloride typically originate from sea salt; bromide and iodide depend on the sea ice extent (Spolaor et al 2013). Some of them also play a role in climate forcing (Toon and Pollack 1980; Satheesh and Krishnamoorthy 2005), exerting a cooling effect by light reflection and forming reflective clouds (especially sulphate). Their role as cloud condensation nuclei (CCN) is also important (Merikanto et al 2009). Since it is relatively easy to determine the concentration of ions, they form a basis for further analyses and have been monitored in Svalbard for a long time. The traditional method of sample collection for the analysis of inorganic ions in air and aerosol includes a combination of denuders (glass and alkaline-carbon-coated) and filters (Beine et al 2001). The filter pack captures both fine and coarse particulate matter (a Teflon filter, 1-µm pore size) and acids evaporated from the front filter (a Nylon filter, 1-µm pore size). The analytical technique best suited for the determination of inorganic ions collected by both denuders and filters is ion chromatography. Collection times applied by Beine et al (2001) were between 12 and 24 hours. Nowadays, sampling and analysis of inorganic ions remains similar, yet with a large variety of modified protocols. For example, Teinilä et al (2003) used polycarbonate films and a sequence of membrane filters with two types of impactors in their NICE campaign (at Ny-Ålesund). In Barentsburg, samples were collected on a four-stage filter pack. The direct accumulation of aerosol took place at the first polytetrafluoroethylene filter (0.8 µm pore size; Golobokova et al 2013; Chernov et al 2016). Three other filters, chemically pre-treated (EANET 2003), collected gases (filter 2: nitric acid, filter 3: sulphur dioxide, hydrochloric acid, filter 4: ammonia). Similarly, Park et al (2017), Becagli et al (2019) and Jang et al (2021) used quartz filters to analyse sulphate and methandsulphonic acid concentration (at Gruvebadet). All the above studies used a variation of 18 MΩ water extraction and ion chromatography as determination technique. The variety of employed filter materials harmonisation of ion analysis with a different particulate impurity monitoring, using filter papers dedicated to that purpose.

Alternatively, copper grids coated with carbon film may be used, combined with a later analysis by electron microscopy (as at the Chinese Yellow River). Nanoscale secondary ion mass spectrometry may the be used to analyse the composition of individual aerosol particles (Chi et al 2015). At Gruvebadet, the equivalent of this approach is using nucleopore polycarbonate membrane filters with a 12-stage low volume impactor and analysis by scanning electron microscopy (see also section 2.1.1), which is also a way to study mineral dust composition.

For mineral dust quantification, most sampling protocols are rather individual and depend on the device used (for active sampling procedures). The passive sampling in Rymer et al (2022) used the standard Marble Dust Collector traps (Hall and Upton 1988). An alternative sample collection strategy involves sampling of snow cover as a substrate for mineral dust deposition. Usually only the upper layer of snow is sampled to avoid contamination from the ground surface.

Sampling for determination of metals and metalloids is very similar to sampling for determination of ions, and sometimes different parts of the same filter are used for both determinations (Zhan et al 2014; Golobokova et al 2020), which is an excellent harmonisation example. Analytical methods, invasive and non-invasive, are used to determine the content of metals and metalloids. The invasive method requires wet digestion of the sample, using e.g. nitric acid and microwaves as an energy source. Subsequently, the content determination is performed using inductively coupled plasma mass spectrometry (Berg et al 2004; Demin et al 2011; Zhan et al 2014; Bazzano et al 2016; Conca et al 2019, 2021; Golobokova et al 2020; Turetta et al 2021). This method can also be used to determine the isotope content of e.g. lead (Bazzano et al 2016). It is also possible to determine the content of the radioisotope ^{210}Pb using the automatic alpha/beta analyser (Paatero et al 2003). A non-invasive

method is to use X-ray fluorescence spectroscopy (Anderson et al 1992; Shpartko et al 2021).

Among metals, mercury is of special importance due to its toxic effects. Hg is determined in the air in three forms: gaseous elemental, gaseous reactive and associated with particulates (Gauchard et al 2005). The most popular device for determining gaseous elemental Hg is a Tekran gas-phase mercury vapor analyser, which uses cold vapour atomic fluorescence spectrometry: atmospheric air is passed through a gold trap, the gold forms an amalgam with mercury, and after a specified sample enrichment time, thermal mercury desorption and final detection as HgO by atomic fluorescence spectrometry is performed. The other two types of mercury must first be isolated from the air stream: for gaseous reactive Hg, a KCl-coated annular denuder or soda lime trap is used, and for Hg on particulates, quartz filters are used. The enriched samples can then be analysed using the same spectrometric technique (Ferrari et al 2005; Osterwalder et al 2021). A detailed description of the repeatability of the method is presented by Aspmo et al (2005).

BC particles have a unique combination of properties, including strong visible light absorption, being refractory with an aggregate morphology, and insoluble in water and common organic solvents (Gilardoni et al 2020). BC mass concentrations are measured directly by incandescent and thermal techniques or indirectly from absorption measurements using appropriate mass absorption cross-section values as the conversion factor (Petzold et al 2013). Different terms are used for black carbon depending on the property being measured. While rBC refers to incandescent measurements, EC is used for thermal techniques and eBC is the term for optical or photoacoustic techniques. The results obtained with different techniques agree within a factor of two. The principal measurement technique for BC is based on single-particle soot photometers, using an online laser-induced incandescent method to determine the size distribution of rBC. Total mass concentrations and information on the mixing state of BC (a ratio of BC to total particle diameters) can also be derived (Schwarz et al 2010; Kondo et al 2011). Long-term monitoring of BC in the atmosphere is based on two other techniques. The first is the thermal-optical methods, which measure elemental and organic carbon at the same time (Caiazzo et al 2021). Active research networks have adopted different protocols to quantify elemental carbon (see WMO/GAW [2016] for details). Elemental carbon measurements may differ by up to a factor of two due to differences in protocols, instruments, laser signals, and corrections for the chemical character of organic carbon (Karanasiou et al 2015). Filter-based optical methods are another approach taken for long-term BC monitoring, providing outputs as eBC. Instrumentation available in Svalbard includes particle soot- and multi-angle absorption photometers and aethalometers (Petzold and Schönlinner 2004). Uncertainties in the filter-based absorption techniques are caused by non-BC aerosol compounds, which can either absorb or scatter the light when deposited on the filter, and by light scattering of the filter itself. Correction schemes have been developed for the Arctic to account for the effects mentioned above in the aethalometer absorption conversion (Backman et al 2017).

Atmospheric POPs monitoring at Zeppelin is a key component of the Arctic Monitoring and Assessment Programme (e.g., AMAP 2016), and its collection and analysis method are therefore well established. In order to generate high quality data and comparable results, a standard operation protocol for air sampling and analysis has been harmonised through the analytical laboratories working within the Programme for classic POPs including PCBs, PBDEs, OCPs and PFAS. Standard operating procedures have been created for both active and passive air sampling for POPs monitoring. Newer studies of POPs aspire to match the standard techniques closely, e.g. at Barentsburg, PAHs and PCBs were determined in particulate matter collected on glass fibre filters (14 m^3 of air collected in 24 hours) (Golobokova et al 2020). The concentrations of PAHs were measured by a GC-MS (GC with mass spectrometric detection) Triple Quadrupole system. In the RPA 'Typhoon' programme, less typically, 16 PAH concentrations were determined with high-performance liquid chromatography with fluorescence and diode array

detectors. PCB analysis was performed with a GC with electron capture detection (Demin et al 2011, E. Yaeski, pers. comm.).

A challenging topic for the sampling and analysis techniques is CEACs, due to variety of the encountered substances, new substances being added to the catalogue, and their relatively low concentration levels. As the concentrations of CEACs in Arctic air are usually at picogrammes to nanogrammes per cubic metre (pg/m^3 to ng/m^3), suitable sampling and pre-concentration techniques are essential to match the sensitivity of the analytical instruments. Active air sampling is performed with a high-volume sampler equipped with glass- or quartz-fibre filters for collecting atmospheric particles (cutoff points vary), and solid adsorbents, e.g. Amberlite XAD-2 resin, polyurethane foam alone in combination with XAD-2 resin combination for the gaseous phase (Röhler et al 2020, 2021). Cellulose nitrate membrane filters (pore size: 1-5 µm) are used to trap microplastics in the air. The sampling of CEACs is typically compatible with the POPs collecting programmes.

Passive samplers (PAS) have been also deployed to monitor the background level and annual trends of POPs and CEACs in Svalbard (Li et al 2022). Sampling media include polyurethane foam discs, XAD-2 resin and semi-permeable membrane devices. PASs are cost-effective, simple in operation, and could be deployed anywhere, e.g. on a glacier or in remote sites without power supply, thus providing data from more locations.

Many other organic compounds are also screened in Svalbard by NILU, as can be ascertained from the EBAS database[6]. Such compounds are collected with a high-volume air sampler (besides selected POPs, including PFAS, also carbohydrates such as levoglucosan, mannitol and sucrose, and other substances, e.g. bisphenol A and triclosan; also total organic carbon), passive airsampler with a polyurethane foam plug (PAHs, PCBs, and organochlorine pesticides – a campaign in 2006), steel canister (chosen alkanes and alkenes), glass flask (selected alkanes), and adsorbent tube (selected aldehydes and ketones).

Given the diverse techniques and configurations developed for monitoring POPs and CEACs in Arctic air, sampling artefacts often occur related to the technical design, sampling material, or air-sampling interval, in particular: breakthrough, microbial or photo degradation, and equilibrium or non-equilibrium states regarding passive sampling (Bohlin-Nizzetto et al 2020; Li and Wania 2021; Hao et al 2021). The concentrations of certain POPs and CEACs could be underestimated by 30-95% (Melymuk et al 2014), which might override their seasonal variations and mislead the assessment of their environmental fate and related risk. Therefore, the current challenge is to validate sampling approaches with a focus on POPs and CEACs through interlaboratory comparison to achieve comparability of air impurity measurements in the Arctic. Detailed information on methodologies for air sampling, chemical analysis, data management and quality assurance/quality control is provided in the literature and annual reports (NILU 2021).

A distinct set of methods is dedicated to aerobiology, even though the basic collection mechanism resembles that for other particulates (Feltracco et al 2021a). Aerobiological sampling methods involve impaction, impingement, membrane filtration (Figure 3) or drop plate mechanisms, which have been extensively reviewed in Griffin et al (2011). Although efforts have been made to establish standard methodologies (Pearce et al 2016; Dommergue et al 2019; Jensen et al 2022), no single ideal method exists. For example, microinvertebrates passively transported by wind are still collected by classical techniques, unchanged for decades. Each methodology has advantages and disadvantages (Table 1) – selecting the right one will depend on the research question. Recent developments in this regard include work by Ferguson et al (2019), who evaluated airborne recovery efficiencies using filtration and liquid impingement and found filtration using polycarbonate filters to give the best recovery, with impingement recommended for shorter duration

6 http://ebas-data.nilu.no

of sampling. Luhung et al (2021) investigated DNA extraction efficiencies from filters and found that direct extraction (by placing sampling filter into extraction kit) underestimated total cell numbers. Instead, they suggested a two-stage approach: first removing biomass from the filter, then re-filtering onto a smaller, thinner membrane. Total bacterial count can be measured by growing cells on agar and counting the total number of colony-forming units and using fluorescence microscopy on filters (combined with staining via a universal DNA stain such as DAPI, or a 16S-rRNA-specific probe such as EUB338) and molecular methods (Mayol et al 2014; Cuthbertson et al 2017). With the development of molecular sequencing methods (PCR, Sanger or Illumina sequencing), and improvements in microscopy, cell culture, and sampling methodology, along with modern sensitive sensors detecting changes in air composition, new possibilities opened up for quantifying the abundance, diversity, and composition of several biological constituents in the air.

Table 1: Typical aerobiology sampling methods.

Method	Advantages	Disadvantages
Membrane filtration	Low cost, easy to use, high capture rate, possibility of combining biological and chemical analysis	Desiccation of microorganisms on the filter surface, filter size can impact particle loading, inefficient extraction of nucleic acids
Impinge-ment	Efficient for culture- and non-culture-based analyses, the liquid matrix can be split for various analyses	Low capture rates, loss of collection fluid to evaporation and violent bubbling, loss of viability, liquid incompatible with chemical analysis
Impaction	Cell death from impaction is insignificant, efficient means of obtaining total counts of fungal spores, ease of use, portability, assessment of culturable populations of bacteria and fungi per volume of air	Restricted use in the analysis of other microbial types (bacteria and viruses), loss of viability due to impact stress, loss of recovery efficiency, small sample volumes due to low flow rates
Sticky traps	Low cost, easy to use and install, perfect for counting of animals and plants directly on the trap.	Dedicated to invertebrates and plant particles, often destroy invertebrate specimens; cannot be used for quantifying bacteria and fungi

3. Contributions to interdisciplinarity

An integral part of this chapter is connecting the chemical, biological and supportive physical measures of atmospheric impurity loading, and certainly more work at this interface is warranted. The analysis of geographical distribution of atmospheric impurity measurements in Svalbard shows the most likely location for interdisciplinary studies is the Ny-Ålesund hub, as co-siting multiple measurements offers vast opportunities for improved understanding of the Arctic environment as a whole. The internal harmoniation of measurements at Ny-Ålesund is already underway. Emerging disciplines, such as aerobiology and CEACs are likely to be enhanced there in the future. However, other locations also offer opportunities for interdisciplinary studies. For example, Longyearbyen could be a site to screen for changes in human impact as mining ceases to be the predominant activity in the area. Furthermore, climate-induced changes in spatial patterns and seasonality of parameters related to atmospheric impurities need to be studied at more than one site to be comprehensively understood, and the Arctic is likely to face multiple non-linear changes (e.g. Song et al 2022). Air impurity interactions with climate are likely to be at the forefront of interdisciplinary issues in Svalbard since multiple components of the atmospheric aerosol – of various origins, and both chemical and biological – can act as CCN and ice-nucleating particles (Varutbangkul et al 2006; Möhler et al 2008; King et al 2012; Abbatt et al 2019). Furthermore, both direct and indirect

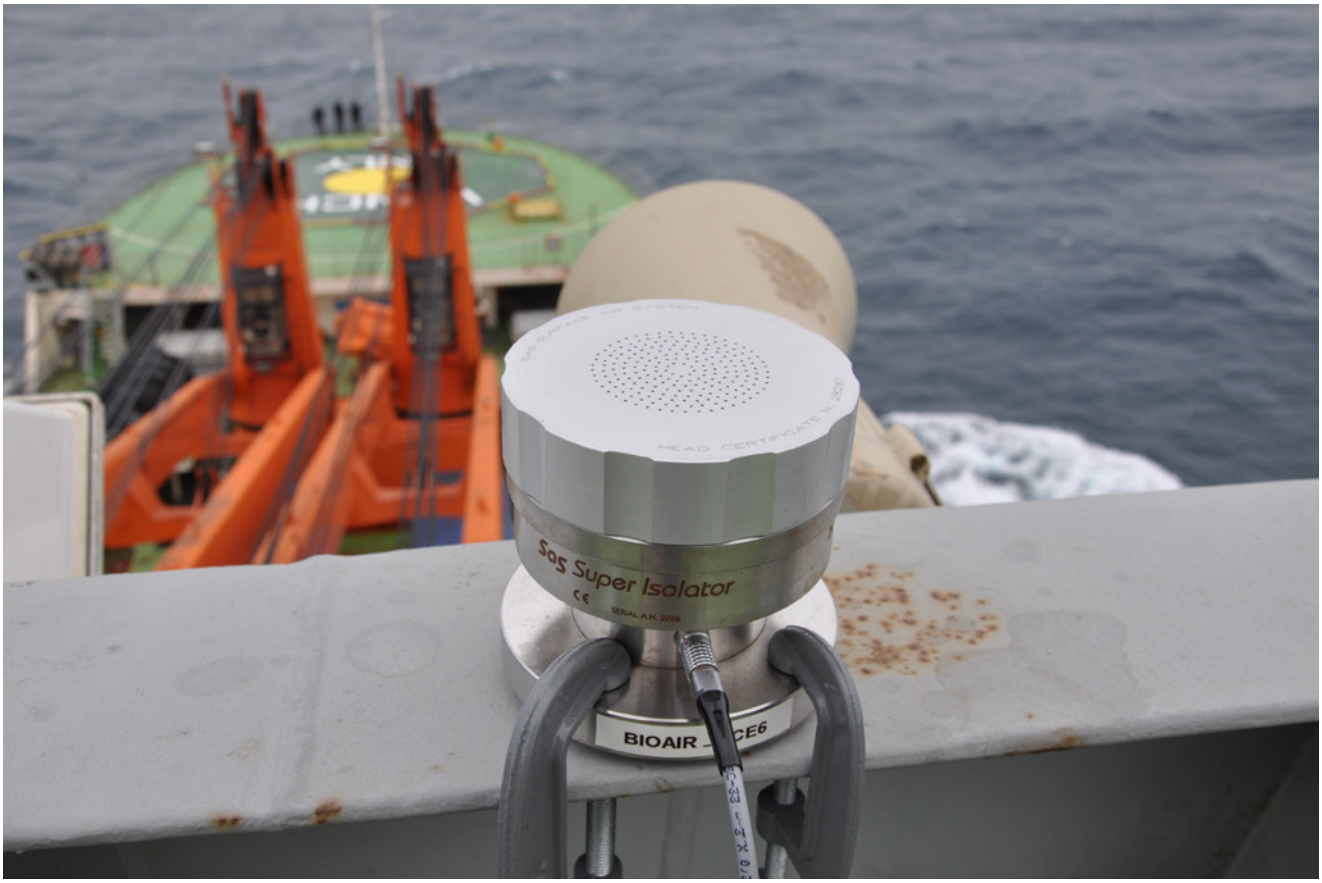

Figure 3: For air sampling for microorganisms, a number of commercial options are available. Key considerations are: a) direct collection or a filter size of 0.2 µm to capture bacteria, b) maximum flow rates for DNA yield, c) ability to withstand the Arctic environment, d) a convenient power source (battery or generator) to enable long sample runs and e) preferably many users to provide data for comparison elsewhere. Pictured is one such example, the SAS Air Sampler as deployed in the field. (Photo: David Pearce)

impacts of aerosol upon radiation and precipitation components of climate have been noted (Toon and Pollack 1980; Satheesh and Krishnamoorthy 2005; Merikanto et al 2009; Burgos et al 2020; Allen et al 2020), and the climate properties change air quality. Interdisciplinary aspects, such as impacts on cryosphere and ecosystems, are inherent in atmospheric impurity studies (Boy et al 2019), as are the well-known connections to human health, social science and economy (IPCC 2021, 2022a, b).

4. Unanswered questions

Within each field of atmospheric impurity research, there remain unanswered questions. For example, researchers investigating mineral dust still ponder the origin of the deposited material, especially whether it is local or long-range transported (e.g. Moroni et al 2016, 2018; Conca et al 2019; Kavan et al 2020; Lewandowski et al 2020). Shrinking glaciers are expected to expose more mineral dust sources locally (Zawierucha et al 2019; Schuler et al 2020; Geyman et al 2022; Rymer et al 2022). Altitude effects on mineral dust deposition are also of concern, as are seasonal changes. Other atmospheric impurities are in principle subject to the same concerns and open questionsrelated to changing origin (what is the proportion of local to long-range sources?), changing seasonality (how do seasonal patterns in impurity concentrations change?), and unknown effects of altitude. An additional concern is the question of how atmospheric impurities impact climate in such changed conditions, through light scattering in the atmosphere, precipitation changes and albedo (surface reflectivity) effects. In aerobiology, rising temperatures in the Arctic along with an increasing

number of tourists spur a question about invasion of Svalbard by non-native pollen and spores. Specifically for CEACs, questions arise about their degradation products and their environmental fate. We believe that the parallel monitoring of multiple impurities would accelerate research progress towards solving such questions, since information provided by various impurity contents will be more comprehensive and thus more likely conclusive.

5. Recommendations for the future

For a harmonised picture of spatial distribution of key atmospheric impurities across Svalbard, we recommend establishing regular measurements of a basic set of variables at ground-based stations, which are logistically available and represent a different level of local human impact (proposed here: Longyearbyen, as the main settlement, and Hornsund, as a relatively remote site with year-round staff). These are also AERONET sites, already measuring AOD. The proposed set of key impurities includes: BC (due to its climate impacts and a large uncertainty in deposition patterns; cf. Zdanowicz et al 2021); CH_4 (due to climate effects and potential local sources), inorganic ions (simple aerosol source markers), pollen (to track the colonisation of Svalbard by new plants), and selected CEACs (e.g. PFAS due to known sources in Svalbard). Such measurements should be performed with consistent methods and be subject to interlaboratory checks. Co-timing of measurements (and matching their time resolutions) at these stations will also be necessary. Regular measurements will also allow detection of changes in **seasonal phenomena** due to climate change.

For several atmospheric impurities, three sites across Svalbard are insufficient to **detect the spatial differences**, especially in bulk atmospheric deposition, which is both more varied and more relevant to the impact on the terrestrial system than pure atmospheric concentrations. For such variables, field campaigns can be used to supplement the existing data, be it with the use of passive air samplers or snow as a natural deposition medium. Impurities we recommend here are: mineral dust, CEACs with an established negative impact on the terrestrial ecosystem, BC and aerobiological parameters (the deposition of pollen, and DNA studies of microbial communities).

The altitudinal transect in Ny-Ålesund between Zeppelin and Gruvebadet should remain in operation, if possible with unified protocols – consistent with SESS report recommendations by Sipilä et al (2020) and Traversi et al (2021); shorter-term experiments on altitude differences in impurity concentrations in the atmosphere and their deposition would be beneficial elsewhere (Viola et al 2019).

Unified or highly comparable measurement methods are desired, which has already been postulated for BC (Gilardoni et al 2020) and microplastics (Singh et al 2021), or harmonised Svalbard-wide sampling strategies (consistent with the conclusions of Petkov et al 2022). Therefore, a long-term experiment involving parallel collection with different sampling protocols at one site is proposed here.

A sample bank should be designed for CEACs, in the form of non-targeted chemical analysis recording (with high-resolution gas- or liquid chromatography and mass spectrometric techniques). It is possible that a future re-analysis of such data from past samples would detect CEACs that have not yet been discovered. This would make it possible to study their temporal trends, testifying to the changing human impact in the Arctic, resulting e.g. from the diversion of shipping routes or increased tourism.

Broadening the spectrum of measured properties also applies as a prospective research area **in aerobiology** as more in-depth characterisation of the gene pool in the aerial microbiome becomes possible. Functional links with the environment are also an important concern for future aerobiology studies (new recommendations compared to Malard et al 2019).

Finally, the breadth of existing data, not all of which is fully available (FAIR-compliant), drives the last recommendation to **make the existing and future datasets findable, accessible, interoperable and reusable** to facilitate solving complex scientific problems connected to atmospheric impurities through collaboration.

6. Data availability

Data availability is shown in Appendix 2.

7. Acknowledgements

This work was funded by the Research Council of Norway, project no. 322387, Svalbard Integrated Arctic Earth Observing System – Knowledge Centre (SIOS), operational phase 2022. The workshop organised within the scope of SSG project no. 311270 (*HERMOSA*) contributed initial ideas. The chapter was supported by a subsidy of the Ministry of Education and Science in Poland for the Institute of Geophysics, Polish Academy of Sciences, which also financed the observations at the Polish Polar Station in Hornsund in the form of SPUB grants and participated in funding SIOS actions. D. Kępski's contribution was supported by the National Science Centre of Poland grant MINIATURA 4 2020/04/X/ST10/02050. J. Kavan was supported by SVELTA project no. 2020/37/K/ST10/02852 (at University of Wroclaw) and project ARCTOS MU (MUNI/G/1540/2019, at Masaryk University).

8. References

Abbatt JPD, Leaitch WR, Aliabadi AA et al (2019) Overview paper: New insights into aerosol and climate in the Arctic. 2527–2560

Åkerman J (1983) Notes concerning the vegetation on deflation surfaces, Knapp Linné, Spitsbergen. Polar Res 1:161-169

Ali AM, Langberg HA, Hale SE et al (2021) The fate of poly- and perfluoroalkyl substances in a marine food web influenced by land-based sources in the Norwegian Arctic. Environ Sci Process Impacts 23:588–604. https://doi.org/10.1039/D0EM00510J

Allen RJ, Turnock S, Nabat P et al (2020) Climate and air quality impacts due to mitigation of non-methane near-term climate forcers. Atmos Chem Phys 20:9641–9663. https://doi.org/10.5194/acp-20-9641-2020

AMAP (2011) Combined Effects of Selected Pollutants and Climate Change in the Arctic Environment. Arctic Monitoring and Assessment Programme, Oslo

AMAP (2016) AMAP Assessment 2015: Temporal Trends in Persistent Organic Pollutants in the Arctic. Oslo

AMAP (2017) AMAP Assessment 2016: Chemicals of Emerging Arctic Concern

Amore A, Giardi F, Becagli S et al (2022) Source apportionment of sulphate in the High Arctic by a 10 yr-long record from Gruvebadet Observatory (Ny-Ålesund, Svalbard Islands). Atmos Environ 270:118890. https://doi.org/10.1016/j.atmosenv.2021.118890

Anderson JR, Buseck PR, Saucy DA, Pacyna JM (1992) Characterization of individual fine-fraction particles from the Arctic aerosol at Spitsbergen, May–June 1987. Atmos Environ Part A Gen Top 26:1747–1762. https://doi.org/10.1016/0960-1686(92)90072-S

Araujo BF, Osterwalder S, Szponar N et al (2022) Mercury isotope evidence for Arctic summertime re-emission of mercury from the cryosphere. Nat Commun 13. https://doi.org/10.1038/s41467-022-32440-8

Aspmo K, Gauchard PA, Steffen A et al (2005) Measurements of atmospheric mercury species during an international study of mercury depletion events at Ny-Ålesund, Svalbard, spring 2003. How reproducible are our present methods? Atmos Environ 39:7607–7619. https://doi.org/10.1016/J.ATMOSENV.2005.07.065

Avango D (2020) Imprints on the Resource Landscape : The Long History of Mining in the Arctic. J North Stud 14:67–82

Backman J, Schmeisser L, Virkkula A et al (2017) On Aethalometer measurement uncertainties and an instrument correction factor for the Arctic. Atmos Meas Tech 10:5039–5062. https://doi.org/10.5194/amt-10-5039-2017

Bazzano A, Ardini F, Grotti M et al (2016) Elemental and lead isotopic composition of atmospheric particulate measured in the Arctic region (Ny-Ålesund, Svalbard Islands). Rend Lincei 27:73–84. https://doi.org/10.1007/S12210-016-0507-9

Becagli S, Amore A, Caiazzo L et al (2019) Biogenic Aerosol in the Artic from Eight Years of MSA Data from Ny-Ålesund (Svalbard Islands) and Thule (Greenland). Atmosphere (Basel) 10:349. https://doi.org/10.3390/atmos10070349

Beine HJ, Allegrini I, Sparapani R et al (2001) Three years of springtime trace gas and particle measurements at Ny-Ålesund, Svalbard. Atmos Environ 35:3645–3658. https://doi.org/10.1016/S1352-2310(00)00529-X

Berg T, Kallenborn R, Manø S (2004) Temporal Trends in Atmospheric Heavy Metal and Organochlorine Concentrations at Zeppelin, Svalbard. Arctic, Antarct Alp Res 36:284–291. https://doi.org/10.1657/1523-0430

Bohlin-Nizzetto P, Melymuk L, White KB et al (2020) Field- and model-based calibration of polyurethane foam passive air samplers in different climate regions highlights differences in sampler uptake performance. Atmos Environ 238:117742. https://doi.org/https://doi.org/10.1016/j.atmosenv.2020.117742

Boy M, Thomson ES, Acosta Navarro J-C et al (2019) Interactions between the atmosphere, cryosphere, and ecosystems at northern high latitudes. Atmos Chem Phys 19:2015–2061. https://doi.org/10.5194/acp-19-2015-2019

Bryś T (2002) Meteorological and orographic conditions of ionic deposition from precipitations and atmospheric depositions in the Hornsund area in the period July 1999 – June 2000. Probl Klimatologii Polarn 12:89–106

Burakowska A, Kubicki M, Mysłek-Laurikainen B et al (2021) Concentration of 7Be, 210Pb, 40K, 137Cs, 134Cs radionuclides in the ground layer of the atmosphere in the polar (Hornsund, Spitsbergen) and mid-latitudes (Otwock-Świder, Poland) regions. J Environ Radioact 240:106739. https://doi.org/10.1016/j.jenvrad.2021.106739

Burgos MA, Andrews E, Titos G et al (2020) A global model-measurement evaluation of particle light scattering coefficients at elevated relative humidity. Atmos Chem Phys 20:10231–10258. https://doi.org/10.5194/acp-20-10231-2020

Burzyk M, Burzyk J, Głowacki P (2001) Comparative chemical characteristics of precipitation in the Hornsund region (SW Spitsbergen) in the years 1993-1994 and 1998-1999. Pol. Polar Res. 22 (3-4):233-247

Caiazzo L, Calzolai G, Becagli S et al (2021) Carbonaceous Aerosol in Polar Areas: First Results and Improvements of the Sampling Strategies. Atmosphere (Basel) 12:320. https://doi.org/10.3390/atmos12030320

Carlsson P, Christensen JH, Borgå K et al (2016) AMAP 2016. Influence of Climate Change on Transport, Levels, and Effects of Contaminants in Northern Areas - Part 2

Chang RYW, Leck C, Graus M et al (2011) Aerosol composition and sources in the central Arctic Ocean during ASCOS. Atmos Chem Phys 11:10619–10636. https://doi.org/10.5194/acp-11-10619-2011

Chernov DG, Kozlov VS, Panchenko MV et al (2016) Investigation of microphysical characteristics and chemical composition of near-ground aerosol in Barentsburg (Spitsbergen) in the spring and summer seasons of 2011-2015. In 22nd International Symposium on Atmospheric and Ocean Optics: Atmospheric Physics 10035:690-695

Chi JW, Li WJ, Zhang DZ et al (2015) Sea salt aerosols as a reactive surface for inorganic and organic acidic gases in the Arctic troposphere. Atmos Chem Phys 15:11341–11353. https://doi.org/10.5194/acp-15-11341-2015

Conca E, Abollino O, Giacomino A et al (2019) Source identification and temporal evolution of trace elements in PM10 collected near to Ny-Ålesund (Norwegian Arctic). Atmos Environ 203:153–165. https://doi.org/10.1016/j.atmosenv.2019.02.001

Conca E, Malandrino M, Giacomino A et al (2021) Chemical Fractionation of Trace Elements in Arctic PM10 Samples. Atmosphere (Basel) 12:1152. https://doi.org/10.3390/atmos12091152

Coulson SJ (2015) The alien terrestrial invertebrate fauna of the High Arctic archipelago of Svalbard: potential implications for the native flora and fauna. Polar Res 34:27364. https://doi.org/10.3402/polar.v34.27364

Coulson SJ, Fjellberg A, Gwiazdowicz DJ et al (2013) Introduction of invertebrates into the High Arctic via imported soils: the case of Barentsburg in the Svalbard. Biol Invasions 15:1–5. https://doi.org/10.1007/s10530-012-0277-y

Coulson SJ, Hodkinson ID, Webb NR et al (2002) Aerial colonization of high Arctic islands by invertebrates: the diamondback moth Plutella xylostella (Lepidoptera: Yponomeutidae) as a potential indicator species. Divers Distrib 8:327–334. https://doi.org/10.1046/j.1472-4642.2002.00157.x

Coulson SJ, Hodkinson ID, Webb NR (2003) Aerial dispersal of invertebrates over a high-Arctic glacier foreland: Midtre Lovenbreen, Svalbard. Polar Biol 26:530–537. https://doi.org/10.1007/s00300-003-0516-x

Cuthbertson L, Amores-Arrocha H, Malard L et al (2017) Characterisation of Arctic Bacterial Communities in the Air above Svalbard. Biology (Basel) 6. https://doi.org/10.3390/biology6020029

Dastoor A, Wilson SJ, Travnikov O et al (2022) Arctic atmospheric mercury: Sources and changes. Sci Total Environ 839:156213. https://doi.org/https://doi.org/10.1016/j.scitotenv.2022.156213

Demin BN, Graevsky AP, Demeshkin AS et al (2011) The state and trends of environmental pollution in the places of economic activity of Russian enterprises on Spitsbergen archipelago (Barentsburg and adjacent territories) for the period 2002-2010. RPA "Typhoon", Saint-Petersburg. 316 p. [In Russian].

Di Mauro B, Cappelletti D, Moroni B, Mazzola M, Gilardoni S, Luks B, Nawrot A, Lewandowski M, Dagsson Waldhauserova P, Meinander O, Wittmann M, Kaspari S, Khan A (2023) Dust in Svalbard: local sources versus long-range transported dust. In: Gevers et al (eds) SESS report 2022, Svalbard Integrated Arctic Earth Observing System, Longyearbyen, pp 62-77. https://doi.org/10.5281/zenodo.7377518

Dommergue A, Amato P, Tignat-Perrier R et al (2019) Methods to Investigate the Global Atmospheric Microbiome. Front Microbiol 10. https://doi.org/10.3389/fmicb.2019.00243

Drotikova T, Ali AM, Halse AK et al (2020) Polycyclic aromatic hydrocarbons (PAHs) and oxy- and nitro-PAHs in ambient air of the Arctic town Longyearbyen, Svalbard. Atmos Chem Phys 20:9997–10014. https://doi.org/10.5194/acp-20-9997-2020

Drotikova T, Dekhtyareva A, Kallenborn R, Albinet A (2021) Polycyclic aromatic hydrocarbons (PAHs) and their nitrated and oxygenated derivatives in the Arctic boundary layer: seasonal trends and local anthropogenic influence. Atmos Chem Phys 21:14351–14370. https://doi.org/10.5194/acp-21-14351-2021

EANET (2003) Technical Document for Filter Pack Method in East Asia. Acid Deposition and Oxidant Research Center, 2003. https://www.eanet.asia/wp-content/uploads/2019/04/techdoc_fp.pdf

EMEP (2001) EMEP manual for sampling and chemical analysis 2001. EMEP Co-operative Programme for Monitoring and Evaluation of the Long-range Transmission of Air Pollutants in Europe. http://www.nilu.no/projects/ccc/manual/index.html

Evenset A, Ottesen R (2009) Norsk og russisk overvaking av PCB-forurensning ved bosettinger pa Svalbard: Sammenligning av felt- og analysemetoder og resultater. Akvaplan-niva. Tromsø, Norway.

Feltracco M, Barbaro E, Hoppe CJM et al (2021a) Airborne bacteria and particulate chemistry capture Phytoplankton bloom dynamics in an Arctic fjord. Atmos Environ 256:118458. https://doi.org/10.1016/j.atmosenv.2021.118458

Feltracco M, Barbaro E, Kirchgeorg T et al (2019) Free and combined L- and D-amino acids in Arctic aerosol. Chemosphere 220:412–421. https://doi.org/10.1016/j.chemosphere.2018.12.147

Feltracco M, Barbaro E, Spolaor A et al (2021b) Year-round measurements of size-segregated low molecular weight organic acids in Arctic aerosol. Sci Total Environ 763:142954. https://doi.org/10.1016/j.scitotenv.2020.142954

Feltracco M, Barbaro E, Tedeschi S et al (2020) Interannual variability of sugars in Arctic aerosol: Biomass burning and biogenic inputs. Sci Total Environ 706:136089. https://doi.org/10.1016/j.scitotenv.2019.136089

Ferguson RMW, Garcia-Alcega S, Coulon F et al (2019) Bioaerosol biomonitoring: Sampling optimization for molecular microbial ecology. Mol Ecol Resour 19:672–690. https://doi.org/10.1111/1755-0998.13002

Ferrari C, Gauchard P, Aspmo K et al (2005) Snow-to-air exchanges of mercury in an Arctic seasonal snow pack in Ny-Ålesund, Svalbard. Atmos Environ 39:7633–7645. https://doi.org/10.1016/j.atmosenv.2005.06.058

Ferrero L, Sangiorgi G, Perrone M et al (2019) Chemical Composition of Aerosol over the Arctic Ocean from Summer ARctic EXpedition (AREX) 2011–2012 Cruises: Ions, Amines, Elemental Carbon, Organic Matter, Polycyclic Aromatic Hydrocarbons, n-Alkanes, Metals, and Rare Earth Elements. Atmosphere (Basel) 10:54. https://doi.org/10.3390/atmos10020054

Gallet JC, Björkman MP, Borstad CP, Hodson AJ, Jakobi H-W, Larose C, Luks B, Spolaor A, Schuler TV, Urazgildeeva A, Zdanowicz C (2019) Snow research in Svalbard: current status and knowledge gaps. In: Orr et al. (eds): SESS report 2018. Svalbard Integrated Arctic Earth Observing System, Longyearbyen, pp 82–107. https://doi.org/10.5281/zenodo.4778366

Gallet JC, Bjorkman MP, Larose C et al (2018) Protocols and recommendations for the measurement of snow physical properties, and sampling of snow for black carbon, water isotopes, major ions and microorganisms. Short report 046, Norwegian Polar Institute, Tromsø, Norway

Gauchard PA, Aspmo K, Temme C et al (2005) Study of the origin of atmospheric mercury depletion events recorded in Ny-Ålesund, Svalbard, spring 2003. Atmos Environ 39:7620–7632. https://doi.org/10.1016/J.ATMOSENV.2005.08.010

Gębica P, Szczęsny R (1988) Symptoms of aeolian accumulation in western Sorkapp Land Spitsbergen. Pol. Polar Res. 9, 447-460.

Geyman EC, van Pelt WJJ, Maloof AC et al (2022) Historical glacier change on Svalbard predicts doubling of mass loss by 2100. Nature 601:374–379. https://doi.org/10.1038/s41586-021-04314-4

Giardi F, Becagli S, Traversi R et al (2016) Size distribution and ion composition of aerosol collected at Ny-Ålesund in the spring–summer field campaign 2013. Rend Lincei 27:47–58. https://doi.org/10.1007/s12210-016-0529-3

Gilardoni S, Lupi A, Mazzola M, Cappelletti DM, Moroni B, Ferrero L, Markuszewski P, Rozwadowska A, Krecji R, Zieger P, Tunved P, Karlsson L, Vratolis S, Eleftheriadis K, Viola AP (2020) Atmospheric black carbon in Svalbard. In: Van den Heuvel et al. (eds): SESS report 2019, Svalbard Integrated Arctic Earth Observing System, Longyearbyen, pp 196–211. https://doi.org/10.5281/zenodo.4707201

Głowacki P, Leszkiewicz J (1994) Physico–chemical properties of precipitation and snow cover in Spitsbergen in winter season 1992/1993. XXI Polar Symp. 60 Years of Polish Research of Spitsbergen, Warsaw: 199-208.

Głowacki P, Pulina M (2000) The physico-chemical properties of the snow cover of Spitsbergen (Svalbard) based on investigations during the winter season 1990/1991. Pol Polar Res 21(2):65-88

Głowacki P, Krawczyk WE (2002) Long range transport of pollutants – evidences from rainfall chemistry in Hornsund (Svalbard). In: Orbaek JB (ed) The Changing Physical Environment. Pro ceedings from the Sixth Ny–Ålesund International Scientific Seminar, Tromsø, Norway, Norsk Polarinstitutt Internrapport 10:65–69.

Golobokova LP, Pol'kin VV, Kabanov DM et al (2013) Studies of atmospheric aerosols in the Russian Arctic regions. Led i Sneg (Ice and Snow). 53(2):129-136.

Golobokova LP, Khodzher TV, Chernov DG et al (2020) Chemical composition of the near-surface atmospheric aerosol in Barentsburg (Spitsbergen) based on the long-term observations. Led i Sneg (Ice and Snow) 60(1):85–97. [In Russian]. https://doi.org/10.31857/S2076673420010025

Hall D, Upton S (1988) A wind tunnel study of the particle collection efficiency of an inverted Frisbee used as a dust deposition gauge. Atmos Environ 22:1383–1394

Hansen G, Kouremeti N, Gilardoni S, Stebel K, Evangeliou N, Ritter C, Zielinski T, Herrero S, Kazadzis S, Mateos D, Mazzola M, Pakszys P, Eleftheriadis K (2023) Long-term observations of aerosol optical depth and their relation to in-situ aerosol properties in the Svalbard region. In: Gevers et al (eds) SESS report 2022, Svalbard Integrated Arctic Earth Observing System, Longyearbyen, pp 44-61. https://doi.org/10.5281/zenodo.7376140

Hao Y, Li Y, Wania F et al (2021) Atmospheric concentrations and temporal trends of polychlorinated biphenyls and organochlorine pesticides in the Arctic during 2011–2018. Chemosphere 267:128859. https://doi.org/10.1016/j.chemosphere.2020.128859

Heintzenberg J, Leck C, Tunved P (2015) Potential source regions and processes of aerosol in the summer Arctic. Atmos Chem Phys 15:6487–6502. https://doi.org/10.5194/acp-15-6487-2015

Hodkinson ID, Coulson SJ, Harrison J, Webb NR (2001) What a wonderful web they weave: spiders, nutrient capture and early ecosystem development in the high Arctic - some counter-intuitive ideas on community assembly. Oikos 95:349–352. https://doi.org/10.1034/j.1600-0706.2001.950217.x

Hung H, Kallenborn R, Breivik K et al (2010) Atmospheric monitoring of organic pollutants in the Arctic under the Arctic Monitoring and Assessment Programme (AMAP): 1993-2006. Sci Total Environ 408:2854–2873. https://doi.org/10.1016/j.scitotenv.2009.10.044

IPCC W (2021) Climate Change 2021. The Physical Science Basis. Summary for Policymakers

IPCC W (2022a) Climate Change 2022. Impacts, Adaptation and Vulnerability. Summary for policymakers

IPCC W (2022b) Climate Change 2022. Mitigation of Climate Change. Summary for Policymakers

Iversen T (1989) Some statistical properties of ground level air pollution at Norwegian Arctic stations and their relation to large scale atmospheric flow systems. Atmos Environ 23:2451–2462

Iversen T, Joranger E (1985) Arctic air pollution and large scale atmospheric flows. Atmos Environ 19:2099–2108

Jacobi H-W, Obleitner F, Da Costa S et al (2019) Deposition of ionic species and black carbon to the Arctic snowpack: combining snow pit observations with modeling. Atmos Chem Phys 19:10361–10377. https://doi.org/10.5194/acp-19-10361-2019

Jang S, Park K-T, Lee K et al (2021) Large seasonal and interannual variations of biogenic sulfur compounds in the Arctic atmosphere (Svalbard; 78.9° N, 11.9° E). Atmos Chem Phys 21:9761–9777. https://doi.org/10.5194/acp-21-9761-2021

Jensen LZ, Glasius M, Gryning S et al (2022) Seasonal Variation of the Atmospheric Bacterial Community in the Greenlandic High Arctic Is Influenced by Weather Events and Local and Distant Sources. Front Microbiol 13:1–13. https://doi.org/10.3389/fmicb.2022.909980

Johansen S, Hafsten U (1988) Airborne pollen and spore registrations at Ny-Ålesund, Svalbard, summer 1986. Polar Res 6:11–17. https://doi.org/10.3402/polar.v6i1.6842

Kallenborn R, Brorström-Lundén E, Reiersen L, Wilson S (2018) Pharmaceuticals and personal care products (PPCPs) in Arctic environments: indicator contaminants for assessing local and remote anthropogenic sources in a pristine ecosystem in change. Env Sci Pollut Res 25:33001–33013. https://doi.org/10.1007/s11356-017-9726-6

Kandler K, Schneiders K, Heuser J et al (2020) Differences and Similarities of Central Asian, African, and Arctic Dust Composition from a Single Particle Perspective. Atmosphere (Basel) 11:269. https://doi.org/10.3390/atmos11030269

Karanasiou A, Minguillón MC, Viana M et al (2015) Thermal-optical analysis for the measurement of elemental carbon (EC) and organic carbon (OC) in ambient air a literature review. Atmos Meas Tech Discuss 8:9649–9712. https://doi.org/10.5194/amtd-8-9649-2015

Karasiński G, Posyniak M, Bloch M et al (2013) Lidar observations of volcanic dust over Polish Polar Station at Hornsund after eruptions of Eyjafjallajökull and Grímsvötn. Acta Geophys 62:316–339. https://doi.org/10.2478/s11600-013-0183-4

Kavan J, Láska K, Nawrot A, Wawrzyniak T (2020) High Latitude Dust Transport Altitude Pattern Revealed from Deposition on Snow, Svalbard. Atmosphere (Basel) 11:1318. https://doi.org/10.3390/atmos11121318

Khan AL, Dierssen H, Schwarz JP et al (2017) Impacts of coal dust from an active mine on the spectral reflectance of Arctic surface snow in Svalbard, Norway. J Geophys Res Atmos 122:1767–1778. https://doi.org/10.1002/2016JD025757

King SM, Butcher AC, Rosenoern T et al (2012) Investigating primary marine aerosol properties: CCN activity of sea salt and mixed inorganic-organic particles. Environ Sci Technol 46:10405–10412. https://doi.org/10.1021/es300574u

Kondo Y, Sahu L, Moteki N et al (2011) Consistency and Traceability of Black Carbon Measurements Made by Laser-Induced Incandescence, Thermal-Optical Transmittance, and Filter-Based Photo-Absorption Techniques. Aerosol Sci Technol 45:295–312. https://doi.org/10.1080/02786826.2010.533215

Kozak K, Kozioł K, Luks B et al (2015) The role of atmospheric precipitation in introducing contaminants to the surface waters of the Fuglebekken catchment, Spitsbergen. Polar Res 34:24207. https://doi.org/10.3402/polar.v34.24207

Krawczyk WE, Głowacki P, Niedźwiedź T (2002) Charakterystyka chemiczna opadów atmosferycznych w rejonie Hornsundu (SW Spitsbergen) latem 2000 r. na tle cyrkulacji atmosferycznych. In: A. Kostrzewski and G. Rachlewicz (eds) Polish Polar Studies. Funkcjonowanie i monitoring geoekosystemów obszarów polarnych. Poznań: 187–202 [in Polish]

Krawczyk WE, Skręt U (2005) Organic compounds in rainfall at Hornsund, SW Spitsbergen: qualitative results. Pol Polar Res 26(1):65–76

Krawczyk WE, Bartoszewski SA, Siwek K (2008) Rain water chemistry at Calypsobyen, Svalbard. Polish Polar Res 29:149–162

Kvello JK, (2004) Store norske Spitsbergen kulkompani: om å arbeide i en politisk bedrift på Svalbard 1970-2000. Store Norske: Longyearbyen, 304 pp

Leck C, Nilsson ED, Bigg EK, Bäcklin L (2001) Atmospheric program on the Arctic Ocean Expedition 1996 (AOE-96): An overview of scientific goals, experimental approach, and instruments. J Geophys Res Atmos 106:32051–32067. https://doi.org/10.1029/2000JD900461

Lewandowski M, Kusiak MA, Werner T et al (2020) Seeking the Sources of Dust: Geochemical and Magnetic Studies on "Cryodust" in Glacial Cores from Southern Spitsbergen (Svalbard, Norway). Atmosphere (Basel) 11:1325. https://doi.org/10.3390/atmos11121325

Li J, Xie Z, Mi W et al (2017) Organophosphate Esters in Air, Snow, and Seawater in the North Atlantic and the Arctic. Environ Sci Technol 51:6887–6896. https://doi.org/10.1021/acs.est.7b01289

Li Y, Wania F (2021) Partitioning between polyurethane foam and the gas phase: data compilation, uncertainty estimation and implications for air sampling. Environ Sci Process Impacts 23:723–734. https://doi.org/10.1039/D1EM00036E

Li Y, Xiong S, Hao Y et al (2022) Organophosphate esters in Arctic air from 2011 to 2019: Concentrations, temporal trends, and potential sources. J Hazard Mater 434:128872. https://doi.org/10.1016/j.jhazmat.2022.128872

Luhung I, Uchida A, Lim SBY et al (2021) Experimental parameters defining ultra-low biomass bioaerosol analysis. npj Biofilms Microbiomes 7:37. https://doi.org/10.1038/s41522-021-00209-4

Lundkvist Q, Pedersen HR, Ottesen RT et al (2008) PCBs in Svalbard: status of knowledge and management, April 2008.

Ma J, Hung H, Macdonald RW (2016) The influence of global climate change on the environmental fate of persistent organic pollutants: A review with emphasis on the Northern Hemisphere and the Arctic as a receptor. Glob Planet Change 146:89–108. https://doi.org/10.1016/j.gloplacha.2016.09.011

Ma J, Hung H, Tian C, Kallenborn R (2011) Revolatilization of persistent organic pollutants in the Arctic induced by climate change. Nat Clim Chang 1:255–260. https://doi.org/10.1038/nclimate1167

Malard L, Avila-Jimenez M, Convey P, Larose C, Hodson A, Øvreås L, Schmale J, Anwar MZ, Pearce D (2019) Microbial activity monitoring by the Integrated Arctic Earth Observing System. In: Orr et al. (eds): SESS report 2018, Svalbard Integrated Arctic Earth Observing System, Longyearbyen, pp 48-81. https://doi.org/10.5281/zenodo.4778348

Markowicz KM, Pakszys P, Ritter C et al (2016) Impact of North American intense fires on aerosol optical properties measured over the European Arctic in July 2015. J Geophys Res Atmos 121. https://doi.org/10.1002/2016JD025310

Marquès M, Sierra J, Drotikova T et al (2017) Concentrations of polycyclic aromatic hydrocarbons and trace elements in Arctic soils : A case-study in Svalbard. Environ Res 159:202–211. https://doi.org/10.1016/j.envres.2017.08.003

Mayol E, Jimenez MA, Herndl GJ et al (2014) Resolving the abundance and air-sea fluxes of airborne microorganisms in the North Atlantic Ocean. Front Microbiol 5. https://doi.org/10.3389/fmicb.2014.00557

Mazzola M, Viola AP, Cappelletti DM, Ritter C, Storvold R (2020) Probing of the Vertical Structure of the lower Atmosphere over Svalbard. In: Van den Heuvel et al. (eds): SESS report 2019, Svalbard Integrated Arctic Earth Observing System, Longyearbyen, pp 212-235. https://doi.org/10.5281/zenodo.4777711

Melymuk L, Bohlin P, Sáňka O et al (2014) Current Challenges in Air Sampling of Semivolatile Organic Contaminants: Sampling Artifacts and Their Influence on Data Comparability. Environ Sci Technol 48:14077–14091. https://doi.org/10.1021/es502164r

Merikanto J, Spracklen D V, Mann GW et al (2009) Impact of nucleation on global CCN. Atmos Chem Phys 9:8601–8616. https://doi.org/10.5194/acp-9-8601-2009

Migała K, Sobik M (1984) Deflation and nival eolian phenomena observed under conditions of congelation in the forefield of the Werenskiold Glacier (SW Spitsbergen). Zeitschrift fur Gletscherkd und Glazialgeol 197–206

Möhler O, Georgakopoulos DG, Morris CE et al (2008) Heterogeneous ice nucleation activity of bacteria: new laboratory experiments at simulated cloud conditions. Biogeosciences 5:1425–1435. https://doi.org/10.5194/bg-5-1425-2008

Moroni B, Arnalds O, Dagsson-Waldhauserová P et al (2018) Mineralogical and Chemical Records of Icelandic Dust Sources Upon Ny-Ålesund (Svalbard Islands). Front Earth Sci 6. https://doi.org/10.3389/feart.2018.00187

Moroni B, Becagli S, Bolzacchini E et al (2015) Vertical Profiles and Chemical Properties of Aerosol Particles upon Ny-Ålesund (Svalbard Islands). Adv Meteorol 2015:292081. https://doi.org/10.1155/2015/292081

Moroni B, Cappelletti D, Ferrero L et al (2016) Local vs. long-range sources of aerosol particles upon Ny-A (Svalbard Islands): mineral chemistry and geochemical records. Rend Lincei 27:115–127. https://doi.org/10.1007/s12210-016-0533-7

Myhre CL, Hermansen O, Fjæraa AM, et al (2010) Greenhouse gas monitoring at the Zeppelin station. Annual report 2008, prepared for Klima- og forurensningsdirektoratet (Klif) by Norsk institutt for luftforskning (NILU), report no. 1071/2010, ISBN 978-82-425-2212-2, Norway.

Mysłek-Laurikainen B, Matul M, Mikołajewski S et al (2006) Air aerosol sampling station AZA-1000 at Polish Polar Station in Hornsund, Spitsbergen. Nukleonika 51:137–140

Nawrot AP, Migała K, Luks B et al (2016) Chemistry of snow cover and acidic snowfall during a season with a high level of air pollution on the Hans Glacier, Spitsbergen. Polar Sci 10:249–261. https://doi.org/10.1016/j.polar.2016.06.003

NILU (2021) Monitoring of environmental contaminants in air and precipitation. Annual report 2020

Oehme M, Ottar B (1984) The long range transport of polyclorinated hydrocarbons to the Arctic. Geophys Res Lett 11:1133–1136. https://doi.org/10.1029/GL011i011p01133

Osterwalder S, Dunham-Cheatham SM, Ferreira Araujo B et al (2021) Fate of Springtime Atmospheric Reactive Mercury: Concentrations and Deposition at Zeppelin, Svalbard. ACS Earth Sp Chem 5:3234–3246. https://doi.org/10.1021/ACSEARTHSPACECHEM.1C00299

Paatero J, Hatakka J, Holmén K et al (2003) Lead-210 concentration in the air at Mt. Zeppelin, Ny-Ålesund, Svalbard. Phys Chem Earth 28:1175–1180. https://doi.org/10.1016/J.PCE.2003.08.050

Paatero J, Vira J, Siitari-Kauppi M et al (2012) Airborne fission products in the high Arctic after the Fukushima nuclear accident. J Environ Radioact 114:41–47. https://doi.org/10.1016/j.jenvrad.2011.12.027

Pakszys P, Zieliński T, Ferrero L et al (2020) Changing Arctic. Firm scientific evidence versus public interest in the issue. Oceanologia 62:593–602. https://doi.org/10.1016/j.oceano.2020.03.004

Park K-T, Jang S, Lee K et al (2017) Observational evidence for the formation of DMS-derived aerosols during Arctic phytoplankton blooms. Atmos Chem Phys 17:9665–9675. https://doi.org/10.5194/acp-17-9665-2017

Pearce DA, Alekhina IA, Terauds A et al (2016) Aerobiology Over Antarctica – A New Initiative for Atmospheric Ecology. Front Microbiol 7. https://doi.org/10.3389/fmicb.2016.00016

Pękala K (1980) Morphogenetic processes and cover deposits of nunataks in the Hornsund area (SW Spitsbergen). Pol Polar Res 1(2–3):9-44

Petkov BH, Vitale V, Hansen GH, Svendby TM, Sobolewski PS, Láska K, Elster J, Viola A, Mazzola M, Lupi (2019) Observations of the solar UV irradiance and ozone column at Svalbard. In: Orr et al. (eds): SESS report 2018, Svalbard Integrated Arctic Earth Observing System, Longyearbyen, pp 170-183. https://doi.org/10.5281/zenodo.4778491

Petkov BH, Vitale V, Di Carlo P, Hansen GH, Svendby TM, Laska K, Sobolewski PS, Solomatnikova A, Pavlova K, Johnsen B, Posyniak MA, Elster J, Mazzola M, Lupi A, Verazzo G (2022) The extreme Arctic ozone depletion in 2020 as was observed from Svalbard. In: Feldner et al (eds) SESS report 2021, Svalbard Integrated Arctic Earth Observing System, Longyearbyen, pp 66-73. https://doi.org/10.5281/zenodo.5751922

Petzold A, Ogren JA, Fiebig M et al (2013) Recommendations for reporting "black carbon" measurements. Atmos Chem Phys 13:8365–8379. https://doi.org/10.5194/acp-13-8365-2013

Petzold A, Schönlinner M (2004) Multi-angle absorption photometry—a new method for the measurement of aerosol light absorption and atmospheric black carbon. J Aerosol Sci 35:421–441. https://doi.org/https://doi.org/10.1016/j.jaerosci.2003.09.005

Pietruczuk A, Karasiński G (2010) LIDAR at Polish Polar Station, instrument design and first results. In: Reviewed Papers of 25th ILRC International Laser Radar Conference. pp 5–9

Pilskog HE, Solhøy T, Gwiazdowicz DJ et al (2014) Invertebrate communities inhabiting nests of migrating passerine, wild fowl and sea birds breeding in the High Arctic, Svalbard. Polar Biol 37:981–998. https://doi.org/10.1007/s00300-014-1495-9

Platt SM, Hov Ø, Berg T et al (2022) Atmospheric composition in the European Arctic and 30 years of the Zeppelin Observatory, Ny-Ålesund. Atmos Chem Phys 22:3321–3369. https://doi.org/10.5194/acp-22-3321-2022

Polunin N (1955) ARCTIC AEROPALYNOLOGY: SPORA OBSERVED ON STICKY SLIDES EXPOSED IN VARIOUS REGIONS IN 1950. Can J Bot 33:401–415. https://doi.org/10.1139/b55-034

Pulina M (1991) Stratification and physico-chemical properties of snow in Spitsbergen in the hydro-glaciological year 1989/1990. — Wyprawy Geograficzne na Spitsbergen. Materiały Sesji Polarnej "Arctic Environment Research", UMCS, Lublin: 191-213

Pusz W, Urbaniak J (2021) Airborne fungi in Longyearbyen area (Svalbard, Norway) — case study. Environ Monit Assess 193:290. https://doi.org/10.1007/s10661-021-09090-2

Reimann S, Kallenborn R, Schmidbauer N (2009) Severe aromatic hydrocarbon pollution in the Arctic town of Longyearbyen (Svalbard) caused by snowmobile emissions. Environ Sci Technol 43:4791–4795. https://doi.org/10.1021/es900449x

Röhler L, Bohlin-Nizzetto P, Rostkowski P et al (2021) Non-target and suspect characterisation of organic contaminants in ambient air – Part 1: Combining a novel sample clean-up method with comprehensive two-dimensional gas chromatography. Atmos Chem Phys 21:1697–1716. https://doi.org/10.5194/acp-21-1697-2021

Röhler L, Schlabach M, Haglund P et al (2020) Non-target and suspect characterisation of organic contaminants in Arctic air -- Part 2: Application of a new tool for identification and prioritisation of chemicals of emerging Arctic concern in air. Atmos Chem Phys 20:9031–9049. https://doi.org/10.5194/acp-20-9031-2020

Ruman M, Szopińska M, Kozak K et al (2014) The research of the contamination levels present in samples of precipitation and surface waters collected from the catchment area Fuglebekken (Hornsund, Svalbard Archipelago). In: Proceedings of the AIP Conference. Athens, pp 297–300

Rymer KG, Rachlewicz G, Buchwal A et al (2022) Contemporary and past aeolian deposition rates in periglacial conditions (Ebba Valley, central Spitsbergen). CATENA 211:105974. https://doi.org/10.1016/j.catena.2021.105974

Sakerin SM, Chernov DG, Kabanov DM et al (2012) Preliminary results of studying the aerosol characteristics of the atmosphere in the region of Barentsburg, Spitsbergen. Problemy Arktiki i Antarktiki. 1(91):20-31. [In Russian].

Sakerin SM, Golobokova LP, Kabanov DM et al (2018) Seasonal and interannual variability of aerosol characteristics in arctic settlement of Barentsburg (Spitsbergen, 2011-1017). Materials of the XXIV International Symposium Optics of atmosphere and ocean. Physical atmosphere, 2-5 July 2018 Tomsk. pp 67-71. [In Russian].

Sakerin SM, Golobokova LP, Kabanov DM et al (2019) Comparison of average aerosol characteristics in neighboring Arctic regions. Atmospheric and Oceanic Optics 32(1):33-40.

Satheesh S, Krishnamoorthy K (2005) Radiative effects of natural aerosols: A review. Atmos Environ 39:2089–2110. https://doi.org/10.1016/j.atmosenv.2004.12.029

Scalabrin E, Zangrando R, Barbaro E et al (2012) Amino acids in Arctic aerosols. Atmos Chem Phys 12:10453–10463. https://doi.org/10.5194/acp-12-10453-2012

Schuler TV, Kohler J, Elagina N et al (2020) Reconciling Svalbard Glacier Mass Balance. Front Earth Sci 8. https://doi.org/10.3389/feart.2020.00156

Schwarz JP, Spackman JR, Gao RS et al (2010) The Detection Efficiency of the Single Particle Soot Photometer. Aerosol Sci Technol 44:612–628. https://doi.org/10.1080/02786826.2010.481298

Sha B, Johansson JH, Tunved P et al (2022) Sea Spray Aerosol (SSA) as a Source of Perfluoroalkyl Acids (PFAAs) to the Atmosphere: Field Evidence from Long-Term Air Monitoring. Environ Sci Technol 56:228–238. https://doi.org/10.1021/acs.est.1c04277

Shpartko VI, Popova SA, Legan MV (2021) The SR-XFA Method Used to Determine the Multi-Element Composition of Arctic Aerosols. IOP Conf Ser Earth Environ Sci 666:052082. https://doi.org/10.1088/1755-1315/666/5/052082

Sierau B, Chang RYW, Leck C et al (2014) Single-particle characterization of the high-Arctic summertime aerosol. Atmos Chem Phys 14:7409–7430. https://doi.org/10.5194/acp-14-7409-2014

Singh N, Granberg M, Collard F, Caruso G, Lu Z, Kögel T, Gabrielsen GW (2021) Microplastics in the realm of Svalbard: current knowledge and future perspective. In: Moreno-Ibáñez et al (eds) SESS report 2020, Svalbard Integrated Arctic Earth Observing System, Longyearbyen, pp 118-141. https://doi.org/10.5281/zenodo.4293836

Sipilä M, Hoppe CJM, Viola A, Mazzola M, Krejci R, Zieger P, Beck L, Petäjä T (2020) Multidisciplinary research on biogenically driven new particle formation in Svalbard. In: Van den Heuvel et al. (eds): SESS report 2019, Svalbard Integrated Arctic Earth Observing System, Longyearbyen, pp 168–194. https://doi.org/10.5281/zenodo.4707175

Skaar JS, Ræder EM, Lyche JL, Ahrens L (2019) Elucidation of contamination sources for poly- and perfluoroalkyl substances (PFASs) on Svalbard (Norwegian Arctic). Env Sci Pollut Res Int 26:7356–7363. https://doi.org/10.1007/s11356-018-2162-4

Song C, Becagli S, Beddows DCS et al (2022) Understanding Sources and Drivers of Size-Resolved Aerosol in the High Arctic Islands of Svalbard Using a Receptor Model Coupled with Machine Learning. Environ Sci Technol. https://doi.org/10.1021/acs.est.1c07796

Spolaor A, Gabrieli J, Martma T et al (2013) Sea ice dynamics influence halogen deposition to Svalbard. Cryosphere 7:1645–1658. https://doi.org/10.5194/tc-7-1645-2013

Spolaor A, Moroni B, Luks B et al (2021) Investigation on the Sources and Impact of Trace Elements in the Annual Snowpack and the Firn in the Hansbreen (Southwest Spitsbergen). Front Earth Sci 8. https://doi.org/10.3389/feart.2020.536036

Teinilä K, Hillamo R, Kerminen V-M, Beine H (2003) Aerosol chemistry during the NICE dark and light campaigns. Atmos Environ 37:563–575. https://doi.org/10.1016/S1352-2310(02)00826-9

Terpugova SA, Zenkova PN, Kabanov DM et al (2018) Results of the Study of Aerosol Characteristics in the Atmosphere of the Kara and Barents Seas in Summer and Autumn 2016. Atmos Ocean Opt 31:507–518. https://doi.org/10.1134/S1024856018050172

Tjernström M, Leck C, Birch CE et al (2014) The Arctic Summer Cloud Ocean Study (ASCOS): overview and experimental design. Atmos Chem Phys 14:2823–2869. https://doi.org/10.5194/acp-14-2823-2014

Toon OB, Pollack JB (1980) Atmospheric Aerosols and Climate: Small particles in the Earth's atmosphere interact with visible and infrared light, altering the radiation balance and the climate. Am Sci 68:268–278

Traversi R, Becagli S, Severi M, Caiazzo L, Mazzola M, Lupi A, Fiebig M, Hermansen O, Krejci R (2021) Arctic haze in a climate changing world: the 2010-2020 trend. In: Moreno-Ibáñez et al (eds) SESS report 2020, Svalbard Integrated Arctic Earth Observing System, Longyearbyen, pp 104-117. https://doi.org/10.5281/zenodo.4293826

Turetta C, Feltracco M, Barbaro E et al (2021) A Year-Round Measurement of Water-Soluble Trace and Rare Earth Elements in Arctic Aerosol: Possible Inorganic Tracers of Specific Events. Atmosphere (Basel) 12:694. https://doi.org/10.3390/atmos12060694

Turetta C, Zangrando R, Barbaro E et al (2016) Water-soluble trace, rare earth elements and organic compounds in Arctic aerosol. Rend Lincei 27:95–103. https://doi.org/10.1007/s12210-016-0518-6

Udisti R, Bazzano A, Becagli S et al (2016) Sulfate source apportionment in the Ny-Ålesund (Svalbard Islands) Arctic aerosol. Rend Lincei 27:85–94. https://doi.org/10.1007/s12210-016-0517-7

Varutbangkul V, Brechtel FJ, Bahreini R et al (2006) Hygroscopicity of secondary organic aerosols formed by oxidation of cycloalkenes, monoterpenes, sesquiterpenes, and related compounds. Atmos Chem Phys 6:2367–2388. https://doi.org/10.5194/acp-6-2367-2006

Vestreng V, Kallenborn R, Økstad E (2009) Climate influencing emissions, scenarios and mitigation options at Svalbard. Rapport from the Climate and Pollution Agency in Norway (KLIF), TA-2552.

Viola AP, Hudson SR, Krejci R, Ritter C, Pedersen CA (2019) The Lower Atmosphere above Svalbard (LAS): Observed long term trends, small scale processes and the surface exchange. In: Orr et al. (eds): SESS report 2018, Svalbard Integrated Arctic Earth Observing System, Longyearbyen, pp 148–169. https://doi.org/10.5281/zenodo.4778471

Węsławski JM, Sagan S (2020) Morskie badania polarne. Acad - Mag Pol Akad Nauk 29–31. https://doi.org/10.24425/academiaPAN.2020.135289

Westby S, Amundsen B, (2003) Store norske Spitsbergen kulkompani 1916-1945. Store Norske: Longyearbyen, 520 pp.

WMO/GAW (2016) WMO/GAW Aerosol Measurement Procedures Guidelines and Recommendations 2nd Edition. WMO No. 1177; GAW Report No. 227. World Meteorological Organization (WMO) Global Atmosphere Watch (GAW), Geneva, Switzerland. vi + 93pp.

Wong F, Hung H, Dryfhout-Clark H et al (2021) Time trends of persistent organic pollutants (POPs) and Chemicals of Emerging Arctic Concern (CEAC) in Arctic air from 25 years of monitoring. Sci Total Environ 775:145109. https://doi.org/10.1016/j.scitotenv.2021.145109

Xie Z, Wang P, Wang X et al (2022a) Organophosphate ester pollution in the oceans. Nat Rev Earth Environ 3:309–322. https://doi.org/10.1038/s43017-022-00277-w

Xie Z, Wang Z, Mi W et al (2015) Neutral Poly-/perfluoroalkyl Substances in Air and Snow from the Arctic. Sci Rep 5:8912. https://doi.org/10.1038/srep08912

Xie Z, Zhang P, Wu Z et al (2022b) Legacy and emerging organic contaminants in the polar regions. Sci Total Environ 835:155376. https://doi.org/10.1016/j.scitotenv.2022.155376

Yu Y, Katsoyiannis A, Bohlin-Nizzetto P et al (2019) Polycyclic Aromatic Hydrocarbons Not Declining in Arctic Air Despite Global Emission Reduction. Environ Sci Technol 53:2375–2382. https://doi.org/10.1021/acs.est.8b05353

Zangrando R, Barbaro E, Zennaro P et al (2013) Molecular Markers of Biomass Burning in Arctic Aerosols. Environ Sci Technol 130716103911002. https://doi.org/10.1021/es400125r

Zawierucha K, Baccolo G, Di Mauro B et al (2019) Micromorphological features of mineral matter from cryoconite holes on Arctic (Svalbard) and alpine (the Alps, the Caucasus) glaciers. Polar Sci 22:100482. https://doi.org/10.1016/j.polar.2019.100482

Zdanowicz C, Gallet J, Björkman MP et al (2021) Elemental and water-insoluble organic carbon in Svalbard snow: a synthesis of observations during 2007 – 2018. Atmos Chem Phys 3035–3057. https://doi.org/10.5194/acp-21-3035-2021

Zhan J, Gao Y, Li W et al (2014) Effects of ship emissions on summertime aerosols at Ny-Ålesund in the Arctic. Atmos Pollut Res 5:500–510. https://doi.org/10.5094/APR.2014.059

Appendix 1: Details of the POPs and CEACs monitoring in the atmospheric air at Ny-Ålesund.

Monitoring efforts for POPs and CEACs in the Svalbard atmosphere, undertaken at the Ny-Ålesund (NyÅ) hub, in chronological order (except Gruvebadet - see Appendix 2 for all Gruvebadet datasets). All data by NILU are available at EBAS[1] , and all data by Z. Xie (Hereon) are available at PANGAEA[2] .

Organic species	Sampling method	Location within NyÅ	Period of sampling	Research unit	Contact person
OCPs, PCNs	HVS	Zeppelin	1993-present	NILU	P. Bohlin-Nizzetto (pbn@nilu.no)
PAHs	HVS	Zeppelin	1994-present	NILU	P. Bohlin-Nizzetto
PCBs	HVS	Zeppelin	2001-present	NILU	P. Bohlin-Nizzetto
PBDEs, PFAS (ionic)	HVS	Zeppelin	2006-present	NILU	P. Bohlin-Nizzetto
OCPs, PCBs, PBDEs, OPEs	PAS (Gas phase)	Ny-Ålesund	2011-2018	RCEES	Q. Zhang (qhzhang@rcees.ac.cn)
PFAS (volatile)	HVS	Zeppelin	2011-present	Hereon	Z. Xie (zhiyong.xie@hereon.de)
OCPs, PBDEs, HCBD, CUPs, novel BFRs, CFRs	HVS	Ny-Ålesund	2012-Present	Hereon	Z. Xie
cVMS	HVS (Gas phase)	Zeppelin	2013-present	NILU	P. Bohlin-Nizzetto
Chlorinated paraffins	HVS	Zeppelin	2013-present	NILU	P. Bohlin-Nizzetto
Phthalate esters, fragrance material, UV-filters, OPEs	HVS	Ny-Ålesund	2014-present	Hereon	Z. Xie
cVMS	HVS (Gas phase)	Ny-Ålesund	2015-Present	Hereon	Z. Xie
Chlorinated paraffins	HVS	Ny-Ålesund	2015-Present	Hereon	Z. Xie
HCBD	HVS	Zeppelin	2020-present	NILU	P. Bohlin-Nizzetto
Novel BFRs	HVS	Zeppelin	2017-present	NILU	P. Bohlin-Nizzetto
CFRs	HVS	Zeppelin	2019-present	NILU	P. Bohlin-Nizzetto
PFAS (volatile)	HVS (Gas phase)	Zeppelin	2017-present	NILU	P. Bohlin-Nizzetto
PFAS (ionic)	HVS (Particle phase)	Ny-Ålesund	2017-Present	Hereon	Z. Xie
OPEs, phthalate esters	HVS	Zeppelin	2017-present	NILU	P. Bohlin-Nizzetto
Alkylphenol	HVS	Ny-Ålesund	2018-Present	Hereon	Z. Xie
Microplastics	HVS (Particle phase)	Ny-Ålesund	2019-Present	Hereon	Z. Xie
Volatile fluorinated substances	HVS (Gas phase)	Zeppelin	2020-present	NILU	P. Bohlin-Nizzetto

Abbreviations

BFRs – brominated flame retardants, CFRs – chlorinated flame retardants, CUPs – current use pesticides, cVMS – cyclic volatile methyl siloxanes, **HCBD** – hexachlorobutadiene, HVS – high-volume air sampling, OCPs – organochlorine pesticides, **OPEs** – organophosphate esters, PAHs – polycyclic aromatic hydrocarbons, PAS – passive sampling, **PBDEs** – polybrominated diphenyl ethers, PCBs – polychlorinated biphenyls, PCNs – polychlorinated naphthalenes, PFAS – per- and polyfluoroalkyl substances.

1 http://ebas-data.nilu.no
2 https://pangaea.de

Appendix 2: Data availability

To access the links, please use the pdf-file of the chapter: https://doi.org/10.5281/zenodo.7406842

Abbreviations used in the table:

Dataset impurity types and methods

AAS = atomic absorption spectrometry; **AOD** = aerosol optical depth; **BC** = black carbon; **CCN** = cloud condensation nuclei; **CEACs** = chemicals of emerging Arctic concern; **CFCs** = chlorofluorocarbons; **COSMOS** = continuous soot monitoring system; **CRDS** = cavity ring-down spectroscopy; **eBC** = equivalent black carbon; **EC** = elemental carbon; **FID** = flame ionisation detector; flue gas **CEM** (continuous emission monitoring); **FTIR spectroscopy** = Fourier-transform infrared spectroscopy; **GC** = gas chromatograph; **HCFCs** = hydrochlorofluorocarbons; **HFCs** = hydrofluorocarbons; **H-NMR** (proton nuclear magnetic resonance); **HR-TOF-AMS** (High-Resolution Time-of-Flight Aerosol Mass Spectrometer); **HVS** = high-volume air sampler; **ICP-MS** (inductively coupled plasma – mass spectrometry); **INP** = Ice Nucleating Particles; LVS (low-volume sampler); **MAX-DOAS** = Multi-AXis Differential Optical Absorption Spectroscopy; **OC** = organic carbon; PAHs = polycyclic aromatic hydrocarbons; **PCBs** = polychlorinated biphenyls; **PFAS** = per- and polyfluoroalkyl substances; **PIXE** = Proton Induced X-ray Emission; **PM** = particulate matter; **POPs** = persistent organic pollutants; **PSAP** = particle soot absorption photometer; **PUF** = polyurethane foam; **SEM** = scanning electron microscope; Skypost (a Sequential Tecora® Skypost low volume sampler with automatic filter change, with PM10 sampling head); **SMPS** = Scanning Mobility Particle Sizer; **SP2** = single-particle soot photometers; ; **TEM grids** = Transmission electron microscopy grids; **TOC** (total organic carbon); **TSP** = total suspended particulate matter; **VOCs** = volatile organic compounds; **WSOC** = water-soluble organic carbon

Parameters

A = Air/aerosol; **P** = Snow/rain

Locations

BAR = Barentsburg; **GVB** = Gruvebadet Atmosphere Laboratory; **HRN** = Hornsund; **LYR** = Longyearbyen; **NyÅ** = Ny-Ålesund; **ZEP** = Zeppelin Observatory

Dataset providers

AARI = Arctic and Antarctic Research Institute; **AWI** = Alfred Wegener Institute; **ISP-CNR** = National Research Council of Italy, Institute of Polar Sciences; **IRET- CNR** = National Research Council of Italy, Institute of Research on Terrestrial Ecosystems; **ISAC-CNR** = National Research Council of Italy, Institute of Atmospheric Sciences and Climate; **HEREON** = Helmholtz-Zentrum Hereon; **IG PAS** = Institute of Geophysics, Polish Academy of Sciences; **INFN** = National Institute for Nuclear Physics (Italy); **KOPRI** = Korean Polar Research Institute; **NILU** = Norwegian Institute for Air Research; **NIPR** = National Institute for Polar Research (Japan); **RAS** = Russian Academy of Sciences; **RPA 'Typhoon'** = Research and Production Association 'Typhoon' (Russia); **AMU** = Adam Mickiewicz University of in Poznan; **UniFI** = University of Florence; **UniTO** = University of Turin; **UniGE** = University of Genoa; **UniMib** = University of Milan Bicocca; **UNIS** = University Centre in Svalbard

No. on the map (Fig. A1)	Dataset (impurity type + method in brief)	Parameter and temporal resolution of measurement (if known)	Period	Location	Metadata access (URL)	Dataset provider
1	POPs (mainly organochlorine pesticides and PCBs) by high-volume sampler	**A**	1980-1983	NyÅ	(Oehme and Ottar 1984)	NILU
2	Black carbon by aethalometer	**A**; every 5 or 10 mins (two devices)	2011	NyÅ, Chinese Yellow River, and three other locations	(Zhan and Gao 2014)	J. Zhan & Y. Gao (Rutgers University)
3	Black carbon by aethalometer	**A**, every 10 mins	2005-2008	NyÅ, Chinese Yellow River	(Chen et al. 2016)	L. Chen (State Oceanic Administration, Xiamen, China) et al
4	Trace gases (O_4, BrO, OClO, NO_2) by MAX-DOAS	**A**, continuous (every 2000 ms)	2017	NyÅ, Chinese Yellow River	(Chen et al. 2022)	D. Chen (Chinese Academy of Sciences, Hefei) et al
5	Mineral dust by copper TEM grids coated with carbon film	**A**, 20 min - 2 h	2012	NyÅ, Chinese Yellow River	(Chi et al. 2015; Yu et al. 2019)	J. W. Chi (Shandong University, Jinan) et al; H. Yu (Hangzhou Normal University) et al
6	Inorganic ions, conductivity (EC) and pH by bulk sampler	**P**, daily in 1980-83, then weekly	1980-2021, EC only in 1984-85, gaps for particular parameters	Ny-Ålesund	LINK	NILU
7	Inorganic ions by filter pack	**A**, weekly	2019-2021	NyÅ, Transformatorbua	LINK	NILU
8	Inorganic ions by filter pack	**A**, daily or weekly, depending on the period	Mid-2008-2018	NyÅ, Nordpolhotellet	LINK	NILU
9	Trace gases (e.g. CO, CH_4, O_3) by FTIR spectroscopy			NyÅ, AWIPEV	Data not directly available	project website: https://www.iup.uni-bremen.de/ftir/cms/
10	Pollen	**A**, weekly	1986	NyÅ	(Johansen and Hafsten 1988)	S. Johansen & U. Hafsten
11	Atmospheric optical depth (AOD) / water vapour in the air column / inversion aerosol products	**A**, depending on cloud cover	Since 2017 (& March-April 2006)	NyÅ	LINK LINK	C. Ritter (AWI), AERONET
12	Bacteria	**A**	2018	NyÅ, GVB	(Feltracco et al. 2021a)	M. Fetracco (ISP-CNR)
13	WSOC, phenolic compounds, trace elements and rare earths; in 6 dimensional classes of aerosol \ Andersen High volume cascade impactor	**A**, weekly	Since 2010	NyÅ, GVB	LINK (Zangrando et al. 2013; Turetta et al. 2016, 2021; Feltracco et al. 2019, 2020, 2021b, a)	E. Barbaro (ISP-CNR, UNIVE)

No. on the map (Fig. A1)	Dataset (impurity type + method in brief)	Parameter and temporal resolution of measurement (if known)	Period	Location	Metadata access (URL)	Dataset provider
14	EC/OC Tecora® LVS	**A**, weekly	Since 2010	NyÅ, GVB	(Caiazzo et al. 2021)	R. Traversi (UniFI) & G. Calzolai (INFN)
15	PM10 for elementary composition (PIXE) \ Skypost	**A**, weekly	Since 2010	NyÅ, GVB	Upon request to R. Traversi	R. Traversi (UniFI)
16	PM10 sampling for ionic compounds determination \ Skypost	**A**, weekly	Since 2010	NyÅ, GVB	(Udisti et al. 2016; Becagli et al. 2019; Traversi et al. 2021; Amore et al. 2022)	R. Traversi (UniFI)
17	Sampling of PM10 - determination of trace elements and lead isotopes \ Tecora® HVS	**A**, four days - now weekly	Since 2010	NyÅ, GVB	(Ardini et al. 2020; Bazzano et al. 2021; Conca et al. 2021)	M. Malandrino (UniTO) & M. Grotti (UniGE)
18	Aerosol sampling in 4 dimensional classes for distribution of ions \ Dekati 4-stage impactor	**A**, weekly	From 2010 to 2018	NyÅ, GVB	(Giardi et al. 2016)	R. Traversi (UniFI)
19	Spore and pollen sampling \ Cyclone	**A**, weekly	From 2018	NyÅ, GVB	Upon request	L. P. D'Acqui (IRET-CNR)
20	Ice Nucleating Particles (INP) \ Tecora® PM10/ PM1	**A**, campaign based	From 2018 to 2020	NyÅ, GVB	(Rinaldi et al. 2021)	M. Rinaldi et al
21	Characterisation of WSOC in sub-micrometric aerosol with H-NMR & HR-TOF-AMS (all offline) \ Tecora® Echo HVS PM1	**A**, weekly	From 2018 - ongoing	NyÅ, GVB	LINK	M. Rinaldi, M. Paglione (ISAC-CNR)
22	Microplastics, CEACs, PAHs \ TSP Tisch HVS	**A**, weekly	From 2021 - ongoing	NyÅ, GVB	upon request	F. Corami, M. Vecchiato (ISP-CNR)
23	Optical properties of the aerosol \ Nephelometer, Radiance Res.	**A**, weekly	From 2010 - ongoing	NyÅ, GVB	upon request	M. Mazzola (ISP-CNR)
24	Optical properties of the aerosol (including eBC) \ Radiance Res. (PSAP)	**A**, daily to weekly	From 2010 - ongoing	NyÅ, GVB	LINK	M. Mazzola, S. Gilardoni (ISP-CNR)
25	Optical properties of the aerosol and BC \ Aethalometer	**A**, daily to weekly	From 2021 - ongoing	NyÅ, GVB	upon request	M. Mazzola, S. Gilardoni (ISP-CNR)
26	Aerosol size distribution, 523 nm-20 µm range \ Aerodynamic Particle Sizer	**A**, daily to weekly	From 2010 to 2020	NyÅ, GVB	(Rader et al. 2021)	M. Mazzola (ISP-CNR); R. Traversi (UniFI)
27	Aerosol size distribution, 10-487 nm range \ SMPS	**A**, daily to weekly	From 2010 - ongoing	NyÅ, GVB	upon request	M. Mazzola (ISP-CNR); R. Traversi (UniFI)
28	Passive sampler for dry deposition – SEM analysis (dimensional & chemical particle characterisation) \ Sigma-2	**A**, month	From 2020 - ongoing	NyÅ, GVB	upon request	P. Ielpo (ISAC-CNR); F. Scoto (ISAC-CNR)

No. on the map (Fig. A1)	Dataset (impurity type + method in brief)	Parameter and temporal resolution of measurement (if known)	Period	Location	Metadata access (URL)	Dataset provider
29	Multiparametric optical characterisation of airborne dust with single particle extinction and scattering	**A**, days	From 2022 - ongoing	NyÅ, GVB	upon request	Marco Potenza (UniMib)
30	CO_2, CH_4, N_2O, SF_6 and O_2/N_2 ratio and stable isotope ratio of CO_2	**A**, weekly	03/2015-03/2019	NyÅ	LINK	D. Goto (NIPR) et al
31	Inorganic ions by filter pack	**A**, daily	1989-2021, with breaks	NyÅ, ZEP	LINK	NILU
32	"Heavy metals" (As, Cd, Co, Cr, Cu, Fe, Pb, Mn, Ni, Ti, V, Zn) by high volume sampler	**A**, weekly	1994-2021, with breaks	NyÅ, ZEP	LINK	NILU
33	Cloud condensation nuclei (CCN) number concentration by a CCN counter	**A**, hourly	2007-2015; 2018-2019	NyÅ, ZEP	LINK	KOPRI
34	Ozone by UV absorption	**A**, hourly	1989-2022	NyÅ, ZEP	LINK	NILU
35	Mercury by Tekran (flue gas CEM), a gold trap denuder, high-volume sampler or mini-trap	**A**, hourly (in 2021 - every 3 hours)	1994-2016; 2021	NyÅ, ZEP	LINK	NILU
36	Halogenated greenhouse gases (CFCs; halons, HCFCs, HFCs, SF_6 and other halogenated compounds) by an online gas chromatograph (GC)	**A**, daily; since 2010 every 2 hours	2001-2021	NyÅ, ZEP	LINK	NILU
37	H_2 by GC-HgO	**A**, every 2 h	2006-2009	NyÅ, ZEP	LINK	
38	CO (carbon monoxide) by GC-HgO	**A**, at least daily (every 2 h 2006-2008; hourly 2009-2012)	2001-2012	NyÅ, ZEP	LINK	NILU
39	CO (carbon monoxide) by online CRDS	**A**, hourly (daily in 2013)	2013-2022	NyÅ, ZEP	LINK	NILU
40	CO_2 and CH_4, N_2O by online CRDS	**A**, hourly	2012-2022	NyÅ, ZEP	LINK	NILU
41	PAHs by high-volume sampler	**A**, weekly	2008	NyÅ, ZEP	LINK	
42	POPs (mainly organochlorine pesticides and PCBs) by passive PUF samplers	**A**, single sample	2006	NyÅ, ZEP	LINK	
43	POPs (mainly organochlorine pesticides and PCBs) by high-volume sampler	**A**, weekly samples, representing 48-72 h	Pesticides regularly since 1994, PCBs since 1998; early measurements in 1984	NyÅ, ZEP	(Hung et al. 2016); 1984 data in (Oehme 1991)	NILU
44	PFAS by high-volume sampler	**A**, weekly samples, representing 48 h	2006-2014	NyÅ, ZEP	(Wong et al. 2018)	P. Bohlin-Nizzetto (NILU)

No. on the map (Fig. A1)	Dataset (impurity type + method in brief)	Parameter and temporal resolution of measurement (if known)	Period	Location	Metadata access (URL)	Dataset provider
45	OC/EC (organic carbon/ elemental carbon) by high-volume sampler (in PM10)	**A**, weekly	2017-2021	NyÅ, ZEP	LINK	NILU
46	Saccharides by high-volume sampler	**A**, weekly	2017-2021	NyÅ, ZEP	LINK	NILU
47	VOCs (volatile organic compounds) by adsorbent tube	**A**, daily	1994-1998	NyÅ, ZEP	LINK	
48	Alkanes by glass flask	**A**, weekly	2003-2016	NyÅ, ZEP	LINK	
49	Organic gaseous compounds by steel canister	**A**, daily	1989-1999 (various periods for various gases)	NyÅ, ZEP	Soon available through the SIOS data access portal	NILU
50	Black carbon, number and mass concentrations by SP2	**P**, daily	09/2012-03/2018	NyÅ	LINK	K. Goto-Azuma (NIPR) et al
51	Black carbon, mass concentration, by SP2	**A**, hourly	03/2017	NyÅ	LINK	S. Ohata (Univ. of Nagoya) et al
52	POPs and CEACs by high-volume sampler	**A**, weekly	2011	NyÅ, AWIPE-V(HERE-ON)	(Xie et al. 2015)	HEREON (Z. Xie)
53	Black carbon, mass concentration, by COSMOS	**A**, hourly (at least the first link, which is a dataset starting in 10/2012)	04/2009-10/2019	NyÅ	LINK	M. Koike (Univ. of Tokyo) et al
54	Microfauna	**A**, weekly	2000, 2001	NyÅ	(Coulson et al. 2003)	S. Coulson (UNIS) et al
55	Pollen, bryophyte spores	**A**, daily	1950	Sarsbukta	(Polunin 1955)	N. Polunin
56	Dust deposition	**A+P**, yearly	2012-2022	Petunia-bukta	(Rymer et al. 2022)	Krzysztof G. Rymer (AMU)
57	Dust deposition	**P**, campaign based	2019	Petunia-bukta	LINK	J. Kavan (Uni. Wroclaw & Masaryk University, Czech Rep.)
58	Bacteria	**A**, once	2015	Billefjorden	(Cuthbertson et al. 2017)	L. Cuthbertson (University of Northumbria at Newcastle) et al
59	Bacteria	**A**, once	2015	Gipsdalen	(Cuthbertson et al. 2017)	L. Cuthbertson (University of Northumbria at Newcastle) et al
60	Bacteria	**A**, once	2015	Sassen-fjorden	(Cuthbertson et al. 2017)	L. Cuthbertson (University of Northumbria at Newcastle) et al
61	Bacteria	**A**, once	2015	Deltaneset	(Cuthbertson et al. 2017)	L. Cuthbertson (University of Northumbria at Newcastle) et al

No. on the map (Fig. A1)	Dataset (impurity type + method in brief)	Parameter and temporal resolution of measurement (if known)	Period	Location	Metadata access (URL)	Dataset provider
62	Bacteria	**A**, once	2015	Advent-fjorden	(Cuthbertson et al. 2017)	L. Cuthbertson (University of Northumbria at Newcastle) et al
63	Bacteria	**A**, once	2015	Isfjorden	(Cuthbertson et al. 2017)	L. Cuthbertson (University of Northumbria at Newcastle) et al
64	Fungi	**A**, daily	2019	Area of LYB	(Pusz and Urbaniak 2021)	W. Pusz & J. Urbaniak
65	Aerosol optical depth (AOD) / water vapour in the air column / inversion aerosol products	**A**, depending on cloud cover	2003-2004; 2018	LYB	LINK	B. Holben (NASA), AERONET
66	PAHs, oxy- and nitro-PAHs, by high-volume sampler	**A**, on days with predicted NW wind direction	28 August - 28 September 2018	LYB (UNIS roof)	(Drotikova et al. 2020)	T. Drotikova (UNIS) et al
67	PAHs, oxy- and nitro-PAHs, by high-volume sampler	**A**, 31 samples in total, 24 h each (~weekly)	Nov 2017 - Jun 2018	LYB (UNIS roof)	(Drotikova et al. 2021)	T. Drotikova (UNIS) et al
68	Aromatic VOCs by GC-FID	**A**, every 15 mins	2007	LYB	(Reimann et al. 2009)	S. Reimann (Empa, Switzerland) et al
69	Bacteria	**A**, four	2015	LYB	(Cuthbertson et al. 2017)	L. Cuthbertson (University of Northumbria at Newcastle) et al
70	Bacteria	**A**, once	2015	Bjørndalen	(Cuthbertson et al. 2017)	L. Cuthbertson (University of Northumbria at Newcastle) et al
71	Fungi	**A**, daily	2019	Area of LYB	(Pusz and Urbaniak 2021)	W. Pusz & J. Urbaniak
72	PAHs, oxy- and nitro-PAHs, by high-volume sampler	**A**, on days with predicted NW wind direction	28 August - 28 September 2018	LYB (Aurora station Advent-dalen)	(Drotikova et al. 2020)	T. Drotikova (UNIS) et al
73	Fungi	**A**, daily	2019	Area of LYB	(Pusz and Urbaniak 2021)	W. Pusz & J. Urbaniak
74	Fungi	**A**, daily	2019	Area of LYB	(Pusz and Urbaniak 2021)	W. Pusz & J. Urbaniak
75	Bacteria	**A**, once	2015	Mine (Gruve) 7	(Cuthbertson et al. 2017)	L. Cuthbertson (University of Northumbria at Newcastle) et al
76	Fungi	**A**, daily	2019	Area of LYB	(Pusz and Urbaniak 2021)	W. Pusz & J. Urbaniak
77	Pollen by sticky trap	**A**, weekly	2022	BAR CALM site	data available by request; RiS projects 11316 and 10855	AARI paleo reconstruction group
78	PAHs, PCBs and trace metals, by multichannel sampler PU-4EP	**A**, twice a year	Since 2002	BAR	data available by request at RPA 'Typhoon', North-West branch	RPA 'Typhoon'

No. on the map (Fig. A1)	Dataset (impurity type + method in brief)	Parameter and temporal resolution of measurement (if known)	Period	Location	Metadata access (URL)	Dataset provider
79	Trace gases (NO_x, NO_2, NO, NH_3, SO_2, H_2S, CO_2, CO, O_3) + PM10 + mercury by Lumex AAS	**A**, continuous, 10 min (Hg)	2017-2021	BAR mountain	data stored at AARI, currently not online; RiS ID 10863	AARI
80	Pollen by sticky trap	**A**, weekly	2017-2019; 2022	BAR	data available by request; RiS projects 11316 and 10855	AARI paleo reconstruction group
81	Pollen by sticky trap	**A**, weekly	2017-2019; 2022	BAR	data available by request; RiS projects 11316 and 10855	AARI paleo reconstruction group
82	Trace gases (NO_x, NO_2, NO, NH_3, SO_2, H_2S, CO_2, CO, O_3) + PM10 + mercury by Lumex AAS	**A**, continuous, 10 min (Hg)	2017-2022	BAR town	data stored at AARI, currently not online; RiS ID 10863	AARI
83	AOD, water vapour content, aerosol concentration and size distribution, BC concentration by sun photometer, photoelectric particle counter, aethalometer	**A**, continuous	2011-2022	BAR	(Chernov et al. 2016; Sakerin et al. 2019)	D. G. Chernov (V.E. Zuev Institute of Atmospheric Optics, Siberian Branch RAS, Tomsk) et al; S. Sakerin et al
84	Inorganic ions (ion chromatography) and dissolved trace metals (ICP-MS) by low-volume sampler	**A**, weekly	2011-2022	BAR	(Golobokova et al. 2015; 2020)	L. P. Golobokova (Limnology Institute, Siberian Branch, RAS) et al
85	PAHs by GC/MS TripleQuad, low volume samler	**A**, campaign based	2017	BAR	(Golobokova et al. 2020)	L. P. Golobokova (Limnology Institute, Siberian Branch, RAS) et al
86	Pollen by sticky trap	**A**, weekly	2017-2019; 2022	BAR	data available by request; RiS projects 11316 and 10855	AARI paleo reconstruction group
87	Fresh snow chemical composition: major ions, HCO_3^-, pH, conductivity	**P**, every fresh snow episode > 5 mm	2005 - 2019	Hansbreen glacier (HRN)	LINK	IG PAS (A. Nawrot)
88	Fresh snow chemical composition: major ions, HCO_3^-, pH, conductivity	**P**, every fresh snow episode > 5 mm	Since 2020 - ongoing	Ariebreen glacier (HRN)	LINK	IG PAS (A. Nawrot)
89	Metals and metalloids in precipitation, by ICP-MS, and TOC by a Shimadzu TOC Analyser	**P**, every event	2010-2012	HRN pre-cipitation gauge	(Kozak et al. 2015)	K. Kozak (Gdansk Tech) et al
90	POPs (organochlorine pesticides and PCBs) in snow	**P**, every event during 1 month; weekly surface snow at environmental chamber	2019	HRN area	LINK (Pawlak et al. 2022)	K. Koziol (Gdansk Tech)
91	Precipitation chemistry: major ions, HCO_3^-, pH, conductivity; sum of the precipitation	**P**, daily	Since 2005 - ongoing	HRN	LINK	IG PAS (A. Nawrot)

No. on the map (Fig. A1)	Dataset (impurity type + method in brief)	Parameter and temporal resolution of measurement (if known)	Period	Location	Metadata access (URL)	Dataset provider
92	Aerosol concentration, and size distribution (0.01-10 µm)	**A**, 1 min (concentration); 10 min (size distribution)	2021	HRN	LINK; LINK; LINK[3]	D. Kępski, M. Posyniak (IG PAS)
92	Aerosol concentration and size distribution in a vertical distribution	**A**, 1 min (concentration); 10 min (size distribution)	2021	HRN	LINK; LINK	D. Kępski, M. Posyniak (IG PAS)
93	Radionuclides: Concentration of: ^{7}Be, ^{210}Pb, ^{40}K, ^{137}Cs, ^{134}Cs [µBq/m^3] PM (dust) [µq/m^3]	**A**, weekly	Since 2002	HRN	(Burakowska et al. 2021)	A. Burakowska, M. Kubicki (IG PAS)
94	Aerosol optical depth (AOD) / water vapour in the air column / inversion aerosol products	**A**, depending on cloud cover	Since March 2005	HRN	LINK	P. Sobolewski (IG PAS), AERONET network
95	POPs (mainly organochlorine pesticides and PCBs) by high-volume sampler	**A**	1980-1983	Hopen	(Oehme and Ottar 1984)	NILU
96	Sulphate and sulphur dioxide concentrations by a filter pack	**A**, daily	1978-1989	Bjørnøya	LINK	NILU
97	Metal concentrations (Cd, Pb, Zn) by bulk sampler	**P**, monthly	1980-1987	Bjørnøya	LINK	NILU
98	Ion concentrations (NH_4^+, Ca^{2+}, Cl^-, Mg^{2+}, K^+, Na^+, NO_3^-, SO_4^{2-}) by bulk sampler; conductivity and pH	**P**, daily	1977-1985 (various periods within that timespan)	Bjørnøya	LINK	NILU
99	POPs (mainly organochlorine pesticides and PCBs) by high-volume sampler	**A**	1980-1983	Bjornoya	(Oehme and Ottar 1984)	NILU
100	POPs (mainly organochlorine pesticides and PCBs) by high-volume sampler	**A**	1980-1983	Jan Mayen	(Oehme and Ottar 1984)	NILU

3 Entire dataset available on the project subpage https://dataportal.igf.edu.pl/group/avseefi; registration on the website is required to download the data; field data were collected inside a polygon defined by the coordinates in Fig. 1; basic measurements in a fixed position are continued with the SPS30 micro sensor

No. on the map (Fig. A1)	Dataset (impurity type + method in brief)	Parameter and temporal resolution of measurement (if known)	Period	Location	Metadata access (URL)	Dataset provider
No marker on the map	AOD	Depending on cloud cover (only during polar day)	RV Oceania 2007	Arctic maritime aerosol optical properties (Arctic circle)	LINK	Project MAN & AERONET
			RV Oceania 2009		LINK	
			RV Oceania 2010		LINK	
			RV Oceania 2011		LINK	
			RV Oceania 2012		LINK	
			RV Oceania 2013		LINK	
			RV Oceania 2014		LINK	
			RV Oceania 2015		LINK	
			RV Oceania 2016		LINK	
			RV Oceania 2017		LINK	
			RV Oceania 2018		LINK	
			RV Oceania 2019		LINK	
			RV Oceania 2020		LINK	
			RV Polarstern 2009		LINK	
			RV Polarstern 2012		LINK	
			RV Polarstern 2015		LINK	
			RV Polarstern 2017		LINK	
			RV Polarstern 2020		LINK	
			RV Polarstern 2021		LINK	
			RV Jan Mayen 2009		LINK	
			RV Akademik Fedorov 2013		LINK	
			USCGC Healy 2011		LINK	
			USCGC Healy 2015		LINK	
			RV Oden 2014		LINK	
			RV Araon 2020		LINK	
			RV Araon 2020-21		LINK	
			RV Araon 2021		LINK	
			RV Alliance 2021		LINK	

References:

Amore A, Giardi F, Becagli S, et al (2022) Source apportionment of sulphate in the High Arctic by a 10 yr-long record from Gruvebadet Observatory (Ny-Ålesund, Svalbard Islands). Atmos Environ 270:118890. https://doi.org/10.1016/j.atmosenv.2021.118890

Ardini F, Bazzano A, Grotti M (2020) Lead isotopic ratios in the Arctic environment. Environ Chem 17:213. https://doi.org/10.1071/EN19227

Bazzano A, Bertinetti S, Ardini F, et al (2021) Potential Source Areas for Atmospheric Lead Reaching Ny-Ålesund from 2010 to 2018. Atmosphere (Basel) 12:388. https://doi.org/10.3390/atmos12030388

Becagli S, Amore A, Caiazzo L, et al (2019) Biogenic Aerosol in the Artic from Eight Years of MSA Data from Ny Ålesund (Svalbard Islands) and Thule (Greenland). Atmosphere (Basel) 10:349. https://doi.org/10.3390/atmos10070349

Burakowska A, Kubicki M, Mysłek-Laurikainen B, et al (2021) Concentration of 7Be, 210Pb, 40K, 137Cs, 134Cs radionuclides in the ground layer of the atmosphere in the polar (Hornsund, Spitsbergen) and mid-latitudes (Otwock-Świder, Poland) regions. J Environ Radioact 240:106739. https://doi.org/10.1016/j.jenvrad.2021.106739

Caiazzo L, Calzolai G, Becagli S, et al (2021) Carbonaceous Aerosol in Polar Areas: First Results and Improvements of the Sampling Strategies. Atmosphere (Basel) 12:320. https://doi.org/10.3390/atmos12030320

Chen D, Luo Y, Yang X, et al (2022) Study of an Arctic blowing snow-induced bromine explosion event in Ny-Ålesund, Svalbard. Sci Total Environ 839:156335. https://doi.org/10.1016/j.scitotenv.2022.156335

Chen L, Li W, Zhan J, et al (2016) Increase in Aerosol Black Carbon in the 2000s over Ny-Ålesund in the Summer. J Atmos Sci 73:251–262. https://doi.org/10.1175/JAS-D-15-0009.1

Chernov DG, Kozlov VS, Panchenko M V., et al (2016) Investigation of microphysical characteristics and chemical composition of near-ground aerosol in Barentsburg (Spitsbergen) in the spring and summer seasons of 2011-2015. In: Matvienko GG, Romanovskii OA (eds). p 1003534.

Chi JW, Li WJ, Zhang DZ, et al (2015) Sea salt aerosols as a reactive surface for inorganic and organic acidic gases in the Arctic troposphere. Atmos Chem Phys 15:11341–11353. https://doi.org/10.5194/acp-15-11341-2015

Conca E, Malandrino M, Giacomino A, et al (2021) Chemical Fractionation of Trace Elements in Arctic PM10 Samples. Atmosphere (Basel) 12:1152. https://doi.org/10.3390/atmos12091152

Coulson SJ, Hodkinson ID, Webb NR (2003) Aerial dispersal of invertebrates over a high-Arctic glacier foreland: Midtre Lovenbreen, Svalbard. Polar Biol 26:530–537. https://doi.org/10.1007/s00300-003-0516-x

Cuthbertson L, Amores-Arrocha H, Malard L, et al (2017) Characterisation of Arctic Bacterial Communities in the Air above Svalbard. Biology (Basel) 6:. https://doi.org/10.3390/biology6020029

Drotikova T, Ali AM, Halse AK, et al (2020) Polycyclic aromatic hydrocarbons (PAHs) and oxy- and nitro-PAHs in ambient air of the Arctic town Longyearbyen, Svalbard. Atmos Chem Phys 20:9997–10014. https://doi.org/10.5194/acp-20-9997-2020

Drotikova T, Dekhtyareva A, Kallenborn R, Albinet A (2021) Polycyclic aromatic hydrocarbons (PAHs) and their nitrated and oxygenated derivatives in the Arctic boundary layer: seasonal trends and local anthropogenic influence. Atmos Chem Phys 21:14351–14370. https://doi.org/10.5194/acp-21-14351-2021

Feltracco M, Barbaro E, Hoppe CJM, et al (2021a) Airborne bacteria and particulate chemistry capture Phytoplankton bloom dynamics in an Arctic fjord. Atmos Environ 256:118458. https://doi.org/10.1016/j.atmosenv.2021.118458

Feltracco M, Barbaro E, Kirchgeorg T, et al (2019) Free and combined L- and D-amino acids in Arctic aerosol. Chemosphere 220:412–421. https://doi.org/10.1016/j.chemosphere.2018.12.147

Feltracco M, Barbaro E, Spolaor A, et al (2021b) Year-round measurements of size-segregated low molecular weight organic acids in Arctic aerosol. Sci Total Environ 763:142954. https://doi.org/10.1016/j.scitotenv.2020.142954

Feltracco M, Barbaro E, Tedeschi S, et al (2020) Interannual variability of sugars in Arctic aerosol: Biomass burning and biogenic inputs. Sci Total Environ 706:136089. https://doi.org/10.1016/j.scitotenv.2019.136089

Giardi F, Becagli S, Traversi R, et al (2016) Size distribution and ion composition of aerosol collected at Ny-Ålesund in the spring–summer field campaign 2013. Rend Lincei 27:47–58. https://doi.org/10.1007/s12210-016-0529-3

Golobokova L, Khodzher T, Chernov D, et al (2020) Khimicheskiy sostav prizemnovo atmosfernovo aerozolya v Barentsburge (Arkhipelag Shpitsbergen) po rezultatam mnogoletnikh issledovaniy [in Russia: *The Chemical composition of near-ground atmospheric aerosol in Barentsburg (Svalbard Archipelago) according to the results of long-term research*] Ice Snow 60:85–97. https://doi.org/10.31857/S2076673420010025

Golobokova LP, Polkin V V., Kabanov DM, et al (2015) Studies of atmospheric aerosols in the Russia Arctic regions. Ice Snow 122:129. https://doi.org/10.15356/2076-6734-2013-2-129-136

Hung H, Katsoyiannis AA, Brorstrom-Lunden E, et al (2016) Temporal trends of Persistent Organic Pollutants (POPs) in arctic air: 20 years of monitoring under the Arctic Monitoring and Assessment Programme (AMAP). Environ Pollut 217:52–61. https://doi.org/10.1016/j.envpol.2016.01.079

Johansen S, Hafsten U (1988) Airborne pollen and spore registrations at Ny-Ålesund, Svalbard, summer 1986. Polar Res 6:11–17. https://doi.org/10.3402/polar.v6i1.6842

Kozak K, Kozioł K, Luks B, et al (2015) The role of atmospheric precipitation in introducing contaminants to the surface waters of the Fuglebekken catchment, Spitsbergen. Polar Res 34:24207. https://doi.org/10.3402/polar.v34.24207

Oehme M (1991) Further Evidence for Long-Range Air Transport of olychlorinated Aromates and Pesticides: North America and Eurasia to the Arctic. Ambio 20:293–297.

Oehme M, Ottar B (1984) The long range transport of polyclorinated hydrocarbons to the Arctic. Geophys Res Lett 11:1133–1136. https://doi.org/10.1029/GL011i011p01133

Pawlak F, Koziol KA, Kosek K, Polkowska Z (2022) Local variability in snow concentrations of chlorinated persistent organic pollutants as a source of large uncertainty in interpreting spatial patterns at all scales. J Environ Qual 51:411–424. https://doi.org/10.1002/jeq2.20343

Polunin N (1955) ARCTIC AEROPALYNOLOGY: SPORA OBSERVED ON STICKY SLIDES EXPOSED IN VARIOUS REGIONS IN 1950. Can J Bot 33:401–415. https://doi.org/10.1139/b55-034

Pusz W, Urbaniak J (2021) Airborne fungi in Longyearbyen area (Svalbard, Norway) — case study. Environ Monit Assess 193:290. https://doi.org/10.1007/s10661-021-09090-2

Rader F, Traversi R, Severi M, et al (2021) Overview of Aerosol Properties in the European Arctic in Spring 2019 Based on In Situ Measurements and Lidar Data. Atmosphere (Basel) 12:271. https://doi.org/10.3390/atmos12020271

Reimann S, Kallenborn R, Schmidbauer N (2009) Severe aromatic hydrocarbon pollution in the Arctic town of Longyearbyen (Svalbard) caused by snowmobile emissions. Environ Sci Technol 43:4791–4795. https://doi.org/10.1021/es900449x

Rinaldi M, Hiranuma N, Santachiara G, et al (2021) Ice-nucleating particle concentration measurements from Ny-Ålesund during the Arctic spring–summer in 2018. Atmos Chem Phys 21:14725–14748. https://doi.org/10.5194/acp-21-14725-2021

Rymer KG, Rachlewicz G, Buchwal A, et al (2022) Contemporary and past aeolian deposition rates in periglacial conditions (Ebba Valley, central Spitsbergen). CATENA 211:105974. https://doi.org/10.1016/j.catena.2021.105974

Sakerin SM, Golobokova LP, Kabanov DM, et al (2019) Comparison of Average Aerosol Characteristics in Neighboring Arctic Regions. Atmos Ocean Opt 32:33–40. https://doi.org/10.1134/S1024856019010147

Traversi R, Becagli S, Severi M, Caiazzo L, Mazzola M, Lupi A, Fiebig M, Hermansen O, Krejci R (2021) Arctic haze in a climate changing world: the 2010-2020 trend. In: Moreno-Ibáñez et al (eds) SESS report 2020, Svalbard Integrated Arctic Earth Observing System, Longyearbyen, pp 104-117. https://doi.org/10.5281/zenodo.4293826

Turetta C, Feltracco M, Barbaro E, et al (2021) A Year-Round Measurement of Water-Soluble Trace and Rare Earth Elements in Arctic Aerosol: Possible Inorganic Tracers of Specific Events. Atmosphere (Basel) 12:694. https://doi.org/10.3390/atmos12060694

Turetta C, Zangrando R, Barbaro E, et al (2016) Water-soluble trace, rare earth elements and organic compounds in Arctic aerosol. Rend Lincei 27:95–103. https://doi.org/10.1007/s12210-016-0518-6

Udisti R, Bazzano A, Becagli S, et al (2016) Sulfate source apportionment in the Ny-Ålesund (Svalbard Islands) Arctic aerosol. Rend Lincei 27:85–94. https://doi.org/10.1007/s12210-016-0517-7

Wong F, Shoeib M, Katsoyiannis A, et al (2018) Assessing temporal trends and source regions of per- and polyfluoroalkyl substances (PFASs) in air under the Arctic Monitoring and Assessment Programme (AMAP). Atmos Environ 172:65–73. https://doi.org/10.1016/j.atmosenv.2017.10.028

Xie Z, Wang Z, Mi W, et al (2015) Neutral Poly-/perfluoroalkyl Substances in Air and Snow from the Arctic. Sci Rep 5:8912. https://doi.org/10.1038/srep08912

Yu H, Li W, Zhang Y, et al (2019) Organic coating on sulfate and soot particles during late summer in the Svalbard Archipelago. Atmos Chem Phys 19:10433–10446. https://doi.org/10.5194/acp-19-10433-2019

Zangrando R, Barbaro E, Zennaro P, et al (2013) Molecular Markers of Biomass Burning in Arctic Aerosols. Environ Sci Technol 130716103911002. https://doi.org/10.1021/es400125r

Zhan J, Gao Y (2014) Impact of summertime anthropogenic emissions on atmospheric black carbon at Ny-Ålesund in the Arctic. Polar Res 33:21821. https://doi.org/10.3402/polar.v33.21821

Appendix 3: Coal mining in Svalbard as the long-term main source of local atmospheric pollution.

Site	Description of mining history	References
Longyearbyen	1906-2018 – seven mines (Mine 1-7) established and operated by the Norwegian company Store Norske Spitsbergen Kulkompani (SNSK); 2028 - planned date to close the last one	(Westby and Amundsen 2003; Kvello 2004; Vågerö et al 2021)
Barentsburg	1939 - mining operation in Grønnfjorden officially taken over by the USSR (from a Dutch operating company); currently, the mine is operated by the Russian governmental agency Trust Artikugol	(Pashkevich 2018)
Grumant/ Colesbay	1912-1961 - operated by the Soviet Union	(Samoĭlovich and Adadurov 1927; Kulikov 1964; Portsel′ 2011)
Pyramiden	1926 - mine facilities bought by the Soviet Union; in the 1960s-1970s it was the largest mine in Svalbard; in 1998 - closed and abandoned	(Andreassen et al 2010)
Ny-Ålesund	1916 - coal mining established by the Kings Bay mining company (Kings Bay Kulkompani); 1962 - a tragic mining accident led to the close of mine operations, after which the facility gradually transformed into an international research station	(Paglia 2020)

References

Andreassen E, Bjerck HB, Olsen B (2010) Persistent memories: Pyramiden, a Soviet mining town in the high Arctic. Tapir Academic Press: Trondheim, Norway, 215 p.

Kulikov IO (1964) Shakhty na Shpit͡sbergene. Nedra, Moskva, p 108-112 [in Russian].

Paglia E (2020) A higher level of civilisation? The transformation of Ny-Ålesund from Arctic coalmining settlement in Svalbard to global environmental knowledge center at 79° North. Polar Rec (Gr Brit) 56:e15. https://doi.org/10.1017/S0032247419000603

Pashkevich A (2018) In Lessons learned: uses of mining and other cultural heritage in the Arctic. Voices from Russian settlements on Svalbard, 6th International Polar Tourism Network (IPTRN) Conference and community tour, 22-28 June, 2018, Yukon, 2018.

Port͡sel′ AK, (2011) Murmanskiĭ gosudarstvennyĭ tekhnicheskiĭ universitet., Ot "Grumanta" do "Arktikugli͡a": ocherk istorii otechestvennoĭ so-t͡si͡al′no-ėkonomicheskoĭ de-li͡at͡el′nosti na Shpit͡sbergene v XX veke. MGTU: Murmansk, 290 p.

Samoĭlovich RL, Adadurov VA (1927) Kamennougol′nai͡a promyshlennost′ Grumanta. 118 pp

Vågerö O, Olsson E (2021) Social Acceptance of the Energy Transition in Longyearbyen.

Ground penetrating radar measurement of snow in Svalbard – past, present, future (SnowGPR)

Dariusz Ignatiuk[1], Thorben Dunse[2], Jean-Charles Gallet[3], Luc Girod[4], Mariusz Grabiec[1], Daniel Kępski[5], Jack Kohler[3], Michał Laska[1], Bartłomiej Luks[5], Ward van Pelt[6], Rickard Pettersson[6], Veijo Pohjola[6], Thomas V Schuler[4]

1 University of Silesia in Katowice, Katowice, Poland
2 Western Norway University of Applied Sciences, Sogndal, Norway
3 The Norwegian Polar Institute, FRAM Centre, Tromsø, Norway
4 University of Oslo, Department of Geosciences, Oslo, Norway
5 Institute of Geophysics, Polish Academy of Sciences, Warsaw, Poland
6 Department of Earth Sciences, Uppsala University, Uppsala, Sweden

Corresponding author: Dariusz Ignatiuk, dariusz.ignatiuk@us.edu.pl
ORCID number: 0000-0002-2947-474X

Keywords: GPR, ground penetrating radar, snow cover, Svalbard

DOI: https://doi.org/10.5281/zenodo.7371725

1. Introduction

The warming of the Arctic climate, which is well documented (IPCC 2019), causes progressive and ongoing changes in the cryosphere (Box et al. 2018; van Pelt et al. 2019; Schuler et al. 2020; Błaszczyk et al. 2021). The seasonal snowpack, which covers ~60% (summer) to 100% (winter) of the land in Svalbard, is very sensitive to the changing climate (Gallet et al. 2019). Large scale snow thickness and snow structural information across Svalbard are needed to better understand the spatial distribution of snow accumulation and its interannual variability. In addition, such measurements provide a snapshot into spatial patterns of seasonal precipitation that are otherwise barely covered by the operational precipitation gauges. Surveys by ground penetrating radar (GPR) are accurate and cost-efficient, and have been conducted in Svalbard for more than 25 years, thus permitting assessment of long-term changes. These data complement the single-point snow monitoring measurements and seasonal measurement campaigns on glaciers and tundra. The campaigns so far have focused on particular areas, so the data are sparse. The purpose of this report is to compile information about the conducted GPR snow cover measurements and to define standards for measurements and data sharing. The activities initiated in this project will be continued in the coming years and extended with a comprehensive data analysis.

2. Fundamentals of radar surveying of snow cover

2.1. Principles of radio-echo sounding

The radio-echo sounding (RES) method uses induced electromagnetic radiation in the wavelength spectrum from 100 m to 100 mm. The survey consists of transmitting an electromagnetic pulse of a certain frequency to the ground (snow in our case), receiving the reflected signal, and recording the return time and amplitude of the signal.

The propagation of electromagnetic waves is determined by the characteristics of the electromagnetic spectrum and electromagnetic properties of the surveyed material defined by its permittivity, permeability, and conductivity. In environmental radar research, it is assumed that the probing is applied to non-conductive and non-magnetic materials (dielectrics).

The sounding depth range depends on many factors, including several processes of loss of transmitted electromagnetic energy, the most important being geometric spreading, scattering, and attenuation. Due to geometric spreading, the power of the radar signal decreases with the square of the distance to the transmitter, while it decreases exponentially with depth due to attenuation. When probing cryospheric systems, intense energy attenuation can occur in water-saturated sediments or sediments containing salt solutions. Energy passing through is also subject to scattering or refraction on the structures and objects present in the surveyed material depending on the sounding wavelength and the size of these objects (Plewes and Hubbard 2001, Neal 2004). The reflection of the radar wave at the boundaries of materials with different dielectric properties is the basis for recognising the internal structure. Such dielectric contrasts are usually found at the bottom of the winter snow cover (interface snow–ground or snow–ice), thus making the technique well suited for mapping the vertical extent of the snowpack. The reflection coefficient (R) is derived from the dielectric contrast of the adjacent layers and ranges between -1 and 1. The probability of properly identifying the boundary between structures increases with the rise of the absolute value of the reflection coefficient.

2.2. Dielectric properties of the snowpack

The dielectric properties of snow (Table 1) are mainly determined by the mutual contribution of the three basic components that build the snow cover, i.e., ice, air, and water. Their individual dielectric properties are significantly different; hence their contribution to the snow cover substantially impacts the course and results of radio-echo sounding. Changing the proportion of the components also changes the dielectric properties of the entire snow cover. The increase in the gaseous fraction (air) translates into an increased radar wave velocity (RWV) in the snow cover, while the increase of the solid fraction (ice), and even more of the liquid fraction (water) decrease the RWV in the snow cover. The RWV is inversely dependent on the square root of the relative permittivity. Spatial and temporal variation in snow cover dielectric characteristics should be considered in the time-to-depth conversion process.

The contrast of the dielectric properties of adjacent materials affects the possibility of their distinction. Table 1 shows a significant discrepancy between the permittivity of dry snow and most of the typical materials that make up the snow cover base. The absolute value of the reflection coefficient is in the range of 0.06 – 0.61 (Grabiec 2017), which indicates a high probability of the recognition of the boundary between the dry snowpack and the base, regardless of its type. When the snowpack contains a significant proportion of water, the contrast with some types of beddings (glacier ice, firn, sea ice, lake ice, basal ice) becomes blurred, making separating these structures difficult.

Table 1: Dielectric characteristics of snowpack components, snowpack of different properties, and formations of snowpack bedding (based on Davis and Annan 1989; Neal 2004; Baker et al. 2007; Grabiec et al. 2011; Grabiec 2017)

Material	Relative permittivity (dielectric constant) (ε_r)	Radar wave velocity (*RWV*) [m ns^{-1}]
SNOWPACK COMPONENTS		
Ice	3.2	0.168
Air	1	0.30
Freshwater	80	0.03
SNOWPACK		
Fresh snow (200 kg m^{-3}, w=0%)	1.36	0.26
Dry snow (350 kg m^{-3}, w=0%)	1.65	0.23
Dry snow (500 kg m^{-3}, w=0%)	2	0.21
Wet snow (500 kg m^{-3}, w=5%)	2.82	0.18
Water-saturated snow (500 kg m^{-3}, w=10%)	3.83	0.15
Slush (500 kg m^{-3}, w=15%)	5.06	0.13
SNOWPACK BASE (selected materials)		
Glacier ice	3-4	0.15-0.17
Firn	2.5	0.19
Dry till (moraine)	7.4-21.1	0.10-0.12
Saturated till (moraine)	24-34	0.10-0.12
Bedrock	4-9	0.10-0.13

Due to the heterogeneous nature of snow and, consequently, different dielectric properties of individual snow layers, RES seems to be an effective tool for identifying the internal structure of snow cover (Harper and Bradford 2003; Yamamoto et al. 2004; Marshall et al. 2007; Heilig et al. 2009). Hard layers, e.g. ice lenses, ice crusts, and ice layers, are particularly helpful in delimiting boundary layers in snow cover (Marshall et al. 2007; Yamamoto et al. 2004; Dunse et al. 2008). The distinction of snow layers based on the difference in their reflectivity requires that the density contrast between the layers be higher than 100 kg m^{-3} (Yamamoto et al. 2004).

The above considerations regarding the possibility of recognising the snow cover's depth and internal structure should also take into account the technical conditions of the radar survey, such as the sounding radar wave frequency, trace-to-trace interval, sampling frequency, etc.

2.3. Snow radio-echo sounders

Commercial impulse radars, referred to as ground penetrating radars (GPR), are commonly used in snow cover soundings. These devices are characterised by a simple, modular structure, intuitive operation and setting of measurement parameters, the possibility of visualising the results in real time, a data collection system, integration with positioning systems (GNSS receivers), and distance measurement devices (odometers). GPR in snow cover surveys applies high-frequency antennas (commonly, 450 MHz – 2.4 GHz), ensuring a sufficient penetration depth with high vertical resolution. GPR systems were used to obtain the majority of data presented in this report.

Frequency Modulated Continuous Wave (FMCW) radars are also applied in snow cover studies. The principle of FMCW radar is based on the difference in the radar wave frequency transmitted and reflected from the object. FMCW radar is characterised by operation in a high-frequency range (above 1 GHz). Therefore, it allows obtaining results with the high vertical resolution required for analyses of the snow cover structure (e.g. Marshall et al. 2007) or identification of glacier facies (Langley et al. 2008).

2.4. Advantages and limitations of radar sounding of snow

The method has several advantages. Due to the non-invasive nature of sounding, GPRs are a desirable method in areas where environmental protection regulations limit field surveys that interfere with the ground (national parks, nature reserves, and other forms of protection). Due to its mobility and quick measurement times, this method is less time-consuming and cost-intensive than the classic methods of manual snow cover probing. It allows for immediate recognition of the two-dimensional image of the surface layer of the ground (snow cover).

Due to snow cover properties (dry snow cover is highly 'transparent' to radar waves), the depth of snow probing is not a critical limitation. With appropriate measurement parameters and equipment selection, it is possible to recognise snow structures, even of extreme depth.

Like any geophysical method, RES also provides indirect information about the varying geophysical properties of the ground. In the case of GPR, the recorded variable is the two-way travel time of the signal transmitted form the radar and reflected from the dielectric discontinuities. A main RES analysis challenge is obtaining reliable calibration and validation data allowing for the time-to-depth conversion. For this purpose, it is common practice to perform control field measurements to determine the actual depth and snow cover structure (snow cores, snow pits). The use of velocity profiling (common mid-point) is more time-consuming and costly compared with classic field methods of snow depth and structure measurement.

An important factor determining the quality of the measurement results is the vertical resolution of the radar sounding, which depends on the centre frequency of the antenna and the dielectric properties of the snow cover. Assuming that most measurements are made in dry snow with an average density of 350 kg m^{-3}, using antennas with a centre frequency between 450 MHz and 2.4 GHz, the vertical resolution calculated as $\lambda/4$ may range

from 0.11 m to 0.04 m. As a result, the accuracy of separating the boundaries and the snow depth and the possibility of distinguishing thin layers remains limited.

Interpretation issues of the GPR image remain challenging. Independent information from snow pit investigations, shallow cores or manual snow probing ease interpretation of GPR data and identification of the internal reflection horizon originating from the last summer surface. The identification of the bottom of the snow cover may pose particular difficulties in areas with similar dielectric properties of the underlying material, e.g. in the firn zone. Despite the attempts made (e.g. Mitterer et al. 2011; Grabiec et al. 2020), a link between the properties of the radar reflection and the physical properties of the snow cover remains a challenge.

3. Survey design and data processing

3.1. Survey design

Defining the purpose of the research: the methodology discussed in this chapter is dedicated to shallow soundings aimed at determining the depth and distribution of seasonal snow cover, deposited mainly on glaciers and in their immediate vicinity. It cannot be considered universal for all types of GPR sounding conducted in polar regions. The precise definition of the purpose and the object being studied should always be the starting point for the correct planning of the survey.

Defining the layout of the radar profiles and their mutual relations: the recorded data consist of continuous points arranged in profiles with defined start and end points. In order to obtain a full view of the snow cover distribution, a grid of longitudinal and transverse profiles (or zig-zag) should be designed after defining the object, area and purpose. This can be problematic in highly crevassed areas (e.g. frontal parts of tidewater glaciers and surging glaciers), snow deposited on unstable sea ice and terrain with a slope angle exceeding 15 degrees. In areas with diversified ground relief, it is recommended to increase the density of the radar profile grid. For example, the profile density on the frequently monitored glaciers on southern Spitsbergen is c. 2000 m of GPR profile per km^2 on Werenskioldbreen and 1650 m of GPR profile per km^2 on Hansbreen (Laska et al. 2017).

Antenna selection: according to the assumed sounding depth, the dimensions of the investigated object and the expected vertical resolution, and the appropriate antenna type and frequency should be selected. In the case of determining the depth of the seasonal snow cover, the key reflection horizons are: in the ablation zone of glacier, the glacier ice surface; in the accumulation zone of glaciers, the top of the firn layer; on the tundra, the ground surface. In relation with the applications on glaciers, shielded antennas with a frequency of about 800 MHz are most common. They allow coverage of a depth range of at least 10 – 20 m, depending on physical properties of the snow and limited by the user-specified time window. For more detailed results, it is recommended to use higher frequency antennas, such as 1.6 GHz. They are especially recommended for sounding snow with a low depth, e.g. on the tundra or lakes. The first measurements using such frequencies were carried out in Svalbard in recent years. However, the results are not published yet. The theoretical vertical measurement resolution is ¼ of the wavelength emitted by the antenna (Hubbard and Glasser 2005; Berthling and Melvold 2008). For example, for an antenna with a frequency of 800 MHz, it has been calculated as 0.066 m.

Construction of the platform for transporting the radar set: depending on the configuration, the complete radar set will consist of a control unit connected to two (or more) individual dipole antennas – transmitting, Tx and receiving, Rx (for unshielded antennas), or Tx-Rx antennas enclosed

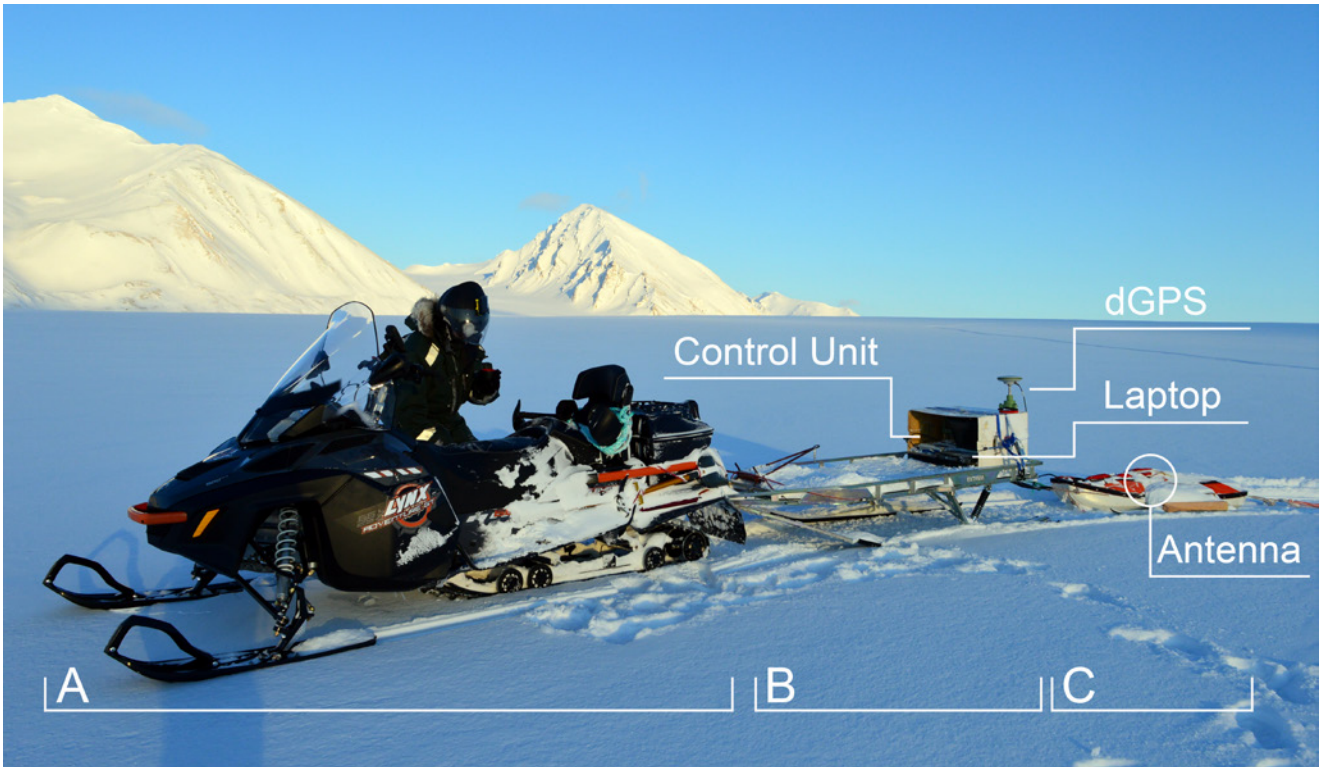

Figure 1: Example of the GPR system configuration: A - snowmobile with navigator, B - sledge with GPR operator, C - pulkas with antenna(s) in a waterproof cover (Photo: Mariusz Grabiec).

in a common housing (for shielded antennas). Shielding makes it possible to separate random, external signals emitted by other neighbouring electronic devices. In both cases, the connection is mainly via optical fibres, which allow fast and undisturbed data streaming. Some designs enable simultaneous sounding with two or more antennas of different frequencies. In addition, the control unit is connected to a portable field computer (or tablet), resistant to moisture, shock, and low temperature, with a battery of sufficiently large capacity. To increase the positioning accuracy, an additional connection to an external GNSS receiver is advised. The entire configuration is shown in Figure 1. Depending on the extent of the area of interest, this set can be transported manually by operator(s), pulled on pulkas, tracked by a snowmobile or installed under a helicopter. There are also designs that can be integrated with unmanned aerial vehicles, UAVs (e.g. Vergnano et al. 2022).

Positioning and measuring the distance: for simple, general surveys, using a laptop built-in or USB standalone GNSS receiver may be sufficient (XY accuracy approx. ± 5 m, Z accuracy approx. 10 m). However, if the objective is focused on a detailed analysis (e.g. determination of the snow cover vertical gradients, glacier surface hypsometry, terrain relief, etc.), a parallel connection with the GNSS receiver is advised. Its sampling interval should be the same as the GPR trace-to-trace time interval. Using differential kinematic mode (dGPS) and a fixed reference station enables XYZ accuracy to be obtained at ±0.1 m. However, this requires additional effort – appropriate post-processing and data synchronisation (described in the section 3.4 'Data processing'). There are various methods of measuring the distance (GNSS receiver, wheel or hip-chain odometers and others) during the GPR survey. Due to the specificity of the research area, common surveys are based on GNSS positioning.

3.2. Measurements settings

Triggering method: there are three ways of triggering the radar signal: manual (practical for single measurements, e.g. RWV measurements by the common midpoint method), distance (using external odometers) and time (used most often in polar surveys). Due to the large diversity of the surface relief, it is recommended to set regular and fast sampling. Most researchers in Svalbard use one in the range 0.2-0.3 s. The most popular setting is

0.2 s (Appendix 1). While maintaining a constant measurement speed of c. 20 km/h, this setting results in a distance of c. 1.0–1.5 m between successive traces.

Time window: it defines the maximum time range of the radar wave recorded for each trace in the investigated substrate. The time window should be set to allow for the arrival of the return signal from the deepest interfaces of interest. This value is usually expressed in nanoseconds, which, with a defined RWV, allows for the determination of the depth. When estimating this parameter, a 30% allowance for error should be applied (Grabiec 2017, after Sensors & Software 1992-1999). For the glaciers of southern Spitsbergen, the time window mostly used is 80 ns (and normally between 45 and 172 ns) when using an 800 MHz antenna. Such a setting makes it possible to fully sample the snow cover, as it implies a penetration depth of c. 7.0–8.4 m.

Sampling frequency: this parameter indicates how often a given trace is sampled. For a given time window, setting the sampling frequency determines how many points will be recorded per trace. Commercial GPR systems generate signals with a frequency in the range of 0.5-1.5 f, where f is the value of the centre frequency (Grabiec 2017). In order to maximise the vertical resolution of the measurement, it is recommended to set the sampling frequency not lower than six times the centre frequency of the antenna being used (Berthling and Melvold 2008).

Number of samples: a single trace consists of a predefined number of samples. They represent digitally the value of the wave amplitude per time unit. The higher the value, the higher the theoretical amplitude resolution. When using 800 MHz antennas, this parameter is most often set to 1024.

3.3. GPR surveying

Depending on the extent of the area of interest, the implementation of the entire survey plan may take up to several hours, which means that it is necessary to properly prepare for it, and fieldwork should be carried out in favourable weather conditions. This is crucial particularly when working in high-risk areas (such as crevassed areas or slopes prone to avalanches). Responsibilities should be divided between at least two people: the equipment operator, who handles the electronics and is focused on its correct operation, and the guide, who leads the team, following the track prepared in advance and trying to maintain a constant speed. In the case of work based on snowmobiles, a reasonable speed is around 20–30 km/h. However, this speed should be much lower in the case of driving on rough terrain or over sastrugi. In difficult terrain such as crevasse fields, it may be necessary to revaluate and adjust the planned survey profiles. Because both the control unit and the antenna electronics are powered with replaceable battery packs, it is recommended to heat spare batteries with body heat. During their replacement, the operator should check that connection plugs are dry and free of snow or ice. Successive profiles should be finished with a noticeable change of the heading. It is recommended to divide long profiles if their length exceeds 5–7.5 km (around 1000 seconds).

3.4. Data processing

Data processing should start with checking the consistency and integrity of the collected data. At the next stage, it is worth defining the course and orientation of the profiles. Applying GIS software for the initial visualisation of profiles' locations could be helpful here. It is also a particularly useful tool for referencing the results of manual point measurements which are used to calibrate the GPR data. When working with GPR profiles, it is recommended to reduce the time window presented on the vertical axis to the range of the analysed reflection horizon. In the next step, the recorded profiles should be cross-checked to remove unnecessary or damaged sections. Those may occur e.g. as a result of antenna rotation during the measurement, weak or drained battery of the antenna electronics, and unplanned stops during data recording. For later analysis, it may be necessary to synchronise the data from the GPR

with the data from the GNSS receiver. This can be done by combining data columns from both independent measurements using the recording time. Some dedicated GPR software packages are able to perform this procedure in a fully automatic way.

There is no single, obligatory set of rules for snow data processing. It is assumed that post-processing of GPR data aims to increase the signal-to-noise ratio, thereby facilitating interpretation of radargrams. When using filters, referring to the applicable instructions for the software being used may be helpful (e.g. ReflexW 3D, RadExplorer, etc.). The mandatory filters include: Time-Zero correction, which allows removing the delay time of first arrivals (direct wave) (especially important when the antenna is located above the investigated surface) and Direct-Current removal (DC removal). In areas with slope exceeding 6°, it is recommended to use Topographic correction (Lehmann and Green 2000). Other filters, such as Dewow, Gain, Background removal or Bandpass filtering, should be used moderately as their overuse may cause misinterpretations and increase measurement errors.

3.5. Validation

Manual point measurements: since GPR is an indirect method, the reliability of the measurements depends on the direct, *in-situ* measurements. For this purpose, an avalanche probe can be used to determine the seasonal snow thickness. The reliability of validation soundings with the use of an avalanche probe is limited in the case of thick internal ice layers. This method, however, has its limitations in the glacier accumulation zone, where it is possible to penetrate into the firn. Validation can also be performed quickly using shallow snow cores collected with a coring system, e.g. Kovacs Mark III. However, it is not trivial to determine the accurate thickness due to strong warming events in Svalbard. A coring system, apart from the snow depth, provides information on the bulk density of the seasonal snow cover, which may contribute to a better estimate of the RWV within the analysed material, and allow construction of a calibration curve between snow-water equivalents (SWE) and RWV, which in turn allows mapping of the SWE over large surface areas for modelling and remote sensing purposes. In addition, an experienced person can detect the snow-firn interface. Full and detailed information about the snowpack stratigraphy, its thickness and density, as well as the snow-firn interface is more precisely determined using traditional snowpit work. However, that procedure requires a lot of effort and time. Regardless of the chosen direct method, point measurements should be made in the immediate vicinity of the GPR profile, at least in several places representing different glacier zones, or evenly distributed over the tundra surface, ultimately capturing the natural variability (thin, thick, soft, and hard snowpacks) so to cover the range of RWV.

3.6. Quality of the data series

A proper identification of the internal reflection horizon originating from the last summer surface on the radar profiles and its accuracy can be estimated by using the standard deviation of a multiple (e.g. five) repetitions of the analysis of the main profile, representing the entire altitude range of the analysed area. For glacial areas, it is worth verifying such a value separately for the ablation and accumulation zones. The correct determination of the appropriate horizon above the equilibrium line may be difficult to perform and only possible through validation with manual point measurements (Laska et al. 2017). Therefore, the largest deviation occurs close to the equilibrium-line altitude (Figure 2).

3.7. Data export formats

Registered data formats and the number of files related to a single profile vary depending on the equipment and software used. Therefore, in the context of exporting the data, it is recommended to focus on the universal data formats, e.g. text file (.csv) with the following columns: X and Y coordinates, trace number, and two-way travel time (TWTT) and depth. Having the TWTT information recorded allows the exported data to be reanalysed if there is a need to modify the RWV. Datasets prepared in this way can be used successfully as input to the GIS software or software/programming language for scientific computing to facilitate the interpretation of the obtained results and their appropriate visualisation.

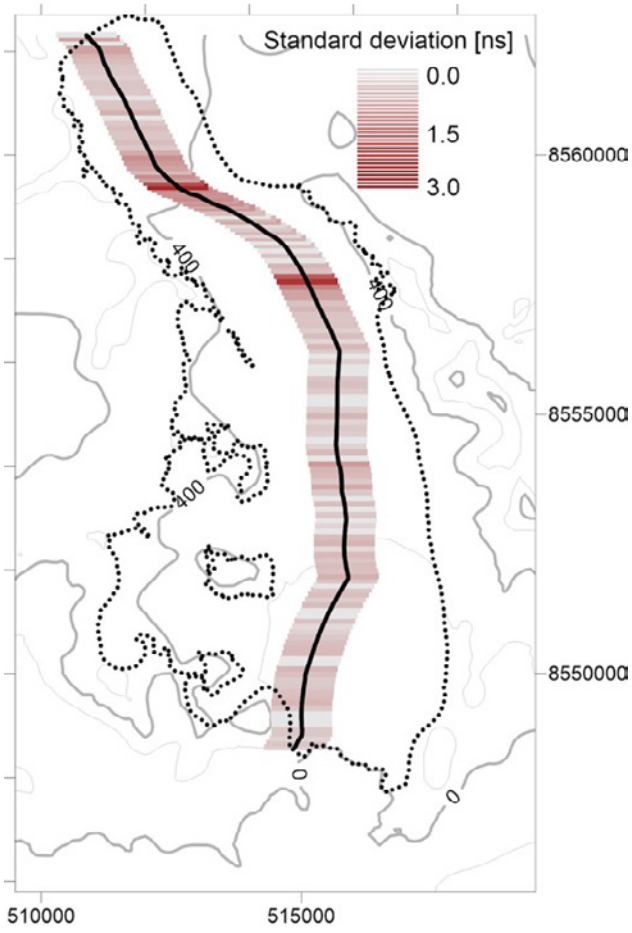

Figure 2: Standard deviation of the identification of the snow base from GPR profiles in the central line of Hansbreen (modified after Grabiec 2017).

4. Overview of radar sounding applications in snow surveys in Svalbard

Snow distribution in high-latitude landscapes plays a key role in defining energy and moisture relationships associated with the Earth's climate system (Melvold 2008). The GPR method has been used in snow measurements for more than four decades. The first snow surveys in Svalbard using GPR date back to the beginning of the 1990s. However, only during the last decade has regular monitoring been carried out in Svalbard using GPR.

GPR is used both for monitoring snow cover on glaciers and on the tundra. Measurements take the form of profiles ranging from a few kilometres to several hundred kilometres long or measurements on a predefined measurement grid (Figure 3). The first measurements were made at the Endalselva catchment in the vicinity of Longyearbyen as well as in De Geerdalen in 1991-1994 (Tveit and Killingtveit, 1994). In De Geerdalen, the measurements were repeated in 2001 (Vonk 2001 after Winther et al. 2003). For the Ny-Ålesund area, the first published results were collected in May 1996 at Kongsvegen (Kohler et al. 2003) and in May 1998 in the lower Bayelva catchment. The measurements in the lower Bayelva catchment were done in the grid and covered an area of 2 x 1.5 km (Bruland et al. 2001; Sand et al. 2001). These measurements were repeated in 2000 (Winther et al. 2003). The first glacial measurements were published by Winther et al. (1998) and Kohler et al.

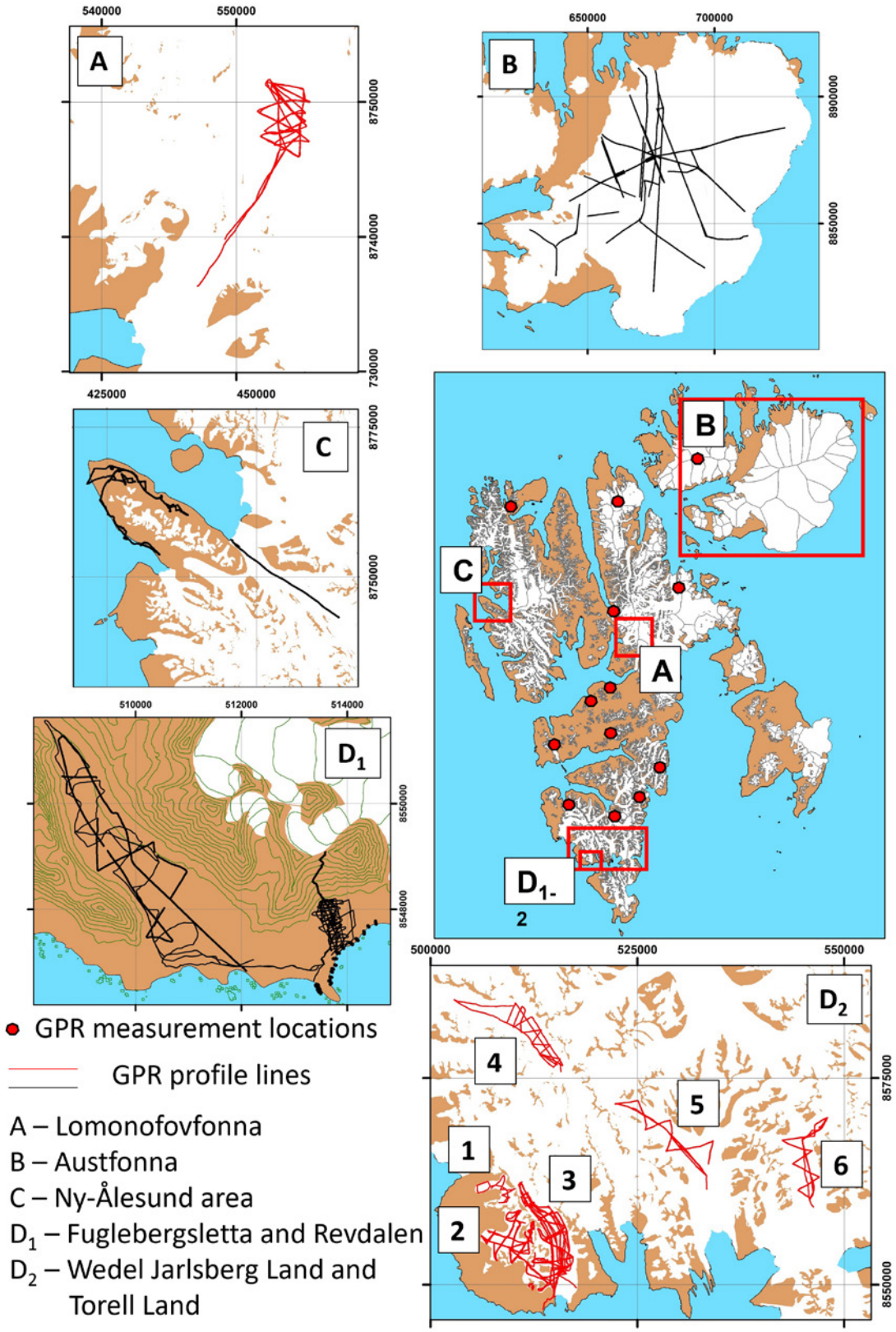

Figure 3: Location of ground penetrating radar measurements of snow cover in Svalbard in 1996-2022. 1- Nannbreen, 2 – Werenskioldbreen, 3 – Hansbreen, 4 – Amundsenisen, 5 – Storbreen and 6 – Flatbreen. Metadata and GPS data (.shp) tracks are available from Ignatiuk et al. (2022).

(2003). These included longitudinal and transverse transects on Slakbreen in 1997, and Kongsvegen in 1996, respectively. Comprehensive GPR surveys were performed between 1997 and 1999 at thirteen sites in Svalbard. Measurements were made on both the tundra and glaciers in the form of four west to east transects (Sand et al. 2003). In 2012, 2014, and 2016-2017, regular measurements were made at Lomonosovfonna (Van Pelt et al. 2014) and in 2013-2015 at Werenskioldbreen (Appendix

1). Currently, the longest observation series are conducted and continued on Austfonna (1999, 2004-2018) (Pinglot et al. 2001; Taurisano et al. 2007; Dunse et al. 2009), which alone accounts for more than 25% of all GPR data from Svalbard, and Hansbeen (2008, 2011, 2013-2019, 2022) (Grabiec et al. 2010; Laska et al. 2017). Snow cover monitoring on Foxfonna close to Longyearbyen (UNIS, personal communication from A. Hodson) is also regularly carried out. At Austre Grønfjordbreen, close to Barentsburg, GPR snow cover observations have been carried out since 2013 (Sosnovsky et al. 2015; Lavrentiev et al. 2018; Singh et al. 2020; Elagina et al. 2021). Occasional campaigns include Amundsenisen (2001, 2006, 2013) (Melvold 2008; Grabiec et al. 2011; Laska et al. 2017), Flatbreen and Storbreen (2013, 2014, 2015 and 2018) (Laska et al. 2017; Barzycka et al. 2020). In the non-glaciated tundra areas, observations are currently carried out in Hornsund (Fuglebekken and Revdalen) (Kępski 2021), Adventdalen close to Longyearbyen (NORCE) and Brøggerhalvøya close to Ny-Ålesund (NPI).

Most of the measurements were made with Malå RAMAC/ProEx survey systems, although at the beginning of the measurements, in the early 1990s, PulseEKKO and GSSI SIR 2 (Appendix 1) systems were sometimes used. Shielded antennas were used for most of the measurements. The 800 MHz antenna has become a standard in the last two decades. Nevertheless, in the 1990s measurements were also made with antennas with a 450-500 MHz centre frequency. In recent years, the first attempts to use high-frequency antennas (e.g. 1.6 GHz) were carried out for more detailed measurements of snowpack stratigraphy. Most measurements were made using GNSS RTK positioning mode. The most popular method of data validation in regards to snow thickness or SWE validation are snowpits and shallow coring. Where there is a permanent network of snow accumulation and ablation stakes (Hansbreen, Werenskioldbreen, Fuglebekken), they are used for data validation.

The GPR snow measurements are a common method for studying large-scale patterns of snow distribution and the gradient of snow accumulation across glaciers in Svalbard (Winther et al. 1998, 2003, Melvold 2008; Bruland et al. 2001; Pinglot et al. 2001; Pälli et al. 2002; Sand et al. 2003; Taurisano et al. 2007; Grabiec et al. 2011; Laska et al. 2017). Observations of the spatial variability of snow cover on glaciers (Figure 4) allow us to determine the seasonal variability of snow cover and to study the factors influencing snow redistribution. Many authors (e.g. Taurisano et al. 2007; Laska et al. 2017) indicate that, despite the annual variability of the snow thickness, its distribution showed the same pattern in different years. Factors contributing to the spatial distribution of snow cover can also be determined for specific glaciers. For example, for Hansbreen, an increase in snow depth towards the north on the western tributary glaciers, and higher snow accumulation in the western part of Hansbreen were found (Figure 5). This suggests that snow distribution is dominated by wind-blown redistribution rather than spatial precipitation variability (Grabiec et al. 2011; Laska et al. 2017). In the case of Austfonna (Figure 6), which has a simple dome shape, the snow distribution is largely controlled both by the distribution of precipitation and the redistribution of snow by wind drift (Pinglot et al. 2001; Taurisano et al. 2007). The analyses carried out based on GPR research show different spatial accumulation gradients for the entire Svalbard region. Winther et al. (1998), based on measurements in the central and northern parts of Svalbard, suggest a gradient of snow accumulation from the west coast towards the east. This pattern was not observed in the Hornsund area (Laska et al. 2017).

The data from shallow GPR surveys (shallow means mainly aimed at snow studies) can be exploited for information about the multi-year sequence of glacier-facies distribution, which provides information for validation of the surface mass balance data (Dunse et al. 2009; Uszczyk et al. 2019; Barzycka et al. 2020). Based on the characteristic signal-reflection pattern dependent on the typical occurrence and strength of dielectric contrasts that occur for different facies on the glacier, it may be possible to identify firn, superimposed ice (SI), and glacial ice zones (Dunse et al 2009). Usually, in such analyses the upper

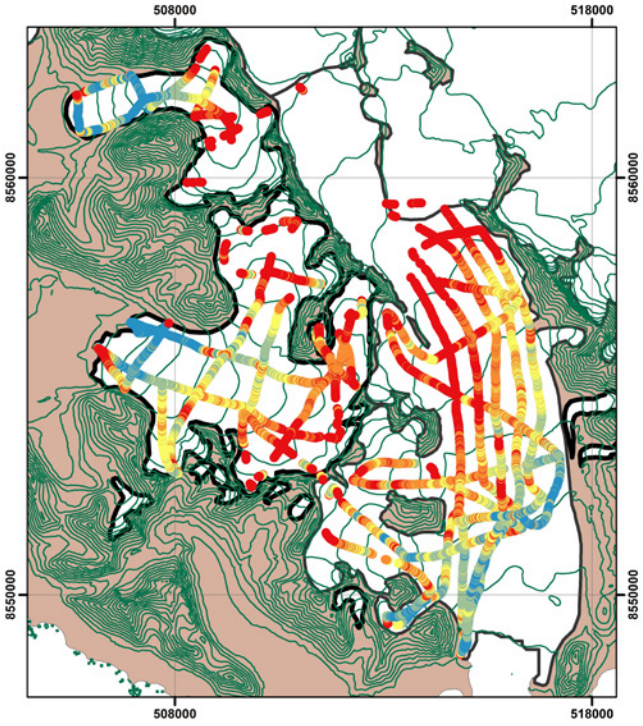

Figure 4: Spatial distribution of the snow cover on Hansbreen, Werenskioldbreen and Nannbreen (modified after Laska et al. 2017).

layer of every profile (corresponding to the snow cover) is excluded from the interpretation and the firn, superimposed ice and ice interface are determined manually in every GPR profile (Barzycka et al. 2020). Validation of the results is based on the comparison between GPR results and SAR images (Dunse et al. 2009; Barzycka et al. 2020). Spatial analysis of glacier facies allows the study of changes of the surface of glaciers caused by a changing climate, as well as distinguishing changes in the mass balance in the southern and northern parts of Svalbard. Observations on Austfonna in the years 2003-2006 show an increase of the extent of the firn zone at the expense of the superimposed ice extent (Figure 7), in contrast with Hansbreen, where the superimposed ice zone disappeared and the extent of the firn zone decreased by 44.5% over 2007-2017 (Figure 8).

Snow depth data from GPR measurements, as well as snow pits, provide important data for calibration and/or validation of models simulating glacier climatic mass balance, snow conditions and runoff (e.g. Schuler et al. 2007; Aas et al. 2016; Østby et al. 2017; Van Pelt et al. 2019, 2021; Schuler and Østby 2020). Observed snow depth in spring can be combined with snow pit (bulk) density to give winter balance estimates. Where snow probing gives local (point) snow depth estimates, GPR has the advantage that it can be used to estimate the spatial average of snow thickness. This is relevant for the validation and calibration of models that

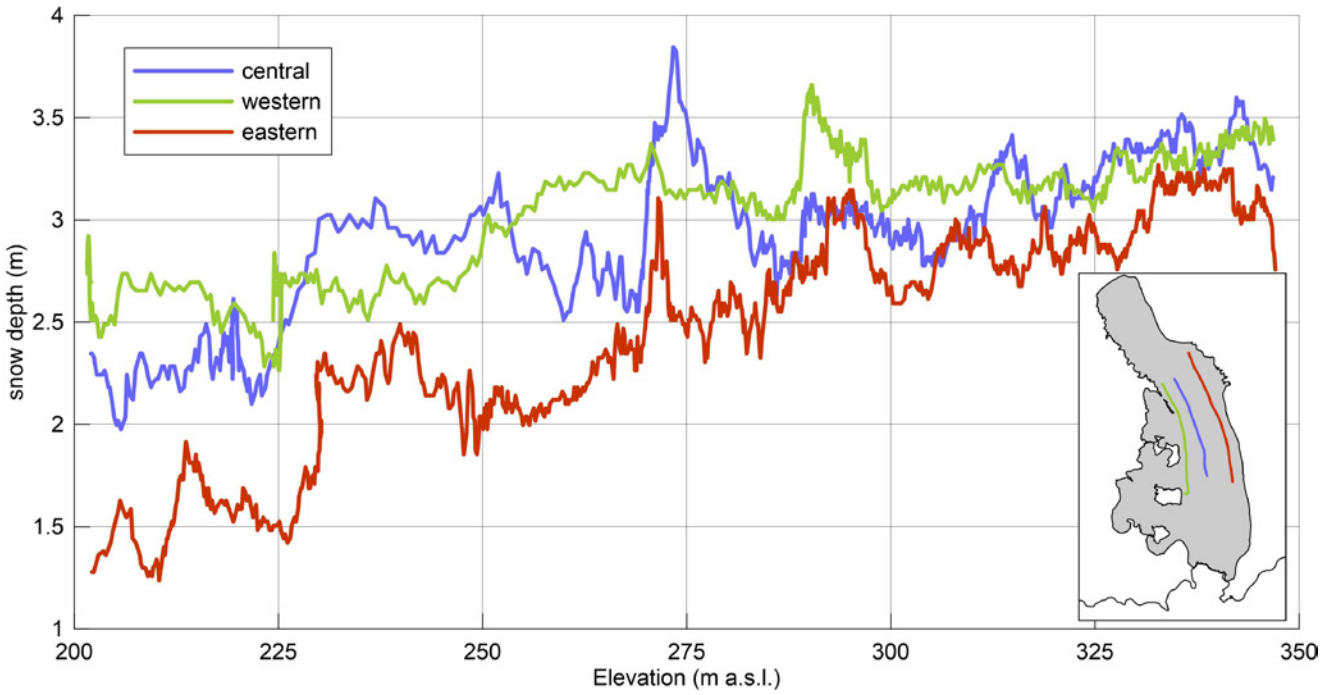

Figure 5: GPR-derived snow depth as a function of elevation on Hansbreen in April 2008, measured along specific parallel profiles: eastern, central and western in the elevation range 200–350 m a.s.l. (modified after Grabiec et al. 2011).

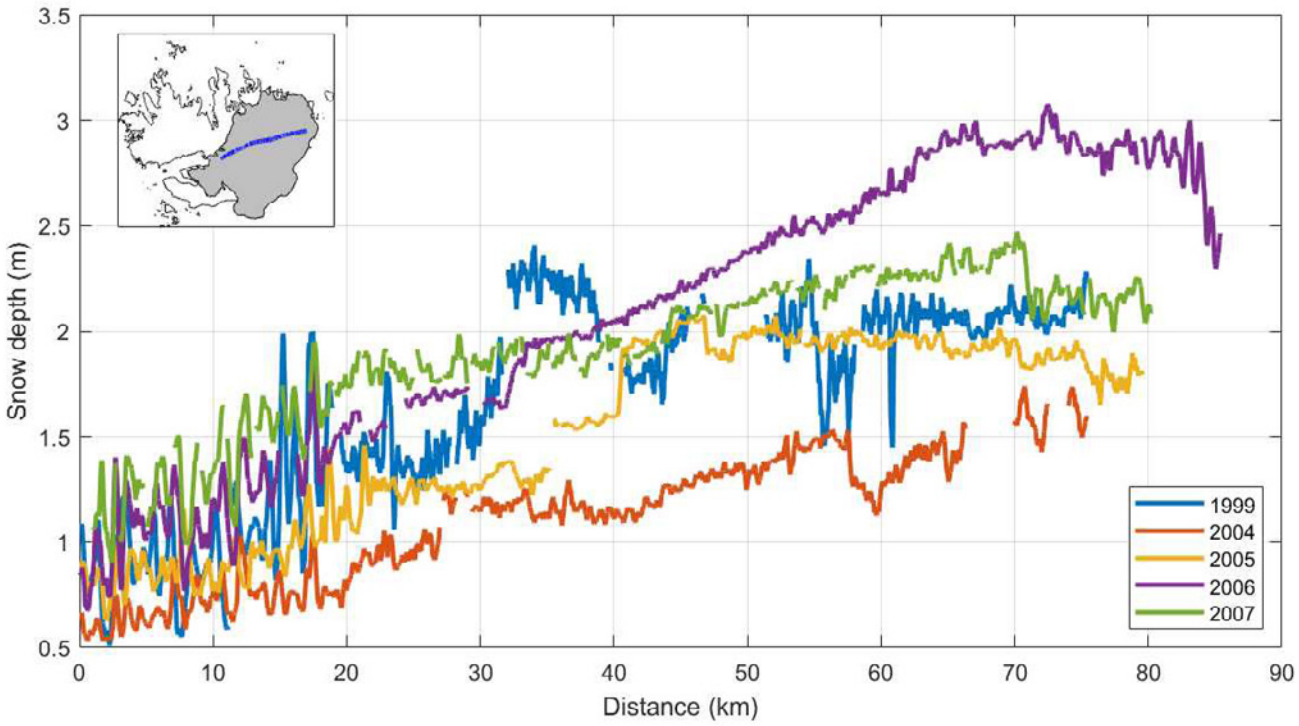

Figure 6: Snow depth profiles along the south-west–north-east transects on Austfonna (modified after Pinglot et al. 2001, Taurisano et al. 2007, and Dunse et al. 2009).

generate gridded (i.e. grid-cell averaged) results. In addition, the data collected by GNSS receivers during GPR measurements are used e.g. for quality assessment of digital elevation models (DEM) derived from space-borne and aerial images (Błaszczyk et al. 2019). It is also possible to use the data to locate crevasses on glaciers, which can be used to improve the safety of fieldwork on glaciers or to monitor changes in glacier dynamics (e.g. Dunse et al. 2015).

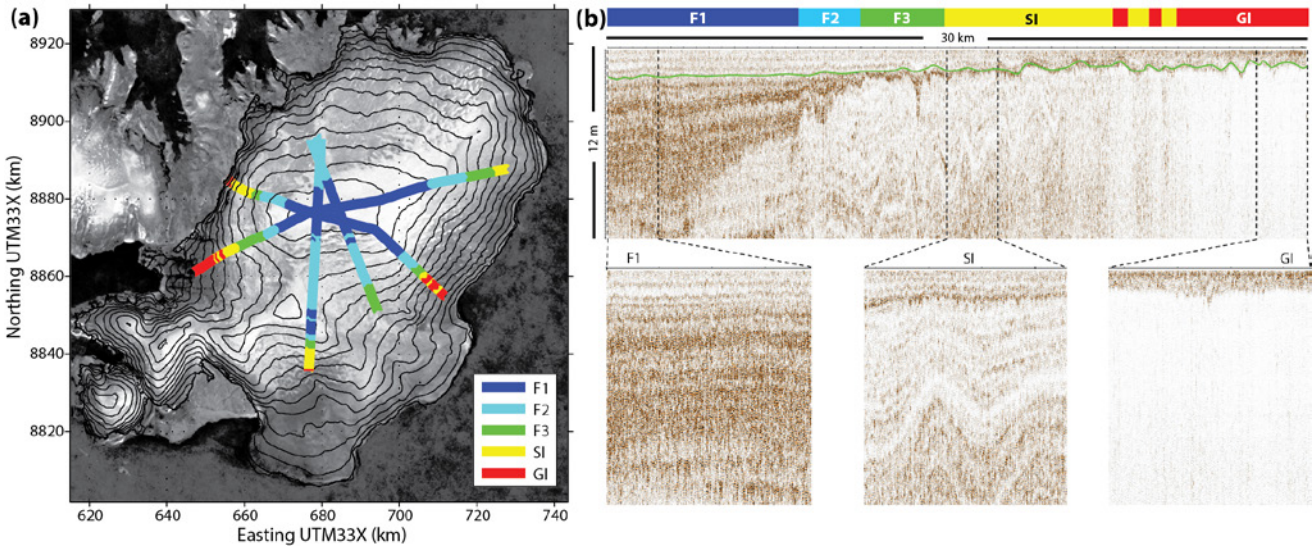

Figure 7: (a) GPR-derived glacier facies across Austfonna, end of summer 2006, distinguishing between firn (F1, F2 and F3), superimposed ice (SI) and glacier ice (GI). The background image shows average SAR backscatter intensity during the winters of 2005 to 2007. (b) Example of the characteristics of GPR signatures from different glacier facies along a 30-km long transect from the summit of Austfonna to the ablation area of Etonbreen. The solid green line indicates the last summer surface 2006 (modified after Dunse et al. 2009).

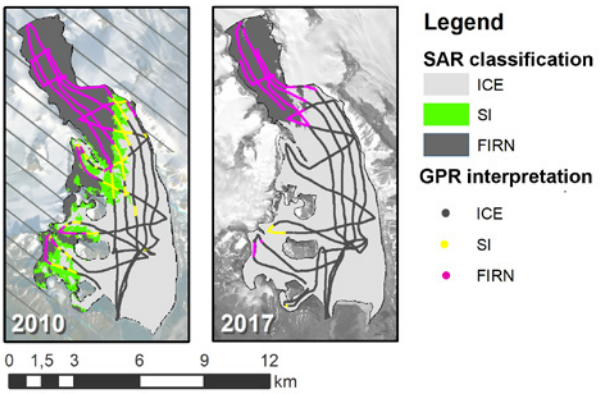

Figure 8: Results of GPR visual interpretation and SAR classification on Hansbreen summer surface in 2010 and 2017. ICE-glacier ice, SI-superimposed ice. Background Landsat 7 and 8 images courtesy of the U.S. Geological Survey, Sentinel-2 images courtesy of the European Space Agency (modified after Barzycka et al. 2020).

5. Contributions to interdisciplinarity

The importance of Svalbard snow cover research, its interdisciplinary potential and its impact on terrestrial, glacier and sea ice research have been widely discussed in SESS reports for snow research (Gallet et al. 2019; Malnes et al. 2021; Killie et al. 2021; Salzano et al. 2021a, 2021b) as well as permafrost monitoring studies (Christiansen et al. 2019, 2020) and Svalbard hydrology (Nowak et al. 2021). Snow cover measurements using GPR, in particular their potential to aid understanding of the spatial distribution of snow, are fundamental for Svalbard ecosystem studies. For example, rain on snow events are currently observed widely in the high Arctic, and particularly in Svalbard. Even if it is very challenging to determine the amount of internal ice within the snowpack or the amount of basal ice (at the ground–snow interface), radar measurements can provide a broad overview of the extent of icing during winter. Thus, large areas where vegetation and ungulates are living can be explored and a better link between climate warming and ecosystem can be made, as well as offering a new strategy to further improve our monitoring and research strategies. Moreover, interest in the type, amount, and activities of the microbial community is growing. Algae and bacteria need nutrients and acceptable temperature to survive: thus, determining the amount of icing (i.e. warming) within the snowpack and the firn is also of interest for microbiological research. Paleoclimate studies are also increasingly focused on the use of radar data for two reasons: first, to find the most appropriate site for drilling ice cores, especially to find a location where the ice is not disturbed so the dating is easy and precise; second, observations of icing inside the snow or the disappearance of firn would show that a site may have been strongly affected by warming in previous years, thus rendering the dating very complex because the signal – often recorded using oxygen isotopes – is flattened (no more seasonality) or even obliterated. Radar measurements are now widely used and provide not only pure glaciological information, but also support data for other disciplines as well as defining the optimal site for a specific research purpose.

6. Unanswered questions/Future challenges

Several challenges must be faced related to the use of GPR in snow research. One of the most important is the use of unmanned aerial vehicles (UAV) for GPR snow cover measurements. Both multi-rotor and fixed-wing drones outfitted with GPR can open up new research horizons. The first tests in the Italian Alps (Vergnano et al. 2022), Quebec (Valence et al. 2022), and Svalbard (carried out by NORCE

(Jenssen and Jacobsen 2021)) show promising results. By performing GPR measurements from UAVs, it will be possible to study snow cover over strongly crevassed glacier areas and on steep mountain slopes. Indeed, many Svalbard glaciers are small and some of their accumulation areas are in basins (or bowls, lobes) with steep terrain. Due to increased melting over summer, areas which were safe in the past are now becoming more hazardous. Old crevasses in these bowls used to be snow filled during springtime, but can now simply be covered by a thin snow bridge, making them dangerous to cross. Measurements in these areas are important to understand water balance and glacier mass balance, and are becoming even more important now that they are sometimes the only part of the glacier where snow remains in summer. In the past, we could interpolate the amount of snow on these parts of the glacier from data collected at lower altitude. Today the inaccessibility of these areas for surface-based measurements and the resulting lack of information increases our uncertainty on snow cover depth and duration. The use of UAVs will allow us to cover these and larger areas of the terrain, making the dataset more representative.

Another challenge is to broaden the areas where measurements have been done so far, to better define the spatial and temporal variability of Svalbard's snow cover. This will allow us to track changes that take place in the cryosphere under a dynamically changing climate. Data with better spatial coverage will also contribute to better validation and calibration of remote sensing products and climate models. It is known that Svalbard has strong north–south and east–west gradients in terms of snow cover, and a glance at a map shows that it is in central Spitsbergen, where precipitation is lowest, that we observe the least glaciation. Changing climate will change the amount of precipitation, in absolute values, with most of it coming in the form of rain and during summer or autumn, enhancing the melt of the glaciers even further. The change of precipitation patterns will strongly affect glacier mass balance and the current link between climate and mass balance may in the future follow different regimes even at the scale of Svalbard if on top of summer melting, autumn melting and/or winter rain events become more frequent. To better understand the long-term variability of snow cover distribution and its future changes, it is thus necessary to conduct regular monitoring using GPR in representative areas of Svalbard, selected to cover most of the precipitation gradient. Monitoring of larger glaciers at higher altitude would also be welcome. These glaciers are still relatively safe to travel on, and thus may not yet require use of UAV-mounted GPR. However, they are also melting, and this is where changes in terms of snow amount and type (dry, wet or icy) will be easiest to detect in a near future. While it is important to continue studying the small glaciers, as this is where we have most of our longer time series, those glacier are sadly destined to disappear in the coming decades. The possibility remains that the larger ones will retreat but adapt to climate change and survive, unless temperatures continue to rise to the point where they will no longer allow any glacier in Svalbard to accumulate ice.

Shallow snowpacks in a tundra environment and on mountain slopes pose another challenge. Relatively popular 500-800 MHz antennas used for snow mapping over the glaciers do not give satisfactory results in shallow (below 50 cm) snow and in areas covered by basal ice. Higher-frequency antennas (over 1.2 GHz) with smaller near-field effects can overcome the problems on the tundra. Their greater vertical resolution allows successful detection, e.g. even 16 cm thin snowpack in the case of the 1.6 GHz antenna. However, it should be noted that in the case of fresh snow, the sledges/pulkas carrying the GPR can significantly compact the surface, causing underestimation of original snow depth (McGrath et al. 2019), which imposes a limitation to the use of GPR in zones with low snow accumulation. One way to address that issue would be to build a very light radar sledge which is attached to the side of a snowmobile, thus measuring over an undisturbed snow surface and limiting the physical impact on it. Nevertheless, higher-frequency antennas can provide insight into snow stratigraphy and be used e.g. for avalanche prediction, and to measure the amount of internal or basal ice. Especially interesting results on shallow

snow may be given by upward-looking ground penetrating radars (upGPR) installed at fixed positions, providing continuous data (Heilig et al. 2009; Mitterer et al. 2011; Schmid et al. 2014; Schmid et al. 2015). These types of studies have not been carried out so far in Svalbard but may provide valuable supplementary data to study the continuous evolution of snow cover at selected specific sites.

Most of the GPR data collected so far is not currently available in any open-access data repository. A comprehensive collection of the studies on which this report is based, and recommendations for metadata and data quality should be the first step to making GPR data more accessible. In the interest of the research community, there should be a will to construct an open-access international database for snow GPR-based data similar to the Glacier Thickness Database (GlaThiDa) hosted by the World Glacier Monitoring Service (WGMS)

7. Recommendations for future

Measurements of snow cover depth using GPR differ depending on whether the measurements are performed on a glacier or on the tundra, as well as on the predicted depth of the snow cover and the purpose of the study. Nevertheless, it is possible to extract some general recommendations regarding fieldwork and data processing and formatting for data exchange, which we have grouped below into appropriate subsections. These are followed by some recommendations for future work under subsection "New Challenges".

Survey:

- Repeated measurements in successive years should be made on the same GNSS tracks whenever safety conditions allow.
- In order to validate the results, it is recommended to perform snow measurements (snow depth, snow pit-stratigraphy, snow water equivalent (SWE)) or shallow coring (snow depth, SWE). It is not recommended to use snow probes or measurements from ablation stakes, as this may result in larger errors.
- The frequency of antennas used for snow cover measurements should not be less than 750 MHz. In the case of surveys of shallow snowpack (tundra environment, mountain slopes) it is recommended to use higher-frequency antennas (above 1 GHz).

Processing:

- For greater accuracy when determining the depth of snow cover, it is recommended use the standard deviation of multiple (e.g. five) repetitions of the analysis of the main GPR profile, representing the entire altitude range of the analysed area.
- The basic processing of the data should include as mandatory steps Time-Zero correction and DC removal filters.
- The RWV used in the data processing and time-to-depth conversion should be derived from the point validation measurements of snow depth (from snow pit or coring) and the corresponding record of the TWTT to the snow base.

Data sharing:

- The shared GPR data should have a full metadata description as proposed in this report (link to data repository). The processed data structure for snow depth should contain a minimum as follows: X and Y coordinates, trace number, TWTT to the snow base and snow depth.

New challenges:

- Adaptation of UAVs to perform autonomous GPR measurements of the snow cover.
- The programmed conducted in the late 1990s for recognition of regional variations in snow accumulation in W–E and N–S transects (Sand et al. 2003) should be repeated for all of Svalbard in order to determine changes in the accumulation of snow cover under ongoing climate change.

- To promote gender balance, the snow GPR research community should encourage women to participate in the GPR campaigns and studies.

8. Data availability

Due to the large number of partners and available data, information is provided in Appendix 2.

9. Acknowledgements

The study presents part of the results from the project the Centre for Polar Studies (the Leading National Research Centre in Earth Sciences for 2014–2018) funding, No. 03/KNOW2/2014; AWAKE2 project Pol Nor/198675/17/2013 (the National Centre for Research and Development within the Polish–Norwegian Research Cooperation Programme); AWAKE project PNRF-22-AI-1/07 (Polish–Norwegian funding); GLACIODYN No. IPY/269/2006 (Polish Ministry of Science and Higher Education); SvalGlac project No. NCBiR/PolarCLIMATE-2009/2-2/2010; ice2sea programme, grant no. 226375,contribution no. 108 (European Union 7th Framework Programme); INTAROS - Integrated Arctic Observing System, grant No. 727890 (European Union's Horizon 2020 Research and Innovation Programme); IPY-KINNVIKA field campaign, grant no. IPY/279/2006 (the Polish Ministry of Science and Higher Education). The studies were carried out with the use of research and logistic equipment (GPR survey system, GNSS receivers, snowmobiles and other supporting equipment) of the Polar Laboratory of the University of Silesia in Katowice. The spring fieldwork in Hornsund 2016 was possible thanks to Svalbard Science Forum funds in the form of Arctic Field Grant No. 2.

This work was supported by the Research Council of Norway, project number 322387, Svalbard Integrated Arctic Earth Observing System – Knowledge Centre, operational phase 2022."

10. References

Aas KS, Dunse T, Collier E, Schuler TV, Berntsen TK, Kohler J, Luks B (2016) Simulating the climatic mass balance of Svalbard glaciers from 2003 to 2013 with a high-resolution coupled atmosphere-glacier model. The Cryosphere, 10:1089-1104. https://doi.org/10.5194/tc-10-1089-2016

Barzycka B, Grabiec M, Błaszczyk M, Ignatiuk D, Laska M, Hagen JO, Jania J (2020) Changes of glacier facies on Hornsund glaciers (Svalbard) during the decade 2007–2017. Remote Sensing of Environment. 251:112060. https://doi.org/10.1016/j.rse.2020.112060

Baker GS, Jordan TE, Pardy J (2007) An introduction to ground penetrating radar (GPR). In: Baker GS, Jol HM (eds) Stratigraphic Analyses Using GPR. The Geological Society of America. Special Paper 432, 1-18.

Błaszczyk M, Jania J A, Ciepły M, Grabiec M, Ignatiuk D, Kolondra L, Kruss A, Luks B, Moskalik M, Pastusiak T, Strzelewicz A, Walczowski W, Wawrzyniak T (2021) Factors Controlling Terminus Position of Hansbreen, a Tidewater Glacier in Svalbard. J Geophys Res Earth Surf 126:e2020JF005763. https://doi.org/10.1029/2020JF005763

Błaszczyk M, Ignatiuk D, Grabiec M, Kolondra L, Laska M, Decaux L, Jania J, Berthier E, Luks B, Barzycka B, Czapla M (2019) Quality Assessment and Glaciological Applications of Digital Elevation Models Derived from Space-Borne and Aerial Images over Two Tidewater Glaciers of Southern Spitsbergen. Remote Sensing 11:1121. https://doi.org/10.3390/rs11091121

Berthling I, Melvold K (2008) Ground-penetrating radar. In: Hauck C, Kneisel C (eds) Applied geophysics in periglacial environments. Cambridge: Cambridge University Press, p. 81—98.

Box JE, Colgan WT, Wouters B, Burgess DO, O'Neel S, Thomson LI, Mernild SH (2018) Global sea-level contribution from Arctic land ice: 1971 to 2017. Environ Res Lett 13:1–11. https://doi.org/10.1088/1748-9326/AAF2ED

Bruland O, Sand K, Killingtveit Å (2001) Snow Distribution at a High Arctic Site at Svalbard. Hydrology Research 32:1-12. https://doi.org/10.2166/nh.2001/0001

Christiansen HH, Gilbert G, Demidov N, Guglielmin M, Isaksen K, Osuch M, Boike J (2019) Permafrost thermal snapshot and active-layer thickness in Svalbard 2016-2017. In: Orr et al. (eds): SESS report 2018, Svalbard Integrated Arctic Earth Observing System, Longyearbyen, pp. 26-47. https://doi.org/10.5281/zenodo.4777825

Christiansen HH, Gilbert G, Demidov N, Guglielmin M, Isaksen K, Osuch M, Boike, J (2020) Permafrost temperatures and active layer thickness in Svalbard during 2017, 2018. In: Van den Heuvel et al. (eds): SESS report 2019, Svalbard Integrated Arctic Earth Observing System, Longyearbyen, pp. 236-249. https://doi.org/10.5281/zenodo.4777728

Davis JL, Annan AP (1989) Ground-penetrating radar for high-resolution mapping of soil and rock stratigraphy. Geophysical Prospecting, 37(5):513–551.

Dunse T, Eisen O, Helm V, Rack W, Steinhage D, Parry V (2008) Characteristics and small-scale variability of GPR signals and their relation to snow accumulation in Greenland's percolation zone. Journal of Glaciology 54(185):333-342. https://doi.org/10.3189/002214308784886207

Dunse T, Schuler TV, Hagen JO, Eiken T, Brandt O, Høgda KA (2009) Recent fluctuations in the extent of the firn area of Austfonna, Svalbard, inferred from GPR. Annals of Glaciology 50:155-162. https://doi.org/10.3189/172756409787769780

Dunse T, Schellenberger T, Hagen JO, Kääb A, Schuler TV, Reijmer CH (2015) Glacier-surge mechanisms promoted by a hydro-thermodynamic feedback to summer melt. The Cryosphere 9:197-215. https://doi.org/10.5194/tc-9-197-2015

Elagina N, Kutuzov S, Rets E, Smirnov A, Chernov R, Lavrentiev I, Mavlyudov B (2021) Mass Balance of Austre Grønfjordbreen, Svalbard, 2006–2020, Estimated by Glaciological, Geodetic and Modeling Aproaches. Geosciences 11:78. https://doi.org/10.3390/geosciences11020078

Gallet JC, Björkman MP, Borstad CP, Hodson AJ, Jakobi H-W, Larose C, Luks B, Spolaor A, Schuler TV, Urazgildeeva A, Zdanowicz C (2019) Snow research in Svalbard: current status and knowledge gaps. In: Orr et al. (eds): SESS report 2018, Svalbard Integrated Arctic Earth Observing System, Longyearbyen, pp. 82-107. https://doi.org/10.5281/zenodo.4778366

Grabiec M, Barzycka B, Laska M, Ignatiuk D, Kachniarz K (2020) Snow Cover Reflection Properties on Hansbreen (South Spitsbergen) based on radio-echo sounding. IASC Workshop on the dynamics and mass budget of Arctic glaciers. Abstracts and program. IASC Network on Arctic Glaciology 43.

Grabiec M, Puczko D, Budzik T, Gajek G (2011) Snow distribution patterns on Svalbard glaciers derived from radio-echo soundings. Polish Polar Research. 32. https://doi.org/10.2478/v10183-011-0026-4

Grabiec M (2017) Stan i współczesne zmiany systemów lodowcowych Svalbardu południowego Spitsbergenu w świetle badań metodami radarowymi [The state and contemporary changes of glacial systems in Svalbard southern Spitsbergen in the light of radar methods] Habilitation Thesis, University of Silesia, 328 pp [in Polish]

Harper JT, Bradford JH (2003) Snow stratigraphy over a uniform depositional surface: spatial variability and measurement tools. Cold Regions Science and Technology 37:289-298. http://dx.doi.org/10.1016/S0165-232X(03)00071-5

Heilig A, Schneebeli M, Eisen O (2009) Upward-looking ground-penetrating radar for monitoring snowpack stratigraphy. Cold Regions Science and Technology 59(2-3):152-162. https://doi.org/10.1016/j.coldregions.2009.07.008

Hubbard B, Glasser N (2005) Field techniques in glaciology and glacial geomorphology. Chichester: John Wiley & Sons, Ltd., 400 pp

Ignatiuk D, Dunse T, Gallet JC, Girod L, Grabiec M, Kępski D, Kohler J, Laska M, Luks B, Van Pelt W, Pettersson R, Pohjola V, Schuler TV (2022) 25 years of high-frequency ground penetrating radar measurements of snow studies in Svalbard – metadata and GPS tracks (Version 2) [Data set]. Zenodo. https://doi.org/10.5281/zenodo.7298986

Jenssen ROR, Jacobsen SK (2021) Measurement of Snow Water Equivalent Using Drone-Mounted Ultra-Wide-Band Radar. Remote Sens 13:2610. https://doi.org/10.3390/rs13132610

Kępski D (2021) The Influence of Topography and Vegetation on the Snow Cover in Tundra: Case Study from the Southern Spitsbergen Area, Publications of the Institute of Geophysics, Polish Academy of Sciences 438:131, ISSN 2299-8020. https://doi.org/10.25171/InstGeoph_PAS_Publs-2021-041

Killie MA, Aaboe S, Isaksen K, Van Pelt W, Pedersen ÅØ, Luks B (2021) Svalbard snow and sea-ice cover: comparing satellite data, on-site measurements, and modelling results. In: Moreno-Ibáñez et al (eds) SESS report 2020, Svalbard Integrated Arctic Earth Observing System, Longyearbyen pp 220-235, https://doi.org/10.5281/zenodo.4293804

Kohler J, Moore J, Isaksson E (2003) Comparison of modelled and observed responses of a glacier snowpack to ground-penetrating radar. Annals of Glaciology 37:293-297. https://doi.org/10.3189/172756403781815528

IPCC (2019) The Ocean and Cryosphere in a Changing Climate 2019, https://www.ipcc.ch/srocc/

Langley K, Hamran SE, Høgda KA, Storvold R, Brandt O, Kohler J, Hagen JO (2008) From glacier facies to SAR backscatter zones via GPR IEEE Transactions On Geoscience and Remote Sensing, 46:2506-2516. https://doi.org/10.1109/TGRS.2008.918648

Laska M, Grabiec M, Ignatiuk D, Budzik T (2017) Snow deposition patterns on southern Spitsbergen glaciers, Svalbard, in relation to recent meteorological conditions and local topography. Geografiska Annaler Series A Physical Geography. https://doi.org/10.1080/04353676.2017.1327321

Lavrentiev II, Kutuzov SS, Glazovsky AF, Macheret YY, Osokin NI, Sosnovsky AV, Chernov RA, Cherniakov GA (2018) Snow thickness on Austre Grønfjordbreen, Svalbard, from radar measurements and standard snow surveys (in Russian). Ice Snow 58:5–20. https://doi.org/10.15356/2076-6734-2018-1-5-20

Lehmann F, Green AG (2000) Topographic migration of georadar data: implications for acquisition and processing. Geophysics 65(3):836–848. https://doi.org/10.1190/1.1444781

Malnes E, Vickers H, Karlsen SR, Saloranta T, Killie MA, Van Pelt W, Pohjola V, Zhang J, Stendardi L, Notarnicola C (2021) Satellite and modelling based snow season time series for Svalbard: Inter-comparisons and assessment of accuracy. In: Moreno-Ibáñez et al (eds) SESS report 2020, Svalbard Integrated Arctic Earth Observing System, Longyearbyen pp 202-219. https://doi.org/10.5281/zenodo.4294072

Marshall H , Schneebeli M, Koh G (2007) Snow stratigraphy measurements with high-frequency FMCW radar: Comparison with snow micro-penetrometer. Cold Regions Science and Technology 47:108-117.

McGrath D, Webb R, Shean D, et al (2019) Spatially Extensive Ground-Penetrating Radar Snow Depth Observations During NASA's 2017 SnowEx Campaign: Comparison With In Situ, Airborne, and Satellite Observations. Water Resour Res 55:10026–10036. https://doi.org/10.1029/2019WR024907

Melvold K (2008) Snow measurements using GPR: example from Amundsenisen, Svalbard. Cambridge (England): Applied Geophysics in Periglacial Environments, Cambridge University Press; 207–216. https://doi.org/10.1017/CBO9780511535628.016

Mitterer C, Heilig A, Schweizer J, Eisen O (2011) Upward-looking ground-penetrating radar for measuring wet-snow properties. Cold Regions Science and Technology 69(2-3):129-138. https://doi.org/10.1016/j.coldregions.2011.06.003

Neal A (2004) Ground-penetrating radar and its use in sedimentology: principles, problems and progress. Earth-Science Reviews 66:261-330.

Nowak A, Hodgkins R, Nikulina A, Osuch M, Wawrzyniak T, Kavan J, Łepkowska E, Majerska M, Romashova K, Vasilevich I, Sobota I, Rachlewicz, G (2021) From land to fjords: The review of Svalbard hydrology from 1970 to 2019. In: Moreno-Ibáñez et al (eds) SESS report 2020, Svalbard Integrated Arctic Earth Observing System, Longyearbyen pp 176-201. https://doi.org/10.5281/zenodo.4294063

Østby TI, Schuler TV, Hagen JO, Hock R, Kohler J, Reijmer CH (2017) Diagnosing the decline in climatic mass balance of glaciers in Svalbard over 1957-2014. The Cryosphere 11:191-215, https://doi.org/10.5194/tc-11-191-2017

Pälli A, Kohler JC, Isaksson E, Moore JC, Pinglot JF, Pohjola VA, Samuelsson H (2002) Spatial and temporal variability of snow accumulation using ground-penetrating radar and ice cores on a Svalbard glacier. Journal of Glaciology 48(162):417–424. https://doi.org/10.3189/172756502781831205

Pinglot JF, Hagen JO, Melvold K, Eiken T, Vincent C (2001) A mean net accumulation pattern derived from radioactive layers and radar sounding on Austfonna, Nordaustlandet, Svalbard. Journal of Glaciology 147(159):555–566. https://doi.org/10.3189/172756501781831800

Plewes LA, Hubbard B (2001) A review of the use of radio-echo sounding in glaciology. Progress in Physical Geography 25(2):203-236.

Salzano R, Aalstad K, Boldrini E, Gallet JC, Kępski D, Luks B, Nilsen L, Salvatori R, Westermann S (2021 a) Terrestrial photography applications on snow cover in Svalbard. In: Moreno-Ibáñez et al (eds) SESS report 2020, Svalbard Integrated Arctic Earth Observing System, Longyearbyen pp 236-251. https://doi.org/10.5281/zenodo.4294084

Salzano R, Killie MA, Luks B, Malnes E (2021b) A multi-scale approach on snow cover observations and models. In: Moreno-Ibáñez et al (eds) SESS report 2020, Svalbard Integrated Arctic Earth Observing System, Longyearbyen pp 252-257. https://doi.org/10.5281/zenodo.4294092

Sand K, Winther J-G, Marechal D, Bruland O, Melvold K (2003) Regional variations of snow accumulation on Spitsbergen, Svalbard in 1997–99. Nord Hydrol 34:17–32. https://doi.org/10.2166/nh.2003.0026

Sensors&Software, 1992—1999: Ground penetrating radar, survey design. Sensors&Software Inc., 18 pp

Schmid L, Heilig A, Mitterer C, Schweizer J, Maurer H, Okorn R, Eisen O (2014) Continuous snowpack monitoring using upward-looking ground-penetrating radar technology. Journal of Glaciology, 60(221):509-525. https://doi.org/10.3189/2014JoG13J084

Schmid L, Koch F, Heilig A, Prasch M, Eisen O, Mauser W, Schweizer J (2015) A novel sensor combination (upGPR-GPS) to continuously and nondestructively derive snow cover properties. Geophysical Research Letters, 42(9):3397-3405. https://doi.org/10.1002/2015GL063732

Schuler TV, Loe E, Taurisano A, Eiken T, Hagen JO, Kohler J (2007) Calibrating a surface mass balance model for the Austfonna ice cap, Svalbard. Annals of Glaciology 46:241-248. https://doi.org/10.3189/172756407782871783

Schuler TV, Kohler J, Elagina N, Hagen JOM, Hodson AJ, Jania JA, Kääb AM, Luks B, Małecki J, Moholdt G, Pohjola VA, Sobota I, Van Pelt WJJ (2020) Reconciling Svalbard Glacier Mass Balance. Front Earth Sci 8:156. https://doi.org/10.3389/feart.2020.00156

Schuler TV, Østby TI (2020) Sval_Imp: a gridded forcing dataset for climate change impact research on Svalbard. Earth Syst Sci Data 12(2):875-885. https://doi.org/10.5194/essd-12-875-2020

Singh G, Lavrentiev I, Glazovsky A, Patil A, Mohanty S, Khromova T, Nosenko G, Sosnovskiy A, Arigony-Neto J (2020) Retrieval of Spatial and Temporal Variability in Snowpack Depth over Glaciers in Svalbard Using GPR and Spaceborne POLSAR Measurements. Water 12:21. https://doi.org/10.3390/w12010021

Sosnovsky AV, Macheret YY, Glazovsky AF, Lavrentiev II (2015) Influence of snow cover on the thermal regime of a polythermal glacier in Western Spitsbergen (in Russian). Ice Snow 131:27. http://dx.doi.org/10.15356/2076-6734-2015-3-27-37

Taurisano A, Schuler TV, Hagen JO, Eiken T, Loe E, Melvold K, Kohler J (2007) The distribution of snow accumulation across the Austfonna ice cap, Svalbard: direct measurements and modeling. Polar Research 26:7-13. https://doi.org/10.3402/polar.v26i1.6204

Tveit J, Killingtveit Å (1994) Snow surveys for studies of water budget on Svalbard 1991–1994. In: Sand K, Killingtveit Å (eds.): Proceedings of the 10th International Northern Research Basins Symposium and Workshop, Spitsbergen, Norway. SINTEF Rep. 22 A96415. pp 489– 509. Trondheim: Norwegian Institute of Technology.

Uszczyk A, Grabiec M, Laska M, Kuhn M, Ignatiuk D (2019) Importance of snow as component of surface mass balance of Arctic glacier (Hansbreen, southern Spitsbergen). Polish Polar Research 40: 311-338. https://doi.org/10.24425/ppr.2019.130901

Valence E, Baraer M, Rosa E, Barbecot F, Monty C (2022) Introducing drone-based GPR in snow hydrology studies, The Cryosphere Discuss. [preprint], 10.5194, tc-2022-42, in review, 2022.

Van Pelt W, Pettersson R, Pohjola VA, Marchenko S, Claremar B, Oerlemans J (2014). Inverse estimation of snow accumulation along a snow radar transect on Nordenskiöldbreen, Svalbard. Journal of Geophysical Research: Earth Surface 119(4):816-835. https://doi.org/10.1002/2013JF003040

Van Pelt W, Pohjola V, Pettersson R, Marchenko S, Kohler J, Luks B, Hagen JO, Schuler TV, Dunse T, Noël B, Reijmer C (2019) A long-term dataset of climatic mass balance, snow conditions, and runoff in Svalbard (1957-2018). The Cryosphere 13:2259-2280. https://doi.org/10.5194/tc-13-2259-2019

Van Pelt W, Schuler TV, Pohjola V, Pettersson R (2021). Accelerating future mass loss of Svalbard glaciers from a multi-model ensemble. Journal of Glaciology 67(263):485-499. https://doi.org/10.1017/jog.2021.2

Vergnano A, Franco D, Godio A (2022) Drone-Borne Ground-Penetrating Radar for Snow Cover Mapping. Remote Sens 14:1763. https://doi.org/10.3390/rs14071763

Vonk JE (2001) Distributed snow modelling—verification in a High Arctic catchment. MSc thesis, Vrije University, Amsterdam

Winther J-G, Bruland O, Sand K, Killingtveit Å, Marechal D (1998) Snow accumulation distribution on Spitsbergen, Svalbard, in 1997. Polar Res 17:155–164. https://doi.org/10.1111/j.1751-8369.1998.tb00269.x

Winther J-G, Bruland O, Sand K, Gerland S, Marechal D, Ivanov B, Głowacki P, König M (2003) Snow research in Svalbard–an overview. Polar Research 22. https://doi.org/10.3402/polar.v22i2.6451

Yamamoto T, Matsuoka K, Naruse R (2004) Observation of internal structures of snow covers with a ground-penetrating radar. Annals of Glaciology 38:21-24. http://dx.doi.org/10.3189/172756404781814834

Appendix 1

Snow cover measurements made using ground-penetrating radar (GPR) from 1997 to 2022 on the basis of collected and published data. A detailed table with metadata can be found in Ignatiuk et al. 2022.

Survey area and coordinates	Date of the survey (YYYY-MM-DD) and total distance [km]	Time window [ns]	Trace-to-trace time interval [s]	Average trace-to-trace distance interval [m]	Snow depth validation method (Positioning mode)	Snow RWV applied [m, ns]
Amundsenisen[3)]	200104XX [20.4]	179	0.2	0.8	snow probe, snow pit (RTK GNSS)	
Amundsenisen[2)]	20060421-27 [44.5]	405		1	(wheel odometer)	0.21
Amundesinsen[1)]	20130505 [56.7]	80	0.2	1.0-1.5	snow pit (RTK GNSS)	0.21
Amundesinsen- Högstebreen[1)]	20110416 [66]	98.9	0.2	1.31	GNSS	
Ariebreen[1)]	2014		0.2	1.0-1.5	snow pit (RTK GNSS)	0.21
Austfonna[3)]	1999 [235]	105			snow pit, core	
Austfonna[1)]	2004 [197] 2005 [140] 2006 [143] 2007 [187] 2008 [109] 2009 [138] 2010 [98] 2011 [291] 2012 [346] 2013 [299] 2014 [191] 2015 [69] 2016 [61] 2017 [219] 2018 [114]	126 (2004-2006, 2008-2009) 145 (2007) 130 (2010) 128 (2011-2012) 139 (2013) 145 (2014) 172 (2015-2018)	0.5 (2004-2005). 0.05 (2006-2007). 0.05, 0.01 (2008-2015)	2 (2004-2005). 0.25 (2006-2007). 0.25, 0.5 (2008-2018)	snow pit, core	
Austfonna[1)]	2006	126	0.05	0.25	snow pit, core	
Austre Grønfjordbreen[6)]	2014					
Brøggerhalvøya[9)]	2021 [40] 2022 [40]		0.05/0.01	0.25/0.5	Snow pit, snow probe	0.21/0.23

Flatbreen[1)5)]	20130420 [11.8] 20140405 [12.2] 20150404 [13] 20180426 [22.8]	80 (2013, 2014) 100 (2015) 800 MHz 80.7/1.6GHz 67 (2018)	0.2	0.8-1.5	snow pit, core (GNSS, RTK GNSS)	0.21
Fuglebekken[1)]	20160419 [12.3] 20160519 [3.7]	61	0.2 (20160419). 0.1 (20160519)	0.85 (20160419). 0.1 (20160519)	snow probe, fixed snow gauges (RTK GNSS)	0.22 (20160419). 0.18 (20160519)
Fuglebekken[5)]	20220429 [8]	67	0.2	0.5	snow probe/fixed snow gauges (GNSS)	
Fugleberget[5)]	20220505 [1.6]	67	0.2		snow probe (GNSS)	
Fuglebergsletta[1)]	20160430 [10.3]	45	0.2	0.85	snow probe (RTK GNSS)	0.22
Hansbreen[1)]	20080426 [63.9], 20110414 [117.5] 20130416 [105.1] 20140403 [103.9] 20140412 [25.9] 20150402 [98.5] 20150511 [78.1] 20150608 [44.5] 20160418 [91.1] 20170420-22 [105.1] 20180418 [105.1] 20190406 [105] 20220407 [94.9]	80 (2014, 2017, 2018), 99 (2015)	0.2	1.0-1.5	snow pit, core, ablation stakes (RTK GNSS)	
Hansbreen[5)]	20180418 [105.1] 20190406 []	67	0.2	1.2	snowpit (RTK GNSS)	
Holtedahlfonna[8)]	20180324 [22.2]	83	0.2		snowpit (GNSS)	
Isbjornhamna[1)]	20150423 [0.7]	100	0.2	0.2	snow probe (RTK GNSS)	
Kongsvegen[3)]	199605					
Kongsvegen[9)]	2016	-	-	-	-	-
Lomonosovfonna[3)]	20120413 [49] 20140403 [35] 20160409 [49] 20170425 [35]	155	0.5	1.5	snow pit, core (RTK GNSS)	average 0.20
Longyearbreen[8)]	20180401 [8.2]	83	0.2		snow pit (GNSS)	
lower Bayelva catchment[7)]	1997/1998 [1.5x2]					
Maritbreen-Philipbreen[8)]	20170327 [15.4]	83	0.2		snow pit (GNSS)	

Survey area and coordinates	Date of the survey (YYYY-MM-DD) and total distance [km]	Time window [ns]	Trace-to-trace time interval [s]	Average trace-to-trace distance interval [m]	Snow depth validation method (Positioning mode)	Snow RWV applied [m, ns]
Nannbreen[1)]	20130516 [20.1]	80	0.2	1.0-1.5	snow pit (RTK GNSS)	0.21
Recherchebreen[1)]	20160412	80	0.2		snow pi, core (GNSS)	
Recherchebreen, Nathorstbreen, Doktorbreen, Polakkbreen, Strong-Nuddbreen, Morsjnevbreen, Grenfjordbreen, Slakbreen, Ulvebreen, Kongsvegen, Mittag-Lefflerbreen, Kvitbreen, Hannabreen, Raufjordbreen, Asgardfonna, Valhallfonna[3)4)7)]	1997-1999	-	-	-	snow pit, snow probe	-
Renardbreen[1)]	20080402 [37]	-		1.5-2	snow pit (RTK GNSS)	0.21
Revdalen[1)]	20160421 [21.6]	45	0.2	0.75	snow probe (RTK GNSS)	0.22
Revdalen[5)]	20160421 [15.7]	67	0.2	0.75	snow probe, snow pit (GNSS)	0.22
Slakbreen[4)]	1997	-	-	-	snow pit	-
Slakbreen[8)]	20180303	83	0.2	-	snow pit (GNSS)	
Storebreen[1)]	20130420 [12.3] 20140405 [15.7] 20140413 [15.7] 20150404 [13] 20180426 [19.7]	100 (2015), 80 (2013-2014, 2018)	0.2	1.0-1.5	snow pit (RTK GNSS)	0.21
Storebreen[5)]	20180426 [19.7]	67	0.2	1.2	snow pit (RTK GNSS)	
Vestfonna[1)]	20090518 20090519 [90]	-	-	1.5-2	(RTK GNSS)	0.21
Werenskioldbreen[1)]	20130515 [57.9] 20140520 [47.7] 20150407 [51.2] 20150515 [52.5]	80 (2013, 2014 100 (2015))	0.2	1.0-1.5	snow pit (RTK GNSS)	0.21
Wilczekodden[1)]	20150423 [0.92]	100	0.2	0.2	snow probe (RTK GNSS)	

1) MALÅ RAMAC survey system, 800 MHz shielded antenna
2) MALÅ RAMAC survey system, 200 MHz unshielded antenna
3) MALÅ RAMAC survey system, 500 MHz shielded antenna
4) PulseEKKO (450 MHz)
5) MALÅ ProEx survey system, 1.6 GHz shielded antenna
6) PulseEKKO PRO (500 MHz)
7) GSSI SIR System 2 (500 MHz)
8) MALÅ ProEx survey system, 800 MHz shielded antenna
9) GNSS Sir 4000

Appendix 2

The data in the repository include parameters such as survey metadata (.csv) and GPX tracks (.shp).

Metadata access: https://doi.org/10.5281/zenodo.7298986.

Dataset Name and Survey Date	GNSS coordinate system	Location	Dataset provider
20060421-27_Amundsenisen_UoS 20110416_Amundsenisen_UoS 20130505_Amundsenisen_UoS	UTM: 33X E511271 N8582040	Amundsenisen	Mariusz Grabiec, Michał Laska, Dariusz Ignatiuk, University of Silesia in Katowice
20140520_Ariebreen_UoS	UTM: 33X E512305 N8549887	Ariebreen	Michał Laska, University of Silesia in Katowice
1999_Austfonna_UiO 2004_Austfonna_UiO 2005_Austfonna_UiO 2006_Austfonna_UiO 2007_Austfonna_UiO 2008_Austfonna_UiO 2009_Austfonna_UiO 2010_Austfonna_UiO 2011_Austfonna_UiO 2012_Austfonna_UiO 2013_Austfonna_UiO 2014_Austfonna_UiO 2015_Austfonna_UiO 2016_Austfonna_UiO 2017_Austfonna_UiO 2018_Austfonna_UiO	UTM: 35X E448113 N8851524	Austfonna	Trond Eiken, Andrea Taurisano,University of Oslo, Thorben Dunse, Western Norway University of Applied Sciences, Kjetil Melvold, NVE
202104_Brøggerhalvøya_NPI 202204_Brøggerhalvøya_NPI	UTM: 33X E431531 N8761203	Brøggerhalvøya	Jean-Charles Gallet, The Norwegian Polar Institute
20130420_Flatbreen_UoS 20140405_Flatbreen_UoS 20150404_Flatbreen_UoS 20180426_Flatbreen_UoS	UTM: 33X E544763 N8564598	Flatbreen	Mariusz Grabiec, Michał Laska, Dariusz Ignatiuk, Barbara Barzycka, University of Silesia in Katowice
20160419_Fuglebekken_IGPAS 20160519_Fuglebekken_IGPAS 20220429_Fuglebekken_IGPAS	UTM: 33X E513703 N8547766	Fuglebekken	Bartłomiej Luks, Daniel Kępski, Institute of Geophysics, Mariusz Grabiec, University of Silesia in Katowice
20220505_Fugleberget_IGPAS	UTM: 33X E513459 N8548511	Fugleberget	Bartłomiej Luks, Institute of Geophysics
20160430_Fuglebergsletta_IGPAS	UTM: 33X E511847 N8547841	Fuglebergsletta	Bartłomiej Luks, Daniel Kępski, Institute of Geophysics, Aleksander Uszczyk, University of Silesia in Katowice

Dataset Name and Survey Date	GNSS coordinate system	Location	Dataset provider
20080426_Hansbreen_UoS 201104_14_17_Hansbreen_UoS 20130416_Hansbreen_UoS 20140403_12_Hansbreen_UoS 20140521_Hansbreen_UoS 20150402_Hansbreen_UoS 20150511_Hansbreen_UoS 20150608_Hansbreen_UoS 20160418_Hansbreen_UoS 20170420_Hansbreen_UoS 20170422_Hansbreen_UoS 20180418_Hansbreen_UoS 20190406_Hansbreen_UoS 20220407_Hansbreen_UoS	UTM: 33X E515758 N8552524	Hansbreen	Mariusz Grabiec, Michał Laska, Dariusz Ignatiuk, Aleksander Uszczyk, University of Silesia in Katowice
20180324_Holtedahlfonna_IGPAS	33X E468703 N8777705	Holtedahlfonna	Bartłomiej Luks, Institute of Geophysics, Polish Academy of Sciences
20150423_Isbjornhamna_UoS_IGPAS	UTM: 33X E514142 N8547348	Isbjornhamna	Michał Laska, University of Silesia in Katowice, Mateusz Moskalik, Institute of Geophysics, Polish Academy of Sciences
2016_Kongsvegen_NPI	UTM: 33X E451639 N8750747	Kongsvegen	Jack Kohler, The Norwegian Polar Institute
20120413_Lomonosovfonna_UU 20140403_Lomonosovfonna_UU 20160409_Lomonosovfonna_UU 20170409_Lomonosovfonna_UU	UTM: 33X E553500 N874900	Lomonosovfonna	Rickard Pettersson, Uppsala University
20180401_Longyearbreen_IGPAS	UTM: 33X E511284 N8678070	Longyearbreen	Bartłomiej Luks, Institute of Geophysics, Polish Academy of Sciences
20180327_Maritbreen_Philipbreen_IGPAS	33X E563357 N8711448	Maritbreen_ Philipbreen	Bartłomiej Luks, Institute of Geophysics, Polish Academy of Sciences
20130516_Nannbreen_UoS	UTM: 33X E507990 N8562080	Nannbreen	Michał Laska, Dariusz Ignatiuk University of Silesia in Katowice
20160412_Recherchebreen_UoS	UTM: 33X E495438 N8596043	Recherchebreen	Mariusz Grabiec, University of Silesia in Katowice
20080402_Renardbreen_UoS	UTM: 33X E484754 N8603965	Renardbreen	Mariusz Grabiec, University of Silesia in Katowice
20160421_Revdalen_IGPAS 20220428_Revdalen_IGPAS	UTM: 33X E510145 N8548676	Revdalen	Bartłomiej Luks, Daniel Kępski, Institute of Geophysics, Aleksander Uszczyk, University of Silesia in Katowice
20180330_Slakbreen_IGPAS	33X E534707 N8657094	Slakbreen	Bartłomiej Luks, Institute of Geophysics, Polish Academy of Sciences
20130420_Storbreen_UoS 20140405_Storbreen_UoS 20140413_Storbreen_UoS 20150404_Storbreen_UoS 20180426_Storbreen_UoS	UTM: 33X E532903 N8563265	Storbreen	Mariusz Grabiec, Michał Laska, Dariusz Ignatiuk, Barbara Barzycka, University of Silesia in Katowice
20090518_19_Vestfonna_UoS	UTM: 34X E600178 N8878889	Vestfonna	Mariusz Grabiec, University of Silesia in Katowice

Dataset Name and Survey Date	GNSS coordinate system	Location	Dataset provider
20130513_Werenskioldbreen_UoS 20140520_Werenskioldbreen_UoS 20150407_Werenskioldbreen_UoS 20150515_Werenskioldbreen_UoS	UTM: 33X E509683 N8554672	Werenskioldbreen	Michał Laska, Dariusz Ignatiuk, Mariusz Grabiec University of Silesia in Katowice
20150423_Wilczekodden_UoS_IGPAS	UTM: 33X E513446 N8546554	Wilczekodden	Michał Laska, University of Silesia in Katowice, Mateusz Moskalik, Institute of Geophysics, Polish Academy of Sciences
1997_WintherSand_UiO 1998_WintherSand_UiO 1999_WintherSand_UiO	-	Svalbard	Jan Gunnar Winther, Knut Sand, University of Oslo

Practical guidelines for scientific application of uncrewed aerial vehicles in Svalbard (UAV Svalbard 3)

Richard Hann[1], Peter Betlem[2,3], Kajetan Deja[4], Marek Ewertowski[5], Barbara Harm-Altstädter[6], Marius Jonassen[2], Astrid Lampert[6], Michał Laska[7], Ireneusz Sobota[8], Rune Storvold[9], Aleksandra Tomczyk[5], Piotr Zagórski[10]

1 Norwegian University of Science and Technology, Trondheim, Norway
2 University Centre in Svalbard, Longyearbyen, Norway
3 University of Oslo, Oslo, Norway
4 Institute of Oceanology of the Polish Academy of Sciences, Sopot, Poland
5 Adam Mickiewicz University in Poznań, Poznań, Poland
6 Institute of Flight Guidance, Technische Universität Braunschweig, Braunschweig, Germany
7 University of Silesia in Katowice, Katowice, Poland
8 Nicolaus Copernicus University in Toruń, Toruń, Poland
9 Norwegian Research Centre, Tromsø, Norway
10 Maria Curie-Skłodowska University, Lublin, Poland

Corresponding author: Richard Hann, richard.hann@ntnu.no
ORCID number: 0000-0002-0577-5812

Keywords: UAV, UAS, drone, RPAS, Svalbard

DOI: https://doi.org/10.5281/zenodo.7371141

1. Introduction

The objective of this report is to develop guidelines and standards for conducting research with uncrewed aerial vehicles[1] (UAVs) in Svalbard. This work follows two previous chapters on the use of uncrewed vehicles in Svalbard in the 3rd (Hann et al. 2021) and 4th (Hann et al. 2022) SESS reports. In accordance with their recommendation, guidelines for data storage and data sharing are collected with the intention to make drone-based research results transparent and usable for long-term studies. Furthermore, we present a comprehensive framework for the planning of drone fieldwork, along with practical recommendations. Last, several recommendations are given on how SIOS could further strengthen the use of UAVs in Svalbard for scientific applications.

2. Data storage and data accessibility

One of the key recommendations from the last SESS chapters on the scientific use of unmanned vehicles in Svalbard was the need to develop guidelines for the storage and accessibility of data. The previous work revealed that, currently, most datasets are not published alongside papers, and remain largely unavailable for further re-use. This is considered as the largest and most important unanswered question in the field. Also, key supplementary information on the acquisition and processing steps in papers that use drone data is frequently missing. The produced data and scientific work thus often fall short of the principles associated with findability, accessibility, interoperability, and reusability (FAIR) data (Wilkinson et al. 2016) and scientific best practices. In consequence, transparency and reproducibility of the work are lost. In particular, the potential for long-term findability, accessibility, interoperability, and reusability of the data is severely reduced. Essentially, this means that the opportunity to build long-term monitoring datasets from ongoing research with drones is severely limited. A theoretical example for this could be a case where a glacier area is mapped in a drone mission and later on, the glacier starts to surge – the availability of pre-surge data would be crucial input to understand the underlying surge mechanics.

In Svalbard, SIOS has well-defined general guidelines for metadata, paradata, and data sharing that provide a first step towards standardising the archiving of scientific (meta)data. Where available, the guidelines draw from community-established standards, whilst relying on custom metadata conventions for fields where no standards exist, e.g. for drone-based mapping.

Clear guidelines also exist for the fields of biology, oceanography, and glaciology. However, such guidelines do not exist yet that address the documentation needs for UAV-derived datasets or processing workflows. To rectify this situation, we recommend the establishment of standardised data structures and para-/metadata formats for UAV-related data, supplementing existing field-specific conventions. In addition, there is a need to establish a standard for the publication of photogrammetry data (James et al. 2019). Photogrammetry-derived data are increasingly important for the digitisation and characterisation of the earth's surface, with digital outcrop models (DOMs), digital elevation models (DEMs), and orthomosaic maps being frequently used in Svalbard for digitisation of landscape geomorphological characteristics, glaciers, geological outcrops, and cultural heritage sites.

The wide-scale applicability of UAVs both complicates the standardisation of (meta) data structures and requires it. The process of standardisation is likely to involve a multi-disciplinary

1 Note: Following the terminology of the original chapters, the terms "UAV" and "drone" are used synonymously. Other common terms are unmanned aerial system, remotely piloted aircraft system (RPAS), unmanned aerial system (UAS), unoccupied aerial vehicle, or uncrewed aerial vehicle.

approach, an effort that requires a scientific platform to connect people and allow for discussions. There is a potential for learning from similar activities in other fields (e.g., CARARE metadata scheme for 3D cultural objects; (D'Andrea and Fernie 2013)).

Until a comprehensive list of standards is developed, we recommend the minimum requirements outlined in Table 1. The list is mainly intended for the most common drone-based results in Svalbard, i.e. generation of DEMs, DOMs, and orthomosaic maps, but is also generally applicable. It is partly based on learnings from the UNIS-led Svalbox project, which aims to compile and acquire key data sets and publications to provide an interactive 3D geoscientific database of Svalbard with a focus on research and education (Senger et al. 2021). DOM data are openly published, and the para-/metadata are made available through the Svalbox Digital Model Database REST services and Svalbox Zenodo group (Betlem et al. 2022). At this stage, we do not suggest specific file types for the data; however, this should be discussed in the future.

As part of the publishing practice, all data sets should include a processing report and/or quality assessment of the data, including a comparison with legacy data. The published digitised Festningen profile is a good example of how this can be done, including the integration with a para-/metadata database and open publication of source and product data (e.g. Senger et al. 2022).

Suitable storage locations of such data need to offer three key characteristics. They must offer free access for the end-users, allow for the storage of large datasets, and guarantee long-term storage. Currently, there are a large number of databases that can be used for this application. The following is a selection of the databases that are most commonly used for the archiving of data from Svalbard; additional data centres are listed in the SIOS guidelines for metadata and data sharing[2].

Table 1: Recommended information to be included in datasets.

Metadata	Acquisition: • Vehicle type: what was the brand and model of the drone • Date & time: when were the data obtained • Location: where were the data obtained (coordinates of all field sites), including the coordinate system (i.e. EPSG code) • Altitude: at which altitude were the data obtained and how was altitude measured • Sensors: what type, brand, and model of sensors were used • Weather: temperatures, precipitation, cloud cover, and wind information • Authorship: role and affiliations of those involved in the acquisition • Coverage: how large an area was mapped • Image overlap: how much horizontal and vertical overlap exists between pictures • Camera angles: at which angle where pictures were taken (nadir or oblique) Processing: • Software: which software was used and which version number • Workflow: documentation of the whole processing sequence, including applied processing parameters • Authorship: role and affiliations of those involved in the processing
Raw data	• Images: especially for mapping and DEM generation missions • Ground control points: type, coordinates, and coordinate system of all points used • Other data: depending on the mission type
Products	• Final products: e.g. orthomosaic maps, digital elevation models, textured mesh • Processing reports: information about what processing settings were used to obtain the final products
Optional	• Flight and attitude data: drone flight logs and/or automated flight plan • Images that display the flight path and selected parameters • Crash or malfunction reports

2 https://sios-svalbard.org/sites/sios-svalbard.org/files/common/sdms-guidelines4providers.pdf

Zenodo: Zenodo is a general-purpose open repository developed under the European OpenAIRE programme and operated by CERN.

NorStore: The goal of NorStore is to develop and operate a persistent, nationally coordinated infrastructure that provides non-trivial services to a broad range of scientific disciplines that have a variety of needs for storing and publishing digital data.

Dataverse.no: A national, generic repository for open research data from researchers from Norwegian research institutions.

PANGAEA: The World Data Center for Earth & Environmental Science, located in Germany, operates as an Open Access library for free publishing.

Arctic Data Centre: The primary data and software repository for the Arctic section of the US National Science Foundation's Office of Polar Programs.

3. Framework for planning drone-based fieldwork

UAVs have emerged over the last couple of decades as a very efficient tool for collecting data for many environmental applications, including landscape mapping, monitoring, and sampling. In Svalbard, the biggest use case is the generation of DEMs and orthomosaic maps. A full overview of all work conducted is given in Hann et al. (2022) and can be accessed online[3]. In this context, the biggest advantage of UAVs is closing the gap between high-resolution satellite data and direct field-based observations. UAVs offer excellent flexibility in terms of temporal and spatial coverage, as well as resolution, with all three aspects controlled by the platform and sensor used, operator experience, weather conditions, and legal regulations. However, there are still applications where high-resolution satellite data will be better suited (e.g. mapping of areas larger than several km^2). Similarly, direct observations or ground-based time-lapse cameras can be more efficient for long-term monitoring (e.g. monitoring of avalanches or ice cliff retreat). Therefore, there is a need for a framework for planning UAV-based activities, first to ensure that UAVs are the optimal solution, and second to propose a uniform approach that will ensure that the gathered result can be compatible with future work (AMAP 2012; Ewertowski et al. 2019). In this section, we focused on a framework consisting of several steps, including (1) a definition of the survey aims; (2) a selection of the appropriate platform in compliance with local air traffic regulations; (3) transportation and preliminary activities; (4) pre-flight checks and setup; (5) conducting the survey; (6) post-flight checks; and (7) data processing and storage. In addition to this, the following references are recommended for planning drone activities: AMAP (2012) and Hann et al. (2021) for an overview of key capabilities of UAVs for science; AMAP (2015) and UNOLS (2021) for practical operational and piloting guidelines; Ewertowski et al. (2019), James et al. (2019) and Śledź et al. (2021) for guidelines for using structure-from-motion photogrammetry in general. As part of the Svalbox project, the UNIS Arctic Geology department also offers an (online) module (unisvalbard.github.io/Geo-SfM) with best practices for the acquisition and processing of photogrammetry data, including DEM, DOM and orthomosaic generation. The best practices include the use of ground control points (GCPs), differential GNSS and Agisoft Metashape.

3.1. Definition of the survey aims

Most UAV surveys include at least some kind of mapping, usually based on a series of images taken by UAV-mounted cameras, and their subsequent processing through the structure-from-motion (SfM) approach. Resultant data include dense cloud points and very detailed (cm to dm resolution) orthomosaic maps and DEMs, which can be used

3 https://sios-svalbard.org/UAV_Svalbard

for further analysis. The first question one needs to address is the purpose of the study, as that will indicate if UAVs are the best tool and will help with the selection of the platform. The main issue to be defined here is the area of the survey and the size of the targeted feature.

Due to limitations related to the combination of altitude, camera focal length, and camera sensor size, UAVs are most efficient at collecting data with ground sampling distance (GSD) between 0.01 and 0.30 m. Data requiring better resolution than 0.01 m can be collected using a UAV, but that will require a very low flying altitude (which translates into low flying speed and overall slow surveys); therefore, ground-based photogrammetry will be a cheaper and more efficient solution here. On the other hand, resolutions coarser than 0.30 m can be obtained from high-resolution satellites (e.g. WorldView or Pleiades series), which are cheaper and more efficient than ground or UAV-based observations.

Similar to GSD, also size of the studied area can potentially make use of UAV inefficient. UAVs' most efficient survey area is from 100 m^2 to 10 km^2. Smaller sites can be more efficiently surveyed using ground-based approaches, whereas satellite and conventional aerial data will be more economical for larger areas. If both the dimension of the targeted feature and the size of the area to be surveyed are within the suitable ranges (0.01 – 0.20 m GSD, 100 m^2 – 10 km^2 area), then it makes sense to use UAVs for surveys.

The definition of the survey aims should also incorporate the character of the survey, e.g. one-time mapping; change detection (in which case it might be worth installing semi-permanent ground control points); process-form geomorphological studies (which usually will include some additional data, e.g. ground-based time-lapse cameras); analysis of spectral signatures (which require multispectral or hyperspectral sensor, and thus typically large UAV platforms).

3.2. Selection of the appropriate platform in compliance with local terrain conditions and aviation traffic regulations

The type of the UAV platform should be selected according to the survey aims and adjusted to local terrain characteristics. More general information on typical UAV types is given in e.g. Hann et al. (2021).

Small multi-rotors (e.g. DJI Phantom and Mavic series) are very compact and can be easily transported in the backpack over large distances; therefore, they can be especially useful in remote parts of Svalbard. Moreover, they can hover over one place and take images even in very low light conditions (common in Svalbard). However, their main limitation is limited operation time (up to 40 minutes per battery pack), which usually means that additional batteries must be brough to the fieldwork, and a lack of ability to mount more sophisticated sensors.

Large multi-rotors (e.g. DJI Matrice series) are more capable in terms of available sensors (including LiDAR and multispectral cameras); however, they are heavier and larger and, therefore, harder to transport to remote locations.

Fixed-wing constructions can cover larger areas, are more resilient to high winds, and have much better battery efficiency; however, they are generally bulkier than small multi-rotors. Moreover, they cannot hang mid-air and usually require larger ground patches for a safe landing. Therefore, they are preferable to surveys that cover large areas (> 1 km^2).

Additional consideration must be given to regulations and the recently introduced EU drone laws. For more detailed information about regulations, refer to Hann et al. (2022). Operations in the "open" category cover flights with visual line of sight (VLOS), low altitudes (below 120 m), with small UAVs (< 4 kg). This type of operation covers most mapping missions. More complex operations, e.g. beyond visual line of sight (BVLOS) or at higher altitudes, are subject to more requirements. Special

notice should be given to the airspace restrictions when operating close to airports, bird cliffs, national parks, or Ny-Ålesund. Also, a process is currently ongoing to introduce new environmental protection act regulations that may limit drone usage in Svalbard in the future.

Preparation of a checklist and printed operation manual is also an element of good practice. We also advise registering and updating all equipment pieces prior to fieldwork. When planning fieldwork, several extra days should be included to allow for bad weather windows. Time for packing and unpacking should also be considered.

The cost level for such platforms is also an consideration. Small off-the-shelf drones are usually quite affordable (ca. 2 000–5 000 EUR). Large multi-rotor platforms are more expensive (ca. 10 000–30 000 EUR). Fixed-wing systems, especially custom-built systems, can be an order of magnitude more expensive than large multi-rotor solutions. Rental prices can range widely and are around 100-300 EUR per day for smaller systems. Pilots can be hired for 200-2 000 EUR a day, depending on the level of qualification required.

3.3. Transportation and preliminary activities

Two aspects of transportation must be taken into account–first, delivery of the UAV to Svalbard, which typically means as checked-in luggage on airlines or as cargo on a ship. Airlines limit the number of LiPo batteries one is allowed to bring, depending on capacity: batteries up to 100 Wh can be brought without limitation; two batteries with 100-160 Wh capacity are allowed per passenger; and batteries larger than 160 Wh must be shipped separately. In addition, some airlines have banned drone transport entirely. Sending UAVs as cargo takes substantial shipping time. The drone must be packed into a solid case that can withstand handling during transport. Overall shipping as cargo comes at high cost and with a substantial risk that the planned research schedule will not hold. Good practice suggests transporting spare equipment (e.g. second UAV, controller, propellers, cables).

The second issue is related to transportation within Svalbard. Depending on the scenario and available transport solution, UAVs might be transported by vehicle (e.g. in the vicinity of Longyearbyen), which allows for the use of large UAVs, or be transported on foot, which instead favours small constructions which fit into a backpack. Watertight and hard-case containers (e.g. Pelicases or Zarges boxes) are advisable for longer transportation. When travelling in the field, one should ensure that the batteries do not get too cold (e.g. by carrying them close to the body, or by using heated transport boxes).

3.4. Pre-flight checks and setup

Technical pre-flight checklists, typically provided by the drone manufacturer, should be used to ensure that the drone is ready for flight. Especially it needs to be ensured that propellers and batteries are mounted securely and that an appropriate home point and return-home altitude are set. Furthermore, the survey area should be explored to familiarise oneself with the local terrain conditions and potential obstacles or hazards. A suitable take-off and landing spot should be carefully selected. Flat areas, with few obstacles and good overview of the survey area are usually a good choice. Potential safe emergency landing spots should be identified in case missions need to be aborted. If automatic flight paths are used (i.e. pre-planned missions) , it should be ensured that the right mission and altitudes are chosen. Before flight, any camera covers and protection must be removed, and one must ensure that there is enough free data storage capacity on the SD card. Before take-off, camera settings should be checked.

For additional accuracy of DEMs, ground control points (GCPs) can be used. The decision if of whether GCPs should be used or not depends on the use case. Typically, GCPs need to be used when low absolute spatial errors are desired, e.g. when comparing between different data sets, looking at very detailed resolutions, or investigating change-processes. There are two basic options for GCPs: artificial targets (preferably machine-readable) that are placed around the survey area, or natural targets such as rocks or outcrops. The coordinates

of GCPs need to be obtained with high precision, ideally with differential use of the Global Navigation Satellite System (GNSS) networks, e.g. GPS, Gallileo.

3.5. Conducting the survey

The fieldwork crew should contain at least two persons: one pilot, operating the drone, and one designated polar bear guard. While the pilot should focus on conducting the mission, the polar bear guard should keep an eye on the surroundings not just for polar bears, but also other hazards, such as birds, weather changes, helicopter/airplane traffic, etc. For more complex missions, e.g. EVLOS or BVLOS, a third person acting as observer or mission operator is useful. During operations, special attention should be paid to the condition of the field crew concerning hypothermia or frostbite. Also, stress and tiredness can lead to carelessness and bad decision-making, and thus increase the risk of losing the aircraft.

3.6. Post-flight checks

After landing, the aircraft should be checked for any damage that might have occurred during flight or landing. If possible, data should be downloaded from the drone immediately and backed up without delay. It is an advantage if data can be reviewed in the field to verify the correct coverage of the survey area. Proper flight logs should be kept that include take-off and landing times, as well as some information about the mission and weather conditions.

3.7. Data processing and storage

For further information on data processing and data storage refer to section above.

3.8. Infrastructure

Limited infrastructure and access to UAVs are important barriers to the use of this emerging technology. Currently, there are several suppliers for UAV infrastructure in Svalbard. The following is a short overview of key stakeholders in this matter:

- The University Centre in Svalbard (UNIS) is offering the rental of drone equipment with optional pilot support for fieldwork, as well as extended support and planning for fieldwork operations (UNIS 2020). They offer a range of UAVs, consisting mostly of DJI systems with RGB and thermal cameras. The Svalbox project furthermore offers RGB-data acquisition and processing services.
- SIOS is offering access and funding to UAV infrastructure. SIOS is collaborating with the Norwegian Research Centre (NORCE) and UNIS to make these systems available to its partners.
- Ny-Ålesund: The first floor of the airport tower in Ny-Ålesund is set up to serve as a drone operation centre. Around Ny-Ålesund, a radio silent zone has been established due to a sensitive radio telescope. This makes it impossible to use the standard 2.4 GHz telemetry range for communication with the UAV within a radius of 20 km around the centre of Ny-Ålesund. Suitable alternatives are the commonly used frequencies of 484 and 868 MHz.
- Polish Multidisciplinary Laboratory for Polar Research (PolarPOL): Offers equipment for comprehensive studies of the structure and dynamics of the cryosphere and polar catchments, including quadcopter UAVs, fixed-wing UAVs, and GNSS systems.
- Polish Polar Station Hornsund: Offers no permanent UAV equipment or certified operators but can be used as a logistics hub. During the spring and summer seasons, the station is visited by seasonal expeditions which often use unmanned vehicles for their purposes.
- Nicolaus Copernicus University Polar Station, Svalbard (NCUPS): The station is equipped with: UAV, UAV real-time kinematic (RTK) system, GNSS system, and software (e.g. UgCS, DroneDeploy, Agisoft Metashape). Precise Digital Terrain Models are developed for the area of Kaffiøyra based on remote sensing sources, supported by UAV and precise GNSS measurements (also RTK and post-processing kinematic (PPK).

- Polar Station of the Maria Curie-Skłodowska University in Calypsobyen (Bellsund), is a seasonal station. Expeditions are equipped with: UAV, fixed-wing GNSS system, and software (e.g. ContexCapture/Bentley, Agisoft Metashape). Professional service with authorisation to use this type of device.
- Adam Mickiewicz University Polar Station (AMUPS), in Petuniabukta, is a seasonal station offering access within the framework of the International Network for Terrestrial Research and Monitoring in the Arctic (INTERACT). Available field equipment: UAVs multirotor, GNSS system, power generator.
- R/V Oceania is a research vessel belonging to the Institute of Oceanology of the Polish Academy of Science, that goes into the Arctic every summer. Expeditions are typically equipped with ROV, drop camera, AUV, and UAV.
- Czech Arctic Research Station operates a GNSS ground station in Longyearbyen and a GNSS ground station in Longyearbyen and Ny-Ålesund is made available via Kartverket.

4. Practical guidelines

Despite the undeniable advantages and versatility of unmanned systems, there are several challenges that responsible operators should be aware of. Using drones in the Arctic and Svalbard is a more difficult task than at mid-latitudes and is also associated with higher risks. From our experiences, the following special issues need to be considered for UAV operations in Svalbard.

Compass and GNSS issues: especially some off-the-shelf products (e.g. DJI Phantoms) are sensitive to any problems with GNSS and the onboard magnetometer compass. Magnetic interference errors occur often in Svalbard. In manuals, DJI frequently informs that their product should not be used in polar regions, which may lead to problems with the warranty in case of an aircraft crash. Solar activity can lead to ionospheric scintillation causing changes in the magnetic field that can confuse the drone's autopilot. The potential for disturbance of the Earth's magnetic field caused by solar winds (Kp-index) should be checked before take-off in polar regions. User experience also shows that the Longyearyben GNSS ground station may be difficult to pair with in RTK mode, yet still provides key data for PPK.

Air temperature and wind speed: low air temperature is a key limiting factor, especially during cold seasons. The operating temperature range of older generations of the most popular platforms starts from 0°C. However, it is possible to use DJI Phantom/Mavic series in sub-zero conditions. There might be a problem with turning on engines if the battery temperature drops below 15°C. It is recommended to keep batteries as warm as possible, also whilst charging, as lower temperatures may prevent the batteries from fully charging. Notice that flight time in low air temperatures is also severely reduced. Solutions can consist of insulation or active heating, as presented in Lampert et al. (2020). Light platforms are also more susceptible to high wind speeds and gusts. Operation in strong winds will draw more energy and reduce flight time. Strong winds can also lead to fly-away of the drone, especially when paired with GNSS issues. Wind profiles in Svalbard may be unpredictable due to large orographic diversity. Plastic, such as that in cables or 3D printed parts, becomes very brittle in the cold and can easily break.

Precipitation and atmospheric icing: due to the interaction between oceanic circulation – land relief, and a large proportion of glacierised areas, Svalbard is characterised by high relative humidity in the atmosphere. Fog or low cloud levels significantly reduce the extent of the VLOS operations. Supercooled water in clouds, fog, drizzle, or rain can cause icing on the vehicle's surface and lead to a rapid crash (Hann and Johansen, 2020). Heavy snowfall can also lead to failures. Additionally,

marine aerosols contain solid impurities (e.g. salt) which harm fragile electronic parts (rusting, rotor damage).

Wildlife: some birds like the black-legged kittiwake (*Rissa tridactyla*), Arctic tern (*Sterna paradisaea*), Arctic skua (*Stercorarius parasiticus*), great skua (*Stercorarius skua*) or glaucous gull (*Larus hyperboreus*) can be aggressive towards aerial platforms or pilots, especially during nesting. Mammals (polar bears, reindeer, foxes, seals) are usually afraid of engine noise (Palomino Gonzalez 2019). All drone operations need to avoid exposing the wildlife in Svalbard to extra stress. Note that there are restrictions to accessing bird cliffs in national parks. Polar bear safety should always be a key consideration for fieldwork planning.

Light conditions: UAVs experience the same limitations of the light conditions as optical satellite remote sensing. In Svalbard, the dark season (also referred to as 'polar night') several months, which means that optical sensors are mostly useless between October and February. Even during polar day surveys, the low solar angle may affect operations by shading (caused by varied land relief). Flying over extremely dark or bright, highly reflective surfaces (e.g. fresh snow cover) may cause problems with obstacle avoidance systems.

Ground Control Points (GCPs): proper distribution of the GCPs may be particularly challenging over inaccessible areas such as glacier crevasse fields. Because glaciers are constantly in motion, it is recommended to place several markers also on unglaciated surfaces. Use of shiny coated markers may obstruct the processing stage because of solar reflection, especially on sunny days. Alternatively, UAVs with GNSS correction technology, e.g. RTK and PPK systems, can be used to eliminate the necessity of large numbers of GCPs across difficult terrain. The use of few points then suffices for the determination of absolute errors.

Variable ground conditions: Ground conditions can vary considerably between seasons in Svalbard, ranging from hard and frozen ground to wet and muddy. This can limit the possibility of UAVs to safely take off and land – in particular larger multicopters or fixed-wing aircraft.

A more general list of technical and operational challenges of using unmanned platforms in polar environments or for scientific purposes was presented by Kramar (2019) and UNOLS (2021). An operational handbook for scientific users of UAVs in the Arctic was produced by the AMAP workgroup (AMAP 2015).

5. Contributions to interdisciplinarity

One of the main findings in previous SESS chapters was that uncrewed vehicles have the potential to be beneficial to a very wide range of scientific disciplines in Svalbard (Hann et al. 2021, 2022). As such, there is a very large interdisciplinary interest in both UAVs and practical guidelines for scientific operations in Svalbard, particularly within the fields of geomorphology, ecology, atmosphere, oceanography, technology, glaciology, snow, cultural heritage, sea ice, and geodesy. As there are a wide range of users with different backgrounds, it is important to establish a common platform to share and discuss results and methods in a Svalbard context. Furthermore, there are key techniques (mainly structure-from-motion photogrammetry) that are used in many fields. There is great potential for synergy with UAVs on sharing platforms, methods, results, and more.

6. Recommendations for the future

6.1. Efforts to lower barriers for specific operations

Most areas in Svalbard are remote and uninhabited. This means that drone missions have lower risks compared to operations on the more densely populated mainland. This offers the potential to push for extending the operational envelope in Svalbard. In particular, the focus should be on the barriers of 120 m maximum altitude and the requirements for extended visual line of sight operation for simple operations. There are several ways this could be achieved within the current EU drone regulations, most easily with the development of special predefined risk assessments (PDRA) for Svalbard. SIOS should take a leading role in developing such frameworks, that will lower the barrier for scientists to conduct complex operations in Svalbard. Based on earlier work, two particular scenarios would be of high relevance for the Svalbard research community:

- Extended visual line of sight operations (with observer) for unmanned aerial vehicles below 4.0 kg and altitude below 120 m. Such operations are relevant for mapping activities to extend the distance the drone can travel from the pilot's location.
- Visual line of sight operations near take-off point with unmanned aerial vehicles below 25 kg and altitudes below 600 m. Pushing the maximum altitude from 120 m to 600 m is relevant for operations involving meteorological measurements and geological outcrop mapping.

6.2. Develop standards for data storage and data accessibility

A common standard for storage and sharing of data that were obtained with drones needs to be developed. This is required to unlock the full potential of such datasets – especially in the context of re-using data and building long-term monitoring datasets. Developing these standards is a community activity and requires dedicated funding and action to achieve. SIOS should facilitate discussions about this topic and take lead in organising a task force to develop a comprehensive standard for the scientific community.

6.3. Develop and provide a forum for drone users in Svalbard

A forum for scientific drone users in Svalbard should be developed. Since a wide and diverse range of scientific disciplines use drones in Svalbard, there is no natural forum. This diversity means that there is a need for an interdisciplinary platform where researchers with different backgrounds can come together to discuss, share experiences, develop best practices, etc. This would benefit experience transfer, development of standards, and help to build a knowledge base. Such a platform could also be combined with education and training activities. We suggest that the Svalbard Science Forum or the SIOS Polar Night Week could be used for this purpose. Also, reaching out to other stakeholders in this area, for example the Sustaining Arctic Observing Networks (SAON), is recommended.

6.4. Provide and fund training for basic and advanced drone use

Unmanned vehicles have a large potential to contribute to a wide range of scientific fields. Currently, there are only a handful of applications that are being used on a wide basis (mapping and surveying). Especially more complex and specific operations are currently only used by a few actors. We recommend that SIOS strive to offer opportunities to further develop drone applications and to lower the barrier for new users to implement drones in their research. This could be achieved, for example, by conducting workshops, offering infrastructure (UAV platforms), and funding for drone missions. This could also include providing information material in more compact form (brochure, website, etc.) about various topics. In particular information about regulations in Svalbard is of interest.

7. Acknowledgments

This work was supported by the Research Council of Norway, project number 322387, Svalbard Integrated Arctic Earth Observing System – Knowledge Centre, operational phase 2022.

Peter Betlem acknowledges the Norwegian CCS Research Centre (Research council of Norway project number 257579 and research partners).

8. References

AMAP (2012) Enabling Science use of Unmanned Aircraft Systems for Arctic Environmental Monitoring. By: W. Crowe, K.D. Davis, A. la Cour-Harbo, T. Vihma, S. Lesenkov, R. Eppi, E.C. Weatherhead, P.Liu, M. Raustein, M. Abrahamsson, K-S. Johansen, D. Marshall, R. Storvold, B. Mulac. AMAP Technical Report No. 6 (2012). Arctic Monitoring and Asessment Programme (AMAP), Oslo. 30 pp.

AMAP (2015) Arctic Science Remotely Piloted Aircraft Systems (RPAS) Operator's Handbook. By: Storvold R, Sweatte C, Ruel P, Wuennenberg M, Tarr K, Raustein M, Hillesøy T, Lundgren T, Sumich M. Arctic Monitoring and Assessment Programme, Oslo. 25 pp

Betlem P, Birchall T, Lord G, Oldfield S, Nakken L, Ogata K, Senger K: High resolution digital outcrop model of faults and fractures in caprock shales, Konusdalen West, central Spitsbergen. Earth Syst Sci Data Discuss [preprint], https://doi.org/10.5194/essd-2022-143, in review, 2022.

D'Andrea A, Fernie K (2013) CARARE 2.0: A metadata schema for 3D cultural objects, In: 2013 Digital Heritage International Congress (DigitalHeritage), pp 137–143. https://doi.org/10.1109/DigitalHeritage.2013.6744745

Ewertowski MW, Tomczyk AM, Evans DJA, Roberts DH, Ewertowski W (2019) Operational Framework for Rapid, Very-high Resolution Mapping of Glacial Geomorphology Using Low-cost Unmanned Aerial Vehicles and Structure-from-Motion Approach. Remote Sens 11(1):65. https://doi.org/10.3390/rs11010065

Hann R, Altstädter B, Betlem P, Deja K, Dragańska-Deja K, Ewertowski M, Hartvich F, Jonassen M, Lampert A, Laska M, Sobota I, Storvold R, Tomczyk A, Wojtysiak K, Zagórski P (2021) Scientific Applications of Unmanned Vehicles in Svalbard. In: Moreno-Ibáñez et al (eds) SESS report 2020, Svalbard Integrated Arctic Earth Observing System, Longyearbyen, pp 78-103. https://doi.org/10.5281/zenodo.4293283

Hann R, Betlem P, Deja K, Hartvich F, Jonassen M, Lampert A, Laska M, Sobota I, Storvold R, Zagorski P (2022) Update to Scientific Applications of Unmanned Vehicles in Svalbard. In: Feldner et al (eds) SESS report 2021, Svalbard Integrated Arctic Earth Observing System, Longyearbyen, pp 74-86. https://doi.org/10.5281/zenodo.5751959

Hann R, Johansen T (2020) Unsettled Topics in UAV Icing. SAE International, SAE EDGE Research Report EPR2020008. https://doi.org/10.4271/EPR2020008

James MR, Chandler JH, Eltner A, Fraser C, Miller PE, Mills JP, Noble T, Robson S, Lane SN (2019) Guidelines on the use of structure-from-motion photogrammetry in geomorphic research. Earth Surf Processes Landforms 44(10):2081–2084. https://doi.org/10.1002/esp.4637

Kramar V (2019) UAS (drone) Arctic Challenges: Next Steps, In: Balandin S, Niemi V, Tutina T (eds) Proceedings of the FRUCT'25, Helsinki, Finland, 5-8 November 2019 (pp 507-514). Helsinki: FRUCT

Lampert A, Altstädter B, Bärfuss K, Bretschneider L, Sandgaard J. Michaelis J et al (2020) Unmanned Aerial Systems for Investigating the Polar Atmospheric Boundary Layer—Technical Challenges and Examples of Applications. Atmos 11(4). https://doi.org/10.3390/atmos11040416

Senger K, Betlem P, Birchall T, Buckley SJ, Coakley B, Eide CH et al (2021) Using digital outcrops to make the high Arctic more accessible through the Svalbox database. J Geosci Educ 69(2):123–137. https://doi.org/10.1080/10899995.2020.1813865

Senger K, Betlem P, Birchall T, Gonzaga Jr L, Grundvåg S-A, Horota RK, Laake A, Kuckero L, Mørk A, Planke S, Rodes N, Smyrak-Sikora A (2022) Digitising Svalbard's Geology: the Festningen Digital Outcrop Model. First Break 40(3):47–55. https://doi.org/10.3997/1365-2397.fb2022021

Śledź S, Ewertowski MW, Piekarczyk J (2021) Applications of unmanned aerial vehicle (UAV) surveys and Structure from Motion photogrammetry in glacial and periglacial geomorphology. Geomorphology, 378:107620. https://doi.org/10.1016/j.geomorph.2021.107620

UNOLS (2021) Uncrewed Aerial Systems (UAS) Operations from the U.S. Academic Research Fleet: Operator's Handbook. Available at: https://www.unols.org/document/uncrewed-aerial-systems-uas-operations-us-academic-research-fleet-operator's-handbook

Wilkinson MD, Dumontier M, Aalbersberg IJ, Appleton G, Axton M, Baak A et al (2016) The FAIR Guiding Principles for scientific data management and stewardship. Sci Data 3(1):160018. https://doi.org/10.1038/sdata.2016.18

Concluding remarks

Melting of glaciers and sea ice, thawing of permafrost, and changes in the extent and thickness of snow cover are some evident ongoing changes of concern in the Arctic. Increases in wind speed and liquid precipitation, changes in the sources and transport patterns of aerosols, including dust and pollutants, and in air–sea–land interaction processes are other notable causes for concern.

The scientific community consistently tracks and quantifies such changes to understand them and to give advice on how they may be regulated. To go forward with these important tasks, precise and timely updates on the Arctic environment are essential. This is what the annual State of Environmental Science in Svalbard (SESS) report series has been doing since 2019, focusing on Svalbard – one of the highly climate-sensitive regions in the Arctic.

The peer-reviewed SESS reports provide an exclusive Earth system approach to research strengthened by thoroughly described research methodologies, inter- and cross-disciplinary approaches, and a strong emphasis on the accessibility of the datasets collected in Svalbard. The report acts as a one-stop source for information on Svalbard's environmental status and existing types of research and datasets. It also highlights current knowledge gaps and provides recommendations for filling them. The report adds value to the research done in Svalbard and provides better understanding regionally and globally.

The fifth issue in this series – the SESS 2022 report – adds six more chapters to the overview of internationally driven interdisciplinary research on the archipelago's environment. The first chapter focuses on temperature trends in the atmosphere and ionosphere (SATS), followed by three chapters on aerosols and impurities in the Svalbard atmosphere (LOAD-RIS, SVALDUST, HERMOSA). The last two chapters thoroughly assess studies of snow cover using Ground Penetrating Radar (SnowGPR) and guidelines and operational standards for uncrewed aerial vehicles (UAV Svalbard 3).

In previous SESS reports, three chapters have been dedicated to upper atmosphere studies (Moen et al. 2019, 2020; Baddeley 2021).[1] This year, SATS connects studies of the upper atmosphere with the lower atmosphere and even the depths of the fjords, revealing the interconnections of space and atmospheric physics with meteorology and oceanography.

The lower atmosphere has been the topic of many earlier SESS report chapters (e.g. Bensi et al. 2019; Viola et al. 2019, Petkov et al. 2019; Sipilä et al. 2020; Gilardoni et al. 2020; Mazzola et al. 2020; Traversi et al. 2021; Petkov et al. 2022). This year's chapter, LOAD-RIS, adds an overview of columnar aerosol observations from two locations over the last two decades. SVALDUST describes both local and long-transported dust sources and current observational and modelling methodologies to study them. HERMOSA compiles information on atmospheric pollutant research and gives an overview of parameters that need to be monitored to understand pollutants' origin and future in the Arctic atmosphere, specifically Svalbard. LOAD-RIS, SVALDUST, and HERMOSA highlight the intrinsic interdisciplinarity of aerosol and impurity studies. Aerosols are important components in the Arctic climate, e.g., cloud formation nuclei and carriers of pollution from lower to higher latitudes. Aerosols and pollutant trace gases deposited on the biosphere and cryosphere critically impact the Arctic ecosystem. With the Arctic likely to face multiple non-linear changes, aerosol–trace gas interactions with climate and subsequent impacts on cryosphere and ecosystems are likely to be at the forefront of interdisciplinary issues in Svalbard, as are the well-known connections to human health, social science and economy.

1 All references refer to previous SESS reports, which can be found here: https://sios-svalbard.org/SESSreport

Snow has an impact on most spheres of the Svalbard environment, and many aspects of snow, snow cover and related topics like permafrost and hydrology have been described in earlier SESS reports (e.g. Gallet et al. 2019; Malnes et al. 2021; Killie et al. 2021; Salzano et al. 2021a, 2021b, Christiansen et al. 2019, 2020, Nowak et al. 2021). As a continuation, SnowGPR, with data from 25 years, allows a long-term perspective in understanding the spatial distribution of snow and its effects, which are crucial for feeding glaciers and the entire ecosystem.

UAV Svalbard 3 is an addition to two previous SESS chapters on scientific and practical issues of using uncrewed aerial vehicles in Svalbard and the Arctic in general (Hann et al. 2021, 2022). UAVs are an affordable and environment-friendly technology useful for many different applications in fieldwork, and thus, relevant for a wide scientific audience.

The first four issues of the SESS report were synthesised in 2022 (Matero et al. 2022), providing an overview of 40 chapters and 169 recommendations. It condenses these into disciplinary recommendations and identifies the major cross-cutting interdisciplinary steps forward for Svalbard Integrated Arctic Earth Observing System (SIOS). These include the further development of the data management system and a variety of ways to make the observing system more integrative – action items also reflected in this year's SESS report.

Standardisation of metadata and accessible data storage to facilitate data sharing are strongly recommended in this SESS report. The importance of involving modellers and the added value of modelling components to improve the understanding of the Earth system are mentioned frequently throughout the report. It is also pointed out that technologies and techniques developed in one discipline can be useful in other disciplines as well, and that advanced technologies are facilitating the reduction of human footprints during data collection.

Challenges connected with interdisciplinarity are also mentioned, e.g. the use of inconsistent units and vocabulary in various disciplines, the diverse forces which are important in different spheres, and the challenges in harmonising data collected in several fields. Common platforms to discuss methods and results, e.g. for various disciplines using uncrewed aerial vehicles, yield an unanticipated but useful pathway around these obstacles. An interdisciplinary approach with multi-institutional and international environmental research collaborations is needed to understand the environmental status of Svalbard. The present report is an important contribution to this effort.

The ambition of SIOS, the publisher of the SESS report, is to become a full-scale interdisciplinary and multidomain Earth observing system for the Svalbard region, with the SESS report describing all aspects of the system and the research conducted within this realm. The SESS report has yet to cover many important topics; every new chapter adds a new puzzle piece to the holistic picture. The editorial board of the current SESS report would like to encourage the research community to contribute with their expertise to present and update the state of their environmental science in Svalbard and make the SESS report series an important and comprehensive knowledge source for both the scientific community and society.

Divya David T, Marjolein Gevers, Roseline C Thakur, Christiane Hübner, Jacek Jania

Frequently Asked Questions

Seasonal asymmetries and long-term trends in atmospheric and ionospheric temperatures in polar regions and their dependence on solar activity (SATS)

What do you mean by 'seasonal asymmetry'?

In this context, a seasonal asymmetry means that there is a shift in time between the day of maximum solar input and the day with maximum temperature.

How big is this 'seasonal asymmetry' in Svalbard?

Maximum solar illumination input is around the summer solstice, but most ground stations in Svalbard reach their maximum temperatures around August, so the shift is 40-50 days.

What causes this seasonal asymmetry?

A combination of heat capacity in the ground, in the ocean and in ice, plus transport of energy through sea currents and wind. Heat capacity determines how long it takes for a substance to change its temperature. The ground, water and ice have high heat capacity and their temperatures change slowly, whereas the atmosphere reacts quickly.

Can this seasonal asymmetry be observed also higher up in the atmosphere?

Yes, the asymmetry can be observed in balloon measurements all the way up to the tropopause. Above the tropopause, the asymmetry largely disappears, and temperatures largely follow seasonal changes in solar illumination.

Do you see any correlations between temperatures in Svalbard and solar activity?

No, our study does not reveal any clear correlations and does not identify any causal links between ground temperatures and solar activity.

Long-term observations of aerosol optical depth and their relation to in-situ aerosol properties in the Svalbard region (LOAD-RIS)

Are aerosols an issue at all in a clean area like the Arctic, and if yes, where do they come from?

Although the Arctic is indeed a rather clean area, aerosols play an important role here and have done so for a long time. Already in the 1960s a phenomenon called Arctic haze was observed and prompted continuous measurement programmes from the 1970s. It turned out to be pollution originating from the densely populated mid-latitudes, which accumulated in the Arctic during the winter. These emissions have declined in recent years, but now one increasingly observes smoke from forest fires at high latitudes, in addition to regional sources.

How do aerosols from lower latitudes get into the Arctic?

During the winter, the natural barrier between the Arctic and mid-latitudes, called the polar front, moves southward so that pollution easily can be transported northward. In the summer, this also happens, but from higher latitudes. In addition, smoke plumes from forest fires can rise high up into the atmosphere and there easily cross over the Arctic.

What effect can aerosols have on the Arctic environment?

Aerosols have a twofold impact on the Arctic environment. First, they can influence the climate system by weakening the incoming radiation of the sun, by formation of clouds and by changing the surface reflectance, especially by darkening the bright surfaces of glaciers and snowy areas. Aerosols from forest fires containing a lot of soot are particularly effective at this. Second, aerosols also carry a wide spectrum of pollution into the

Artic which then accumulates in the region and affects all life forms.

Dust in Svalbard: local sources versus long-range transported dust (SVALDUST)

What are the main sources of dust in Svalbard?

In the Svalbard archipelago, dust can have both local and long-range sources. In Ny-Ålesund, local dust dominates in the summer–fall period, while Hornsund reports local dust as early as late spring and throughout the melting season. Dust storms have been reported in Longyearbyen, in Pyramiden and Ebba Valley, as well as at the forefield of the Werenskioldbreen glacier.

Long-range transport to Spitsbergen involves dust from high- to low-latitude regions. According to global transport model simulations, the largest contribution to Svalbard comes from Africa, Asia and, above all, Eurasia, while the contribution from Iceland, North America and, especially, from Greenland is much smaller. In addition, dust from remote sources shows a marked seasonal trend with highs in late winter/spring and lows in summer/autumn.

How dust can modify the cryosphere?

When dust is deposited on snow and ice, it is able to modify their optical properties. In fact, dark particles absorb solar radiation more efficiently and consequently they alter the properties of surface snow and ice. Darker snow/ice will absorb more energy and will melt faster. This particular mechanism has been studied in polar and nonpolar glaciers, but in Svalbard this has not been analysed in detail.

Harmonising environmental research and monitoring of priority pollutants and impurities in the Svalbard atmosphere (HERMOSA)

Where does pollution in Svalbard come from – shouldn't the air be clean so far away from civilisation?

For a long time, scientists studying the Arctic have known that air currents can carry pollution very far away from its source, so smoke produced in Europe, America, or Asia can still reach Svalbard. However, after the year 2000 researchers gave more thought to the pollution produced locally by power plants, engines and other man-made sources in Svalbard, and they are important near the settlements in Svalbard as well.

Is there one way to measure all pollutants/impurities/parameters in the Svalbard air at once?

Unfortunately, no, because there are so many of them. But several are similar enough that it is possible to collect one sample which can be then divided up in a lab and analysed for many parameters. Moreover, there may be pollutants in the air we don't know about – new substances may turn out to be harmful to wildlife, for example UV filters used in cosmetics. That's why we think it would be good to have an air sample bank preserved for future research.

Why bother about pollution, if it is literally everywhere?

It may be everywhere, but not at the same level (typically we call that level concentration). Also, some substances are more harmful than others, and there may be interactions between pollutants. The best research these days is combining data on many types of pollution (or many air measurements) at once to tell us about processes happening in the Arctic. And believe me, there is a lot happening, and we don't know the half of it yet with climate change destabilising things!

Ground penetrating radar measurement of snow in Svalbard - past, present, future (SnowGPR)

Is it possible to find objects buried by snow using a ground penetrating radar system, such as a snowmobile?

GPR detects differences in electrical properties within the ground. A buried object can be detected if its electrical properties are different enough from those of the ground and the GPR system is

sensitive enough. The shape/orientation of the object also matter as the GPR signal must be reflected back towards the ground surface. The object's size in relation to the wavelength of the GPR signal may also influence detectability. The electrical properties of a snowmobile buried in snow and the complexity of its shape would make it detectable with GPR.

How can ground penetrating radar be used to detect layering in snow and firn?

Natural snow/firn is subject to seasonal melting and refreezing, and its surface is exposed to changes in weather. These can make the snow surface denser, creating layers of ice that are subsequently covered by new snow. The buried ice layers have electrical properties similar to those of solid ice, whereas the surrounding snow has pockets of air. This difference in density between ice and snow makes their electrical properties distinct enough that they can be detected with GPR.

Is it possible to obtain information about permafrost by examining snow cover on the tundra?

Yes, indirectly and sometimes directly. Snow cover depth is highly correlated with the thermal regime of the underlying ground. In places where snow cover remains for a long time, the active layer of permafrost (the top layer of soil, which thaws in summer), is often thin. On the other hand, deep snow cover insulates the ground beneath it. In the first case, the ground is frozen down to the full depth of the permafrost. In the second case, it is frozen only at the top, with no permafrost below. GPR waves can penetrate quite deep and reveal the structure of the ground under the snow cover. Frozen and unfrozen ground reflect the GPR signal differently.

How deep does a layer of snow have to be before its thickness and structure can be studied with GPR?

The short answer is 10 cm.

The long answer is that it depends on the type of antenna and the structure of the snow. Soft snow is difficult to measure accurately because it is compressed by the weight of the snowmobile and the antenna. Hard snow tolerates the weight better and is therefore easier to measure.

Practical guidelines for scientific application of uncrewed aerial vehicles in Svalbard (UAV Svalbard 3)

What are the biggest challenges to flying drones in the Arctic?

The main challenge is low air temperatures, which make piloting drones difficult and reduces their battery capacity.

Svalbard's high latitude can mean interference in the magnetic field and low GPS coverage, perturbing the drone's positioning system.

Wildlife can pose problems. Seabirds can attack drones and pilots operating near breeding or feeding grounds. Mammalian wildlife may be frightened by the rotor noises. Stressing Svalbard's fauna is prohibited.

High winds, low visibility, and icing can cause problems, restricting operations to fair weather.

What do I have to do to fly a drone on Svalbard?

Norwegian regulations for drone operations currently apply to Svalbard. For simple missions this means:

- Follow the EU drone regulations
- Disturbing Svalbard's wildlife is prohibited
- Fly no higher than 120 metres above ground
- Keep 150 metres away from people, buildings, boats, etc
- You must always be able to see your drone
- Familiarise yourself with rules about filming and photographing other people
- Flying drones in the dark is prohibited

Stay at least 5 km away from airports in Longyearbyen and Svea. Obey the 20 km no-fly zone around Ny-Ålesund

How are drones used for science in Svalbard?

Drones are used scientifically in many ways. Most scientists use simple drones to take pictures from above. This method can generate maps and 3D landscape models that are useful for many scientific disciplines in Svalbard. Examples include assessing vegetation covers, counting reindeer, mapping glacier crevasses, identifying geohazards, digitising geological outcrops, etc. Some scientists use more sophisticated drones, such as fixed-wing drones, for more advanced purposes, like atmospheric measurements or mapping of large areas.

I want to use drones in Svalbard. How can I get access to drone infrastructures?

Several facilities can be used to obtain access to drones on Svalbard. The University Centre in Svalbard (UNIS) and the Svalbard Integrated Arctic Earth Observing System (SIOS), both offer drone and pilot rental services.

I am using drones for science in Svalbard. Why should I share and long-term store my results?

Data collected with drones can potentially be useful for others in ways that the original drone operators cannot easily predict. For example, a drone campaign mapping glacier surfaces to study crevasses could be used in the future to monitor long-term changes in the glacier's volume and extent. Researchers must share their results with the scientific community and ensure long-term storage of their data. Most university libraries can help with long-term storage of research data and open access, and can advise on general data management strategies.

Would you like to be part of the SESS report?

SIOS frequently publishes calls for contributions to the SESS report. Subscribe to our newsletter and follow us on social media to stay updated.

www.sios-svalbard.org/Newsletter

twitter.com/sios_kc

facebook.com/SIOSKnowledgeCentre

instagram.com/sios_svalbard/

You can find this and previous SESS reports on our webpage:
https://sios-svalbard.org/SESSreport

Visit the SIOS data access portal to find metadata and datasets described in this report: https://sios-svalbard.org/metsis/search

SIOS
SVALBARD INTEGRATED ARCTIC EARTH OBSERVING SYSTEM

ISSN 2535-809X (printed)
ISSN 2535-6321 (pdf)
ISBN 978-82-93871-07-1 (printed, stapled)
ISBN 978-82-93871-06-4 (pdf)